



UNIVERSITY OF CALGARY

The author of this thesis has granted the University of Calgary a non-exclusive license to reproduce and distribute copies of this thesis to users of the University of Calgary Archives.

Copyright remains with the author.

Theses and dissertations available in the University of Calgary Institutional Repository are solely for the purpose of private study and research. They may not be copied or reproduced, except as permitted by copyright laws, without written authority of the copyright owner. Any commercial use or publication is strictly prohibited.

The original Partial Copyright License attesting to these terms and signed by the author of this thesis may be found in the original print version of the thesis, held by the University of Calgary Archives.

The thesis approval page signed by the examining committee may also be found in the original print version of the thesis held in the University of Calgary Archives.

Please contact the University of Calgary Archives for further information,

E-mail: uarc@ucalgary.ca

Telephone: (403) 220-7271

Website: <http://www.ucalgary.ca/archives/>

UNIVERSITY OF CALGARY

Structural Characterization of *Escherichia coli* Periplasmic Ferric Siderophore

Binding Proteins

by

Teresa E. Clarke

A THESIS

SUBMITTED TO THE FACULTY OF GRADUATE STUDIES
IN PARTIAL FULFILMENT OF THE REQUIREMENTS FOR THE
DEGREE OF DOCTOR OF PHILOSOPHY
DEPARTMENT OF BIOLOGICAL SCIENCES

CALGARY, ALBERTA

APRIL 2001

© Teresa E. Clarke 2001

Abstract

To overcome iron deficiency, a wide variety of microbes synthesize and secrete low molecular weight organic chelators called siderophores. Siderophores complex iron from host proteins or insoluble ferric hydroxide. In *E. coli* and other Gram-negative strains, transport of siderophores involves a specific outer membrane receptor, a periplasmic transport protein and several inner membrane associated proteins. This arrangement is similar to other ATP-binding cassette (ABC) transporters, which transport amino acids, peptides and sugars into the cell. Although there are specific outer membrane receptors in *E. coli* for each type of siderophore, common systems within the periplasm and inner membrane are encoded by the *fhu*, *fep* and *fee* operons. FhuD is the periplasmic binding protein involved in the uptake of hydroxamate-type siderophores. The three dimensional x-ray crystal structure of FhuD from *E. coli* complexed with the ferrichrome homolog gallichrome was determined at 1.9 Å resolution using MAD phasing. This represents the first structure of an ABC-type binding protein involved in the uptake of siderophores. The protein is shaped like a kidney bean, with two globular domains connected by a long α -helix. This is unlike most periplasmic ligand binding proteins (PLBPs), which have several β -strands linking two domains. This helix forms a rigid architecture that may lack the ability to undergo the large conformational changes typically observed in PLBPs upon ligand binding. Gallichrome binds in a shallow hydrophobic pocket between the two domains of the protein. Crystal structures of FhuD complexed with other siderophores, including coprogen, the iron chelation drug Desferal® and the antibiotic albomycin were also solved by x-ray crystallography. These show that binding occurs in a similar manner, with movement of amino acid side chains within the binding pocket. Conformational changes experienced by FhuD and the other *E. coli* periplasmic siderophore binding proteins FepB and FecB were analyzed by a variety of spectroscopic methods. These studies also showed that site-directed mutagenesis decreases the ability of FhuD to bind its ligands. This study allows for the rational design of novel bacteriostatic agents, including

siderophore-antibiotic conjugates that act as "Trojan horses", using the siderophore uptake system to deliver antibiotics directly into targeted pathogens.

Acknowledgements

Not many careers integrate so many different aspects of other professions as does science. To be a successful scientist, you must also learn to wear other hats; as a writer, lecturer, politician, teacher and researcher. During my time at the Vogel lab, there are many people who have given me support and encouragement to strive towards these goals. There is no question that this list is incomplete and I apologize for any omissions.

I would especially like to thank my supervisor, Dr. Hans J. Vogel, for the privilege to work in his laboratory. His guidance and insight have been invaluable over the past few years. I would also like to thank "The Boss" for providing the lab with the best equipment and personnel available.

The help from the other members of the Structural Biology Research Group has also been important during my graduate studies. Many thanks go to my best friend Dave Schibli for his patience, support and enthusiasm. Special thanks also go to Aalim "the Aaliminator" Weljie, Andriyka Papish, Craig "the Sheep" Shepherd, Doug Dougan, Donghui Li, Dr. Hui Ouyang, Karla Krewulak, Peter Hwang, Phoebe Franco, Dr. Rich Brox (of the "Rich salute"), Rob "Maverick" Skene, Sean "S-Club" Peacock, Steve Shouldice, Dr. Tao Yuan, Dr. Tung "the fish pimp" Hoang, Tara "Mimi" Winstone for all the great times inside and outside the lab. Thanks to Elke Lohmeier-Vogel for the jokes, the ski trips and for being a good mentor. I would like to acknowledge Deane McIntyre for his maintenance of the NMR equipment and Kirsten Bagh for keeping the lab in order. I would like to also thank the new members of the Vogel lab for their understanding over the past few months.

The guidance of my supervisory committee is also appreciated. Thank you to Dr. Michael Boorman and Dr. Pam Sokol for their helpful suggestions. Dr. Ray Turner and Dr. Les Tari are thanked for participating in my candidacy examination and for numerous interesting discussions. I would also like to thank Dr. Barry Phipps, Dr. Andrew Braun and Dr. Dick van der Helm (University of Oklahoma) for being a part of my oral examination

committee. I wish to acknowledge the generous financial support from the Canadian Institutes for Health Research (CIHR).

Some aspects of my work would not have been possible without the help of collaborators. Thank you to Dr. Wolfgang Koster (Swiss Federal Institute for Environmental Science and Technology, Switzerland), Dr. Martin Rorhbach and Dr. Volkmar Braun (Universitat Tubingen, Germany) for providing me with bacterial strains used during this project and their analysis of mutant FhuD proteins (Chapter 4). I would also like to thank Dr. G. Winkelmann for providing siderophores (Universitat Tubingen, Germany). For their maintenance of the CD spectrometer, Dorothy Fox, Qiao Wu and Dr. Yamdagni are appreciated. Ryan Deedo is thanked for his help cloning *fepB* (Chapter 6). Thanks to the original synchrotron team, Dr. Les Tari, Doug Dougan and Anjali Relan for showing me the ropes and to Dr. Barry Phipps, Shao-Yang Ku and Rob Skene for having such a great time the next time around. Thanks to the support staff at the NSLS at BNL for their help. I am also indebted to David Hosfield for data collection at SSRL.

There are also other people who have kept me entertained during my studies in Calgary. Our honorary lab member Valerie Brown is thanked for her friendship and encouragement. Thanks also to my friends Jill Hudson and Scott Taylor, Donna Moritsugu, Alison McCray, Nikki Budak for visiting me in Calgary and for all the e-mails. The hockey team and slo-pitch team have also kept me amused and in shape over the years. Thanks to the Ecology and Botany people for including me in their many activities. Finally, I would like to thank my family for their continuous support. I am happy to make my parents John and Linda and their new spouses, Evangeline and John, so proud.

Table of Contents

Approval page	ii
Abstract	iii
Acknowledgements	v
Table of Contents	vii
List of Tables	xiii
List of Figures	xiv
Abbreviations	xvii
Chapter 1: Structural Biology of Iron Uptake Systems	1
Introduction	2
Iron availability	2
Overview of bacterial iron uptake systems	3
Transport across the outer membrane	11
Structure of Receptor Proteins	12
Structure and function of HasA	12
Structure and function of FepA and FhuA	14
Energy requirement for transport via the TonB system	21
ABC Transport Systems	25
Structure of periplasmic ligand binding proteins	26
Biochemistry of inner membrane associated proteins	29
Energy requirement for transport using ATP	31
Regulation of Gene Expression	32

Regulation by Fe ²⁺ -Fur	33
Other types of regulation	36
Storage of Iron	40
Summary	41
Scope of this Dissertation	42
Chapter 2: X-ray Crystallographic Structure of FhuD bound to Gallichrome	44
Introduction	45
General principles of x-ray crystallography	45
MAD phasing	46
Application of MAD phasing	50
Methods	51
Purification of His-tag FhuD	51
Crystallization and data collection	51
Phasing and model refinement	52
Analysis	53
Coordinates	53
Results	54
Overall structure	54
Siderophore binding	59
Structures of the FhuD ferrichrome and FhuD alumichrome complexes	63
Discussion	65

Relation to other periplasmic binding proteins	65
Siderophore binding to FhuD	67
Implications for siderophore transport	70
Chapter 3: X-ray Crystallographic Structures of the <i>Escherichia coli</i> Periplasmic Protein FhuD bound to Various Hydroxamate-type Siderophores	73
Introduction	74
Methods	78
Purification of FhuD	78
Crystallization and data collection	78
Phasing and model refinement	79
PDB coordinates	80
Results	81
Overall structures	81
Siderophore binding	90
Comparison of the binding mode	92
Discussion	97
Recognition of hydroxamate-type ferric siderophores by FhuD	97
Relation to other periplasmic ligand binding proteins	98
Proposed mechanism for ferric siderophore transport	100
Rational design of siderophore-antibiotic conjugates	100
Chapter 4: Ferric Hydroxamate Binding Protein FhuD: Mutants in Conserved and Non-conserved Regions	102
Introduction	103

Methods	106
Construction of the FhuD mutants	106
Functional analysis of the FhuD mutants	106
Identification of the locations of the point mutations in FhuD	106
Sequence analysis and multiple alignments	105
Results	107
Phenotype of the FhuD mutants	107
Location of the point mutations in the crystal structure of FhuD	109
Evolutionary relationships	112
Conserved sequence patterns	112
Discussion	116
Chapter 5: Spectroscopic and biochemical studies of the <i>E. coli</i> periplasmic binding protein FhuD and mutants	119
Introduction	120
Methods	122
Construction of FhuD mutants	122
Purification of FhuD and mutants	123
Fluorescence spectroscopy	123
Circular dichroism spectroscopy	124
Band shift assays	124
Proteolytic protection assays	125
Results	126

Purification of mutant FhuD proteins	126
Fluorescence spectroscopy	127
Circular dichroism spectroscopy	136
Native PAGE band shift assays	145
Protease protection assays	147
Discussion	150
Chapter 6: Characterization of the <i>E. coli</i> periplasmic ferric siderophore binding proteins FepB and FecB	153
Introduction	154
Methods	158
Cloning and Expression of FepB	158
Purification of FepB	158
Purification of enterobactin	159
Cloning and Expression of FecB	161
Purification of FecB	161
Circular dichroism spectroscopy	162
Non-denaturing PAGE	162
Proteolytic protection assays	162
Crystallization of FepB	162
Results	164
Overproduction of FepB and FecB	164
Circular dichroism spectroscopy	166

Band shift assays

Protease protection assays

Crystallization trials

Discussion

Chapter 7: Concluding Remarks

References

List of Tables

1.1	Iron uptake systems of pathogenic bacteria	6
2.1	Summary of crystallographic data for FhuD gallichrome	55
2.2	Summary of crystallographic data for FhuD ferrichrome and alumichrome	64
3.1	Summary of crystallographic data	82
4.1	Phenotype of FhuD mutants	108
4.2	Location of the FhuD mutant residues	111
7.1	FhuB peptides used in crystallization	177

List of Figures

1.1	Overview of bacterial iron uptake systems	4
1.2	Representative structures of the different classes of siderophores	10
1.3	Ribbon diagram of the structure of the hemophore HasA	14
1.4	Structures of FepA and FhuA	15
1.5	Dendrogram of outer membrane receptors	17
1.6	Transmitting energy to the outer membrane in <i>E. coli</i>	21
1.7	Space filling models of the apo- and holo-forms of <i>H. influenzae</i> Fbp	28
1.8	Structure of the ATP-binding subunit of the ATP permease	31
1.9	Alignment of Fur from various bacteria	34
1.10	Structure of DtxR bound to the <i>tox</i> gene operator DNA	39
2.1	Fluorescence spectrum of gallium of gallichrome bound to FhuD	48
2.2	The Harker diagram for determination of phase angles	49
2.3	Crystals of the FhuD gallichrome complex	56
2.4	$2 F_o - F_c $ electron density map at 1.9 Å resolution	56
2.5	A stereo ribbon diagram of the FhuD gallichrome complex	57
2.6	A topology diagram of FhuD	58
2.7	A detailed stereo view of gallichrome binding to FhuD	60
2.8	A space filling model of the FhuD gallichrome complex	61
2.9	A GRASP diagram of the binding pocket of FhuD	62
2.10	Comparison of the structures of periplasmic binding proteins	67

2.11	A comparison of the residues involved in binding in FhuD and FhuA	69
3.1	Chemical structures of various hydroxamate-type siderophores	76
3.2	2 Fo - F _c Oc electron density maps of the FhuD siderophore complexes	83
3.3	Ribbon diagrams of the FhuD siderophore complexes	85
3.4	A close-up view of the binding sites of the FhuD siderophore complexes	87
3.5	Comparison of the conformations of the FhuD siderophore complexes	89
3.6	A schematic comparison of hydrogen bonding	94
3.7	A comparison of the binding modes of albomycin in FhuA and FhuD	96
4.1	Map of the mutations on the structure of FhuD	110
4.2	An unrooted evolutionary tree of periplasmic binding proteins	114
4.3	Sequence alignment of periplasmic binding proteins	115
5.1	A 12% SDS-PAGE following the purification of <i>E. coli</i> FhuD mutants	126
5.2	Fluorescence spectra of FhuD	128
5.3	A Stern-Volmer plot of acrylamide quenching of FhuD	130
5.4	Fluorescence spectra of mutant FhuD proteins	131
5.5	Decrease in the fluorescence intensity of mutant FhuD proteins	133
5.6	Fluorescence spectra of PI 67 A	134
5.7	Far-UV circular dichroism spectra of FhuD	137
5.8	Far-UV CD spectra of R84Q	139
5.9	Far-UV CD spectra of Y106A	141
5.10	Far-UV spectra of P167A	143
5.11	Native PAGE of FhuD complexed with ferrichrome	146

5.12	Native PAGE of mutant FhuD proteins	146
5.13	Protection of FhuD from degradation	147
5.14	Protection of mutant FhuD proteins from degradation	149
6.1	Chemical structures of enterobactin and TREN CAM	155
6.2	A 12% SDS-PAGE following the purification of <i>E. coli</i> FepB	165
6.3	A 12% SDS-PAGE monitoring the purification of <i>E. coli</i> FecB	166
6.4	Far-UV CD spectra of FepB and FecB	167
6.5	Mobility differences between apo and holo proteins on a native PAGE	170
6.6	Protection of FepB from degradation	171
6.7	FepB crystals grown in a hanging drop	172
7.1	Siderophore-antibiotic conjugates used in crystallization	180
7.2	Key interaction sites in the binding pocket of FhuD	182
7.3	The seed structure used by GROW	183

Abbreviations

ABC-type	ATP-binding cassette type
ATP	adenosine triphosphate
BLAST	basic local alignment search tool
BNL	Brookhaven National Laboratories
CD	circular dichroism
CM	cytoplasmic membrane
CNS	crystallography and NMR system
DALI	distance matrix alignment
DBS	dihydroxybenzylserine
DEAE	diethylaminoethyl
DNA	deoxyribonucleic acid
Ent	enterobactin/enterochelin
FeDBS	ferric dihydroxybenzylserine
FeEnt	ferric enterobactin/enterochelin
Hb	hemoglobin
HEPES	N-[2-hydroxyethyl]piperazine-N'-[2-ethanesulfonic acid]
HPLC	high pressure liquid chromatography
IPTG	isopropyl-(3-D-thiogalactopyranoside)
LB	Luria broth
Lf	lactoferrin

MAD	multiwavelength anomalous dispersion
MECAM	1,3,5-tris(N,N',N"-2,3-dihydroxybenzoyl)aminobenzene
MoFe	moybdenum-iron
NMR	nuclear magnetic resonance
NSLS	National Synchrotron Light Source
NTP	nucleoside triphosphate
OM	outer membrane
OMR	outer membrane receptor
PAGE	polyacrylamide gel electrophoresis
PCR	polymerase chain reaction
PDB	Brookhaven Protein Data Bank
PEG	polyethylene glycol
p _i	isoelectric point
PLBP	periplasmic ligand binding protein
PMSF	phenylmethylsulfonylfluoride
PP	periplasm
Q Sepharose	quaternary amine Sepharose
rmsd	root mean square deviation
SD	standard deviation
SDS	sodium dodecyl sulfate
SLAC	Stanford Linear Accelerator Center
Tf	transferrin

tris(hydroxymethyl)aminomethane

ultraviolet

Chapter 1

Structural Biology of Bacterial Iron Uptake Systems

Numerous bacterial proteins are involved in microbial iron uptake and transport and considerable variation has been found in the uptake mechanisms used by different bacterial species. However, whether extracting iron from host proteins such as transferrin, lactoferrin or hemoglobin or importing low molecular weight iron-chelating compounds such as heme, citrate or siderophores, Gram-negative pathogenic bacteria typically employ a specific outer membrane receptor, a periplasmic binding protein and two inner membrane associated proteins: a transporter coupled with an ATP-hydrolyzing protein. Often, studies have shown that proteins with similar function but little amino acid sequence homology are structurally related. Elucidation of the structures of the *Escherichia coli* outer membrane siderophore transport proteins FepA and FhuA have provided the first insights into the conformational changes required for ligand transport through the bacterial outer membrane. The variations between the structures of the prototypical periplasmic ferric binding protein FbpA from *Neisseria* and *Haemophilus influenzae* and the *E. coli* periplasmic siderophore binding protein FhuD reveal that the different periplasmic ligand binding proteins exercise distinct mechanisms for ligand binding and release. The structure of the hemophore HasA from *Serratia marcescens* shows how heme may be extracted and utilized by the bacteria. Other biochemical evidence also shows that the proteins that provide energy for iron transport at the outer membrane, such as the TonB-ExbB-ExbD system, are structurally very similar across bacterial species. Likewise, the iron-sensitive gene regulatory protein Fur is found in most bacteria. Together, these three-dimensional structures provide us with detailed knowledge of iron transport systems from various pathogenic bacteria. More importantly, the current structures for iron transport proteins provide rational starting points for design of novel antimicrobial agents.

Introduction.

In recent years, elucidation of the mechanisms used by bacteria to procure iron from their environment has reached new levels. Many comprehensive reviews have been published about various aspects of bacterial iron transport (Mietzner and Morse, 1994; Braun, 1998; Braun and Killmann, 1999; Schryvers and Stojiljkovic, 1999; Vasil and Ochsner, 1999; Ratledge and Dover, 2000; Wandersman and Stojiljkovic, 2000; Clarke *et al.*, 2001). Here, we will focus our discussion on those iron uptake systems for which biochemical and structural information is available. Over the last few years, several structures of bacterial iron uptake proteins have been solved by x-ray crystallography. These provide detailed insights into bacterial iron uptake mechanisms. The best-characterized iron uptake systems are those from *Escherichia coli*, and they can be reliably used as model systems for other bacteria, since it appears that on the basis of amino acid homology, the various systems are evolutionary related.

Iron availability. Iron is absolutely required by most biological systems due to its diverse role in the biochemistry of the cell. Although iron is the most abundant transition metal on Earth, the solubility of iron is very low at physiological pH in aerobic environments and therefore, the bioavailability of iron is poor. Insoluble ferric hydroxide complexes form in solution, severely limiting the amount of free iron (Crichton, 1991). Within a mammalian host, the majority of the iron is intracellular, where it is sequestered within heme compounds and iron-sulphur clusters in various proteins and in the storage molecule ferritin. Extracellular iron is complexed to transferrin and lactoferrin, and sometimes to citrate (Griffiths, 1991; Payne, 1993). In order for iron to be used by the bacterium, it must be extracted from the environment or host by specialized uptake mechanisms. Once inside the bacterial cell, the iron is involved in enzymatic redox reactions. However, iron can also play a structural role in proteins as well as acting to change the reactivity of active site residues.

Even though the reactivity of the iron atom makes it useful in many different biological applications, undesirable side reactions can occur. Through Fenton-type chemistry, iron catalyzes the production of toxic hydroxyl radicals from hydrogen peroxide, which arises from the spontaneous combination of superoxide anions created by oxidative metabolism in cells (Arroyo *et al.*, 1994). Oxygen radicals and peroxides are highly destructive, damaging lipids, proteins and nucleic acids in the cell. Radicals induce the formation of unsaturated bonds in lipids, decreasing membrane fluidity and causing cell lysis. They also react with thiol groups in proteins, causing cross-linking and inactivation. Hydroxyl radicals can also extract hydrogen atoms from DNA and RNA, causing mutations or cleavage of the phosphodiester backbone.

A collection of different mechanisms has evolved in order to deal with toxic radicals. A number of enzymes and cofactors function in prokaryotes to detoxify oxygen radicals. However, a simpler method to reduce radical formation by iron is to limit the availability of the iron atom itself, by sensing adequate iron levels, limiting uptake and sequestering excess iron in storage proteins.

Overview of bacterial iron uptake systems. A variety of high-affinity iron uptake systems exist in bacteria to obtain iron from the environment or an animal host, by directly binding iron or iron-binding proteins or by utilizing iron chelators (Figure 1.1; Table 1.1) (Mietzner and Morse, 1994; Braun and Killmann, 1999; Schryvers and Stojiljkovic, 1999; Vasil and Ochsner, 1999; Clarke *et al.*, 2001). Most pathogenic bacteria can procure iron directly from the host iron binding proteins, transferrin (Tf) and lactoferrin (Lf) (Wolz *et al.*, 1994; Cornelissen and Sparling, 1994), or indirectly through heme from hemoglobin (Hb) (Dyer *et al.*, 1987). Insoluble ferric iron (Fe^{3+}) can sometimes also be reduced to ferrous iron (Fe^{2+}) for microbial use (Coulanges *et al.*, 1997). Often, iron can be chelated by siderophores, which are small molecular weight compounds produced by the bacteria itself or by neighbouring microorganisms (Neilands, 1995), then transported into the cell by specific acquisition pathways (Table 1.1). Although the primary sequences of many of these

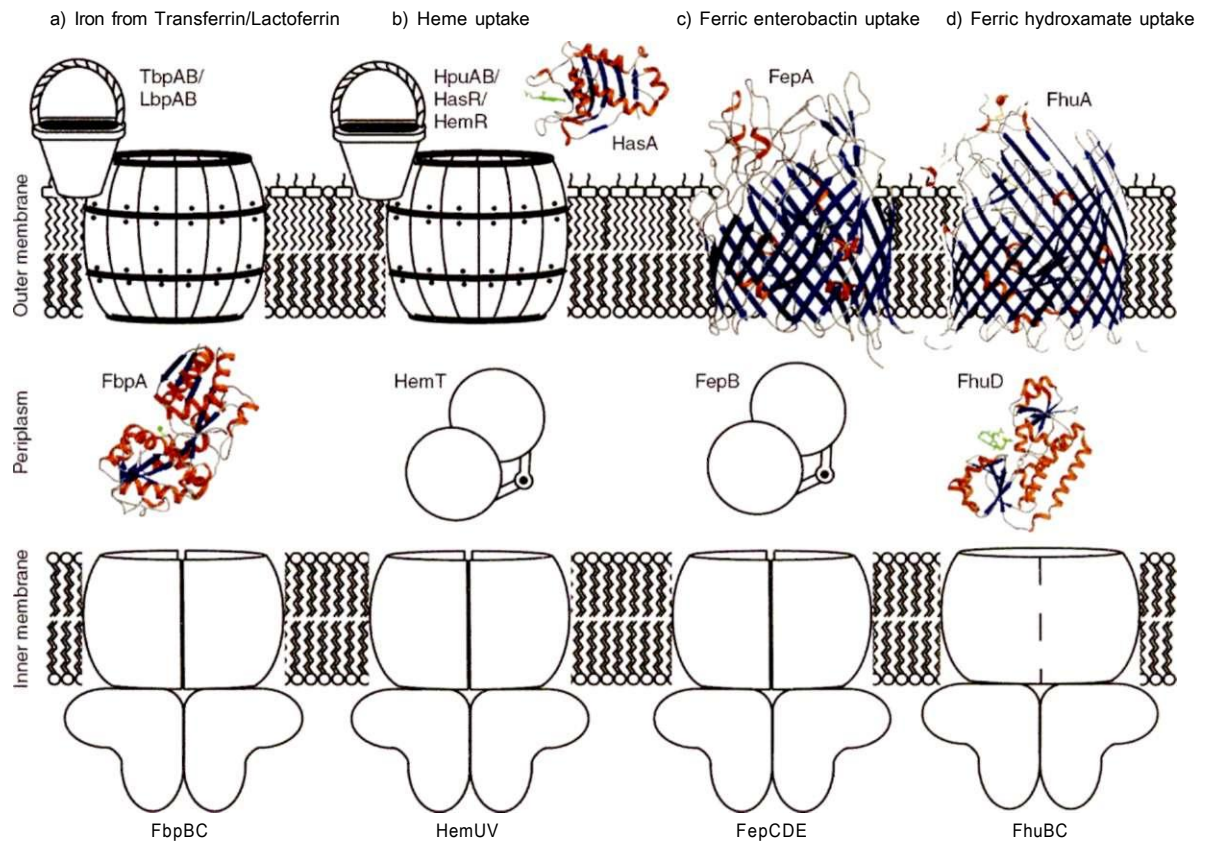


Fig. 1.1 (previous page) Overview of bacterial iron uptake systems. Proteins with known structures are inserted into their appropriate locations in the cell, a) Iron acquisition from transferrin or lactoferrin involves direct binding to a bipartite outer membrane receptor, where Fe^{3+} is extracted. The ferric iron atom is transported across the periplasm by FbpA (Bruns *et al.*, 1997) then transferred to the cytoplasm by an FbpBC complex, b) Heme can either be extracted from hemoglobin at the cell surface by a bipartite receptor (HpuAB) or in the extracellular milieu by a hemophore (HasA (Arnoux *et al.*, 1999)). An outer membrane receptor, HasR, can either bind the hemophore or heme itself for transfer to the periplasm. The detailed mechanism for transport of heme into the cell from the periplasm has yet to be elucidated and may involve an ABC transporter (Stojiljkovic and Hantke, 1992). Ferric siderophores chelate iron from transferrin, lactoferrin or other host proteins and are then transported through outer membrane receptors specific for c) catecholate (FepA (Buchanan *et al.*, 1999)) or d) hydroxamate siderophores (FhuA (Ferguson *et al.*, 1998; Locher *et al.*, 1998)). The FepB and FepCD complex transport catecholate ferric siderophores across the periplasm and inner membrane, respectively. Hydroxamate-type siderophores are transported across the periplasm by FhuD (Clarke *et al.*, 2000) and across the inner membrane by the FhuBC complex.

Table 1.1 Iron uptake systems of pathogenic bacteria

Iron Source	Bacteria	Protein	Function	References
transferrin or lactoferrin	<i>Haemophilus influenzae</i>	LbpAB	LfOMR'	(Ogunnariwo and Schryvers, 1996)
		TbpAB HitABC	Tf OMR Fe ²⁺ ABC system	(Gray-Owen <i>et al.</i> , 1995) (Adhikari 1995)
	<i>Neisseria</i> spp.	LbpAB	LfOMR	(Schryvers and Morris1988b Pettersson <i>et al.</i> 1993; 1994)
		TbpAB	Tf OMR	(Schryvers and Morris1988a; Schryvers and Lee, 1989)
		FbpABC	Fe ³⁺ ABC system	(Berishe/ <i>al.</i> , 1990ab; Adhikariefa/., 1996)
<i>Yersinia enterocolitica</i>	Yfu	Fe ³⁺ ABC system	(Saken <i>et al.</i> , 2000)	
<i>Actinobacillus pleuropneumonia</i>	Afu	Fe ²⁺ ABC system	(Chin <i>et al.</i> , 1996)	
lactoferrin	<i>Helicobacter pylori</i>		ABC system	(Hussone^a/., 1993)
heme	<i>E.coli</i> 0157	ChuA	heme OMR	(Torres and Payne, 1997)
	<i>Neisseria</i> spp.	HmbR	heme/Hb OMR	(Stojiljkovic <i>et al.</i> , 1996)
		HpuAB SfuABC	heme/Hb OMR Fe ²⁺ ABC system	(Lewis <i>et al.</i> , 1997) (Letoffeer <i>al.</i> , 1998; Angerere?a/., 1990)
	<i>Serratia marcescens</i>			
	<i>Shigella dysenteriae</i>	ShuA	heme OMR	(Mills and Payne, 1995)
	<i>Vibrio cholerae</i>			(Stoebner and Payne, 1988)
	<i>Yersinia enterocolitica</i>	HemPRST		(Stojiljkovic and Hantke, 1994)
<i>Yersinia pestis</i>	YbtPQ		(Fetherstone:a/., 1999)	
haemoglobin	<i>Neisseria gonorrhoeae</i>	HpuAB	heme/Hb OMR	(Lewis <i>et al.</i> , 1997)
	<i>Neisseria meningitidis</i>	HmbR	heme/Hb OMR	(Stojiljkovic <i>et al.</i> , 1996)
	<i>Pseudomonas aeruginosa</i>	PhuR	heme/Hb OMR	(Ochsner <i>et al.</i> , 2000)
		PhuSTUV	heme ABC system	(Ochsner <i>et al.</i> , 2000)
		HasRADE	heme receptor, hemophore, HasA ABC transporter	(Ochsner <i>et al.</i> , 2000)
haemoglobin or hemopexin	<i>Haemophilus influenzae</i>			(Braun <i>et al.</i> , 1998)
reduced iron	<i>E.coli</i>	FeoAB	Fe ²⁺ transport	(Kammlere/a/., 1993)
	<i>Pseudomonas aeruginosa</i>	FeoAB	Fe ²⁺ transport	(Vasil and Ochsner, 1999)

siderophores	<i>Azotobacter vinelandii</i>			(Page and Huyer, 1984)
	<i>Bacillus subtilis</i>	FhuBCDG	ferrichrome	(Braun <i>et al.</i> , 1998)
	<i>Bordetella pertussis</i>	BfeA	ferrienterobactin	(Beall and Sanden, 1995)
		BfrABC	siderophore OMR	(Beall and Hoenes, 1997;
		FauA	alcaligin OMR	(Brickman and Armstrong,
	<i>Camphylobacter coli</i>	CeuBCDE	ABC enterobactin transport	(Richardson and Park, 1995)
	<i>Erwinia chrysanthemi</i>	Fct	chrysobactin OMR	(Sauvage <i>et al.</i> , 1996)
		CbrABCD	achromobactin ABC transporter	(Mahe <i>et al.</i> , 1995)
	<i>Escherichia coli</i>	FecABCD	ferric citrate	(Staudenmaier <i>et al.</i> , 1989)
		FepABCD	ferrienterobactin	(Shea and McIntosh, 1991; Ozenberger <i>et al.</i> , 1987; Pierce and Earhart, 1986)
		FhuABCD	ferrichrome, rhodoturulate and coprogen	(Fecker and Braun, 1983)
		Cir, Fiu	dihydroxybenzyl serine OMR	(Hantke, 1981, 1983)
		IutA	aerobactin OMR	(de Lorenzo <i>et al.</i> , 1986)
	<i>Morgenella morgani</i>	RumAB	rhizoferrin transport	(Kuhne/a/., 1996)
	<i>Neisseria</i>	FrpB	siderophore OMR	(Thulasiraman <i>et al.</i> , 1998)
	<i>Pseudomonas aeruginosa</i>	FptA	pyochelin OMR	(Ankenbauer, 1992)
		FpvA	pyoverdine OMR	(Poole <i>et al.</i> , 1993)
		FiuA	ferrioxamine	(Ochsner and Vasil, 1996)
		PfeA (E?),	enterobactin OMR	(Dean and Poole, 1993ab; Ochsner and Vasil, 1996)
		PiuA, PfuA,	unknown OMR	(Ochsner and Vasil, 1996)
	<i>Pseudomonas putida</i>	PupAB	pseuobactin	(Bitter <i>al.</i> , 1991; Kostere/a/., 1993)
	<i>Rhizobia</i>	FhuA	siderophore OMR	(Yeoman <i>et al.</i> , 2000)
	<i>Vibrio</i>			(Sigel and Payne, 1982)
	<i>Vibrio cholerae</i>	ViuA	vibriobactin OMR	(Buttertone/a/., 1992)
	<i>Vibrio anguillarum</i> .	FatDCBA	ferric anguibactin transport	(Tolmaskye/a/., 1988; Crosa, 1989)
	<i>Yersinia enterocolitica</i>	FyuA	yersiniabactin OMR	(Heesemann <i>et al.</i> , 1993)
		FoxA	ferrioxamine B OMR	(Baumler and Hantke, 1992)
		FcuA	ferrichrome OMR	(Koebnikera/., 1993a)

'OMR, outer membrane receptor

proteins are distinctive and their sizes vary widely, consensus sequences for families of proteins can be identified. As more complete bacterial genomes are sequenced, our knowledge about the relationship between these proteins will undoubtedly increase. As the structural database grows, we will gain deeper insights into the molecular mechanisms of pathogenic iron uptake.

In Gram-negative bacterial strains, transport of iron involves a specific outer membrane receptor whereas in Gram-positive organisms, which lack an outer membrane, the receptor protein is anchored by a covalently linked lipid (Cockayne *et al*, 1998). A periplasmic transport protein and several inner membrane associated proteins complete the transport of iron into the cell (Figure 1.1) (Braun and Killmann, 1999; Schryvers and Stojiljkovic, 1999). This arrangement of proteins from periplasm to cytoplasm is similar to other bacterial periplasmic protein dependent systems, termed ABC transporters (for ATP binding cassette-type transport), which transport amino acids, peptides and sugars into the cell (Ames, 1986; Higgins, 1992; Tarn and Saier, 1993; Quioco and Ledvina, 1996). ABC proteins are also found in many mammalian cells, such as the P-glycoprotein involved in drug secretion (Schneider and Hunke, 1998).

In pathogenic *Neisseria* and *Haemophilus*, specific receptors for the serum glycoprotein Tf, TbpA and TbpB (Gray-Owen and Schryvers, 1996; Schryvers and Morris, 1988a) and the structurally related mucosal protein Lf, LbpA and LbpB (Schryvers and Morris, 1988b; Bonnah and Schryvers, 1998; Pettersson *et al*, 1998) remove iron from these proteins for subsequent transport into the periplasm. TbpA and LbpA are integral membrane proteins with large surface loops predicted to extend into the outer milieu that promote iron extraction from Tf and Lf. They also interact with the lipoproteins TbpB or LbpB, which are thought to facilitate Tf binding and iron release. The periplasmic protein FbpA then shuttles the ferric ion across the periplasm to the inner membrane associated proteins FbpB and FbpC for transport into the cytoplasm.

Host heme can be utilized as an iron source in *Pseudomonas aeruginosa* by the *phu* system, which is related to the heme uptake system of *Yersinia*, where PfuR is the heme

receptor and PfuSTUVW forms an ABC transport system (Ochsner *et al.*, 2000). Alternately, heme can be bound by the extracellular hemophore HasA, then taken up into the cell by the receptor HasR (Letoffe *et al.*, 1998; Ochsner *et al.*, 2000). In *Neisseria*, iron in the form of heme or as Hb can be used via the receptor HmbR (Stojiljkovic *et al.*, 1996) or as haptoglobin-hemoglobin by HpuA and HpuB (Lewis *et al.*, 1997). However, heme may also passively diffuse through the outer membrane, or through a porin, since mutants defective in these receptors can grow using heme as the sole iron source (Chen *et al.*, 1996; Stojiljkovic *et al.*, 1996; Stojiljkovic and Srinivasan, 1997). Currently, the proteins involved in the transport of heme across the periplasm and inner membrane are not well characterized, but presumably the existence of an ABC transport system would not be an unreasonable prediction.

Many types of hydroxamate and catechol siderophores, as well as citrate, are utilized by bacteria (Figure 1.2). Although a specific bacterial strain may produce only a few types of siderophores, uptake systems for several different siderophores may be expressed. *Pseudomonad* species synthesize yellow-green, water-soluble fluorescent siderophores called pyoverdines or pseudobactins (Abdallah, 1991). Pyoverdines have a common chromophore derived from 2,3-diamino-6,7-dihydroxyquinoline but different peptides are attached and these are specific for each species. *Pseudomonas aeruginosa* potentially has eight different outer membrane receptors for ferric siderophores. FpvA (Poole *et al.*, 1993) and FptA (Ankenbauer and Quan, 1994) are the receptors for its two endogenously produced siderophores, ferripyoverdine and ferripyochelin, respectively. Ferric enterobactin is taken up by PfeA (Dean and Poole, 1993a; Dean and Poole, 1993b; Dean *et al.*, 1996) and the lower affinity PirA receptor where the FiuA receptor is responsible for ferrioxamine B uptake (Vasil and Ochsner, 1999). The functions of the remaining receptors PiuA, PfuA and UfrA have not yet been characterized. Similarly, in *Escherichia coli*, only the catecholate siderophore enterobactin is actually synthesized by the bacteria itself but there are specific receptors for hydroxamate-type siderophores

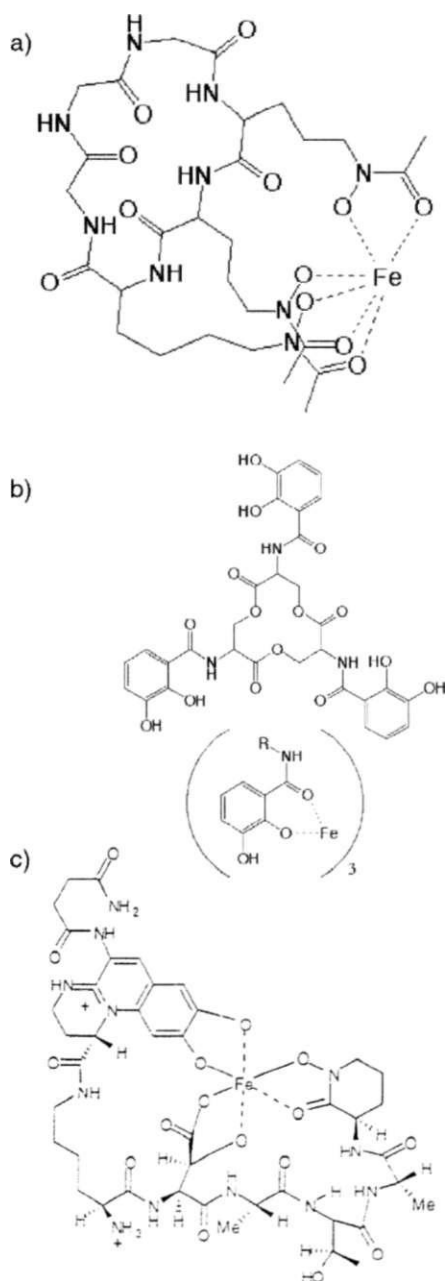


Fig. 12 Representative structures of the different classes of siderophores. a) Hydroxamate (Clarke *et al.*, 2000), b) catechols (Cohen *et al.*, 1998), and c) pyoverdins (Roosenberg *et al.*, 2000) remove iron from host proteins such as transferrin, lactoferrin or hemoglobin or outside the host from the natural environment.

(aerobactin, ferrichrome, rhodoturulate, coprogen and ferrioxamine B) and catechol-type compounds (enterobactin and dihydroxybenzylserine). Common systems within the periplasm and inner membrane are used which are encoded by the *fhu* (Fecker and Braun, 1983) and *fep* (Pierce and Earhart, 1986; Ozenberger *et al*, 1987; Shea and McIntosh, 1991) operons for hydroxamate and catecholate siderophores, respectively. Ferric citrate is internalized in *E. coli* via the transport system encoded by the *fee* genes (Staudenmaier *et al*, 1989).

Under anaerobic conditions, ferric iron (Fe^{3+}) can be reduced to the more soluble ferrous form (Fe^{2+}) by reductases produced by Enterobacteriaceae. The *feoABC* genes identified in *E. coli* are attributed to ferrous iron uptake, where *feoB* is described as a inner membrane associated ATP binding protein, but the functions of *feoA* and *feoC* are presently unknown (Kammler *et al*, 1993). Other *feo* genes have also been identified in *Salmonella typhimurium* (Tsolis *et al*, 1996) and *Methanococcus jannaschii* (Bult *et al*, 1996), however ferrous iron uptake genes have yet to be identified in other pathogenic bacteria. It is still unclear how bacteria coordinate Fe^{3+} versus Fe^{2+} . It is believed that the uptake of Fe^{3+} is the major pathway so that will be the focus of the following sections.

Transport Across the Outer Membrane. Iron uptake does not necessarily begin with transport of iron by the requisite outer membrane receptors. Siderophores and hemophores can be synthesized and secreted by the bacteria in order to chelate iron or heme, respectively, and deliver them to the outer membrane receptors. The genes involved in the biosynthesis and export of siderophores are numerous, and the reader is encouraged to explore several comprehensive reviews on the topic (Braun *et al*, 1991; Wooldridge and Williams, 1993; Crosa, 1989). The chemical structures of many different siderophores are well known (Neilands, 1995) and the three-dimensional structures of some of these have been determined. However, structural information about hemophores and outer membrane receptor proteins is quite limited. Thus, we will examine the recent structures of HasA, a hemophore secreted by *Serratia marcescens* (Arnoux *et al*, 1999) and the outer membrane

siderophore receptors, FepA (Buchanan *et al*, 1999) and FhuA (Ferguson *et al*, 1998; Locher *et al*, 1998) from *E. coli*.

A number of factors contribute to the existence of specific outer membrane receptors for iron uptake. Numerous receptors, between 75 and 85 kDa in size, expressed under iron limiting conditions, have been identified in many different organisms. These receptors bind their ligands with a very high affinity and specificity to transport compounds against a concentration gradient using energy from the inner membrane associated TonB-ExbB-ExbD complex (Braun, 1995; Braun *et al*, 1998). Tf, Lf and heme protein receptors function to recruit these proteins to the cell surface and extract their iron. Although most substrates can diffuse through open porin channels in the outer membrane, heme complexes and ferric siderophores are too large to pass into the periplasm through this route, so outer membrane receptors are required to facilitate their transport. Since the concentration of ferric siderophores and heme in the external media is low, high affinity receptor proteins are utilized by the bacterium, thereby concentrating them at the cell surface and increasing their rate of transport. Competition with other microorganisms for the same siderophore also favours having a receptor with high affinity. Since the receptor is usually rather specific for a particular compound, the bacteria can avoid taking up compounds that have antimicrobial effects, such as siderophore mimetic antibiotics.

Structure of Receptor Proteins.

Structure and function of HasA. Extracellular chelation of iron and heme allows the bacteria to solubilize otherwise unavailable iron sources. Extracellular heme-binding proteins have only been identified thus far in three bacterial species; in *Haemophilus influenzae*, HuxA is required to sequester heme from the heme-hemopexin complex (Hanson *et al*, 1992; Cope *et al*, 1995) while in *S. marcescens* and *P. aeruginosa*, HasA steals heme from hemoglobin (Letoffe *et al*, 1998). Other genes related to *hasA* have been

al., 1999). Arnoux and coworkers (Arnoux *et al.*, 1999) suggest that the affinity of HasA for heme could be modulated by a receptor protein that could control the protonation state of the N8 of His83 of HasA. The N8 of His83 is involved in the formation of a hydrogen bond with the phenolate group of Tyr75, which is in the deprotonated state when it coordinates the iron of heme. Any protein that could stabilize the protonated state of the N8 of His83 would promote the transfer of the His83 N8 proton to the phenolate group, weakening the Tyr75 oxygen and iron bond and facilitating heme release by HasA.

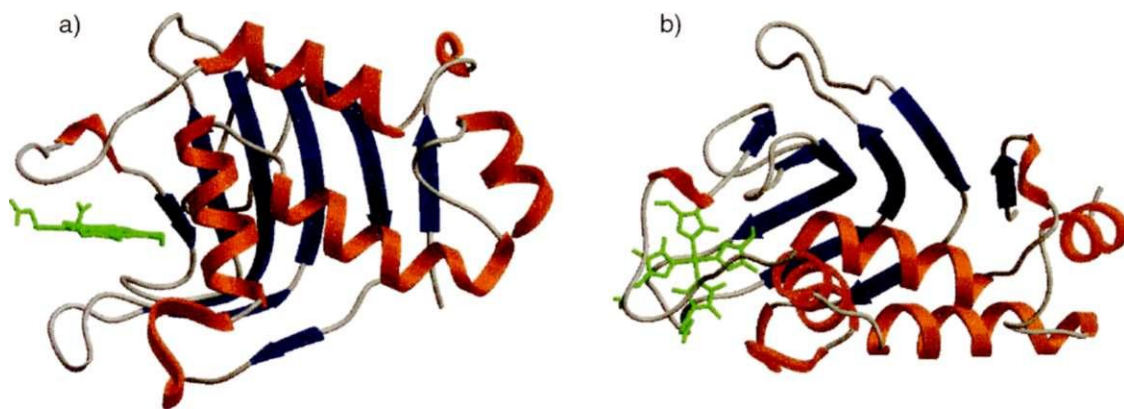


Fig. 1.3 Ribbon diagram of the structure of the hemophore HasA from *Serratia marcescens* (PDB accession code: 1BZV (Arnoux *et al.*, 1999)). a) Side view, illustrating the similarity to a fish shape. Helices are coloured in red, strands in blue and the heme group is represented by ball-and-stick in green, b) Top view showing the distorted strands in the β -sheet, which curve around to meet the α -helices. All figures of protein structures were drawn using SETOR (Evans, 1993).

Structure and function of FepA and FhuA. The crystal structures of two siderophore outer membrane receptors, FepA (Buchanan *et al.*, 1999) and FhuA (Ferguson *et al.*, 1998; Locher *et al.*, 1998) from *E. coli* (Figure 1.4), reveal interesting features that are likely

related to their function and mechanism of transport utilized by other outer membrane receptors involved in ligand uptake. Both proteins form similar monomeric transmembrane P-barrels with large extracellular loops that function in ligand binding. As well, in both proteins, the N-terminal domain folds in from the periplasmic side, almost filling up the space inside the barrel and contributing sites for ligand binding.

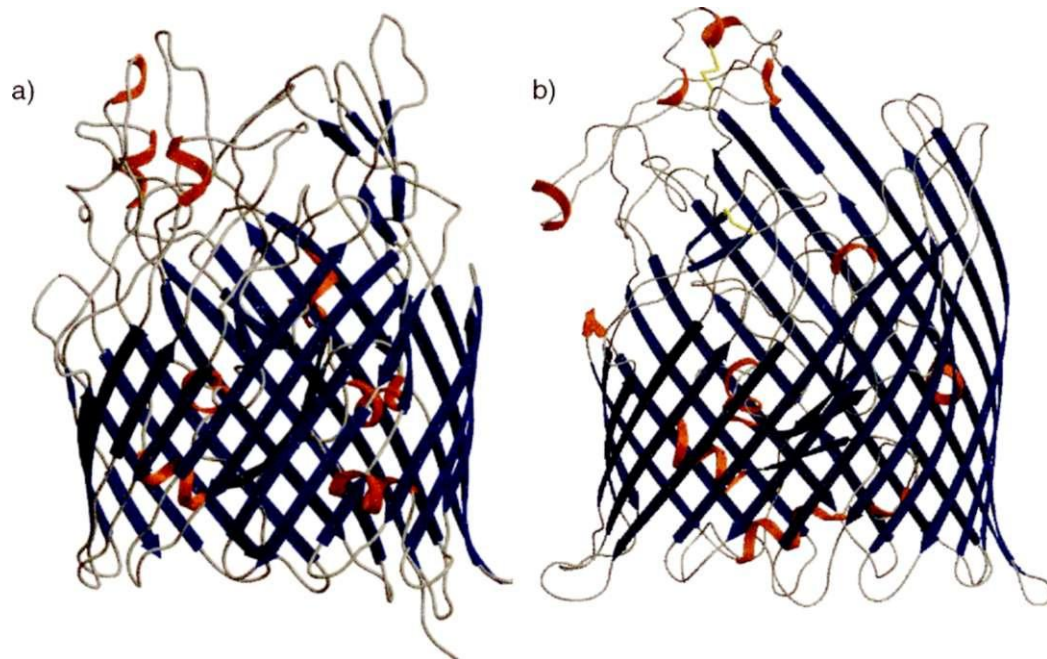


Fig. 14 Structures of a) FepA (PDB accession code: 1FEP (Buchanan *et al*, 1999)) and b) FhuA (PDB accession code: 2FCP (Ferguson *et al*, 1998; Locher *et al*, 1998)). Each consists of a large 22-stranded (3-barrel with large extracellular loops.

The ferric enterobactin receptor FepA and the ferrichrome receptor FhuA form P-barrels of 22 antiparallel strands, larger than any other known porin. FepA contains a wide ribbon of hydrophobic residues on its outer surface while FhuA has two bands of aromatic residues, corresponding to potential sites for interaction with lipids. Interestingly, FhuA co-crystallized with a single molecule of the lipopolysaccharide lipid A positioned such that

the alkyl chains of the lipid are parallel with the barrel axis (Ferguson *et al*, 1998). Analysis of the residues involved in lipopolysaccharide binding in FhuA shows that a common motif of four residues can be found in other lipopolysaccharide binding proteins (Ferguson *et al*, 2000a). Many of the extracellular loops of the receptors continue 30-40 Å above the membrane bilayer, which is considerably greater than for other porins. The function of the sizable loops on the extracellular surface is unknown, but presumably play an important role in ligand recognition. Deletion of a large portion of an extracellular loop (residues 335 to 355) transforms FhuA into an open channel (Killmann *et al*, 1993; Killmann and Braun, 1994). Similarly, deletion of a large loop of FepA (residues 202-340) also creates an open channel (Rutz *et al*, 1992). Previous identification of this area as a "gating loop" was inappropriate, however, it is now suggested that it can affect proper folding of the receptor (Locher *et al*, 1998). Nonetheless, these extracellular loops are recognized by specific bacteriophages or colicin toxins, as revealed by peptide mapping studies of FhuA (Killmann *et al*, 1995; Bonhivers *et al*, 1996).

The unusual N-terminal cork domain found in both structures has been implicated in both siderophore recognition and binding. The domain sits in the 3-barrel, anchored by more than 40 hydrogen bonds and several salt bridges with the barrel strands, blocking the pore. The unique fold of the domain allows several loops to rise above the bilayer interface extending towards the extracellular loops of the barrel. Previous insertion and deletion studies of FepA (Armstrong and McIntosh, 1995), FhuA (Carmel *et al*, 1990), and the related vitamin B₁₂ receptor BtuB (Lathrop *et al*, 1995) indicate that the N-domain is important for function and the highest degree of sequence homology between these active transport proteins is found in this region (Buchanan *et al*, 1999). Although the N-domain appears to block the pore, a narrow water filled channel in the FhuA structure connects the binding site to the periplasm (Ferguson *et al*, 1998). Several residues in a loop of the cork domain (Killmann *et al*, 1998) and along the inner wall of the barrel (Ferguson *et al*, 1998) are highly conserved between FhuA proteins in other bacteria (Figure 1.5).

Structural biology of iron uptake systems

a)

- *S_dysenteriae*_Shu A
- *V_vulnificus*_HupA
- *P fluorescens* PfhR
- *P aeruginosa* PhuR
- *C freundii*LB-tuB
- *E coli*_Btu
- *E coli*_Cir
- *V cholerae*_IrgA
- *P stutzeri*_PfeA
- *B_brevis* BfrA
- "*P aeruginosa*_CirA
- *B pertussis*_BfeA
- *P aeruginosa*_PirA
- *E coli*_IroN
- *S enterica*_IroN
- *P aeruginosa* PfeA
- *E coli*_FepA
- "*P gingivalis*_HmuR

Structural biology of iron uptake systems

b)

— Alteromonas,,FhuA
— V_vulnificus_HupA
— P_fluorescens_PfhR
— P_aeruginosa_PhuR
— Y_enterocolitica_FyuA
— E_coli_FhuE
— B_pertussis_FauA
— P_putida_PupB
— P_aeruginosa_FpvA
— P_putida_PupA
— P_aeruginosa_FptA
— Pseudomonas_Pbu A
— E_coli_YbiL
— P_aeruginosa_Fiu
— P_aeruginosa_PfuA
— P_sp_ferrisiderophore
— Synechocystis_sp__FhuA
— Synechocystis_sp_Fhu A
Synechocystis_FhuA
— R_leguminosarum_FhuA
— B_japonicum_FegA
- P_aeruginosa_FiuA
— S_typhimurium_FoxA
— Y_enterocolitica_FoxA
— E_amylovora_FoxR
— E_chrysanthemi_Fct
- P_agg]oraerans_FhuA
- S_typhimurium_Fhu A
- S_paratyphi_Fhu A
— E_coli_FhuA
— B_bronchiseptica_BfrC
— V_anguillarum_FatA
— P_ac_ruginosa_UfrA
- B_bronchiseptica_BfrB
" E_coli_FecA

Fig. 1.5 (previous pages) Dendrogram of outer membrane receptor proteins, a) Relationship between FepA and other related outer membrane proteins, b) Relationship between FhuA and other outer membrane proteins. This figure was generated using ClustalX and NJPlot (Thompson *et al*, 1997).

A clear picture of the residues involved in siderophore binding to the outer membrane receptors is provided by the structure of ferrichrome-bound FhuA. Ferrichrome is found bound above the bilayer interface by interactions with residues from both the extracellular loops and the N-domain. The shape of the binding pocket, lined with aromatic residues, is highly complementary to the three dimensional conformation of ferrichrome. Three residues from the N-domain as well as two residues from the barrel form hydrogen bonds to ferrichrome, contributing to tight binding (Ferguson *et al*, 1998; Locher *et al*, 1998). Four hydrogen bonds are formed with the hydroxamic acid portion of the ferric siderophore while two more bonds form with the peptide backbone. Tentative identification of the binding site residues in FepA involved in ferrienterobactin binding is based on the characteristics of the siderophore. From the position of putative iron sites in the crystal structure (Buchanan *et al*, 1999) and mutagenesis studies (Newton *et al*, 1997) residues important in the binding site include aromatic and positively charged residues from both the extracellular loops and the N-domain loops. In the same way, residues from receptors involved in binding other siderophores would possess chemical and structural characteristics complementary to the ligand. In addition, receptors for the same siderophore in different species could possibly be structurally related. For example, the enterobactin receptor in *P. aeruginosa* which shares significant homology to FepA (Figure 1.5), likely contains a similar constellation of key amino acid side chains that are involved in the binding site. Highly homologous receptors (Figure 1.5), such as the ferric pyoverdine receptor FpvA of *P. aeruginosa* and the ferric pseudobactin receptor PupA of *P. putida* (41.3% identity) (Poole *et al*, 1993), are also expected to have a very similar overall structure as well as a similar siderophore binding mode.

The mode of ferrichrome binding to FhuA, with the peptide backbone portion of the siderophore partially solvent exposed, immediately suggests that antibiotics could be conjugated to this portion of the siderophore. Pioneering work by the Miller lab has established that chemical synthesis and utilization of siderophore-drug conjugates is feasible (reviewed in (Roosenberg *et al*, 2000). These "Trojan horses" are actively taken up into the cell by the specific iron uptake systems. Once they have entered the cell, the antibiotic portion can kill the cell. FhuA takes up the naturally occurring siderophore-antibiotic conjugate albomycin, a structural analogue of ferrichrome.

The crystal structure of albomycin bound to FhuA (Ferguson *et al*, 2000b) shows the tri-8-A^hhydroxy-8-V-acetyl-L-ornithine peptide coordinating the iron in the same position as the ferrichrome. The covalently linked thioribosyl pyrimidine antibiotic is found in two conformations, extended and compact, due to the flexibility of the linker region. Numerous hydrogen bonds and contacts are made between the antibiotic portion and extracellular loops and the barrel of FhuA in both conformations. The structures of other ferrichrome analogues, ferricrocin and phenylferricrocin, bound to FhuA (Ferguson *et al*, 1998; Ferguson *et al*, 2000b) show that it is the iron chelating hydroxamic portion and key groups on the peptide backbone of the siderophore which are preferentially recognized. Since the remainder of the siderophore is bound less stringently, some variation is tolerated, although it needs to fit within the spatial confines of the binding site. By comparison, the fluorescent hydroxamate-type siderophore pyoverdine contains a conserved dihydroxyquinoline group linked to the N-terminal end of a peptidic moiety of different structure particular to individual *Pseudomonas* strains (Briskot *et al*, 1986; Cornells *et al*, 1989). Uptake of pyoverdine siderophores likely involves specific interactions between the variable peptide and the receptor. Subsequent transport of the siderophore through the receptor across the outer membrane involves interactions along the inside of the receptor, with energy for transport provided by the Ton complex.

Energy requirement for transport via the TonB system. Iron transport across the outer membrane is an energy dependent process (reviewed in Postle, 1993; Moeck and Coulton, 1998). Yet, there is no source of energy in the form of an electrochemical gradient in the outer membrane nor are there any high-energy compounds, such as ATP, in the periplasm. In mutants lacking the ability to transport ferric siderophores or vitamin B₁₂ across the inner membrane, these compounds accumulate in the periplasm (Fischer *et al*, 1989; Koster and Braun, 1990a; Bradbeer, 1993). However, their initial transport across the outer membrane utilizes the electrochemical potential of the inner membrane. Its energy is coupled to the outer membrane by the TonB-ExbB-ExbD complex (Figure 1.6).

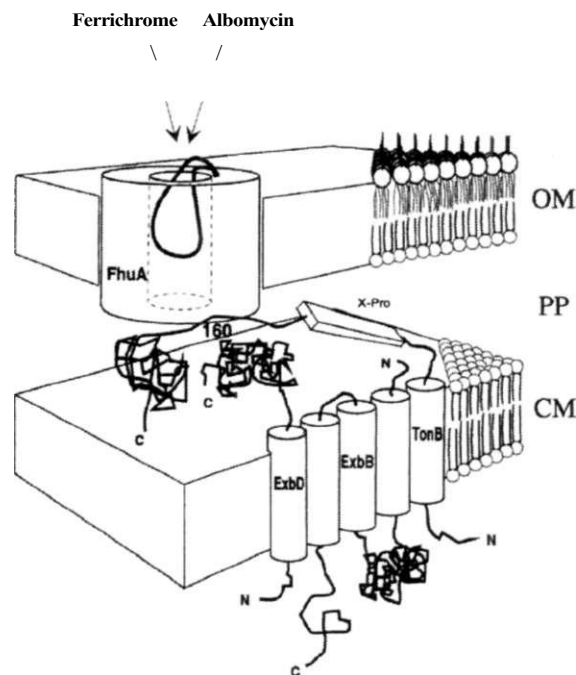


Fig. 1.6 Transmitting energy to the outer membrane receptor in *E. coli*. The TonB-ExbB-ExbD complex is anchored in the cytoplasmic membrane (CM) of the cell. TonB spans the periplasm (PP) via a proline rich region to the TonB-box of the FhuA receptor in the outer membrane (OM). This figure is slightly modified from (Braun, 1995).

Receptors that require the TonB complex as a source of energy contain a common "conserved" five amino acid sequence in their N-terminus, called the TonB box (Figure 1.6). This sequence can vary in the receptors and is tolerant to mutations with no effect to activity. It appears that the secondary structure of this area may be more important than the actual sequence. The TonB box in the crystal structure of the FepA receptor is in an extended conformation while in the structure of the FhuA receptor it is disordered and not visible in the electron density map (Ferguson *et al.*, 1998; Locher *et al.*, 1998; Buchanan *et al.*, 1999). Several conformational changes involving the cork domain of FhuA are evident when the structures of the apo- and holo-protein are compared (Ferguson *et al.*, 1998; Ferguson *et al.*, 2000b; Locher *et al.*, 1998). These changes are consistent with the observed decrease in tryptophan fluorescence when ferrichrome is bound (Locher and Rosenbusch, 1997). Movement facilitates the formation of hydrogen bonds between the ferrichrome and residues found on a loop of the N-domain upwards, while the β -sheet of the domain remains motionless. This disturbs interactions between a hydrophobic pocket and a small helix (residues 24 to 29) found near the periplasm, disrupting the secondary structure of the helix. However, contrary to what one would expect, if the entire N-domain of FhuA (residues 5 to 160) including the TonB box is deleted, transport of ferrichrome still requires TonB (Braun *et al.*, 1999). Thus, additional sites of interaction between TonB and FhuA exist, possibly on the periplasmic surface of the β -barrel, which can discern the ligand-loaded state.

Originally, TonB was identified in a class of phage T1-resistant mutants of *E. coli*, where only energy depleted cells and these *tonB*⁻ mutants could bind T1 reversibly (Hancock and Braun, 1976). FhuA might exist in different conformations depending on the energized state of the inner membrane and TonB (Hantke and Braun, 1978). Studies have shown that TonB activity was required for receptor uptake of all ferric siderophores, vitamin B₁₂, and the group B colicins (Braun *et al.*, 1980). TonB from *E. coli* is a 26 kDa protein which is anchored in the inner membrane by its hydrophobic N-terminus (Postle and Good, 1983; Postle and Skare, 1988). The amino acid sequences of TonB proteins in

many other bacterial species {*Salmonella typhimurium* (Hannavy *et al*, 1990), *Serratia marcescens* (Gaisser and Braun, 1991), *Yersinia enterocolitica* (Koebnik *et al.*, 1993b), *Enterobacter aerogenes* (Bruske and Heller, 1993), *Klebsiella pneumoniae* (Bruske *et al*, 1993), *Vibrio cholerae* (Goldberg *et al*, 1992), *Pseudomonas putida* (Bitter *et al*, 1993) are all very similar. The homologous Tol system (Sun and Webster, 1987; Braun, 1989; Webster, 1991; Kampfenkel and Braun, 1993 a) in *E. coli* appears to function similarly, although no ligands are presently known for this system. Potentially, the TonB and Tol systems, which provide energy at the outer membrane from the inner membrane, could be used for other outer membrane transport functions, which are as yet unknown.

Many attempts have been made to identify the important functional regions of TonB. While anchored in the inner membrane by the N-terminal end, the protein is predicted to span the periplasmic space with a proline rich region (Hannavy *et al*, 1990), which can be modified (Traub *et al*, 1993) or deleted (Larsen *et al*, 1994) without abolishing activity. Since mutations at residue 160 of TonB can suppress mutations at the N-terminal end of the receptors, TonB is thought to directly interact with the outer membrane receptors (Heller *et al*, 1988; Schoffler and Braun, 1989; Bell *et al*, 1990). Deletion of 15 residues of the C-terminal end shows that this area is important for TonB activity (Anton and Heller, 1991). Other mutations in the C-terminal region of TonB also affect colicin sensitivity (reviewed in Braun, 1995), suggesting that the overall structure of the protein is important for activity.

Two other proteins, ExbB and ExbD, located in the cytoplasmic membrane (Postle and Skare, 1988), form a complex with TonB (Fischer *et al*, 1989; Braun and Herrmann, 1993; Skare *et al*, 1993). Formation of the TonB-ExbB-ExbD complex is required for function (Figure 1.6). The N-terminal region of ExbB is predicted to span the inner membrane three times, with the remainder of the protein facing the cytoplasm (Kampfenkel and Braun, 1993b). ExbD has a periplasmic domain anchored in the inner membrane by the N-terminal region (Kampfenkel and Braun, 1992). TonB is stabilized by ExbB and in turn, ExbB is stabilized by ExbD, as shown by proteolytic protection experiments (Fischer *et al*,

1989; Skare and Postle, 1991). Identification of the area of the N-terminal region of TonB which interacts with ExbB also emphasizes the importance of the membrane spanning region in TonB for activity (Karlsson *et al*, 1993; Traub *et al*, 1993; Jaskula *et al*, 1994; Larsen *et al*, 1994). Since TolQ and TolR can partially substitute for ExbB and ExbD, respectively (Braun, 1989; Braun and Herrmann, 1993; Bradbeer, 1993), these are likely structurally related.

The mechanism by which the TonB complex functions *in vivo* is still sketchy. How the TonB complex responds to the energized state of the cell is unknown. Since there are many different receptors that utilize the cytoplasmic proton motive force via the proteins TonB, ExbB and ExbD (reviewed in Braun, 1995), signaling of ligand-loaded status of the receptor is required for effective energy transfer and active transport of iron compounds across the outer membrane. Currently, the most popular theory has the energized TonB complex inducing a conformational change of the receptor once the ligand has bound. This decreases the affinity of the receptor for the ligand and allows its passage to the periplasm. The conformational changes observed in the outer membrane receptor FhuA, and possibly other membrane receptors, when ligand binds likely constitutes the signal used by the TonB complex to distinguish between ligand-free and ligand-loaded forms. Even transfer of the heme group from the hemophore HasA to its receptor HasR appears to require energy from the TonB complex, since *tonB'* strains seem unable to convert holo-HasA to apo-HasA (Letoffeefa/., 1999).

Taken together, biochemical data as well as the structural information for the outer membrane receptors point to a potential mechanism for ferric siderophore movement through the receptor. Ferguson *et al* (1998) suggest that an induced fit mechanism caused by ferrichrome binding to FhuA initiates an allosteric change in the N-domain of the receptor. This change is important for interaction with the TonB complex, which in turn, reduces the stability of the ferrichrome binding site and allows the ferrichrome to be passed down the water-filled channel to the periplasm. This putative channel-forming region, lined with highly conserved residues, could open with slight changes within the loops of the N-

domain, allowing ferrichrome to pass along several low affinity binding sites. FhuA does not form an open channel; rather, the cork domain may undergo changes to block access to the external medium.

A reasonable suggestion is that the energy input from the TonB complex induces the widening of the channel to allow ferric siderophore transport. However, recent copurification of FpvA, the ferric pyoverdine receptor of *P. aeruginosa*, with its iron-free ligand suggests that a cofactor, perhaps TonB, may be required for iron binding to the receptor (Schalk *et al*, 1999). Since FpvA binds ferric and apo pyoverdine with equal affinities, this cofactor functions to stimulate iron loading of the siderophore or exchange of the apo form with ferric siderophores. The authors indicate that this could be a particular mechanism for the class of receptors involved in signal transduction and may not occur for all receptors (Schalk *et al*, 1999). In any case, the role of TonB may be more complicated than originally determined, and could be involved in the siderophore binding event as well as translocation of the siderophore to the periplasmic protein of the ABC transport system.

ABC Transport Systems.

ABC transport systems (ATP-dependent transport systems), consisting of a soluble periplasmic protein, a transmembrane permease and an ATP-binding lipoprotein, are used for the uptake of many different ligands (Nikaido and Saier, 1992). These proteins share consensus sequences which identify them as belonging to a particular family (Tarn and Saier, 1993) but they cannot replace each other in different systems. In addition to those systems for transporting iron and iron complexes, similar ABC transport systems are found for amino acids, peptides, sugars, and other essential nutrients (Higgins, 1992). To date, a significant amount of structural data is available for the periplasmic components, with information about the inner membrane associated proteins gleaned mostly from various sequence analysis and a few biochemical experiments. However, valuable insight into the

mechanism of transport across the inner membrane can be extracted and related to other homologous systems.

Structure of periplasmic ligand binding proteins. Although the periplasmic proteins in ABC transport systems share very little sequence homology and recognize diverse ligands, most are closely related in structure (Quioco and Ledvina, 1996). Periplasmic proteins can be grouped into distinct classes based on similarities in primary sequence (Tarn and Saier, 1993). Many consist of two globular domains connected by short stretches of polypeptide chain, which allow movement of the two lobes by a hinge mechanism. Each lobe consists of a central β -sheet flanked by α -helices and molecular recognition of ligands arises from slight differences in the number and arrangement of the β -strands and α -helices in the two globular domains. As a result of the differences in domain structure and sequence of the periplasmic receptors, the structure of the binding site is highly variable. In most periplasmic proteins, crossovers of the polypeptide chain between the two domains form the hinge region and the base of the binding cleft. The manner of closure around the substrate in the deep binding cleft formed by the two domains is suggestive of a "Venus fly trap" (Mao *et al*, 1982; Ames, 1986) or "Pac-man" motion. This mode of binding gives rise to many interactions between the protein and substrate, conferring ligand binding selectivity to the protein.

Moreover, the final conformation of the receptor-ligand complex is important for making the proper interactions with the inner membrane permease protein and release of the tightly bound ligand. Although the liganded structures of periplasmic proteins are useful for examining interactions important for substrate binding, comparison to the unliganded structures can reveal changes that occur upon ligand binding. Evidence for ligand-induced conformational changes can also be found from low angle x-ray scattering, kinetic, theoretical, and site-directed mutagenesis studies (Shilton *et al*, 1996). For those proteins for which both holo- and apo-forms have been solved by x-ray crystallography, the two domains have rotated away from each other in the unliganded structure (open

conformation) while in the liganded structure (closed conformation), the lobes are drawn together. Each lobe does not significantly change its structure; rather there is a rotation of the two domains about the hinge region. Domain closure is thought to be a dynamic process, with little expenditure of energy involved in the process (Gerstein *et al*, 1994; Hayward, 1999). The hinge angle bends due to small changes in the ϕ and ψ angles of only two or three residues in the 13-sheets connecting the two domains.

The topology of typical periplasmic binding proteins is represented by the homologous iron binding proteins FbpA from *N. gonorrhoeae* and HFbp from *H. influenzae* (Bruns *et al*, 1997). At first glance, their structures are very similar to one lobe of human transferrin and moreover, the coordination of the iron by the oxygens of two tyrosines, an imidazole nitrogen from histidine and a carboxylate oxygen from a glutamic acid is the same. However, HFbp completes the octahedral coordination of Fe^{3+} with oxygens from phosphate and a water molecule, where transferrins utilize the two oxygens from a carbonate anion (Bruns *et al*, 1997). Although the nature of the amino acid side chains coordinating the iron are similar in FbpA and transferrin, they arise from different regions of FbpA than in transferrin. The iron is also more solvent exposed in FbpA than it is in the transferrins, since the iron binding site is deeper within the protein and the loop covering the binding site is missing. As such, HFbp shares more structural similarity with other anion binding periplasmic proteins such as the phosphate binding protein, sulphate binding protein, maltodextrin binding protein, and spermidine binding protein. Thus, the evolutionary descent of periplasmic and iron binding proteins can be traced more accurately based on a combination of structural and sequence information. The apo form of HFbp has the same overall fold but the two lobes of the protein are rotated approximately 20° with respect to each other (Figure 1.7). Changes in the dihedral angles of the (3-sheets lining the bottom of the binding site opens the binding cleft to the solvent. In contrast to FbpA, the periplasmic ferric siderophore binding protein FhuD does not possess the typical periplasmic protein topology (Clarke *et al*, 2000), yet it is able to function in a similar

capacity. In the following chapters, a detailed analysis of the structure of this protein is presented hence specific characteristics of this protein will not be discussed here.

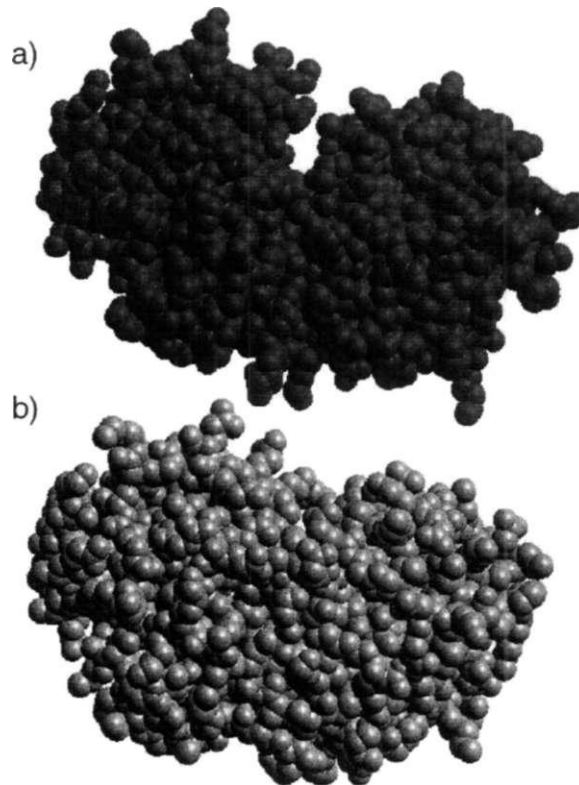


Fig. 1.7 Space filling models of the apo- and holo-forms of the *Haemophilus influenzae* Fbp; (a) apo Hfbp (PDB accession code: 1D9V) and b) holo HFbp (PDB accession code: 1MRP) (Bruns *et al*, 1997). The domains rotate with respect to each other to close around the Fe in the holo-form.

Biochemistry of inner membrane associated proteins. Transport across the inner membrane requires two proteins, one to span the membrane to act as a permease and a second one that can hydrolyze ATP to provide the energy for transport. Typically, two closely associated proteins are found in the inner membrane of iron uptake systems, although the stoichiometry of these proteins varies. Although the inner membrane proteins differ in sequence for each of the iron uptake systems, the mode of transport is very similar. These proteins must first recognize the cognate ligand-loaded periplasmic protein, extract and transport the ligand across the cytoplasmic membrane while utilizing the energy of the third ATP hydrolyzing protein component. Identification and tentative analysis of the structure of inner membrane associated proteins for iron transport relies on similarities of the primary structure with other ABC transport systems (Higgins, 1992).

The permease component is typically a hydrophobic protein (65%) with many transmembrane segments as identified by prediction programs such as that by Persson and Argos (Persson and Argos, 1994). The majority of biochemical data about the inner membrane proteins for iron transport has been collected for the ferric hydroxamate uptake system (FhuB and FhuC) of *E. coli*. The integral membrane protein FhuB was found to be twice the size of most permeases (70 kDa), with the similar N- and C-domains both being essential for transport (Koster and Braun, 1986; Koster and Braun, 1989). An alignment of FhuB N- and C-terminal domains with other proteins identified as permeases reveal a highly conserved region in all proteins found near the C-terminal end (Koster, 1991; Saurin *et al*, 1994). Analysis of mutant proteins FhuB(P60L) and FhuB(G426R) shows that these residues play a role in interdomain interaction (Bohm *et al*, 1996). The two domains are thought to assemble into a complex, but they do not have to be covalently attached (Koster and Braun, 1990b). The topology of FhuB, identified by fusions to (3-lactamase, suggests that each domain spans the membrane 10 times, with the N- and C-termini in the cytoplasm (Groeger and Koster, 1998). Other inner membrane associated proteins involved in siderophore and heme uptake homologous to FhuB are thought to have a similar topology, with the two proteins forming a complex (Braun *et al*, 1998). Interaction studies between

the periplasmic protein FhuD and FhuB indicate that the ligand-loaded FhuD preferentially associates with FhuB (Rohrbach *et al*, 1995; Mademidis *et al*, 1997). Peptide mapping studies suggest that several external loops may exist in FhuB which are important for physical interaction with FhuD (Mademidis *et al*, 1997). In contrast to the siderophore family, FbpB, HitB and SfuB, potential permeases for Fe³⁺ uptake from transferrin/lactoferrin in *Neisseria*, *Haemophilus* and *Serratia*, respectively, are predicted to have 11 transmembrane α -helices with two permease signature sequences, which interact with the nucleotide-binding component, exposed to the cytoplasm (Mietzner *et al*, 1998).

The ATP-binding proteins are identified by a homologous domain common to ATP-dependent transporters of about 200 amino acids, flanked by "Walker A" and "Walker B" consensus sequences. Analysis of the amino acid sequence of FhuC of the siderophore uptake system of *E. coli* showed that it was similar to other ATP-binding proteins (Burkhardt and Braun, 1987; Coulton *et al*, 1987). Changes in the consensus sequences in FhuC abolished activity, confirming that it possessed ATP-hydrolyase activity (Becker *et al*, 1990). Interaction between FhuC and FhuB, important for energizing the transport across the inner membrane, was shown by the effects of single mutations in the ATP-binding regions of FhuC (Schultz-Hauser *et al*, 1992) and mutations in the conserved regions of FhuB (Braun *et al*, 1998). The sequence alignment of the FbpC, HitC and SfuC proteins for Fe³⁺ transport shows the presence of this ATP-binding region (Mietzner *et al*, 1998). It seems likely that the ATP binding region is exposed to the cytoplasm, where ATP is found (Braun and Killmann, 1999). Recently the structure of HisP, the ATP-binding subunit of the histidine permease from *Salmonella typhimurium* has been reported (Hung *et al*, 1998) (Figure 1.8). The ATP-binding loop, which contains the Walker A motif, wraps around the P-phosphate of ATP. Two 'L' shaped subunits form a dimer, with hydrophobic interactions between β -sheets on the outside of arm I. HisP shares 27.2% sequence identity with FhuC, especially in the Walker A/B motifs and the glutamine rich sequence (bacterial consensus sequence LSGGQQQRV), suggesting that FhuC is likely to have a similar structure.

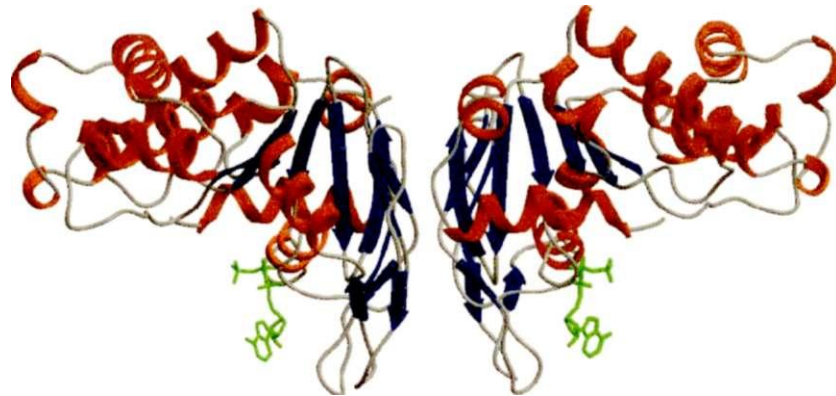


Fig 18 Structure of the ATP-binding subunit of the ATP permease from *Salmonella typhimurium* (PDB accession code: 1BOU (Hung *et al*, 1998)). The overall structure of the monomer protein is that of an 'L', with the dimer interface between (3-sheets of one arm of each of the monomers).

Energy requirement for transport using ATP. Subsequent transport of ferric siderophores across the inner membrane is dependent upon the energy provided by respective cytoplasmic membrane associated components. For example, the complete FhuB protein was found to be essential for iron (III) hydroxamate transport across the inner membrane (Koster and Braun, 1990b), and likely interacts with the other membrane bound component FhuC (Koster and Bohm, 1992; Bohm *et al*, 1996) and the periplasmic protein FhuD (Rohrbach *et al*, 1995). Studies of ABC transport systems for maltose and histidine show that the ligand-loaded binding proteins initiate ATP hydrolysis (Boos and Lucht, 1996), preventing wasteful hydrolysis. This implies that a signal from the periplasmic protein to the ATPase component of the ABC transport system must occur at some point to allow ATP hydrolysis.

Once inside the cytoplasm, siderophore reductases reduce the ferric iron to Fe²⁺, lowering its affinity for the siderophore (Fischer *et al.*, 1990; Fontecave *et al.*, 1994). The siderophore then can be recycled to the outside of the cell (Matzanke *et al.*, 1991). In some cases hydrolysis of the siderophore (i.e. enterobactin) has also been reported, which can aid in the release of bound Fe³⁺ (Brickman and McIntosh, 1992).

So far, limited attention has been paid to the uptake of Fe³⁺ in Gram-positive bacteria. Hantke and coworkers (Schneider and Hantke, 1993) have reported the presence of a three component system for ferrichrome uptake in *Bacillus subtilis*. In this case, the periplasmic component is anchored to the membrane, through attachment of an N-terminal lipid anchor (Schneider and Hantke, 1993). Otherwise, this ABC transport system appears to be quite similar to those discussed above for *E. coli*. Inspection of the complete genome sequence of *Bacillus* reveals the presence of three such systems, presumably responsible for the uptake of different siderophores. Some pathogenic Gram-positive bacteria can use the host protein transferrin as its source of iron. *Staphylococcus aureus* expresses a 42 kDa transferrin receptor on its surface, which has a fairly broad specificity for transferrins from different species. Surprisingly, this protein is also a glyceraldehyde-3-phosphate dehydrogenase, making it multifunctional. Further studies are warranted to determine whether this glycolytic activity is required for iron uptake (Modun *et al.*, 1998; Modun and Williams, 1999; Modun *et al.*, 2000).

Regulation of Gene Expression.

The expression of the genes of the bacterial iron uptake systems is regulated at the level of transcription. In many cases, the transcription of the genes involved in iron uptake is negatively regulated by the Fur repressor protein, producing high levels of expression only under iron-deficient conditions. In addition, a number of iron uptake systems simultaneously utilize another induction system, which requires the presence of the ligand. Many comprehensive reviews have been published about iron regulation, and the reader is

encouraged to peruse these for detailed information (Litwin and Calderwood, 1993 a; Braun, 1997; Escolar *et al*, 1999; Vasil and Ochsner, 1999). Nonetheless, the complete three-dimensional structures of these proteins involved in regulation are unknown, but some information exists regarding the secondary structural features essential for function.

Regulation by Fe^{2+} -Fur. Most iron responsive genes are under the control of the transcriptional repressor, Fur, which binds DNA under iron replete conditions and negatively regulates transcription of iron transport genes (Bagg and Neilands, 1987a; deLorenzo *et al*, 1987; Escolar *et al*, 1997; Escolar *et al*, 1998). The *E. coli* Fur protein (17 kDa (Bagg and Neilands, 1987a; Saito *et al*, 1991)), has homologs in both Gram-negative {*Salmonella* (Ernst *et al*, 1978), *Yersinia* (Staggs and Perry, 1995), *Vibrio* (Litwin *et al*, 1992; Litwin and Calderwood, 1993b; Tolmasky *et al*, 1994; Yamamoto *et al*, 1997), *Neisseria* (Berish *et al*, 1993; Thomas and Sparling, 1994; Thomas and Sparling, 1996), *Pseudomonas* (Prince *et al*, 1993; Venturi *et al*, 1995a), *Campylobacter* (Wooldridge *et al*, 1994), *Legionella* (Hickey and Cianciotto, 1994), *Bordetella* (Brickman and Armstrong, 1995), *Haemophilus* (Carson *et al*, 1996), *Helicobacter pylori* (Bereswill *et al*, 1998), *Acinetobacter baumannii* (Daniel *et al*, 1999), and *Erwinia chrysanthemi* (Franza *et al*, 1999)) and Gram-positive bacteria {*Staphylococcus* (Heidrich *et al*, 1996) and *Bacillus subtilis* (Bsat *et al*, 1998)) (Figure 1.9). Most of these can complement an *E. coli fur* mutant. Interestingly, Fur may have different obligations in each bacterium since *Neisseria* (Berish *et al*, 1993; Thomas and Sparling, 1994), *Pseudomonas* (Prince *et al*, 1993; Venturi *et al*, 1995b), *Rhizobium* (de Luca *et al*, 1998) and *Vibrio anguillarum* (Tolmasky *et al*, 1988) absolutely require Fur while *E. coli* (Hantke, 1981), *Yersinia* (Staggs and Perry, 1995), *Vibrio cholerae* (Litwin and Calderwood, 1993b; Litwin and Calderwood, 1994) and *Bacillus* (Bsat *et al*, 1998) do not. The number of genes found regulated by Fur in *E. coli* and other bacteria has increased (Stojiljkovic *et al*, 1994; Tsolis *et al*, 1995; Ochsner and Vasil, 1996) and not all of these are directly related to iron metabolism (Escolar *et al*, 1999 and references therein). In *P. aeruginosa*, Fur may also

• A_aeolicus
 — H_pylori
 — C_upsaliensis
 -C Jejuni
 — M_tuberculosis
 — M_fortuituin
 S_aureus^
 -T_maritima
 — B_subtilis
 — S_aureusl
 — B_abortus
 — B_japonicum
 "RJeguminosarum
 N_meningitidis
 - B_pertussis
 B_cepacia
 — A_eutrophus
 — H_ducreyi
 — H_influenzae
 "P_multocida
 V_parahaemolyticus
 rC V_vulnificus
 V^cholerae
 Vanguillarum
 - Y_pestis
 -E_crysanthemi
 - K_pneumonia
 -E_coi
 — L_pneumophila
 — A_baumannii
 — A_calcoaceticus
 — X_campestris
 -P_fluorescens
 -P_stutzeri
 — P_putida
 -P_aeruginosa

Fig. 19 Alignment of Fur from various bacteria. Fur from *P. aeruginosa* lacks a highly conserved Gly-X-Cys-(2-5)X-Cys sequence present in the C-terminus and a His-(2X hydrophobic)-Cys-(2X)-Cys motif of other species (Vasil and Ochsner, 1999).

control the expression of a sigma factor PvdS, which affects the expression of other iron regulated genes, including those for the synthesis of pyoverdine (Cunliffe *et al*, 1995; Miyazaki *et al*, 1995; Leoni *et al*, 1996; Stintzi *et al*, 1999) and regA and ptxR for the expression of toxA, encoding exotoxin A (Stintzi *et al*, 1999).

Structurally, very little is known about Fur. In solution, Fur seems to be a dimer in the presence or absence of Fe²⁺ (Coy and Neilands, 1991; Michaud-Soret *et al*, 1997) and it has the ability to multimerize (Wooldridge *et al*, 1994). Metal binding may affect the conformation of Fur since increased rates of proteolysis occur in the presence of excess metal (Coy and Neilands, 1991). The protein is proposed to have two domains, with the N-domain for DNA binding and the C-domain for dimerization (Coy and Neilands, 1991; Stojiljkovic and Hantke, 1995). However, specific amino acids involved in the function of Fur have yet to be determined even though several mutant Fur proteins have been discovered (Coy and Neilands, 1991; Hall and Foster, 1996). Likely possibilities for iron coordination are the 12 His and 4 Cys residues present in the amino acid sequence (Schaffer *et al*, 1985; Wee *et al*, 1988). Yet, results from a variety of spectroscopic techniques, including paramagnetic NMR experiments (Saito *et al*, 1991), spin-label studies and electronic absorption spectra (Coy and Neilands, 1991) are inconclusive and disagree about what type of coordination occurs. Fur can also bind other divalent metal ions such as Mn(II), Co(II), Cu(II) and Cd(II) *in vitro* when binding to DNA (Bagg and Neilands, 1987a; deLorenzo *et al*, 1987). Zn(II) has also been found bound to Fur during the purification process, with one zinc atom bound weakly and another strongly, and it may be involved in stabilizing the protein structure (Althaus *et al*, 1999). As such, previous work to identify the coordinating ligands of Fe²⁺ may have actually been examining two different metal binding sites (Althaus *et al*, 1999). There appears to be some conservation of residues in the putative metal binding sites (His and Cys clusters) in Fur (Althaus *et al*, 1999) with the homologous Zur protein, which regulates zinc uptake in *E. coli* (Patzer and Hantke, 1998). In light of the recent developments, the mechanism by which Fur senses

iron levels becomes more complicated, and may also involve equilibrium with zinc in the cell.

Other types of regulation. A very different transcription initiation process can also occur where the genes for transport are positively regulated. In this case, the inducer does not enter the cytoplasm but remains bound to the outer membrane receptor. A specific σ -factor which controls the operon for the genes for iron uptake is activated in response to ligand binding to the receptor. In the ferric citrate and pseudobactin transport systems, the TonB complex is important for signal transduction across the outer membrane. The conformational change of the receptor and the TonB complex associated with ligand binding likely initiates the signal for increased transcription of the other proteins required for transport.

The regulatory genes *feci* and *fecR* encode a σ factor (Angerer *et al*, 1995; Enz *et al*, 1995) and a protein which spans the inner membrane, respectively. The expression of these genes is regulated by Fur; so when cells require iron, the FecIR proteins are synthesized. When ferric citrate is available, it binds to FecA, which signals to FecR. The topology of FecR, examined by sequence analysis (Van Hove *et al*, 1990), fusion proteins and truncated proteins (Ochs *et al*, 1995), shows that the C-terminus (101-317) is located in the periplasm, the hydrophobic central region (residues 85-100) spans the inner membrane and the N-terminus (residues 1-84) is in the cytoplasm. FecR activates Feci, which can then bind to DNA allowing more transport genes to be transcribed. Feci forms a complex with RNA polymerase which binds to the *fecA* promoter (Angerer *et al*, 1995). Point mutations in the predicted helix-turn-helix DNA binding motif decrease the inducing activity (Ochs *et al*, 1996).

Induction of the *fee* transport genes in *E. coli* via Feci and FecR by ferric citrate requires the receptor FecA as well as the TonB-ExbB-ExbD system (Killmann *et al*, 1993). Studies of FecA which can bind ferric citrate at the cell surface but are defective for transport indicate that the signal is transmitted through the TonB complex to FecR in the

periplasm (Harle *et al.*, 1995). It has been suggested that an extra 40 residues located at the N-terminus of FecA, which are not found in other siderophore receptors, is located in the periplasm and is involved in signaling but not transport across the outer membrane (Kim *et al.*, 1997). FecR interacts with the ligand loaded receptor FecA using its periplasmic C-terminal domain. FecR then signals through the inner membrane via its N-domain to Feci in the cytoplasm, which subsequently binds to the *fee* transport promoter.

Expression of siderophore receptors in other bacterial species also appears to be regulated by the presence of the siderophores themselves. For example, uptake of ferric enterobactin is regulated by a two-component regulatory system in *P. aeruginosa*. The sensor protein PfeS (homology to FecR) passes the signal by phosphorylating the regulatory protein PfeR (homology to Feci), which binds DNA and induces expression of the enterobactin receptor PfeA (Dean and Poole, 1993a; Dean and Poole, 1993b; Dean *et al.*, 1996). Likewise, the lower affinity ferrienterobactin PirA receptor and its regulatory system PirR-PirS have high identity to PfeA and PfeR-PfeS. In *P. putida*, a similar regulatory system for uptake of ferric pseudobactins BN7 and BN8 exists. In this case, the expression of the PupB outer membrane receptor is repressed by PupI (43% identity with Feci) and PupR (48% identity with FecR) (Koster *et al.*, 1994). The receptor PupB, in particular, the N-terminal residues, and TonB are required for induction by the pseudobactins (Koster *et al.*, 1994). Other regulatory genes for pyoverdinin uptake with some sequence homology to *feci* are found in *P. putida* WCS358 (*pfrA* for pseudobactin 358 biosynthesis), *P. aeruginosa* (*pvdS* for pyoverdinin biosynthesis) and *P. fluorescens* M14 (*pbrA* for pseudobactin M14 biosynthesis) (Venturi *et al.*, 1995b; Venturi *et al.*, 1995a), among others.

Regulation of expression of iron transport systems is a complex process. There appears to be a number of feedback mechanisms present in the bacteria for sensing the iron status of the cell and availability of each siderophore in the environment. In *P. aeruginosa*, besides increasing PfeA expression, ferric enterobactin also decreases the levels of pyochelin and pyoverdinin receptors (Dean and Poole, 1993a). Only the pyochelin genes are

directly regulated by Fur while the pyoverdine genes are indirectly regulated in response to iron through the Fur-controlled sigma factor PvdS. For the pyochelin receptor FptA, a combination of negative regulation by Fur and transcriptional activation by a member of the AraC gene regulator family, PchR, determines its levels in the cell (Ankenbauer and Quan, 1994; Heinrichs and Poole, 1993; Heinrichs and Poole, 1996). Another AraC-like transcriptional activator is found in *Yersinia pestis* (Fetherston *et al*, 1996). Presumably, the bacterium is able to preferentially utilize the "best" siderophore available, without expending needless energy producing other receptors.

Iron also is found to regulate other cellular processes that are not directly involved in iron acquisition. For example, adequate iron status in a bacterium can be sensed by regulatory proteins that signal other cellular operations to cease. A number of virulence factors, such as toxins, are linked to the iron status within the bacteria. In many Gram-positive bacteria, the DtxR protein serves to repress the transcription of toxin genes when

⁹⁺

loaded with Fe³⁺. DtxR homologues are found in *Corynebacterium diphtheriae*, *Brevibacterium lactofermentum* (Oguiza *et al*, 1995; Oguiza *et al*, 1996), *Streptomyces lividans* and *S. pilosis* (Gunter-Seeboth and Schupp, 1995) as well as *Mycobacterium tuberculosis* and *M. leprae* (Doukhan *et al*, 1995) and represents a large family of iron-dependent negative regulators (IdeR (Schmitt *et al*, 1995; Pohl *et al*, 1999)). DtxR and Fur can regulate genes such as the *Serratia marcescens* hemolysin, *Shigella dysenteriae* shiga toxin, *Pseudomonas aeruginosa* exotoxin A and *Corynebacterium diphtheriae* diphtheria toxin. Although Fur and DtxR are not homologous, and their target sequences vary, in the absence of a structure for Fur, it is interesting to examine the DtxR structure (Figure 1.10). Like Fur, DtxR and IdeR appear to function as dimers and play a role in controlling the expression of siderophores (Schmitt and Holmes, 1993) and components of the iron uptake system (Schmitt *et al*, 1997). The N-terminal domain of DtxR contains the helix-turn-helix DNA-binding domain and metal binding sites (Qiu *et al*, 1995; Qiu *et al*, 1996; Schiering *et al*, 1995; Pohl *et al*, 1999; Pohl *et al*, 1998; Pohl *et al*, 1997; White *et al*, 1998). Only the structure of Zn-IdeR from *M. tuberculosis* shows occupation of both metal binding sites

(Pohl *et al.*, 1999). The presence of an anion binding site near metal site 1 could allow co-repression by phosphate ions *in vivo* (Qiu *et al.*, 1996). Comparison of the structures of the apo- and holo-DtxR from *Corynebacterium diphtheriae* shows that the DNA-binding domain moves with respect to the dimerization domain (Pohl *et al.*, 1999; Pohl *et al.*, 1998).

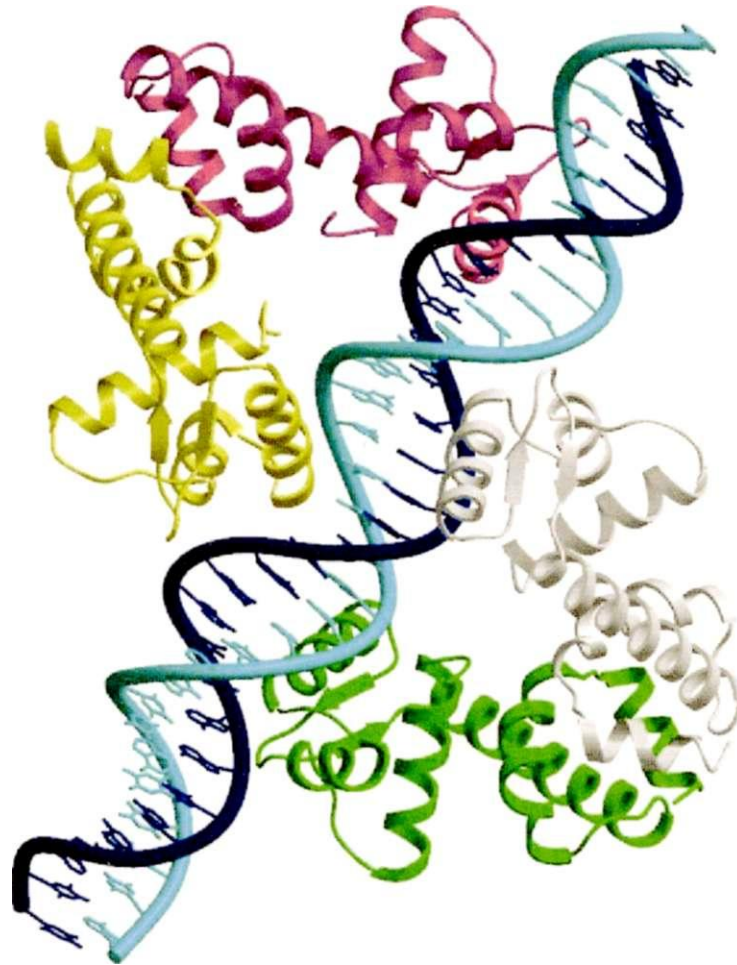


Fig. 1.10 Structure of DtxR bound to the *tax* gene operator DNA (PDB accession code: 1DDN (White *et al.*, 1998)).

Storage of Iron.

Once iron reaches the cytoplasm, the mechanism of distribution within the bacterial cell is not well understood. Of course, iron is required as heme in cytochromes (5%), functions in iron-sulfur proteins (10%) and is sequestered in bacterioferritins (10%). In addition, part of the cellular iron appears to be in a "low molecular weight mobile iron pool" and it has been estimated that up to 40% is bound as Fe^{2+} by an acidic carbohydrate (Bohnke and Matzanke, 1995). Iron homeostasis is also maintained *via* movement of iron in and out of storage proteins. The major iron storage protein found in mammals, invertebrates, fungi, and prokaryotes is ferritin (reviewed in Theil, 1987; Harrison and Arosio, 1996; Andrews, 1998). This soluble protein can bind up to 4500 atoms of iron in a non-toxic form (Crichton, 1991). Ferric iron is bound in the core of the protein in a disordered octahedral coordination, while the core is surrounded by phosphate. Bacterioferritin from *E. coli* has a single type of subunit, forming a spherical shell of 24 proteins and 12 hemes around the polynuclear mineral iron core. The presence of the heme group is unique to bacterioferritin. The crystal structure of bacterioferritin shows that a binuclear metal site is present in each subunit and each heme is bound by Met 52 from symmetry related protein subunits (Frolow *et al*, 1994). In contrast, *P. aeruginosa* has two bacterioferritin genes, *bfrA* and *bfrB*, which encode the a and b subunits which are present in variable proportions in the 24mer (Moore *et al*, 1994; Ma *et al*, 1999). The mechanism for release of iron from the core is unknown. However, it is proposed that the iron enters ferritin by the reduction of Fe^{3+} to Fe^{2+} by the apoprotein and subsequent transport into the core of the protein occurs through channels in the protein. The formation of the iron core occurs in three phases, as demonstrated by electrode oximetry with pH stat measurements (Yang *et al*, 2000).

Summary.

What would life be like without iron? Certain lactic acid bacteria have adapted to conditions with a very low iron availability and apparently survive without iron (Archibald, 1983), utilizing cobalt and manganese instead as catalysts. Other transition metal ions such as copper could serve as redox centres in cellular electron transfer reactions and other metals such as zinc can function as structural cofactors in proteins. Then the question remains, why is iron utilized by so many other organisms? The most likely explanation may be that it was abundant in the reducing conditions in the primordial soup and that the beneficial redox properties of iron outweighed effects of iron toxicity.

Although bacteria can be found in a variety of environments and exhibit a variety of mechanisms to acquire iron, there are common themes in iron transport across species. Iron homeostasis is regulated by controlling its transport through the membrane (Bagg and Neilands, 1987b; Crosa, 1997). The presence of high affinity iron uptake systems is considered to be an important virulence factor for bacteria (Cox, 1982; Payne, 1988; Payne, 1993; Byers and Arceneaux, 1998). For example, *P. aeruginosina* is a versatile bacterium, found in soils, medical equipment and lungs of cystic fibrosis patients. It has the ability to acquire iron from host proteins (Litwin and Calderwood, 1993a; Ochsner *et al.*, 1995; Bearden and Perry, 1999; Franza *et al.*, 1999) as well as produce the siderophores pyoverdine and pyochelin during infection (Sokol and Woods, 1984; Ankenbauer *et al.*, 1985; Cox, 1985; Sokol, 1987).

The iron status in bacteria seems to influence a number of cellular processes in addition to the regulation of iron uptake *per se*. Mechanisms in place to regulate iron acquisition components are not limited in their function and have broad effects on cellular metabolism. Fur and DtxR can play a larger role in bacterial physiology due to the large number of genes they can regulate. Since Fur proteins from different species can complement mutants, a similar mechanism of regulation is shared among bacteria. The

additional level of control provided by other positive regulatory cascades, especially those resulting directly from siderophore binding, can also control other functions in the cell.

Since many bacterial iron uptake systems appear to be related in function as well as in the structures of their components, design of broad-spectrum antibiotics that abolish or interfere with active iron transport systems might be feasible in the next decade.

Scope of this Dissertation.

The research presented in this thesis characterizes the periplasmic ferric siderophore binding protein FhuD by x-ray crystallography and several other spectroscopic methods. Interestingly, the three-dimensional structure of FhuD is unusual for a periplasmic ligand binding protein and represents a new class of periplasmic proteins. FhuD can accommodate a number of hydroxamate-type ligands and the structures of FhuD complexed with a number of different siderophores show that the binding site is fairly malleable. I have also studied the dynamic nature of the protein by various spectroscopic means, hopefully to clarify the mechanism for function of this protein. In addition, several important residues for ligand interaction were mutated and the effects on the protein were studied spectroscopically.

In the following chapter, a brief introduction to x-ray crystallography is presented, including the structure of FhuD, solved by multiwavelength anomalous dispersion methods. Chapter three reveals how FhuD can bind a number of different siderophores by examining the crystal structures of complexes with albomycin, coprogen and Desferal . In chapter four, a thorough evaluation of the effects of various point mutations with respect to their location in the secondary and tertiary structure of FhuD is presented; relating functional experimental data collected by Dr. Wolfgang Koster and Dr. Martin Rohrbach to the structure of the protein. This chapter also evaluates the conservation of polypeptide regions in other siderophore-binding proteins of the FhuD family. Chapter five focuses on spectroscopic studies to examine the dynamics of ligand binding to FhuD, including

circular dichroism spectroscopy and fluorescence measurements. This chapter includes analysis of ligand binding to FhuD mutants. The final chapter summarizes the major findings of this work and draws some conclusions about the significance and future prospects of this project.

Chapter 2**X-ray Crystallographic Structure of FhuD bound to Gallichrome**

The crystal structure of FhuD, an ATP-binding cassette-type (ABC-type) binding protein involved in the uptake of hydroxamate-type siderophores from *Escherichia coli*, complexed with the ferrichrome homolog gallichrome has been determined at 1.9 Å resolution using MAD phasing techniques. This represents the first structure of an ABC-type binding protein involved in the uptake of siderophores. Unlike most periplasmic ligand binding proteins (PLBPs), the two domains of FhuD are connected by a long α -helix with the gallichrome bound in a shallow hydrophobic pocket between the two domains of the protein. This rigid architecture may lack the ability to undergo the large conformational changes typically observed in PLBPs upon ligand binding. The structures of the FhuD ferrichrome and FhuD alumichrome complexes, solved by molecular replacement, are identical to the FhuD gallichrome complex. This study provides a basis for the rational design of novel bacteriostatic agents, including siderophore-antibiotic conjugates that can act as "Trojan horses", using the ferrichrome uptake system to deliver antibiotics directly into targeted pathogens.

Introduction.

Our knowledge of protein biochemistry is enhanced with the detailed three-dimensional information gleaned from NMR (nuclear magnetic resonance) spectroscopy and x-ray crystallography. Although NMR also provides useful information about the dynamics of proteins, currently, detailed structural analysis is limited to proteins of less than 30 kDa. On the other hand, x-ray techniques can be used with much larger proteins, giving a static view of the protein in a crystal. The periplasmic siderophore binding protein FhuD, at 32 kDa, is in the upper limit of structural determination by NMR spectroscopy. Fortunately, it could readily be co-crystallized with a ferric siderophore. Now that the development of MAD (multiwavelength anomalous dispersion) techniques at synchrotron radiation facilities has increased the ease of x-ray structure determination, once data was collected, the structure of the FhuD complex could be completed in a few weeks.

General principles of x-ray crystallography. Understanding the mathematics underlying the principles of x-ray structure determination is not a simple task. However, a working knowledge of the theory of protein x-ray crystallography is essential for performing experiments. Here, we will briefly explore the properties of x-ray diffraction and focus on solving the "phase problem" by MAD techniques (Drenth, 1999).

Diffraction patterns occur when an x-ray is scattered by an ordered array such as a protein crystal. These can be directly used to determine the size of the unit cell, the molecular weight and the symmetry of the packing. Fourier transforms can be used to convert between the coordinates of the array of the diffraction pattern (reciprocal space, hkl) and coordinates of the atoms in real space (xyz). From the diffraction pattern, the intensity of the diffracted spots can be measured ($I(hkl)$), and is proportional to the square

91

of the structure factor amplitude of the reflection (hkl), $|F(hkl)|$. The equation relating the electron density in the crystal $p(xyz)$, to the structure factor amplitude $|F(hkl)|$ is:

$$p(xyz) = \frac{1}{V} \sum_{hkl} |F(hkl)| \exp[-2\pi i(hx + ky + lz) + ia(hkl)] \quad [1]$$

where $a(hkl)$ is the phase angle and K is a scaling factor. It is obvious that in order to calculate the electron density of the molecule from the diffraction pattern, phase information as well as the intensity must be known. The phase angle for each reflection can be determined by MIR (multiple isomorphous replacement), where heavy metals are incorporated into the protein crystal, molecular replacement, where the protein is modeled against a similar protein for which the structure is known, or by MAD techniques, where anomalous scattering nuclei are present in the protein crystal.

MAD phasing. If all the atoms in a crystal have the same scattering behavior, then the intensities for reflections (hkl) and $(-h-k-l)$, Friedel pairs are equal and $|F(hkl)| = |F(-h-k-l)|$ (Friedel's Law). In the case of light atoms such as C, N and O, the frequency of the incident x-ray's wavelength (λ) is large in comparison to the resonance frequencies of the electron shells of the atom (λ_A, λ_B) when calculating atomic scattering factors. However, for heavier atoms, the frequency of the incident radiation is similar to the resonance frequency of the electron shell. In this case, an electron is ejected from the electron shell by the photon energy of the x-ray beam. If a crystal contains a few atoms that scatter in a different phase than other atoms because they are near an absorption frequency, this can be detected in the diffraction pattern. Resonance scattering of radiation by the bound inner electrons of a heavy atom changes the atomic structure factor f by two parts, a real part f' and an imaginary part if . In other words, whereas free electrons have a phase difference of 180° with respect to the incident x-ray wave, bound electrons do not differ by 180° . In this case, the anomalous scattering atoms cause a breakdown of Friedel's Law and $|F(hkl)| \neq |F(-h-k-l)|$. The differences between the amplitudes of the Bijvoet pairs $|F(hkl)| - |F(-h-k-l)|$ is given in equation 2.

$$\Delta|F|_{ano} = (|F(hkl)| - |F(-h-k-l)|) \frac{f'}{2f''}$$

and f' and f'' vary with each element and chemical environment.

With the anomalous Patterson map, calculated with $(a^{TM},,)^2$, the location of the anomalous scattering atoms within the crystal can be determined. Either heavy atoms attached to the protein or already present in the protein structure can be used. However, the amount of anomalous scattering obtained for each element varies. Typically, larger atoms are more efficient at producing anomalous scattering. Unfortunately, the anomalous scattering by sulfur atoms of methionine in the protein is relatively weak. Thus, selenium, in the form of selenomethionine, is often biosynthetically incorporated into the protein to obtain a more intense anomalous signal. A characteristic absorption spectrum can be obtained for each element, measured by a fluorescence detector. Figure 2.1 shows the experimental data for the real (f) and imaginary (f'') components of the anomalous scattering of gallium around its K-edge of 1.19 Å. The two components of the anomalous scattering factor are related by the Kramers-Kronig equation

$$f'(\omega) = \frac{2}{\pi} \int_0^{\infty} \frac{\omega' f''(\omega') \delta\omega'}{\omega^2 - \omega'^2} \quad [3]$$

Intensity differences between Friedel mates for a given wavelength and data sets at different wavelengths result from a change in scattering by variation of the wavelength around the K-edge. Measurement of the differences between Friedel pairs, known as Bijvoet differences, as well as differences between data sets collected at different wavelengths, known as dispersive differences, provides phase information. From the absorption spectrum, wavelengths are chosen for the minimum of f' ("edge" or "inflection point") and maximum of f'' ("peak" or "white line") Another wavelength is chosen on the high energy side of the absorption edge ("remote point"), where f'' is close to zero. The peak position gives large Bijvoet differences within the data while dispersive differences are used between the inflection point and remote wavelength, and the peak wavelength and remote point. A Harker diagram can illustrate how anomalous scattering by heavy atoms can determine the protein phase angles. If three circles are drawn in the diagram, with radii $|F_p|$, $|F_{PH}(+)|$ and $|F_{PH}(-)|$, the structure factor amplitudes for the native protein, and those for the Friedel mates, respectively (Figure 2.2), the correct phase angle is found at the

intersection of these circles.

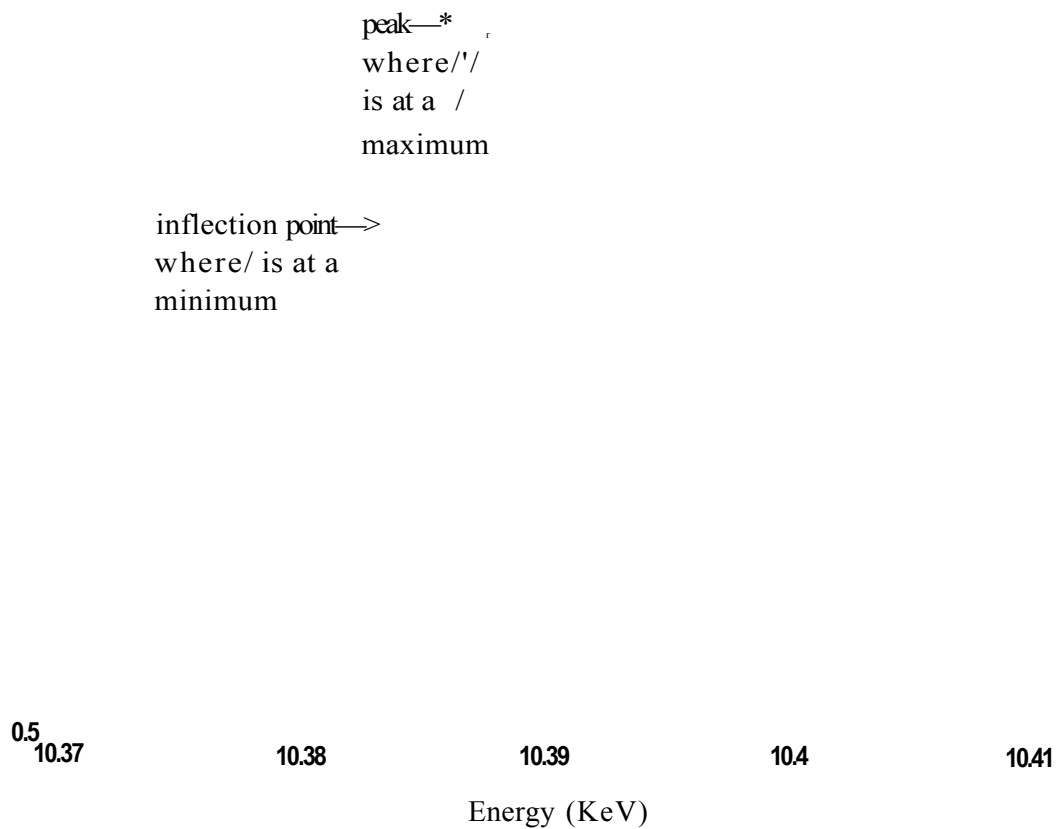


Fig. 2.1 Fluorescence spectrum of gallium of gallichrome bound to FhuD. The wavelengths for data collection of the MAD data set were obtained from the inflection point and peak of this absorption spectrum.

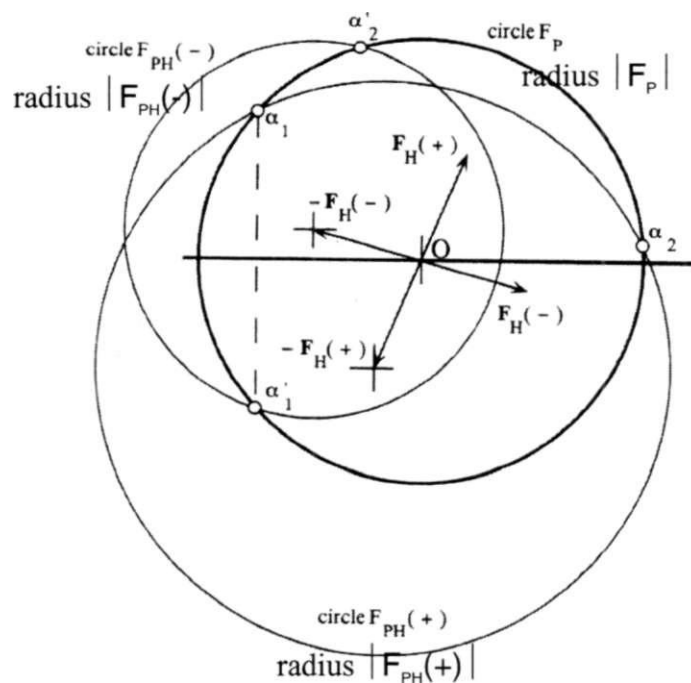


Fig. 22 The Harker diagram for determination of protein phase angles by anomalous scattering. The contribution to the structure factor by the heavy atom is $F_H(+)$ for one member of the Friedel pair and $F_H(-)$ for the other. The two structure factors are not symmetric with respect to the horizontal axis due to an anomalous component. The F_P circle has its centre at the origin, while the centre of the $F_{PH}(+)$ circle originates at $-F_H(+)$ and the $F_{PH}(-)$ circle occurs at $-F_H(-)$. The intersection of the F_P and $F_{PH}(+)$ circles at α_1 and α_1' indicate two possible phase angles. Two other possibilities occur at α_2 and α_2' , where the F_P and $F_{PH}(-)$ circles intersect. The positions of the intersection points α_1 and α_1' are symmetric with respect to the horizontal axis because the structure factor of the native protein does not have an anomalous component. The correct choices for the phase angles are α_1 and α_1' , since the reflections $\{hkl\}$ and $(-h-k-l)$ of the native protein have opposite phase angles. Figure adapted from Drenth (1999).

Application of MAD phasing. The structure of His-tag FhuD complexed with gallichrome was determined using MAD techniques at the absorption edge of gallium. This study appears to represent the first example of the use of gallium as a centre for MAD phasing.

Ga^{3+} has a very similar ionic radius to Fe^{3+} (0.62 Å vs 0.64 Å for iron), and like aluminum, will isomorphously replace iron in iron binding proteins like transferrins (Aramini *et al*, 1994) and *Neisseria* periplasmic ferric binding protein (Leontiev, V. and Vogel H.J., unpublished results). In solution studies and crystallographic studies where iron has been substituted by gallium or aluminum in ferrichrome from the fungus *Ustilago sphaerogena*, no detectable structural perturbations were observed in the structure (Llinas *et al*, 1976; Llinas *et al*, 1977; Llinas and Wuthrich, 1978; De Marco and Llinas, 1979). In addition, a comparison of the structures of the gallichrome ligand described in this study and the ferrichrome ligand observed in the crystal structure of the FhuA-ferrichrome complex (Ferguson *et al*, 1998; Locher *et al*, 1998), reveals that they are virtually identical, with an overall root mean square (r.m.s.) deviation of 0.27 Å in atomic positions for the overlapped structures. In the context of a MAD experiment the properties of gallium make it a superior choice over iron as a phasing vehicle. The anomalous signal from gallium at its absorption edge is slightly greater than that for iron, allowing for the phasing of larger protein structures. The K_{α} edge of gallium is at an easily accessible, higher energy compared to the same edge for iron (-1.19 Å vs. -1.74 Å for iron), so that radiation damage in gallium containing crystals should be much less of a problem than it is for iron containing crystals during a MAD experiment. Therefore, it would appear that for the determination of crystal structures of iron binding proteins, gallium presents itself as the phasing tool of choice.

The structure of FhuD is the first structure of a periplasmic ferric siderophore binding protein. The topology is atypical among structurally characterized periplasmic ligand binding proteins and thus represents a new class of iron-binding ABC transport proteins. Characteristics of the gallichrome binding site reveal the mechanism by which FhuD can accommodate a broad range of hydroxamate siderophores, as well as siderophore-antibiotic conjugates. The structures of FhuD bound to ferrichrome and alumichrome were subsequently solved by molecular replacement using the structure of

FhuD bound to gallichrome as a model. These structures were identical to the original FhuD gallichrome complex.

Methods.

Purification of His-tag FhuD. The overexpression strain *E. coli* BL21(DE3) pLysS pMR21 was obtained from Dr. W. Koster (Zurich, Switzerland) and Dr. V. Braun (Universitat Tübingen, Germany) and His-tag FhuD was purified similarly to the protocol previously described (Rohrbach *et al.*, 1995b). After cell lysis in 50 mM HEPES, 0.5 M NaCl pH 7.6, the protein was bound to a metal chelate column charged with nickel on the BioCad HPLC system. The column was washed with 10 volumes of 50 mM HEPES, 0.5 M NaCl pH 7.6 to remove unbound proteins and eluted with a gradient of 0-0.5 M imidazole. The protein was then dialyzed extensively against 10 mM Tris pH 7.5 at 4 °C. The His-tag was not cleaved off by enterokinase since previous studies showed that the modified protein was functional (Rohrbach *et al.*, 1995b).

Crystallization and data collection. To prepare gallichrome, ferrichrome or alumichrome, a stoichiometric amount of gallium (III) nitrate (99.9%, Aldrich Chemicals), ferric (III) nitrate (99.9%, Aldrich Chemicals) or aluminum nitrate (99.9%, Aldrich Chemicals), respectively, was added to commercially available iron-free ferrichrome (Sigma Fine Chemicals) at acidic pH. The resulting complex was added to apo His-tag FhuD in a 1:1 molar ratio at pH 7.5. Crystals of His-tag FhuD complexed with gallichrome were grown at 20 °C by hanging drop vapour diffusion from 5 μ l drops containing 7 mg ml⁻¹ of the FhuD-gallichrome complex, 0.4 M sodium monophosphate, 0.4 M potassium monophosphate and 0.1 M HEPES pH 7.5. The drops were equilibrated against a 1 ml reservoir containing 0.8 M sodium monophosphate, 0.8 M potassium monophosphate and 0.2 M HEPES pH 7.5. Large, diffraction quality crystals grew within two weeks. For cryo-crystallography experiments, crystals were soaked for 10 minutes in a stabilizing solution identical to the reservoir solution with a final concentration of 30 % (v/v) glycerol.

Preliminary data on His-tag FhuD complexed with gallichrome and ferrichrome

were collected on a Rigaku RUH3RHB rotating copper anode x-ray generator equipped with Osmic confocal multilayer x-ray focusing optics and a MAR345 image plate scanner. Data were collected on crystals frozen to -160 °C in a cold gas stream generated by an Oxford Cryostream crystal cooling device. Data were indexed, integrated and scaled using DENZO/SCALEPACK (Otwinowski and Minor, 1997). The MAD data on the His-tag FhuD complexed with gallichrome were collected at the X8C x-ray beamline at the National Synchrotron Light Source (NSLS, Brookhaven National Laboratories, BNL) using an ADSC Quantum 4R CCD detector. All three data sets were collected on a single crystal frozen using an Oxford Cryosystem cooling device. An x-ray fluorescence detector, mounted at 90° to the beam was used to determine the absorption edge of the gallium. Three x-ray wavelengths similar to the calculated values for a gallium absorption edge were selected to maximize the Bijvoet and dispersive differences (Table 2.1). The maximum of f'' was chosen at 1.19302 Å (white line or peak), the minimum of f' at 1.19387 Å (inflection), and the remote point at 1.17098 Å. Data on the FhuD alumichrome complex was also collected at the X8C x-ray beamline at the National Synchrotron Light Source (NSLS, Brookhaven National Laboratories, BNL) using an ADSC Quantum 4R CCD detector and an Oxford Cryosystem cooling device. Data were indexed, integrated and scaled using DENZO/SCALEPACK (Otwinowski and Minor, 1997). Statistics are given in Table 2.1.

Phasing and model refinement. All phasing calculations, density modification and refinement were carried out using the CNS suite of programs (Brunger *et al.*, 1998). Bijvoet and dispersive difference Patterson maps were used to locate the single gallium ion bound within the His-tag FhuD complex. A single FhuD-gallichrome complex was observed in the crystallographic asymmetric unit. Initial phases were calculated to 2.5 Å, and the electron density map was improved by solvent flattening. The quality of the resulting electron density map was excellent, allowing for the unambiguous tracing of most of the polypeptide chain using TURBO-FRODO (Roussel and Cambillau, 1989) for interactive model building. The nearly complete model was refined using CNS with maximum likelihood refinement against structure factors. Five percent of the reflections

were set aside for calculation of a free-R factor, and the same set of test reflections was maintained throughout the refinement. Iterative cycles of interactive manual refitting of the model and refinement were carried out to complete and correct the model. At this point, most of the water molecules and the gallichrome complex were incorporated into the model manually, using $2|F_o|-|F_c|ac$ and $|F_o|-|F_c|(Xc$ maps. The structure was then refined by two rounds of molecular dynamics using standard protocols and annealing using CNS. A final inspection of $2|F_o|-|F_c|(Xc$ and $JF_o|-|F_c|otc$ maps were used to locate all remaining ordered solvent molecules. The His-tag of the protein (residues 1-26) is not visible in the electron density map, as are some residues of the C-terminus (residues 294-296). Several side chains of surface exposed residues are also missing (residues 86, 111, 115, 136, 171, 186, 226, 231, 243, and 244) and were built as alanines.

The structures of the FhuD complexes with ferrichrome and alumichrome were determined using the coordinates of the FhuD gallichrome complex (without water molecules) using the CNS suite of programs (Brunger *et al.*, 1998). Rigid body refinement followed by CNS maximum likelihood refinement against structure factors was carried out until convergence was reached. Five percent of the reflections were set aside for the calculation of a free R-factor and the same set of reflections was maintained throughout refinement. The structures were refined by the same procedure defined for the FhuD gallichrome complex. At this point, the water molecules were incorporated into the model manually, using $2|F_o|-|F_c|oCc$ and $|F_o|-|F_c|(Xc$ maps.

Analysis. Sequence similarity searches were initiated by the BLAST search tool at the NCBI web site (www.ncbi.nlm.nih.gov) (Altschul *et al.*, 1997). The Predator program (www.embl-heidelberg.de/predator) was used to predict secondary structures (Frishman and Argos, 1996; Frishman and Argos, 1997). The DALI server (www2.ebi.ac.uk/dali) was used to find structurally similar proteins in the FSSP database (Holm and Sander, 1993; Holm and Sander, 1996).

Coordinates. The refined coordinates of His-tag FhuD complexed with gallichrome have been deposited in the Protein Data Bank (accession code 1EFD).

Results.

Overall structure. The FhuD gallichrome complex crystallized in the hexagonal space group P6₃, (cell dimensions $a = 86.57$ Å, $b = 86.57$ Å, and $c = 91.83$ Å) with one FhuD gallichrome complex in the crystallographic asymmetric unit (Figure 2.3). These crystal conditions were obtained from Hampton crystal screen I reservoir 35 by Shao-Yang Ku. The crystals were yellow, indicating that some iron is present in the complex. The final structure was refined to an R-factor of 0.217 against 20-1.9 Å data. Phasing and refinement statistics are reported in Table 2.1. The overall quality of the structure is excellent, with 90% of the amino acid residues occupying the most favourable region of a Ramachandran plot. With the exception of the first 26 N-terminal amino acids (containing the His-tag and the enterokinase cleavage site) and the last three C-terminal residues, neither of which reside near the binding site, the electron density describing the remainder of the polypeptide chain is continuous. The gallichrome and gallium ion were also clearly defined and could be unambiguously fit into the electron density (Figure 2.4). 114 ordered solvent molecules were also visible in the electron density maps and were included in the model.

FhuD is a kidney bean shaped bilobate protein (Figure 2.5) with approximate dimensions of 60 Å x 30 Å x 40 Å. The binding site lies in a shallow groove between the N- and C-terminal domains about 10 Å deep which cuts across the narrowest dimension of the protein. The polypeptide chain only crosses between the N- and C-terminal domains once, connecting the domains by a kinked 23-residue α -helix (residues 142-165) that runs the entire length of the protein. The long connecting helix has partial amphipathic character, with the side chains orientated so that the aromatic amino acids are against the N- and C-domains and the hydrophilic amino acids are solvent exposed. There is one hydrogen bond near the middle of the helix between the hydroxyl of Tyr204 and the carbonyl of the peptide bond of Ile182. Otherwise, hydrogen bonding between residues of the helix and either domain is limited to either end of the helix.

Table 2.1 Summary of crystallographic data

	Inflection point	Peak	Remote
Data collection			
Wavelength (Å)	1.19387	1.19302	1.17098
Resolution (Å)	30-1.9	30-1.9	30-1.9
Completeness (%) ^{1,2}	98.7 (96.4)	98.4 (95.2)	98.7 (93.0)
I/a (I)	27.7(10.4)	32.7(8.1)	30.1 (15.2)
R _{sym} (%) ³	0.047 (0.113)	0.045 (0.167)	0.040 (0.119)
Overall figure of merit			
before solvent flattening	0.5907		
after solvent flattening	0.9660		
Refinement statistics			
Resolution (Å)	20-1.9	Rms deviation from ideality	
Number of Reflections ⁴	60580	bonds (Å)	0.007
working set	52106	angles (°)	1.453
free set	2612	dihedrals (°)	22.77
R factor ⁵	0.218	Mean B-factors	
Free R factor	0.250	protein (Å ²)	23.88
Model composition		gallichrome (Å ²)	25.54
Amino Acids	261	gallium (Å ²)	27.03
Total atoms	2148	solvent (Å ²)	29.55
Water molecules	114		

¹Number in parentheses is the statistic for highest resolution shell.

² $I > aI$

³ $R_{sym} = \sum_h (X_j | I_{j,h} - \langle I_h \rangle | / I_{j,h})$, where h = set of Miller indices and j = set of observations of reflection h .

⁴ $F > 2.0 \sigma$

⁵ $R \text{ factor} = \sum_k | | F_o - F_c | | / \sum_k | F_o |$



Fig. 23 Crystals of the FhuD gallichrome complex. The FhuD complex forms large yellow crystals in about two weeks.

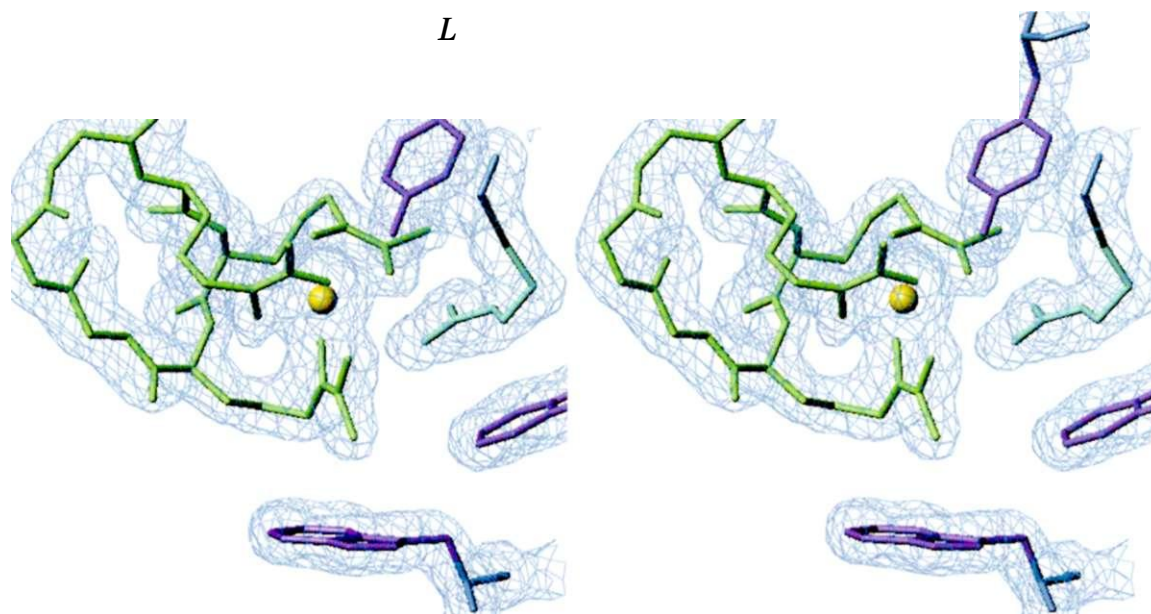


Fig. 24 A stereo $2[F_o - F_c]$ electron density map at 19 Å resolution contoured at 1σ around gallichrome and proximal residues found in the binding pocket. The siderophore is shown in green while the gallium is yellow. Aromatic side chains are purple and the Arg is light blue. This figure was generated with TURBO-FRODO (Roussel and Cambillau, 1989).

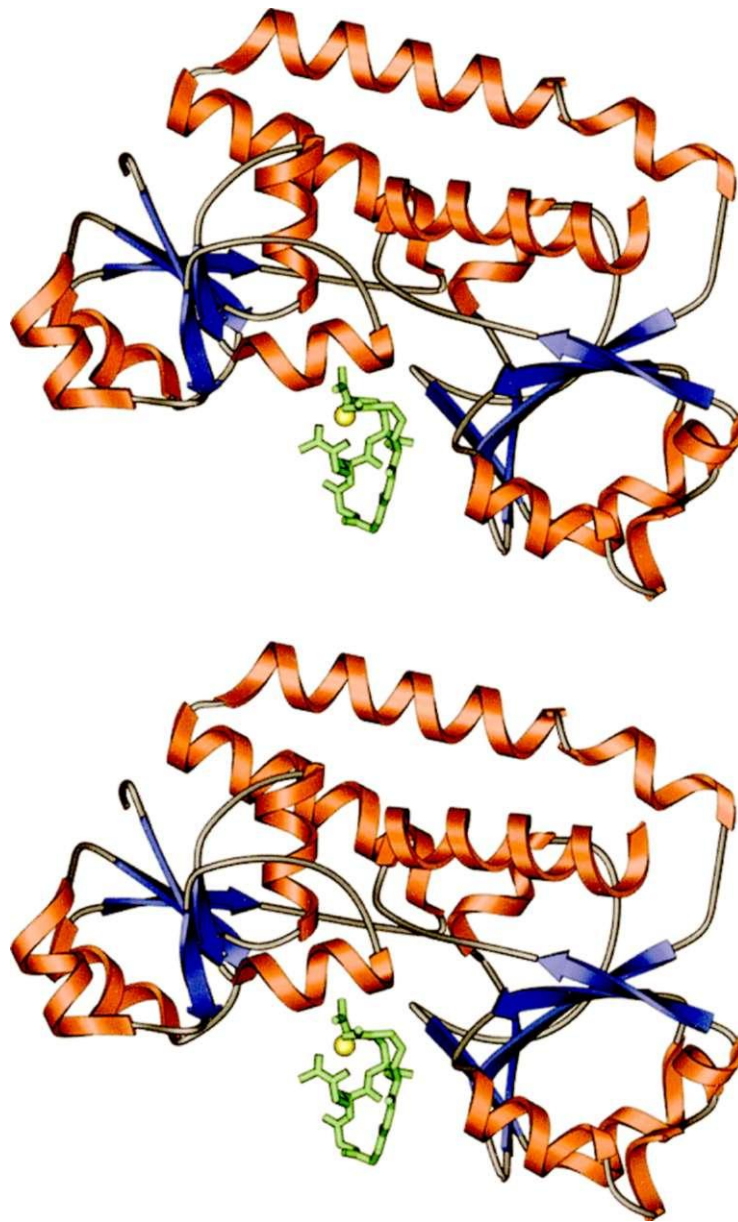


Fig. 25 A stereo ribbon diagram showing the overall structure and the secondary structure elements in the FhuD gallichrome complex. The N-domain is at the top of the figure. The gallichrome is shown in green, with the gallium ion in yellow. Helices are red, p-strands are blue and random coil regions are grey. The binding cleft is a shallow pocket between the N- and C-domains. This figure was drawn using Setor (Evans, 1993).

The N-terminal domain (residues 27-141) consists of a twisted five stranded parallel **(3**-sheet with 3-2-1-4-5 linking topology while the C-terminal domain (residues 166-288) has a five-stranded mixed **(3**-sheet with 3-2-1-4-5 linking topology, with both surrounded by α -helices (Figure 2.6). The contact surface between the two domains of FhuD is extensive, encompassing 1266 Å² of both the N- and C-terminal domains. The domain interface of the protein is lined with many hydrophobic residues and several hydrogen bonds are present between the two domains of the protein. One oxygen of the side chain of Glu47 makes hydrogen bonds to the side chain of Ser280 and the nitrogen of the peptide bond of Ala277 while the other oxygen makes hydrogen bonds to the nitrogen of the peptide bonds of Ala277 and Ser280. One oxygen of the side chain of Glu71 makes a hydrogen bond with one of the nitrogens of the side chain of His283, while the other nitrogen of His283 makes a hydrogen bond with the carbonyl of the peptide bond of Ala271. Other hydrogen bond contacts through water molecules occur between the peptide backbone of the N-domain and the peptide backbone of the C-domain.

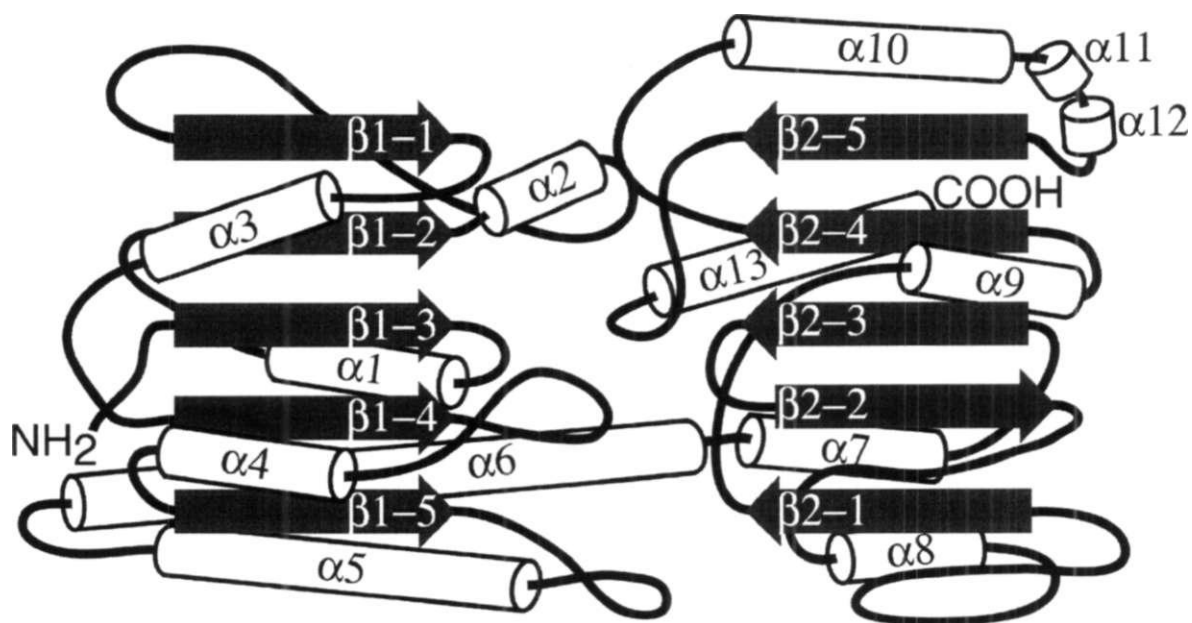


Fig 2.6 A topology diagram of FhuD, showing that the N-terminal and C-terminal domains do not share a similar fold. α -Helices are depicted as cylinders and **(3**-strands as arrows.

A search using the DALI server for proteins in the PDB with similar three dimensional folds (Holm and Sander, 1993; Holm and Sander, 1996) to FhuD showed that the periplasmic zinc-binding protein TroA from *Treponema pallidum* (PDB entry 1TOA) has the most similar overall fold, including the unique connecting cc-helix (Lee *et al.*, 1999). 181 Ca atoms were overlaid (in 22 segments, Z-score 8.5) onto TroA with an r.m.s. deviation of 3.5 Å. An overlay of FhuD (22 segments, Z-score 6.6) on the **3**-subunit of the nitrogenase molybdenum-iron (Mo-Fe) protein involved in the electron transfer process of dinitrogen reduction (PDB entry 2MIN) (Kim and Rees, 1992) gave a r.m.s. deviation of 4.8 Å. Visual inspection of the structure of the related surface manganese-binding lipoprotein PsaA from Gram-positive *Streptococcus pneumoniae* also shows that it is similar to FhuD, with the unusual backbone helix connecting the two domains (Lawrence *et al.*, 1998).

Siderophore binding. A detailed view of the gallichrome binding site is displayed in Figure 2.7. Gallichrome is the Ga³⁺ chelate of the cyclic hexapeptide, (Gly)₃-(A^{1s}-acetyl-N⁵-hydroxy-L-ornithine)**3**. The central gallium atom is coordinated octahedrally by six oxygen donor atoms of the hydroxamic acid moieties of three TV-acetylated hydroxyornithine residues. The gallium coordination is distorted from perfect octahedral symmetry, with distances ranging from 2.13 Å to 2.16 Å between gallium and five of the six coordinating oxygen atoms, with the remaining oxygen lying 2.28 Å from the gallium. The binding of the siderophore to FhuD is mediated by hydrophilic and hydrophobic interactions. Only 45% (246 Å² out of 498 Å²) of the molecular surface of gallichrome is buried in this complex (Figure 2.8), and only three direct hydrogen bonds are formed between the gallichrome and FhuD in the receptor site. Arg84 forms hydrogen bonds with two of the three carbonyl oxygen atoms of the hydroxamic acid moieties while the carbonyl oxygen of the third hydroxamic acid moiety is hydrogen bonded to Tyr106. The peptide backbone of the gallichrome is further stabilized by water-mediated hydrogen bonds to Asn215 and Ser219. One side of the binding pocket is lined with a "band" of hydrophobic residues (Figure 2.7) consisting of the Trp residues Trp43, Trp68, Trp217 and Trp273, as well as Tyr275, Thr85,

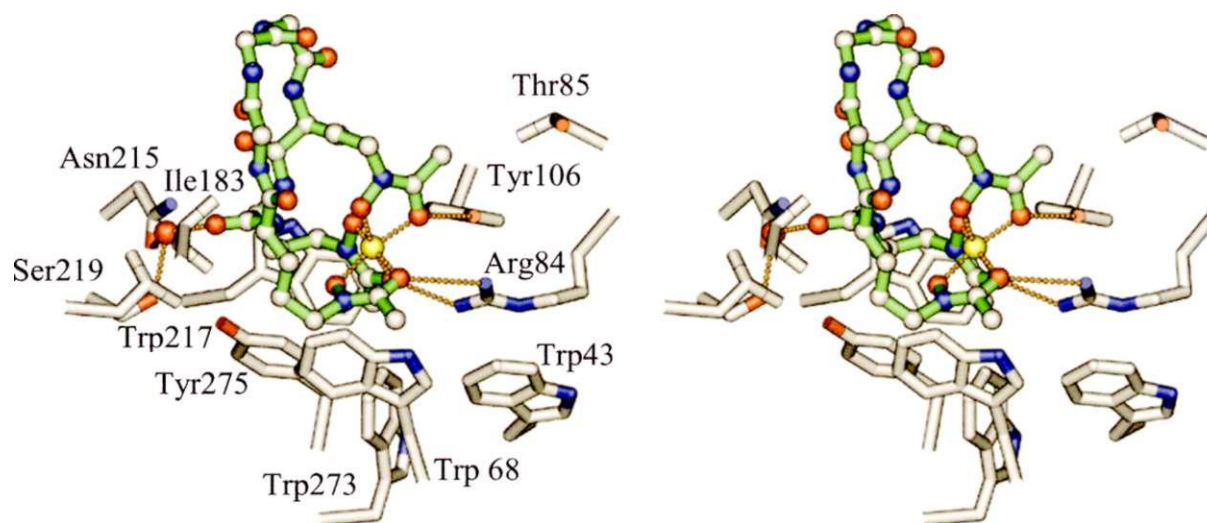


Fig. 2.7 A detailed stereo view of gallichrome binding to FhuD. The gallium ion is displayed as a yellow sphere and the siderophore is displayed as a ball-and-stick model with green bonds to distinguish it from the protein side chains, which are drawn with grey bonds. Carbon atoms are coloured grey, oxygens are red while nitrogen atoms are blue. Dashed green lines show potential hydrogen bonds and electrostatic interactions. All hydrophobic and hydrophilic residues from FhuD which interact either directly or through water mediated interactions are shown. The distorted octahedral coordination of gallium by the siderophore is clearly visible in this view. The gallium ion is completely "caged" by the siderophore and makes no direct contacts with the protein. Arg84 and Tyr106 residues bind the hydroxamate portion of the siderophore and hydrophobic residues line the binding pocket around the siderophore. This figure was generated with Setor (Evans, 1993).

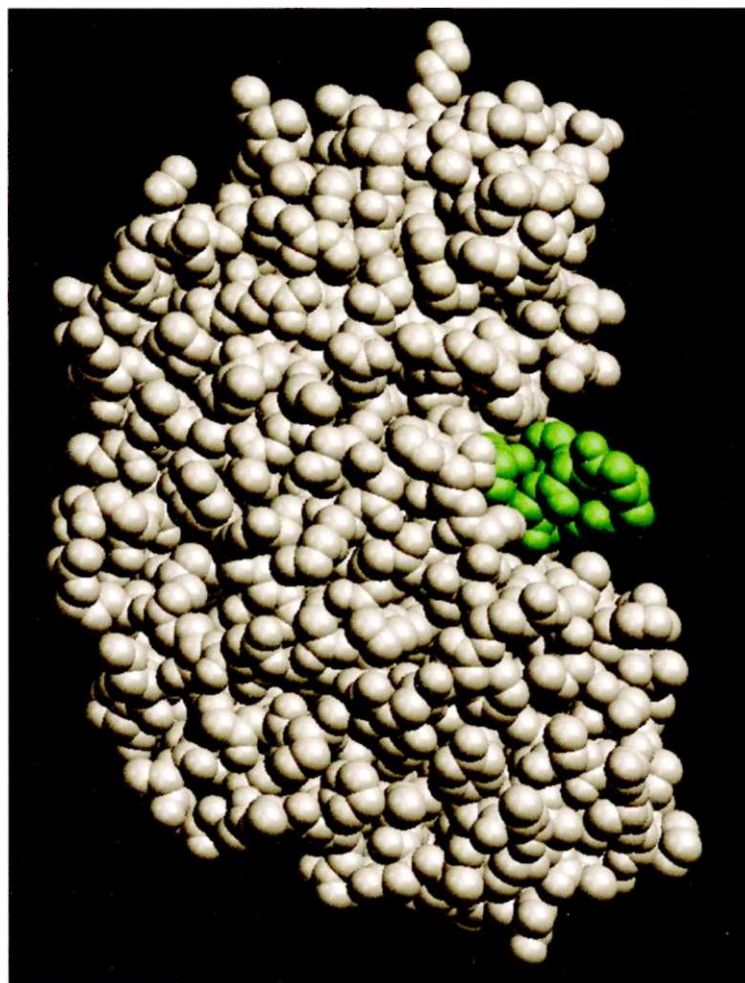


Fig 28 A space filling model of the FhuD gallichrome complex. The protein is shown in grey with the gallichrome in green. This figure was created with GRASP (Nicholls *et al.*, 1992).

He 183 and Leu189. These residues contact the hydrophobic portions of the siderophore and create a cavity the correct shape and size for gallichrome (Figure 2.9). Seven Asp residues lie on the periphery and underside of the siderophore binding pocket, imparting a negative electrostatic potential on the surface of the binding pocket (Figure 2.9).

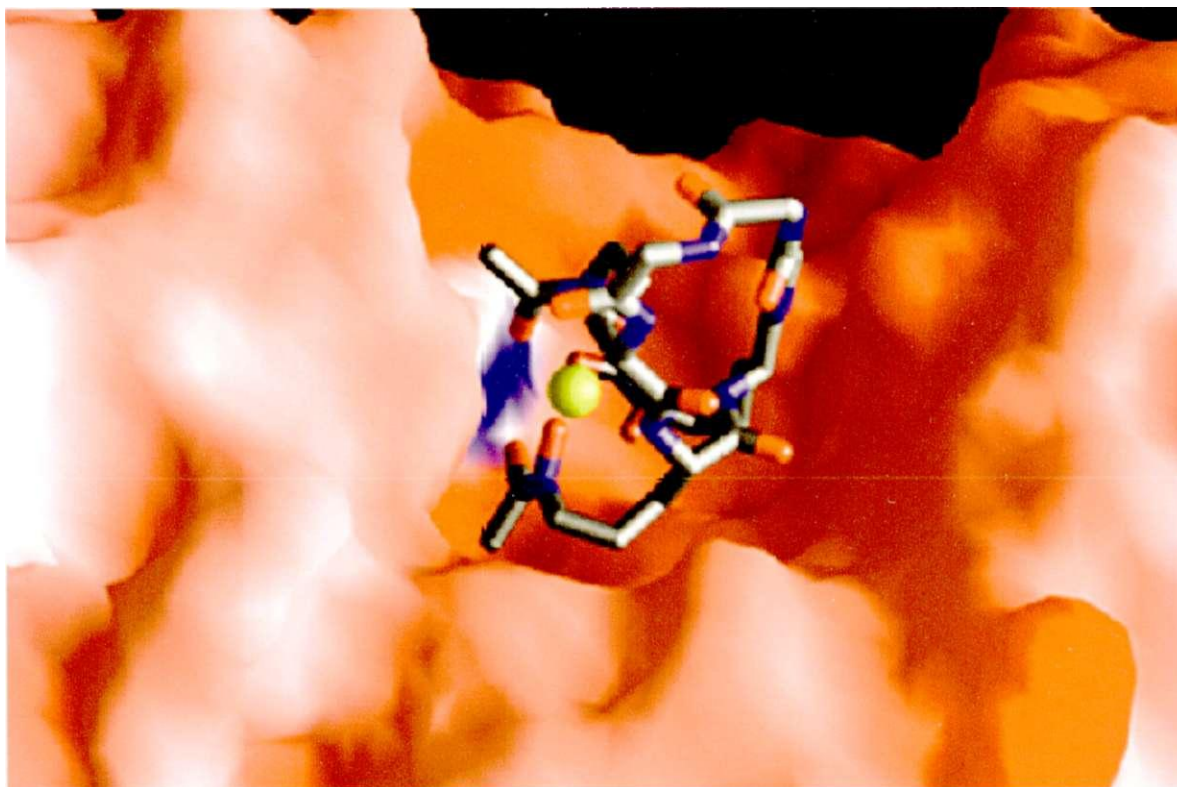


Fig. 2.9 A GRASP (Nicholls *et al.*, 1992) diagram, showing a close-up view of the molecular surface of the gallichrome-binding pocket of FhuD, coloured by electrostatic potential. Regions of negative electrostatic potential are coloured red while regions of positive electrostatic potential are shown in blue. The electrostatic potential of the binding pocket is predominantly negative, with a small locus of positive potential in the vicinity of the hydroxamate oxygen atoms. The molecular surface of the binding pocket has a high amount of structural complementarity with the hydroxamate portion of the siderophore, but leaves the remainder of the siderophore largely exposed to solvent.

Structures of the FhuD ferrichrome and FhuD alumichrome complexes. Although ferrichrome is the natural substrate for iron acquisition by bacteria, other metal ions can isomorphously substitute for the iron when desired for experimental studies. As demonstrated, the substitution of gallium for iron in ferrichrome provides an excellent centre for MAD phasing studies. The iron in ferrichrome can also be substituted by diamagnetic metal ions such as aluminum for NMR spectroscopy. Since the structure of alumichrome is identical to the structure of ferrichrome (Llinas *et al*, 1976; Llinas *et al*, 1977; Llinas and Wuthrich, 1978; De Marco and Llinas, 1979), this molecule can be reliably used in place of ferrichrome.

Each FhuD complex crystallized in the space group P63 with very slight differences in cell dimensions than the FhuD gallichrome complex. Phasing and refinement statistics are reported in Table 2.2. As in the FhuD gallichrome complex, the structures in each complex were missing the N-terminal His-tag (first 26 amino acids of the protein sequence) and the last three amino acids of the C-terminus. Electron density of several surface exposed side chains were missing in each protein and were modeled as alanines. The siderophore in each crystal structure was in the same orientation as in the FhuD gallichrome complex. The hydrogen bonding distances between the siderophore and the side chains of FhuD did not change significantly. The structures of the siderophores were also identical to gallichrome. The temperature factor for aluminum in the alumichrome molecule is elevated compared to the other B factors in the structure. The aluminum ion may be mobile within the cage of hydroxamate ligands since the radius of the ion is smaller.

Table 2.2 Summary of crystallographic data

	FhuD ferrichrome	FhuD alumichrome
Data collection		
Wavelength (Å)	1.5418	1.1005
Resolution (Å)	30-2.3	30-2.3
Unit cell dimensions (Å)	$a = b = 86.57$ $c = 91.82$	$a = b = 86.21$ $c = 92.28$
Completeness (%) ¹	98.2 (94.2)	98.4 (93.6)
I/σ(I)	28.7 (7.1)	23.0(13.8)
R _{sym} (%) ²	0.045 (0.166)	0.053 (0.118)
Refinement statistics		
Resolution (Å)	30-2.3	30-2.3
Number of reflections ³	16881	16276
Working set	16064	15571
Free set	817	796
R-factor ⁴	0.209	0.213
R _{free}	0.232	0.234
Mean B-factors		
Protein (Å ²)	26.19	26.75
Ligand (Å ²)	29.07	28.64
Metal ion (Å ²)	34.88	77.87
Solvent (Å ²)	32.84	32.92

Number in parentheses is the statistic for highest resolution shell.

¹ I > a I

² R_{sym} = $\sum_h (\sum_j |I_{j,h} - \langle I_h \rangle| / \sum_j I_{j,h})$, where h = set of Miller indices and j = set of observations of reflection h.

³ F > 2.0 CT

⁴ R factor = $\sum_k |F_o - F_c| / \sum_k |F_o|$

Discussion.

Although the periplasmic proteins in ABC transport systems share very little sequence homology and recognize diverse ligands, most are closely related in structure (Quiocho and Ledvina, 1996). Many consist of two globular domains connected by short stretches of β -strands, which allow movement by a hinge mechanism. Molecular recognition of ligands arises from slight differences in the number and arrangement of the β -strands and α -helices in the two globular domains. The unique features of the periplasmic protein FhuD, namely the backbone helix and hydrophobic domain interface, are indicative of a novel structure/function relationship related to siderophore binding.

Relation to other periplasmic binding proteins. The overall organization of secondary structure in FhuD, TroA, PsaA and nitrogenase MoFe protein are all similar, with each possessing a pair of β/α sandwich domains spanned by a long helix that is tightly packed against the rest of the protein. TroA and PsaA, which bind the smallest ligands (uncomplexed metal ions), have pseudo two-fold symmetry with 2-1-3-4 linked parallel (P/ α)⁴ topologies in their N- and C-domains. Domain II of the β -subunit of the nitrogenase MoFe protein also contains a 2-1-3-4 linked parallel topology while domain III has 3-2-1-4-5 linked parallel topology. It appears that the larger P-sheet in domain III is required to accommodate the $Fe_7MoS_9O_7C_7$ cluster binding in the cleft between domains II and II. FhuD, which binds the largest ligand of the related proteins, has 3-2-1-4-5 linked topologies (parallel and mixed β/α) in its two domains. The binding clefts of TroA and PsaA are much narrower and deeper than the binding sites of FhuD and nitrogenase MoFe protein and their ligands are much more deeply buried (Figure 2.10). In this respect, the smaller domain interface of TroA is rather hydrophilic, whereas that of FhuD is hydrophobic. This suggests that TroA and PsaA may utilize a different mechanism for ligand binding and release than FhuD. In addition, amino acid sequence alignments of all known PLBPs show that FhuD and TroA fall into separate clusters, distinct from each other and other PLBPs (Tarn and Saier, Jr., 1993; Quiocho and Ledvina, 1996). On the basis of this analysis, FhuD and TroA appear to be representatives of two new, related

structural classes within the PLBP family.

Amino acid sequence homology (23% identity) suggests that FepB and FecB, the periplasmic proteins involved in the uptake of catecholate siderophores and citrate, respectively, could also be structurally related to FhuD. The metal-binding periplasmic proteins, including PsaA and TroA, and the ferric siderophore binding proteins are grouped in two separate classes based on sequence homology (Tarn and Saier, Jr., 1993). The amino acid sequences of the *E. coli* periplasmic ferric siderophore binding proteins FhuD, FepB and FecB are not significantly homologous to any other bacterial proteins involved in the uptake of amino acids or sugars. However, they share some sequence homology to the periplasmic vitamin B12 binding protein, BtuE, the anguibactin binding protein of *Vibrio anguillarum*, FatB and the siderophore binding protein, FhuD, of *Bacillus subtilis* (Koster W, 1991), with most of the homology in the N-terminal domains of FhuD, FepB, FecB and FatB (Tarn and Saier, Jr., 1993). A sequence alignment of FhuD, FepB and FecB shows that a variety of residues are conserved among these periplasmic proteins (Koster W, 1991), however this does not include any of the residues involved in the binding pocket. This is perhaps not surprising since the charge, shape and size of the siderophores bound by these different periplasmic proteins vary. Interestingly, the periplasmic proteins FhuD and FepB have less specificity for ferric hydroxamates and catechols, respectively, than the outer membrane receptors (Stephens *et al*, 1995; Rohrbach *et al*, 1995b). FecB, thus far, appears to only transport ferric citrate (Pressler *et al*, 1988). Very likely, a hydrogen bond network may exist in these proteins, which would act to dissipate the charge of the siderophore, such as that found in other PLBPs (Quioco, 1990).

Tentative identification of residues which may play a role in binding ferric enterobactin in the receptor FepA included Arg and those with negatively charged side chains (Newton *et al*, 1997; Buchanan *et al*, 1999). A cursory inspection of residues in the FepB sequence in the vicinity of the residues in the binding site of FhuD reveals several residues that meet these criteria. However, the correct identification of residues lining the binding pockets of FepB and FecB is awaiting determination of their complexed structures. Nevertheless, a secondary structure prediction of these proteins shows that a long α -helix may be present in similar locations as in FhuD (Frishman and Argos, 1996; Frishman and

Argos, 1997). This suggests that these proteins could have a similar overall fold to FhuD, PsaA and TroA. Together, these proteins represent a new class of structurally similar metal binding proteins.

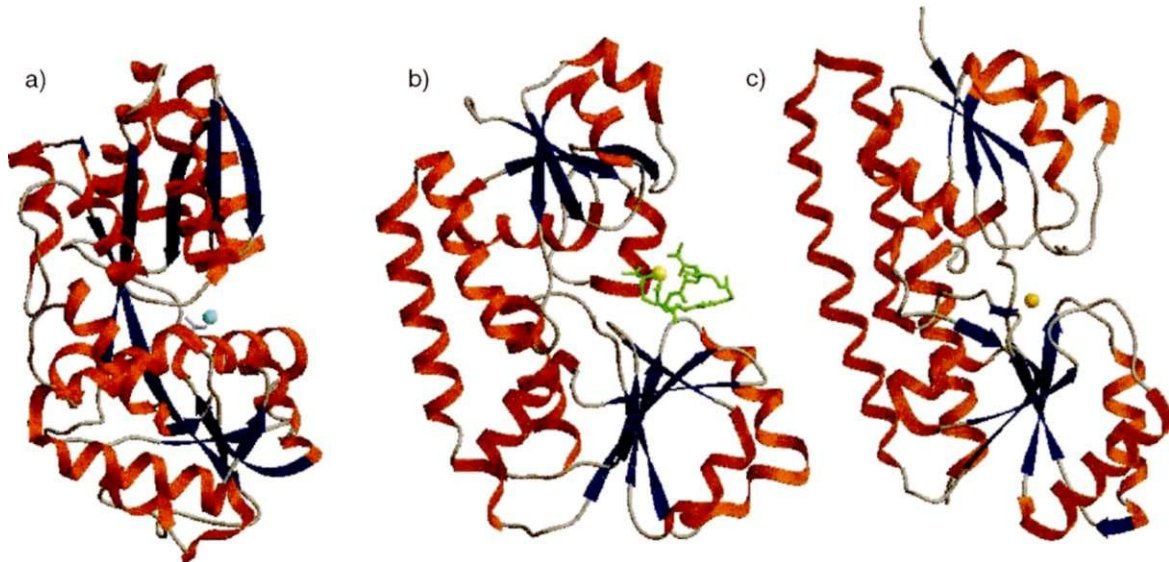


Fig. 2.10 Comparison of the structures of periplasmic binding proteins, a) HFbp, the Fe^{3+} -binding protein from *H. influenzae* (PDB accession code: 1MRP (Bruns *et al*, 1997)) represents a typical periplasmic binding protein, with two domains connected by P-strands, where b) FhuD, the ferric siderophore binding protein from *E. coli* (PDB accession code: 1EFD (Clarke *et al*, 2000)) and c) TroA, a zinc-binding protein from *Treponema pallidum* (PDB accession code: 1TOA (Lee *et al*, 1999)) have two domains connected by a long α -helix. In each ribbon diagram, α -helices are red and β -strands are blue.

Siderophore binding to FhuD. Analysis of gallichrome, ferrichrome and alumichrome binding in these structures reveals that FhuD should be able to accommodate a variety of related hydroxamate siderophores, with its shallow, open binding pocket. It is well known that FhuD can bind ferric hydroxamate complexes transported into the periplasm, including aerobactin, rhodoturulate, coprogen and ferrioxamine B as well as natural siderophore antibiotics like albomycin (Koster and Braun, 1990; Koster W, 1991; Rohrbach *et al*, 1995b). The essential structural and chemical features of the siderophores that are

recognized by FhuD are the hydroxamate moieties and adjacent hydrophobic linkers. It is surprising that most of the backbone of the siderophore is not involved in recognition since ferrichrome binds with a relatively high affinity to FhuD (binding constant is 0.1 μ M) (Rohrbach *et al.*, 1995b). Clustering of aromatic groups in the binding pocket of FhuD likely contributes to the high-affinity binding of gallichrome and other hydroxamate complexes. These form a non-polar environment of the correct size and shape. Stacked aromatic residues are also found in the binding sites of periplasmic amino acid binding and sugar binding proteins (Quioco, 1990; Quioco and Ledvina, 1996). Previous studies show that mutating Trp63 influences the binding of hydroxamates, decreasing ferrichrome binding (Rohrbach *et al.*, 1995b). Hydrogen bonds are useful since they are stable yet have a low energy barrier for release of the ligand. Co-operative multiple hydrogen bonds between the Arg84 and the carboxyl oxygens of the gallichrome are analogous to those found in the binding sites of periplasmic sugar binding proteins (Quioco, 1990; Quioco and Ledvina, 1996). Arg84 and Tyr106 also appear to be essential siderophore-recognition/binding factors. A water molecule also hydrogen bonds to the gallichrome peptide backbone, coordinating with Ser219 and Asn215. With these key features present, the open binding pocket of FhuD could potentially accommodate ligands where the remainder of the compound possesses considerable structural and chemical diversity. An additional property of FhuD, which likely confers some degree of specificity to ligand binding, becomes apparent when the electrostatic potential of the binding pocket is examined (Figure 2.9). This group of negative charges presumably does not hinder the binding of the neutral hydroxamate siderophores, but negatively charged siderophores, like the negatively charged catecholate siderophore enterobactin, would be repelled.

A similar siderophore-binding motif is observed in the FhuA outer membrane ferrichrome receptor (Ferguson *et al.*, 1998; Locher *et al.*, 1998), with a tyrosine and an arginine binding the three hydroxamic acid groups in a similar fashion (Figure 2.11). However, the similarity between the binding pockets of FhuA and FhuD ends there, since FhuA also uses an additional Tyr and a Trp residue to hydrogen bond with the hydroxamate moieties, as well as other hydrophilic groups to interact with the (Gly)₃ backbone of the siderophore. Hydrophobic interactions between the methylene carbon

atoms of the ornithine moieties of gallichrome and the receptor site play an important role in siderophore recognition and binding. Overall, FhuA covers the surface of ferrichrome to a much greater extent than FhuD. The receptor presents a different constellation of hydrophobic residues and utilizes a greater number of hydrogen bonds to interact with the siderophore, which explains the much greater selectivity exercised by FhuA in siderophore binding.

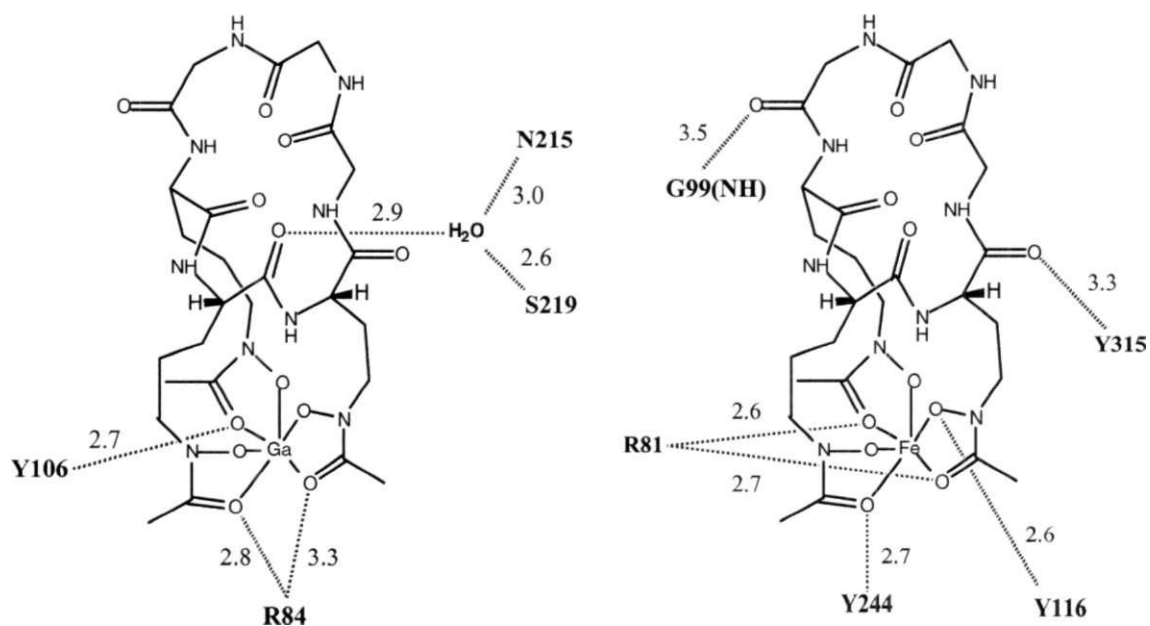


Fig. 2.11 A comparison of the residues involved in hydrogen bonds in the binding pockets of a) FhuD and b) FhuA, with distances indicated. FhuA utilizes a more extensive network of hydrogen bonds to interact with the siderophore, and covers the surface of the siderophore to a greater extent than FhuD.

When bound to FhuD, a large portion of the gallichrome molecule with hydrogen-bonding potential, encompassing six imino groups and six carbonyl oxygens, are largely solvent exposed, with some involved in water-mediated interactions with the receptor site or intramolecular hydrogen bonds (Figures 2.7 and 2.8). The unused potential hydrogen binding surface on the siderophore provides an appealing target that could allow recognition of the FhuD-ferrichrome complex by the inner membrane receptor protein FhuB *in vivo*. However, it is more likely that protein-protein interactions between FhuD

and FhuB are essential for the transfer of the siderophore across the inner membrane for a number of reasons. Firstly, it has been demonstrated the *fhud*⁻ bacterial strains are unable to transport hydroxamates into the cytoplasm (Koster W, 1991), indicating that FhuD is necessary for mediating interactions with the inner membrane receptor. Secondly, it is well established that FhuB can transport siderophore-antibiotic conjugates with a bulky substitution on the glycine backbone, such as albomycin, into the cytoplasm (Rohrbach *et al.*, 1995a). Thirdly, peptide mapping studies reveal external loops in FhuB can physically interact with FhuD (Mademidis *et al.*, 1997). Finally, interaction between the periplasmic protein FhuD and FhuB indicates that the ligand-loaded FhuD preferentially associates with FhuB (Rohrbach *et al.*, 1995a; Mademidis *et al.*, 1997). All available evidence supports a model where a dissociation event occurs to release the ligand from FhuD and deliver it to FhuB, and not one in which ferrichrome is removed directly from FhuD *via* interactions with the backside glycines of the siderophore.

The ability of FhuD to tightly bind its cognate ligands while leaving them largely solvent exposed make it an attractive target for use as a delivery vehicle for antibiotics. Work by the Miller lab has established that chemical synthesis and utilization of siderophore-drug conjugates is feasible (reviewed in Roosenberg *et al.*, 2000). These "Trojan horses" are taken up into the cell by the specific iron uptake systems, where the antibiotic has its effect. Characterization of the important chemical attributes involved in siderophore recognition by the proteins of the iron uptake system is invaluable. A comparison of the structures of FhuA and FhuD clearly indicates how one could create the minimal siderophore scaffold required for recognition by both proteins. However, due to increased interactions with the ferrichrome peptide backbone, the outer membrane receptor will place more limitations on the variety of antibiotic-siderophore conjugates which could be imported into Gram-negative cells. The structure of the FhuD-gallichrome complex, in conjunction with the recently solved FhuA-ferrichrome complex structure (Ferguson *et al.*, 1998; Locher *et al.*, 1998) should aid in the rational development of novel siderophore-antibiotic conjugates.

Implications for Siderophore Transport. The long backbone helix which joins the N- and

C-terminal domains, which is slightly distorted at Ser158, as well as the predominantly hydrophobic character of the domain interface found in FhuD suggests that it exercises an unusual mechanism of ligand exchange, which may not involve opening and closing of the binding site. All other known PLBP structures contain flexible P-strand interdomain linker regions that act as hinges, allowing for opening of the proteins for ligand exchange. The interdomain helix found in FhuD would greatly restrict interdomain opening compared to a P-strand hinge. For those proteins for which both holo- and apo-forms have been solved by x-ray crystallography, the unliganded structure adopts an open conformation while in the liganded structure (closed conformation), the lobes are drawn together by a "Venus fly-trap" like mechanism. Each lobe does not significantly change its structure, rather there is a rotation of the two domains about the hinge region. The opening and closing of these proteins, or "breathing", is thought to be a dynamic process, with a small associated energy barrier (Gerstein *et al*, 1994; Hayward, 1999). The hinge bends due to small changes in the ϕ and ψ angles of the P-sheets connecting the two domains. In FhuD, PsaA and TroA, the single long helix connecting the two domains likely limits domain movement between open and closed states. The hydrophobic domain interface in FhuD would also greatly restrict domain opening. Therefore, binding and release of hydroxamate siderophores from FhuD, and metal ions from PsaA and TroA, would involve a conformational change dissimilar to that observed in other periplasmic proteins. Since these proteins must both recruit substrates from the periplasm with high affinity and deliver them to inner membrane proteins, a conformational change is likely associated with this process. For FhuD, there is some preliminary experimental evidence for a conformational change. Crystallization of the apo form of FhuD occurs under very different conditions compared to the gallichrome bound form (unpublished results) and analysis of the gallichrome complex of FhuD reveals that there are no crystal packing contacts involving the siderophore. However, this conformational change is probably far less dramatic than that observed for the other characterized periplasmic proteins. Dynamic light scattering studies of FhuD in the absence and presence of ferrichrome and analogues showed no significant changes in the hydrodynamic radius of the protein (unpublished results). It is possible that a large scale interdomain movement does not occur, but instead, a loop or segment of the protein near

the receptor site moves to accommodate ligand binding. No obvious candidates for this sort of phenomenon were apparent from the structural analysis, since there are no loops or structural elements that cover the siderophore or display conspicuously large B-factors. Since the domain interface is hydrophobic, any process, such as hinge bending, which would open the domain interface and expose it to solvent, is unlikely. A more plausible mechanism of structural change would allow the two domains to slide with respect to one another, or twist, through bending of the backbone α -helix. An unwinding of the α -helix could also occur, as in the case of the ubiquitous calcium signalling protein calmodulin when it binds peptide (Ikura *et al*, 1992; Meador *et al*, 1992, 1993; Elshorst *et al*, 1999; Osawa *et al*, 1999), but again there is no evidence, such as high B-factors in the atoms comprising the helix, that this occurs. More likely, a flexible loop region on the C-terminal end of the long connecting α -helix could allow the two domains to slide or twist from each other, keeping the long α -helix intact. This effect could cause the slight distortion seen in the helix near this loop. In either case, the substrate would stabilize the closed conformation of the protein since residues from both lobes are involved in tight binding of the ligand. The favourable entropic effect of substrate binding, likely by expulsion of water molecules from the hydrophobic binding pocket, would also stabilize the ligand-bound conformation of the protein. We await determination and analysis of the structure of the apo-form of FhuD to conclusively resolve this issue.

Chapter 3

X-ray Crystallographic Structures of the *Escherichia coli* Periplasmic Protein FhuD bound to Various Hydroxamate-type Siderophores

Siderophore-binding proteins play an essential role in the uptake of iron in many Gram-positive and Gram-negative bacteria. FhuD is an ATP-binding cassette-type (ABC-type) binding protein involved in the uptake of hydroxamate-type siderophores in *Escherichia coli* and is considered to be a potential drug target. Structures of FhuD complexed with different siderophores, including the antibiotic albomycin, coprogen and the drug Desferal® have been solved to high resolution by x-ray crystallography. FhuD has an unusual structure for a periplasmic ligand binding protein, with two p7a domains connected by a long α -helix. The binding site for hydroxamate-type ligands is a shallow pocket that lies between these two domains. These structures of protein-siderophore complexes show that binding occurs in a similar manner with each siderophore, with slight movement of amino acid side chains within the binding pocket. The iron-hydroxamate centre of each siderophore is specifically bound to the protein by a number of hydrogen bonds to the side chains of the residues in the binding pocket. This study provides a basis for the rational design of novel bacteriostatic agents, including siderophore-antibiotic conjugates that can act as "Trojan horses", using the ferrichrome uptake system to deliver antibiotics directly into targeted pathogens.

Introduction.

Since the bioavailability of iron is very low (10^{-18} M), there is an intense competition between a host and bacteria for soluble iron. Low molecular weight compounds called siderophores serve to scavenge iron from the environment for bacterial uptake. Two broad classes of siderophores exist, hydroxamates and catecholates, of which at least one is used by every group of bacteria. Although *Escherichia coli* itself produces only one siderophore, enterobactin, it can utilize siderophores from a variety of sources. Several ferric siderophore uptake systems have been characterized from *E. coli*. Each system consists of a specific outer membrane receptor, a periplasmic protein and several inner membrane associated proteins. The energy for transport of the ferric siderophore across the outer membrane is provided by interaction of the receptor with the TonB complex (reviewed in Braun, 1995). Subsequently, the energy for ferric siderophore transport across the inner membrane is provided by hydrolysis of ATP by the inner membrane associated proteins. This arrangement of protein components and mechanism of transport is typical of systems for uptake of amino acids, sugars and other nutrients in Gram-negative bacteria (Guerinot, 1994; Braun *et al.*, 1998; Schryvers and Stojiljkovic, 1999).

The uptake of hydroxamate-type siderophores in *E. coli* is the most structurally characterized system to date. *E. coli* has several distinct receptors for each different siderophore including FhuA for ferrichrome, FhuE for coprogen, and FoxA for ferrioxamine B. However, a common periplasmic protein, FhuD, can bind and shuttle a variety of hydroxamate siderophores to the inner membrane associated proteins FhuB and FhuC. Fungal hydroxamate siderophores generally consist of similar structural units (8-*N*-hydroxy-orinithine, *α*-anhydromevalonic acid and acetic acid), but the number and arrangement of these units can vary (Figure 3.1). Ferrichrome, originally identified from the smut fungus *Ustilago maydis*, is likely the most studied hydroxamate-type siderophore thus far (Llinas *et al.*, 1970; Llinas *et al.*, 1972; Constantine *et al.*, 1990). The apo and holo

structures of the *E. coli* receptor FhuA, which transports ferrichrome and the structurally related antibiotic albomycin, have recently been solved (Ferguson *et al*, 1998; Locher *et al*, 1998; Ferguson *et al*, 2000). The receptor forms a 22-stranded β -barrel in the bacterial membrane, with a N-terminal domain that fills the inside of the barrel. A short helix at the N-terminus, located near the periplasmic side of the membrane, unravels in the holo complex and is implicated in recruiting the TonB complex to the receptor. In addition, the periplasmic protein FhuD has also been solved as a complex with the ferrichrome analogue gallichrome, where the iron atom coordinated to ferrichrome is replaced with gallium (Clarke *et al*, 2000). The structure of the periplasmic protein is unusual for its function, forming a bilobate structure connected by a long α -helix, in contrast to the typical two domain structure connected by several β -sheets found in most other periplasmic ligand binding proteins. In FhuD, a shallow pocket is located between the two domains for ferric siderophore binding. In both the FhuA receptor and FhuD periplasmic protein, ferrichrome is cradled in a pocket lined with aromatic residues, with a few specific hydrogen bonds from the hydroxamate portion of the siderophore to side chains in the binding site. Similarly to ferrichrome, in other hydroxamate-type siderophores, six oxygen atoms of the hydroxamate portion coordinate a ferric iron, although the overall structures vary considerably (Figure 3.1). Presumably, this is the portion of the iron complex that is important for recognition by the bacterial proteins involved in iron uptake.

Conjugation of an antibiotic to a siderophore is a promising technique for therapeutic control of bacterial infections. The naturally occurring antibiotic albomycin has a thioribosyl pyrimidine antibiotic group attached to an iron binding moiety similar to that of ferrichrome. This antibiotic enters the cell by the ferrichrome uptake system, then the antibiotic group is cleaved off the remainder of the molecule by peptidase N (Hartmann *et al*, 1979; Braun *et al*, 1983). Although the intracellular target of albomycin is unknown, the minimal inhibitory concentration (0.005 μ g/ml) is very low compared to other antibiotics, such as ampicillin (0.1 μ g/ml) (Pugsley *et al*, 1987). In recent years, development of synthetic conjugates of antibiotics and siderophores has been successful in

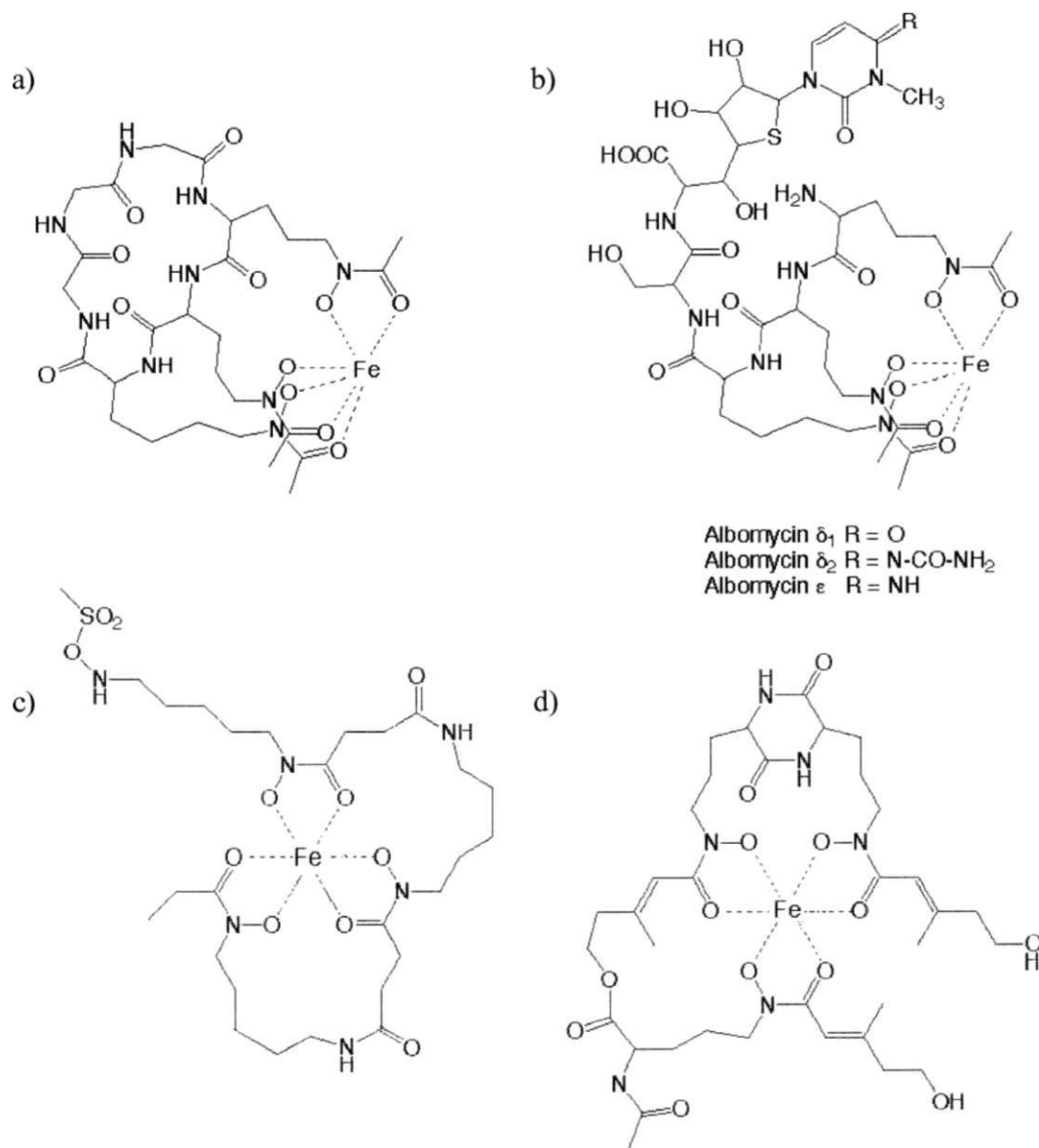


Fig. 3.1 Chemical structures of various hydroxamate-type siderophores. Structures of a) ferrichrome, b) albomycin, c) Desferal®, the dihydroxy mesylate of desferrioxamine B from *Streptomyces pilosus*, and d) coprogen, first isolated from *Neurospora crassa* (Atkin and Neilands, 1968), have octahedral coordination of the ferric ion by oxygen ligands.

limiting the growth of certain bacteria (Roosenberg *et al.*, 2000). The siderophore acts as a "Trojan horse", actively carrying the antibiotic across the cell membrane via the specific ferric siderophore uptake system into the cell.

However, rational design of a novel, effective antibiotic by chemical conjugation is challenging. Many chemical and biological factors pertaining to the effect on the bacteria and impact on the host must be considered. Chemical properties important for drug design include structural similarity to siderophores, solubility and lipophilicity. Biological considerations for development of novel bacteriostatics involve toxicity to the bacteria and host and repercussions from the metabolism of the conjugate. Criteria for broad-spectrum use of the antibiotic and for overcoming the resistance mechanisms of the bacteria must also be met.

Identification of the important structural features for siderophore recognition by bacteria would be one of the first steps in design of a novel bacteriostatic agent. In this chapter, the structures of different FhuD siderophore complexes have been solved by x-ray crystallography. Molecular replacement was used to determine the protein phase angles using the structure of FhuD from the FhuD gallichrome complex as a model. If the new complex is isomorphous with the model protein, then the phases from the model can be used to create an electron density map. However, if the new complex is non-isomorphous with the model protein, the method finds the correct rotational orientation of the model in the unit cell using the fast direct method then the translational position in the unit cell is determined (Drenth, 1999).

The crystal structures of FhuD complexed to the antibiotic albomycin, coprogen, and the drug Desferal® show that although structurally diverse, each siderophore is bound to the protein by specific bonds to the hydroxamate iron core. This is the first characterization of the different binding modes present in a protein that can accommodate a large number of siderophores.

Methods.

Purification of FhuD. The overexpression strain *E. coli* BL21(DE3) pLysS pMR21 was obtained from Dr. W. Koster (Swiss Federal Institute for Environmental Science and Technology, Switzerland) and Dr. V. Braun (Universitat Tubingen, Germany). His-tag FhuD was purified by metal chelate chromatography (POROS 20MC) charged with nickel, similarly as previously described (Rohrbach *et al.*, 1995b) except that the BioCad HPLC metal chelate system (PerSeptive Biosystems) was used. After cell lysis in 50 mM HEPES, 0.5 M NaCl pH 7.6, the protein was bound to the column and washed with 10 volumes of 50 mM HEPES, 0.5 M NaCl pH 7.6 to remove unbound proteins and eluted with a gradient of 0-0.5 M imidazole. The protein was then dialyzed extensively against 10 mM Tris pH 7.5 at 4 °C. The His-tag of the protein was not cleaved off by enterokinase since previous studies showed that the modified protein was functional (Rohrbach *et al.*, 1995b).

Crystallization and data collection. Albomycin 82 and coprogen were gifts from Dr. G. Winkelmann (Universitat Tubingen, Germany). Desferal® (desferrioxamine mesylate) was obtained from CIBA-GEIGY Canada. For each siderophore, a 1 mM stock solution of the ferric siderophore complex was made using Fe₂(NO₃)₆ (99.9%, Aldrich Chemical Company) at acidic pH. Albomycin, coprogen, and Desferal® each bind iron in a 1:1 siderophore to iron molar ratio. The ferric siderophores were added to apo FhuD in a 1:1 ratio in 10 mM Tris, pH 7.5. Crystals of His-tag FhuD complexed with coprogen and Desferal® were grown at room temperature by hanging drop vapour diffusion from 5 μ l drops containing 8.3 mg ml⁻¹ of the FhuD-ferric siderophore complex, 0.8 M di-Na/K phosphate and 0.05 M HEPES, pH 7.5. The drops were equilibrated against a 1 ml reservoir containing 1.6 M di-Na/K phosphate and 0.1 M HEPES, pH 7.5. In a similar manner, crystals of His-tag FhuD complexed with albomycin were grown at room temperature in 5 μ l drops containing 8.3 mg ml⁻¹ of the FhuD-albomycin complex, 8% PEG 4000 and 0.05 M Na acetate, pH 5.2 and equilibrated against a 1 ml reservoir containing 16% PEG 4000 and 0.1 M Na acetate,

pH 5.2. Large, diffraction quality crystals grew within two weeks. For cryo-crystallography experiments, crystals were soaked in a stabilizing solution identical to the reservoir solutions with a final concentration of 30 % (v/v) glycerol.

Data on the FhuD albomycin complex was collected on a Rigaku RUH3RHB rotating copper anode x-ray generator equipped with Osmic confocal multilayer x-ray focusing optics and a MAR 345 image plate scanner. Data on the FhuD coprogen complex was collected at the X12-C x-ray beamline at the National Synchrotron Light Source (Brookhaven National Laboratories, BNL) using a Brandeis B4 CCD detector. Data for the FhuD Desferal® complex was collected at the 7-1 x-ray beamline at the Stanford Synchrotron Radiation Laboratory (Stanford Linear Accelerator Center, SLAC) using an ADSC Quantum 4R CCD detector. All data were collected on crystals frozen to 100 K in a cold gas stream generated by an Oxford Cryostream crystal cooling device. Each FhuD ferric siderophore crystal was found to belong to the space group P63, with small variations in unit cell dimensions. Data were indexed, integrated and scaled using DENZO/SCALEPACK (Otwinowski and Minor, 1997). Statistics are given in Table 3.1.

Phasing and model refinement. All phasing calculations, density modification and refinement were carried out using the CNS suite of programs (Brunger *et al.*, 1998). The structure of the FhuD protein from the FhuD gallichrome complex (Clarke *et al.*, 2000) (PDB accession code: 1EFD) was used as a model for molecular replacement. In each crystal, a single FhuD-ferric siderophore complex was observed in the asymmetric unit. For each structure, initial phases were calculated to 2.5 Å and the electron density was improved by solvent flattening. The quality of the electron density map was excellent, allowing for the unambiguous tracing of most of the polypeptide chain using TURBO-FRODO (Roussel and Cambillau, 1989) for interactive model building. The nearly complete model was refined using CNS maximum likelihood refinement against structure factors. Five percent of the reflections were set aside for the calculation of a free R-factor and the same set of reflections was maintained throughout refinement. Iterative cycles of

interactive manual fitting of the model and refinement were carried out to complete and correct the model. At this point, most of the water molecules and the ferric siderophore could be incorporated into the model manually, using $2|F_o|-|F_c|$ and $|F_o|-|F_c|$ maps, as well as OMIT maps. The structures of similar ferric siderophores were found in the Cambridge Structural Database (www.ccdc.cam.ac.uk/prods/csd/csd.html) and their structures were modified accordingly. For albomycin, the structure of gallichrome from the FhuD gallichrome complex (PDB accession code: 1EFD) was slightly modified. The model of coprogen was based on the structure of the neocoprogen I molecule (Cambridge Structural Database accession code: COFDIK10 (Hossain *et al*, 1987)), which was modified to include a *trans*-anhydromevalonic acid group attached to the ornithine backbone. Desferal®, based on ferrioxamine (Cambridge Structural Database accession code: DUPJON (Hossain *et al*, 1986), was modeled into the binding site using TURBO-FRODO (Roussel and Cambillau, 1989). Topology and parameter files for the ferric siderophores were generated using the Hic-Up server (xray.bmc.uu.se/hicup (Kleywegt and Jones, 1998)) and adjusted appropriately. The structure of each complex was refined by several rounds of molecular dynamics and annealing using standard protocols by CNS (Brunger *et al*, 1998). A final inspection of $2|F_o|-|F_c|$ and $|F_o|-|F_c|$ maps were used to locate all remaining ordered solvent molecules. The stereochemical quality of the final structures were evaluated using PROCHECK Version 3.4.4 (Laskowski *et al*, 1993; Morris *et al*, 1992).

PDB coordinates. The refined coordinates of FhuD complexed with coprogen have been deposited in the Protein Data Bank (accession code: 1ESZ). Deposition of the coordinates of FhuD complexed with albomycin and Desferal® are forthcoming.

Results.

Overall structures. Each FhuD siderophore complex crystallized in the hexagonal space group P6₃ with slightly different cell dimensions than the FhuD gallichrome complex (Table 3.1), with one complex in each asymmetric unit. Phasing and refinement statistics are reported for each complex in Table 3.1. The structures for the FhuD protein in each complex were missing the first 26 N-terminal amino acids (containing the His-tag and the enterokinase cleavage site) and the last three C-terminal amino acids (residues 294-296), while the electron density describing the remainder of the protein is continuous. Several side chains of surface exposed residues were also missing and were built as alanines in the model. The electron density for the iron atom coordinated to each siderophore was well defined. However, the electron density for the siderophores in each case were incomplete and only portions of each molecule were included in the model. The electron density for the antibiotic portion of the albomycin was missing, the density for a methyl group of the coprogen was missing as well as the mesylate (OSO₂CH₃) group of the Desferal® (Figure 3.2).

The overall structures of the FhuD proteins in each complex were very similar to the protein found in the gallichrome complex (Figure 3.3). In each complex, the overall quality of the protein structure is excellent, with 90% of the amino acid residues occupying the most favourable region of a Ramachandran plot (data not shown). The protein is a bilobate kidney bean shape, with two domains connected by a 23-residue kinked α -helix (residues 142-165) (Clarke *et al*, 2000). The N-terminal domain has a twisted five stranded parallel P-sheet while the C-terminal domain has a mixed five stranded P-sheet, with both surrounded by α -helices. The binding site for the siderophores lies in the shallow cleft between these two domains and several side chain residues form hydrogen bonds with each siderophore (Figure 3.4). An overlay of the C _{α} backbone of FhuD from the gallichrome complex with the other siderophore complexes gives root mean square deviations (rmsd) of 0.25 Å with albomycin, 0.27 Å with coprogen and 0.20 Å with Desferal (Figure 3.5).

Table 3.1 Summary of crystallographic data

	FhuD albomycin	FhuD coprogen	FhuD Desferaf
Data collection			
Wavelength (Å)	1.5418	0.9787	1.0800
Resolution (Å)	30-2.6	30-2.0	30-2.0
Unit cell dimensions (Å)	$a = b = 85.48$ $c = 92.47$	$a = b = 86.09$ $c = 91.94$	$a = b = 85.57$ $c = 91.60$
Completeness (%) ^{1,2}	94.8 (95.5)	95.6 (90.1)	99.1 (97.8)
I/O ³	14.0(1.6)	35.1 (6.6)	21.8(3.8)
Rsym (%) ³	0.099 (0.646)	0.043 (0.102)	0.049 (0.205)
Refinement statistics			
Resolution (Å)	30-2.6	30-2.0	30-2.0
Number of reflections ⁴	11873	25292	22886
Working set	8900	22625	21789
Free set	484	1165	1097
R-factor ⁵	0.203	0.219	0.220
Rfree	0.262	0.241	0.242
Mean B-factors			
Protein (Å ²)	43.28	28.69	33.26
Ligand (Å ²)	45.68	31.46	44.74
Metal ion (Å ²)	42.84	23.44	42.50
Solvent (Å ²)	38.62	35.48	43.08

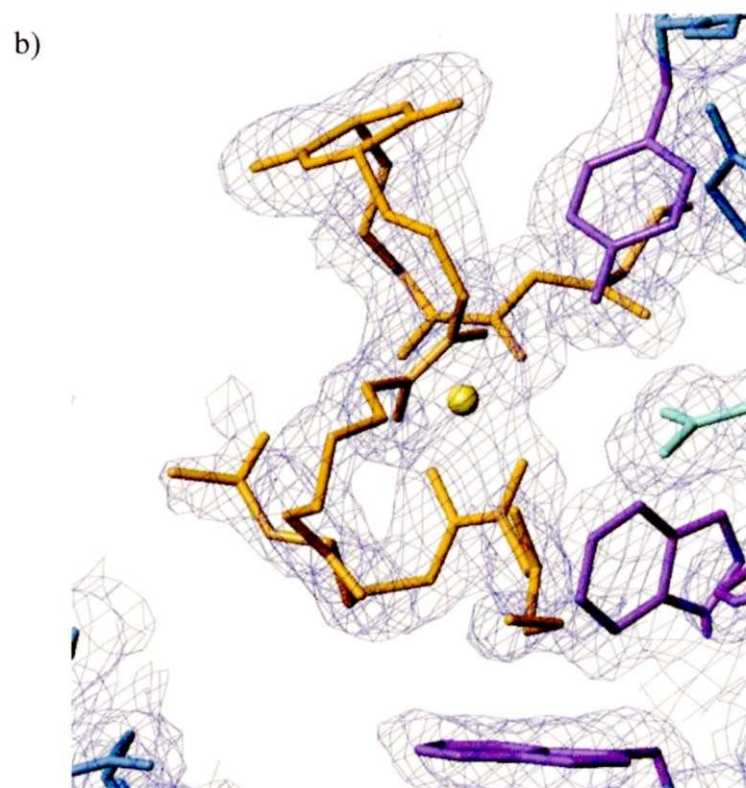
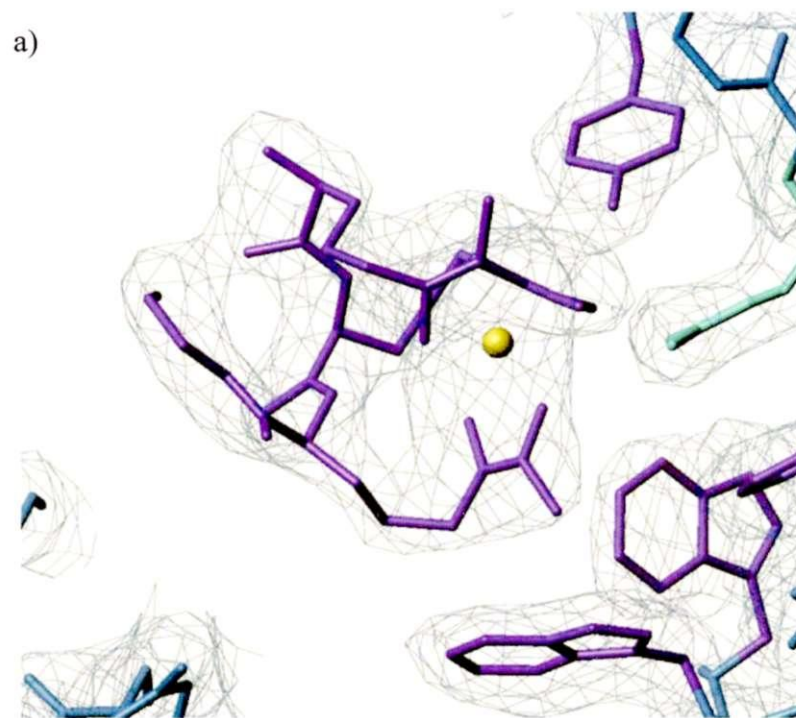
Number in parentheses is the statistic for highest resolution shell.

¹ $I > aI$

³ $R_{sym} = \sum_h (\sum_j |I_{jh} - \langle I_h \rangle| / \sum_j I_{jh})$, where h = set of Miller indices and j = set of observations of reflection h .

⁴ $F > 2.0 \sigma$

⁵ $R \text{ factor} = \sum_k |I_{ki} - F_o - F_d| / \sum_k I_{ki}$



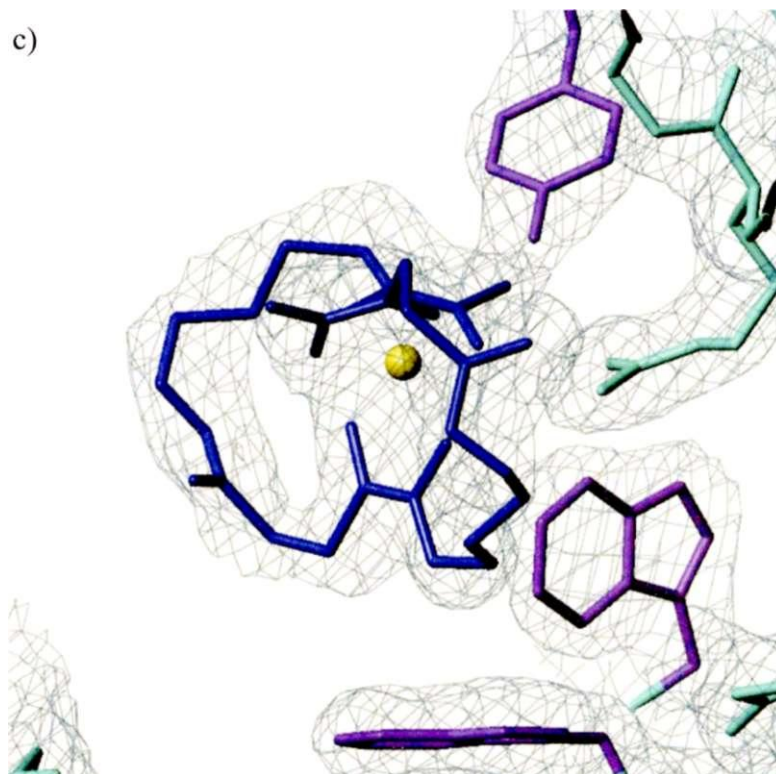
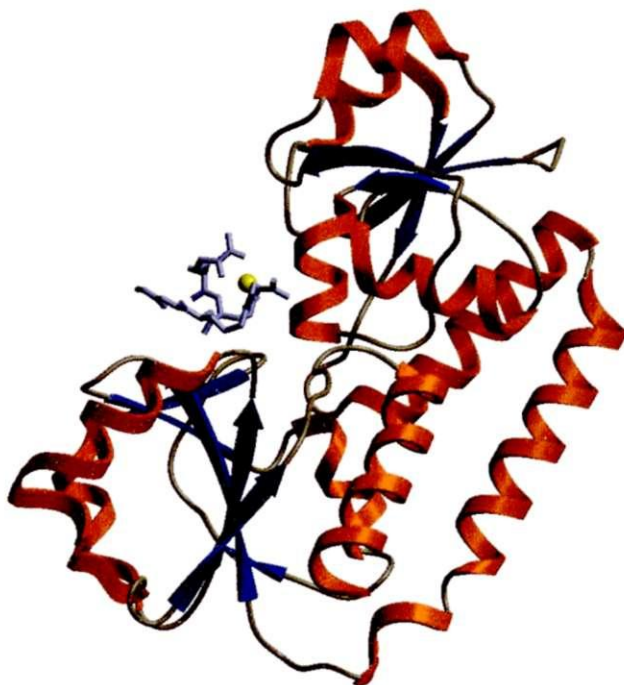


Fig. 3.2 $2|F_o|-|F_c|$ electron density maps of the FhuD siderophore complexes, a) Electron density surrounding the albomycin (purple), b) Electron density surrounding the coprogen (orange), c) Electron density surrounding the Desferal® (blue). In each picture, the iron is shown in yellow, aromatic side chains are purple and Arg84 is light blue. These figures were generated by TURBO-FRODO (Roussel and Cambillau, 1989).

a)



b)



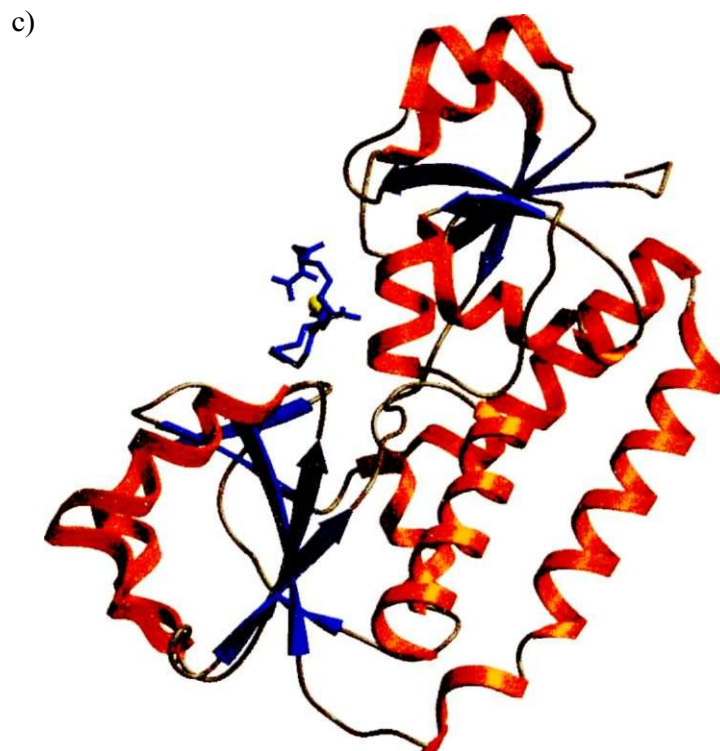
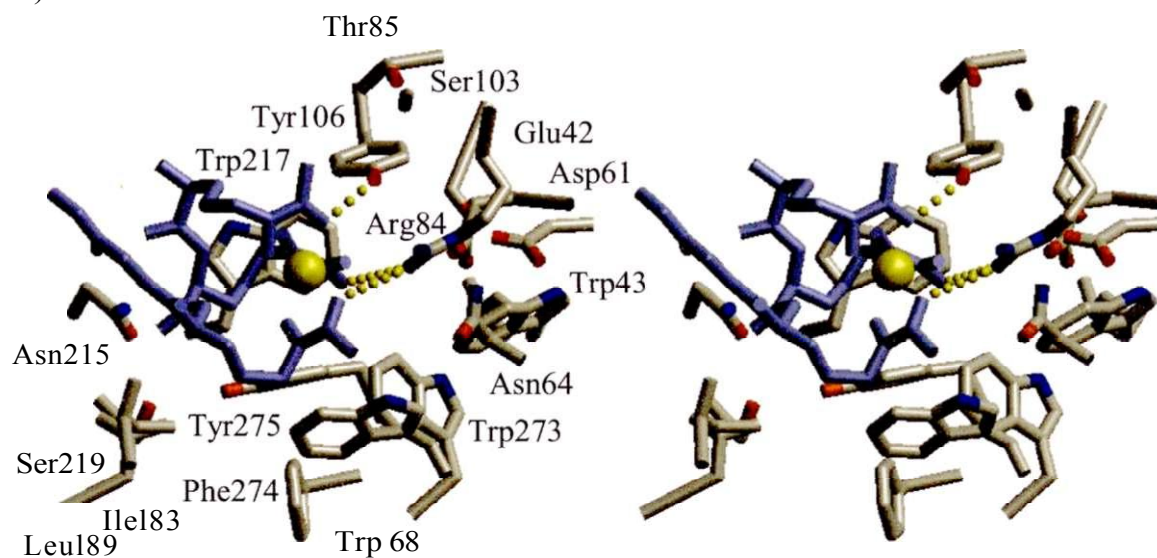
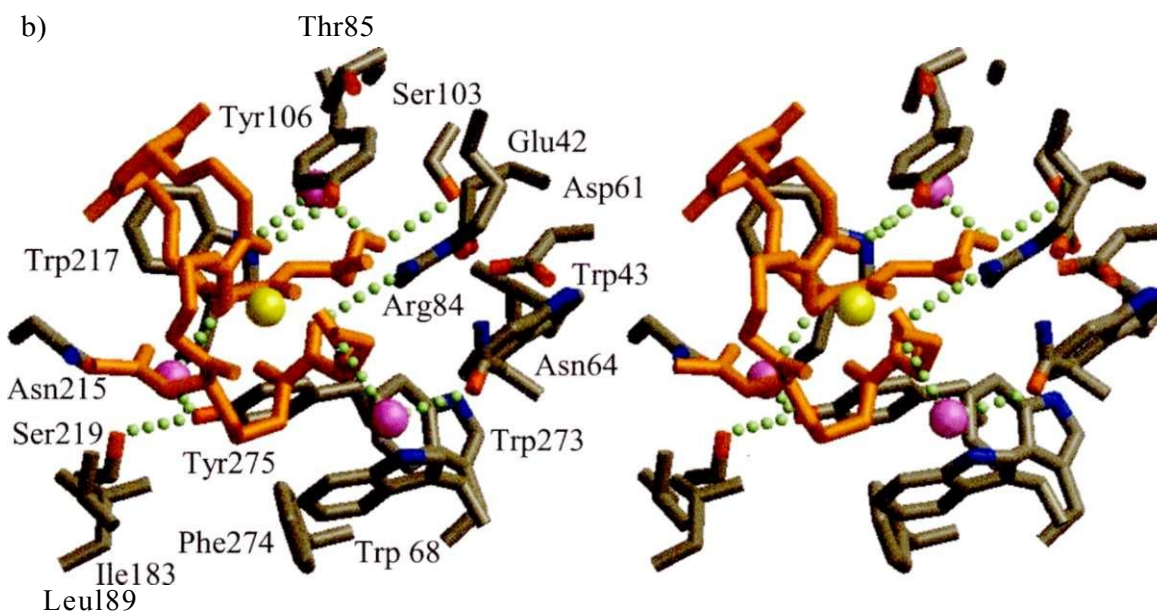


Fig. 33 Ribbon diagrams showing the overall secondary and tertiary structures in the FhuD siderophore complexes; a) FhuD albomycin, b) FhuD coprogen and c) FhuD Desferal®. The albomycin is shown in purple, the coprogen is in orange and the Desferal® is blue, while the iron atom in each is yellow. Helices are red, (β-strands are blue and random coil regions are gray. The binding cleft in each structure is a shallow pocket between the N- and C-domains. These figures were drawn using Setor (Evans, 1993).

a)



b)



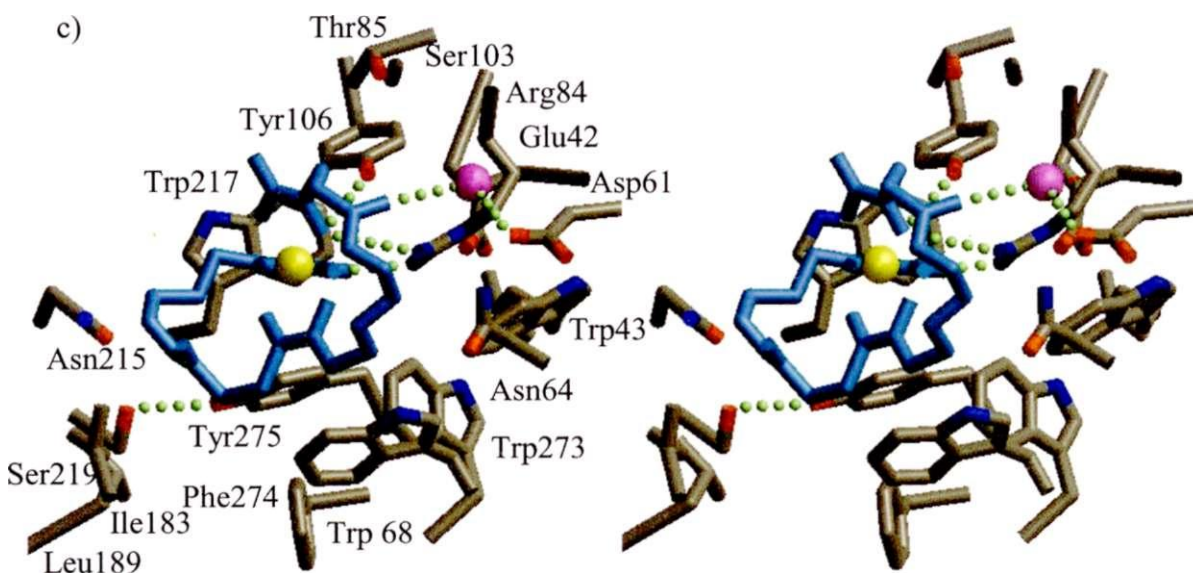


Fig. 3.4 A close-up stereo view of the residues involved in the binding site in the a) albomycin, b) coprogen, and c) Desferal® complexes. The gallichrome is shown in green while the albomycin is purple, coprogen is orange and Desferal® is blue. Important side chain residues involved in hydrogen binding are labeled. These figures were drawn using Setor (Evans, 1993).

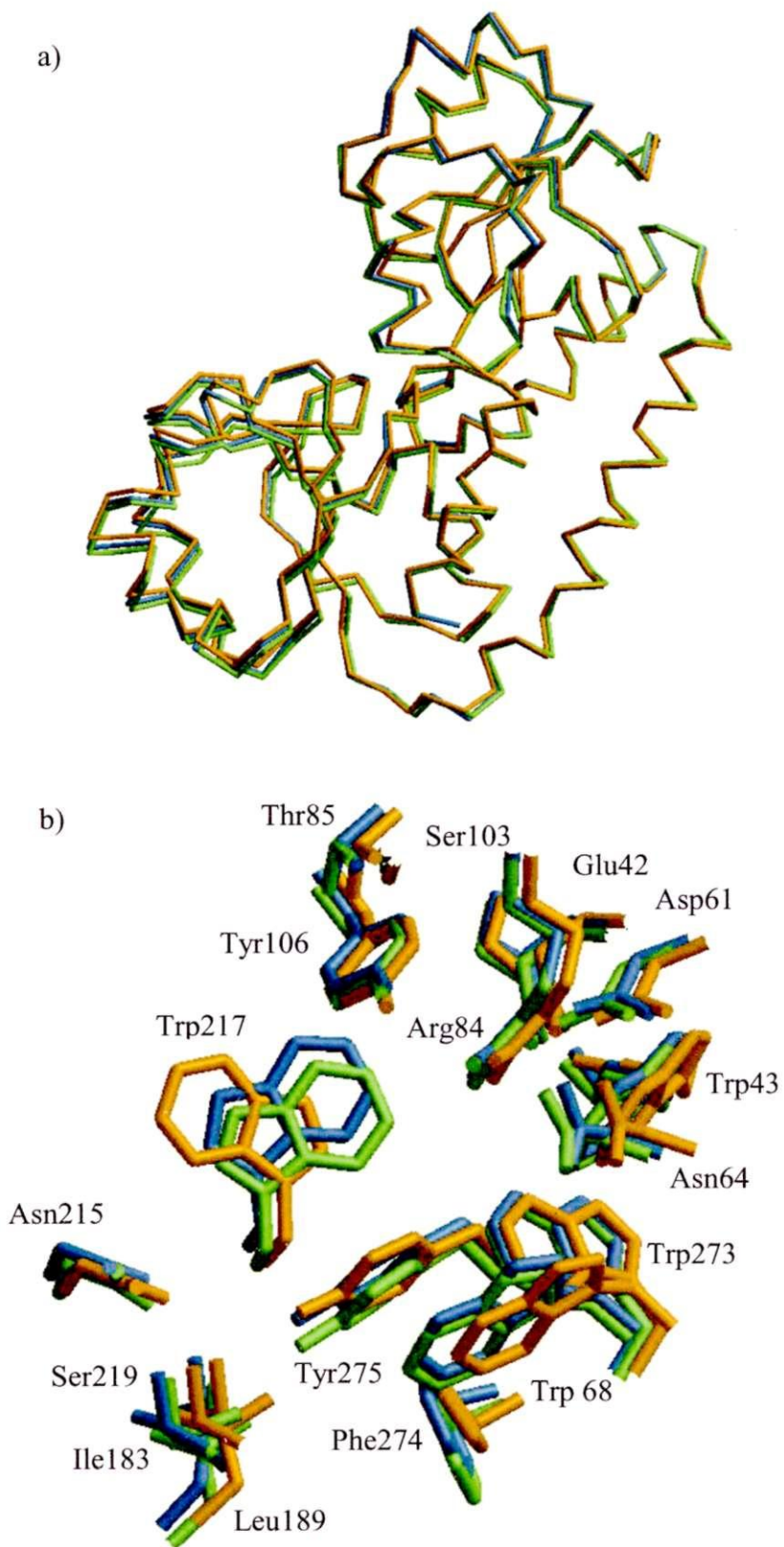


Fig. 3.5 (previous page) Comparison of the conformations of the FhuD structures in each complex. The overlay of the C_α backbone of the FhuD siderophore complexes is shown in a), while the overlay of the side chain residues in the binding pocket is shown in b). The backbone and side chain residues for the albomycin complex are coloured green, the backbone and side chain residues for the coprogen complex are orange and the backbone and side chain residues for the Desferal® complex are blue. These figures were drawn using Setor (Evans, 1993).

Siderophore binding. The ligand binding site of FhuD is lined with hydrophobic residues, forming a hollow large enough to accommodate the hydroxamate portion of each of the siderophores. Hydrogen bonds between several residues in the binding site and the siderophore also play a key role in stabilizing the complex. However, small differences in the position of the amino acid side chains help to accommodate the various ligands.

When albomycin binds (Figure 3.4a), the tri-8-A[^]-hydroxy-8-A[^]-acetyl-L-ornithine peptide which coordinates the ferric iron is found in a similar orientation to gallichrome. The coordination geometry around the iron atom is slightly distorted from octahedral symmetry with distances ranging from 2.08 to 2.43 Å from the oxygen atoms to the metal ion. Three hydrogen bonds form between the protein and the ligand; two from the carbonyl oxygens of the siderophore to the nitrogen atoms of Arg84 and another from the remaining carbonyl oxygen to the oxygen atom of Tyr106, similar to the interactions found with gallichrome. However, the water mediated hydrogen bond present in gallichrome between the peptide backbone of the siderophore and the protein is not found with albomycin. Hydrophobic aromatic residues lining the binding pocket, surrounding the siderophore, are in a similar position to gallichrome. Unfortunately, there is no electron density for the thioribosyl pyrimidine antibiotic group, which is covalently attached to the peptide portion of the siderophore by an amino acetyl linker. This may be because this group is free to move in the crystal structure.

Unlike gallichrome and albomycin, coprogen is a linear chain of three N⁻-hydroxy-

N -acylated ornithines. In this siderophore, two amino acids join to form a diketopiperazine ring, while the third is attached by an ester linkage. Two *trans*-anhydromevalonic acid groups are attached to either end of the molecule. Coprogen binds to FhuD in a slightly different orientation than gallichrome and albomycin (Figure 3.4b). The iron atom is in the same place but the hydroxamic acid moieties are rotated a few degrees clockwise from those of gallichrome. The oxygen atoms coordinating the iron atom are distorted from octahedral symmetry, with distances ranging from 1.98 to 2.05 Å. Within the iron center, one hydrogen bond is formed between the carbonyl oxygen opposite to the diketopiperazine ring and a nitrogen atom of Arg84. The oxygen atom of Tyr106 makes a hydrogen bond to the other carbonyl oxygens on the side of the ring system and a water mediated hydrogen bond to Tyr275 is formed with the remaining carbonyl oxygen. In addition, water mediated hydrogen bonds form between a nitroxyl oxygen of the coordinating group of the siderophore and an oxygen of the peptide backbone of the siderophore to Ser219, which in turn hydrogen bonds to Asn215. The positions of most of hydrophobic residues within the binding site shift slightly, compared to the FhuD gallichrome complex, but the most dramatic change in position involves the reorientation of Trp217. This movement allows the *trans*-anhydromevalonic acid group to insert into the center of the protein. The oxygen atom on the end of this group forms a hydrogen bond with Ser103, as well as a water mediated hydrogen bond to Trp217 and the carbonyl of the peptide backbone of Ala104, stabilizing the complex. Another hydrogen bond forms between Ser103 and Glu42, which bonds to the nitrogen of the peptide bond of Leu44 and has water-mediated hydrogen bonds to the side chain of Trp273 and the carbonyl of the peptide bond of Tyr275. The other *trans*-anhydromevalonic acid group is hydrogen bonded to Asn64 through a water molecule. Since the methyl group is missing in the structure, it may be possibly due to movement in the crystal, as indicated by increased temperature factors in this area.

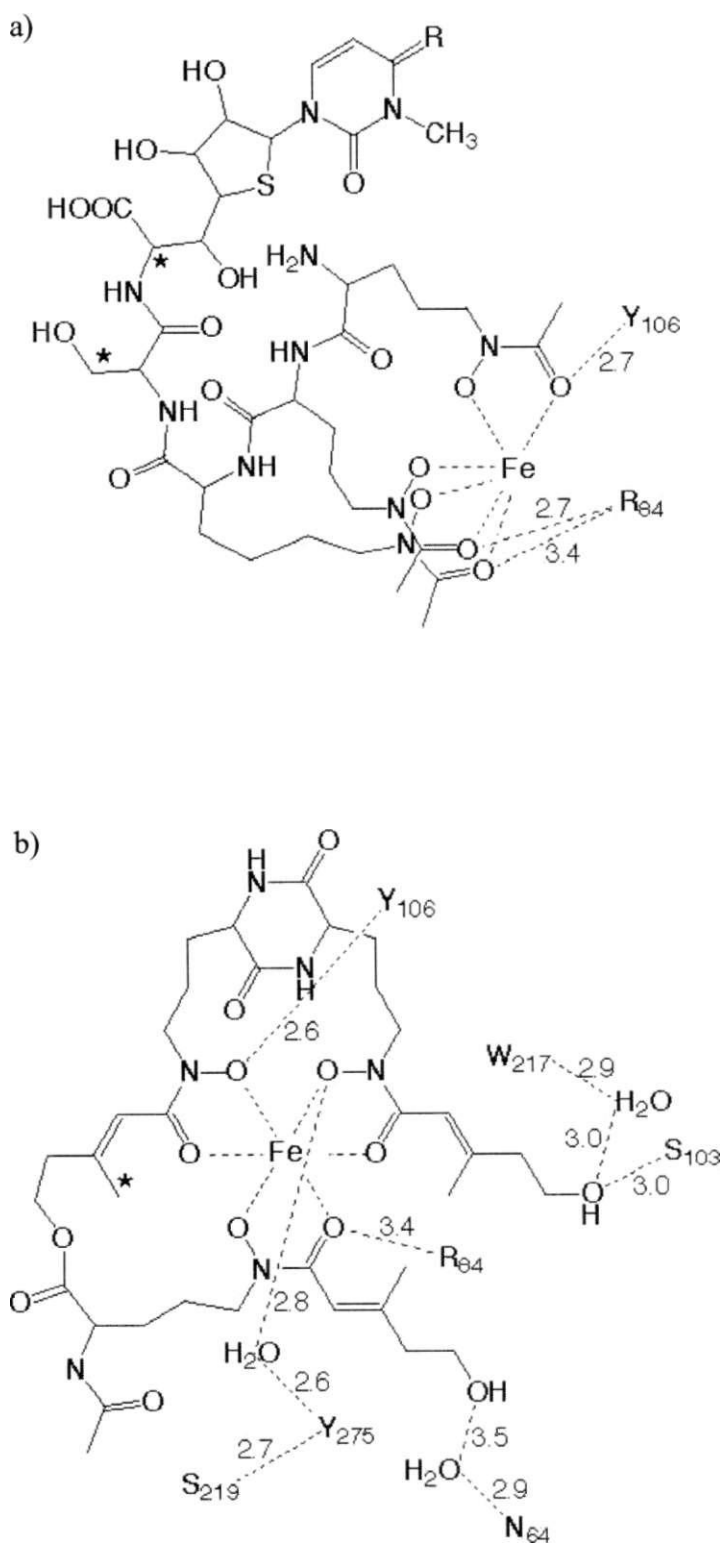
Desferal® has a very high affinity for Fe³⁺ ($K_D = 10^{-31}$ M) and is used to treat iron overload in thalassemia and transfusion patients (Ftershko, 1992) and has been shown to retard progressive neurological degeneration in Alzheimer's patients (McLachlan *et al*,

1991). In the body, it can remove iron from the C-terminus of human skeletal transferrin (Flajtan and Chasteen, 1982) and *E.coli* can utilize iron loaded Desferal® as an iron source. Desferal® binds to FhuD with the ferrioxamine portion of the drug enveloped by the binding site to a greater extent than the other siderophores (Figure 3.4c). This may be due to the absence of bulky functional groups on the peptide backbone, so the smaller size can be accommodated. Coordination of the iron atom is slightly distorted, with distances to the oxygen atoms ranging from 1.95 to 2.00 Å. One carbonyl atom is hydrogen bonded to Arg84, with another carbonyl atom sharing a hydrogen bond with Tyr106. Unlike the other siderophores, the third carbonyl oxygen does not appear to have any hydrogen bonds to the protein. There are two additional hydrogen bonds to the peptide backbone of the ligand; one from a nitrogen to Tyr275 and another from an oxygen via a water molecule to Asp61. The orientation and position of the hydrophobic residues lining the binding pocket are similar to that of gallichrome and albomycin. Since the electron density for the mesylate (OSO₂CH₃) portion of the molecule is not present in this model, it could be mobile in the crystal.

Comparison of the binding mode. An overlay of the binding site residues in each of the FhuD complexes shows that many of the side chains are in a similar position for siderophore binding, with the exception of Trp217 (Figure 3.5b). Since there is very little movement of the side chains, the shape of the binding site is very similar for each siderophore. The hydrogen bonds formed between each siderophore and the side chain residues of FhuD vary in length and number (Figure 3.6). In addition, not all of the hydrogen bonds are to similar oxygens of the iron coordinating region of the siderophore. The number of hydrogen bonds to each siderophore also appears to be related to the relative affinity of FhuD for each siderophore. For example, there are more hydrogen bonds between FhuD and coprogen than there are for ferrichrome and the binding constant for coprogen (0.3 pM) is lower than that for ferrichrome (1.0 pM) (Rohrbach *et al.*, 1995).

A comparison between the binding modes of the outer membrane receptor FhuA

and the periplasmic protein FhuD for albomycin is shown in Figure 3.7. The interactions between the atoms of the ornithine backbone and iron coordination center of the extended conformation of albomycin in FhuA (Ferguson *et al*, 2000) are more numerous and involve more of the molecule compared to the interactions found in FhuD. The orientation of the coordinating Arg and Tyr residues in FhuA is not the same as in FhuD, and contacts form between different oxygens of the coordination sphere of the siderophore. As well, FhuA uses an additional Tyr side chain as well as a Trp and the backbone carbonyl of a Phe to hydrogen bond to the hydroxamate portion of the siderophore.



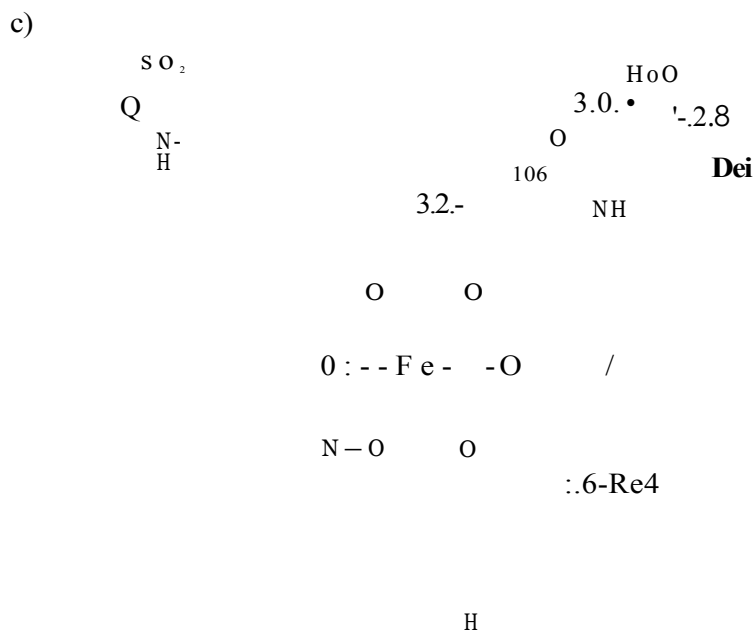


Fig. 3.6 A schematic comparison of the hydrogen bonding between the various siderophores and FhuD. The chemical structures of a) albomycin, b) coprogen, and c) Desferal® are shown with FhuD side chain residues, with interactions indicated by dotted lines (distances indicated). The * indicates the portion of the molecule for which the electron density was missing.

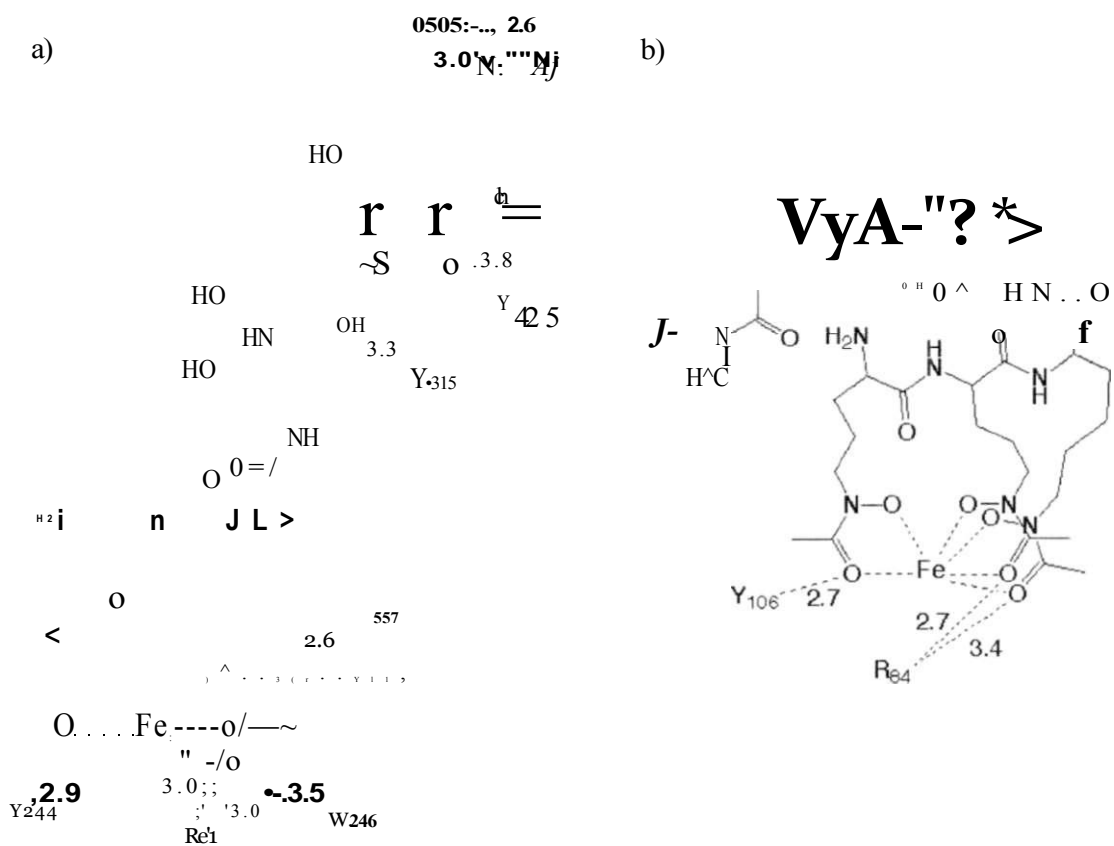


Fig. 3.7 A comparison of the binding modes of albomycin in a) the outer membrane receptor FhuA and b) the periplasmic protein FhuD. The hydrogen bonds from the side chain residues to the chemical structures are shown. The * indicates the portion of the molecule for which the electron density was missing.

Discussion.

High affinity uptake of ferric siderophores in bacteria is aided by specific interactions with proteins along the uptake pathway. Although distinct receptors exist in the outer membrane to extract various siderophores from the environment, it has proven evolutionarily advantageous to utilize a common ABC transport system that recognizes a certain class of siderophore to transport the siderophore from the periplasm through the inner membrane. Although the periplasmic protein FhuD is known to bind a number of hydroxamate-type ferric siderophores with high affinity, as seen from the crystal structures of several of these complexes, there are few limitations on the variety of hydroxamate-type siderophores it could accommodate.

Recognition of hydroxamate-type ferric siderophores by FhuD. The periplasmic binding protein FhuD appears to bind various hydroxamate-type siderophores with a similar binding mode. Many of the interactions between the siderophore and protein are contained within the iron coordinating components of the siderophore. These are mediated by a few hydrogen bonds with key amino acid residues in the binding pocket, namely Arg84 and Tyr106. Slight movement of these key residues involved in hydrogen binding permit a variety of different structures to bind. These hydrogen bonds are present for specificity and directing the siderophore into the binding site for correct fit.

It is interesting to note that FhuD can bind different geometrical isomers of the hydroxamate-type siderophore family. Ferrichromes crystallize in a A-cis coordination geometry (van der Helm *et al.*, 1980), coprogen forms a A-trans geometry (Hossain *et al.*, 1987) and ferriferrioxamines can form racemic mixtures of A-cis and A-cis geometry (Raymond and Carrano, 1979). When bound to FhuD, ferrichrome, albomycin and Desferal® crystallize as the A-cis complex and coprogen forms the A-cis configuration. The large size and malleable shape of the binding site in FhuD allows either stereoisomer to bind.

Since the charge of the residues surrounding the binding site is predominantly negative, the uncharged hydroxamic-type siderophores would not be unable to bind like the negatively charged catechol-type siderophores (Clarke *et al*, 2000). Since Desferal® could have a negative charge on the sulfate group, this drug has a decreased affinity for FhuD (36 pM) (Rohrbach *et al*, 1995a). Aromatic residues lining the binding pocket stack around the siderophore, providing a non-polar environment the correct size and shape for the ligand. In FhuD, the position of aromatic groups, in particular the re-orientation of Trp217, appear to be the defining factor for allowing various siderophores to bind.

Albomycin binding appears to be less specific in the periplasmic protein FhuD than in the receptor FhuA. There are many more interactions between the thioribosyl ring and the outer membrane receptor protein than in the periplasmic binding protein (Figure 3.7). In FhuA, the flexible amino acetyl linker group allows albomycin to be found in both a compact and an extended conformation (Ferguson *et al*, 2000). However, in the FhuD albomycin crystal structure, the thioribosyl moiety is solvent exposed and not visible in the electron density map. Likely, the antibiotic portion adopts a great number of conformations in the crystal structure of the FhuD albomycin complex, due to the flexibility in the linker region, thus static electron density cannot be defined.

There are interesting parallels in the binding of coprogen and Desferal® to FhuD compared to the binding of ferrichrome and albomycin. Coprogen, first isolated from *Neurospora crassa* (Atkin and Neilands, 1968), has a unique diketopiperazine ring not found in the other siderophores. However, the general shape of iron bound coprogen is very similar to linear ferrioxamines, especially in the orientation of the peptide backbone around the iron centre (Hossain *et al*, 1987). The two loops of peptide backbone in each of these structures are positioned in the binding site perpendicularly to the peptide backbone of ferrichrome and albomycin. In this way, the solvent exposure of the peptide backbone is reduced, although the number of hydrogen bonds between the siderophore and FhuD is not increased. The unusual insertion of the α -carboxyanhydromevalonic acid group of coprogen into the interior of FhuD suggests that this functional group may be important for

recognition by the proteins of the coprogen uptake pathway. FhuD may recognize other hydroxamate-type siderophores such as aerobactin and rhodoturulate in a similar manner. FhuD seems to recognize the hydroxamic acid groups coordinating the iron centre of hydroxamate-type siderophores.

Relation to other periplasmic ligand binding proteins. Although the overall structure of FhuD is distinctive for a periplasmic ligand binding protein, the characteristics of the binding pocket and binding mode of the ligands is not uncommon. Most periplasmic proteins from ABC transport systems form two domains, connected by several p-strands, with the binding pocket located in a deep cleft between these two domains. However, the binding pocket is larger and shallower in FhuD than in other periplasmic ligand binding proteins. This could be due to the larger size of the siderophore compared to some of the other types of nutrients transported into the cell.

Hydrogen bonding between the binding protein and ligand are common. Hydrogen bonds are more directional than dispersion forces and are of sufficiently low strength to allow fast ligand dissociation (Quioco, 1990; Quioco and Ledvina, 1996). Stacked aromatic residues lining the binding pocket are also found in other periplasmic proteins which bind amino acids and sugars (Quioco and Ledvina, 1996; Quioco, 1990).

Other ferric siderophore binding proteins may have a similar structure to FhuD to make up a distinct class of ligand binding proteins. Although most of these proteins share little sequence homology (Koster W, 1991; Tarn and Saier, Jr., 1993), previous secondary structure analysis (Clarke *et al.*, 2000) suggests that the *E. coli* periplasmic proteins FepB and FecB could possess a long α -helix in the middle of their sequence. Identification of the key residues involved in ligand binding would be difficult as many of the residues belong to different sections of the polypeptide chain. However, several characteristics could be retained, including hydrophobicity and hydrogen bonding potential. When charged ligands are bound, complimentary charges would also exist in the binding site.

Proposed mechanism for ferric siderophore transport. Once the ferric siderophore has passed through the outer membrane receptor, it is transferred to the periplasmic protein. However, there is no evidence that the periplasmic protein FhuD actually interacts with the outer membrane receptor FhuA. Presumably, the high affinity of the periplasmic protein for ferric siderophores is sufficient for sequestering the ligand and transporting it to the inner membrane associated proteins. Rearrangement of the hydrogen bonding and aromatic residues lining the binding pocket occurs in order to accommodate the siderophore; this is likely accompanied by a conformational change in the protein structure. Recognition of the holo form of FhuD by the inner membrane associated complex would also be aided by change in conformation. Release of the ligand to the inner membrane associated proteins would involve breaking the hydrogen bonds between the ligand and periplasmic protein.

Several periplasmic ligand binding proteins have been found to exist in an open apo form and as a closed holo form. Small changes in the P-strands connecting the two domains allow this conformational change to occur. However, the long α -helix in FhuD may preclude a significant conformational change. Since there are different crystal conditions for the apo form and dynamic light scattering shows very small differences in the hydrodynamic radius of the two forms of the protein (unpublished results), there may be some flexibility in the structure. Since the structure of holo FhuD does not immediately suggest a mechanism by which domain opening could occur, we can only postulate where the hinge would be located.

Rational design of siderophore-antibiotic conjugates. This type of analysis of the factors involved in recognition of siderophores by the outer membrane receptors and ABC transport proteins aids in the rational design of siderophore-antibiotic conjugates. For hydroxamate-type siderophore uptake systems, it appears that the common structural basis for ligand recognition is the iron coordination moieties. In lieu of structures of the entire repertoire of outer membrane receptors in *E. coli*, the structures of the FhuD complexes show that the mode of binding hydroxamate-type siderophores, including those not in the

ferrichrome family, is very similar. Of course, the outer membrane receptor makes more specific contacts to the siderophore and is more spatially restrictive, but it appears that a variety of structures can be accommodated in the receptor binding site (Ferguson *et al*, 1998; Locher *et al*, 1998; Ferguson *et al*, 2000). Requirements of the periplasmic binding protein for transport are less confining and the vast amount of solvent exposed regions of the siderophore may be a good target for antibiotic conjugation. Similarly, in other iron transport systems, it also seems that it is the iron chelating component of the siderophore which is recognized by the uptake proteins. In the crystal structure of the outer membrane receptor FepA, the putative enterobactin binding site shows possible interactions with the iron centre (Buchanan *et al*, 1999).

Chapter 4

Ferric Hydroxamate Binding Protein FhuD: Mutants in Conserved and Non-conserved Regions

Uptake of iron complexes into the bacterial cell requires an outer membrane receptor and an ATP-dependent transport system involving a periplasmic protein and several inner membrane associated proteins. To date, there is little structural information about the components of ATP-dependent (ABC) transport systems involved in iron complex transport. The recently determined structure of the *Escherichia coli* periplasmic ferric siderophore binding protein FhuD is unique for an ABC transport system (Clarke *et al*, 2000). Unlike other periplasmic binding proteins, FhuD has two domains connected by a long α -helix. The ligand binds in a shallow pocket between the two domains. *In vivo* and *in vitro* analysis of single amino acid mutants of FhuD identified several residues that are important for proper functioning of the protein (performed by Dr. M. Rohrbach and Dr. W. Koster, Swiss Federal Institute for Environmental Science and Technology, Switzerland). In this study, the mutated residues were mapped to the protein structure to define special areas and specific amino acid residues in *E. coli* FhuD that are vital for correct protein function. A number of these important residues are found to be conserved in the multiple alignment of *E. coli* FhuD with other periplasmic binding proteins that transport other siderophores, heme, and vitamin B12. The alignment and structure prediction of the siderophore binding family of proteins indicate that these proteins form a distinct family, different from most other periplasmic proteins.

Introduction.

Iron is an essential nutrient for most living bacteria. Moreover, it has been shown for a number of bacterial pathogens that iron sufficiency contributes to their virulence (Cox, 1982; Payne, 1988, 1993; Byers and Arceneaux, 1998), yet little is known about bacterial iron transport mechanisms at the molecular level. Since the bioavailability of iron is very low, bacteria have developed a number of strategies to procure iron from their environment. The import of ferrous iron, ferric iron in its ionic form and of ferric iron coupled to siderophores or heme is mediated by specific TonB energy-dependent outer membrane receptors, and subsequently by an ATP-dependent (ABC) transport system (Braun, 1998; Braun and Killmann, 1999; Schryvers and Stojiljkovic, 1999; Vasil and Ochsner, 1999; Ratledge and Dover, 2000; Wandersman and Stojiljkovic, 2000). The ABC transport systems consist of a periplasmic binding protein and two inner membrane associated proteins; a transporter coupled with an ATP-hydrolyzing protein.

Although a specific bacterial strain may produce only a few types of siderophores, uptake systems for several different siderophores may be expressed. For example, hydroxamate type siderophores (i.e. ferrichrome, aerobactin and coprogen) have individual receptors on the outer membrane of *Escherichia coli*. The structure of the ferrichrome outer membrane transport protein FhuA reveals that its N-terminal domain forms a plug inside the 22-strand (3-barrel (Ferguson *et al*, 1998; Locher *et al*, 1998), similar to the enterobactin outer membrane receptor FepA (Buchanan *et al*, 1999). The ferrichrome and the structurally related antibiotic albomycin nestle in a hydrophobic binding pocket, stabilized by several hydrogen bonds (Ferguson *et al*, 1998; 2000b). Uptake of ferric hydroxamates across the periplasm and inner membrane is mediated by the common *fhu* system. FhuD, the periplasmic binding protein, accepts a number of structurally different siderophores as ligands and transports them to the inner membrane components FhuB and FhuC. The structure of FhuD forms two distinct domains linked by a long α -helix (Clarke *et al*, 2000). The ligand binding pocket lies in a shallow groove between these two domains and slight movements of the amino acid side chains allow a variety of hydroxamate type siderophores to bind. Although there are no crystallographic structures

of the inner membrane associated proteins, peptide mapping studies of FhuB suggest that several external loops may exist that are important for physical interaction with FhuD (Bohm *et al*, 1996; Mademidis *et al*, 1997).

Periplasmic proteins of the ABC system can be grouped into distinct classes based on similarities in primary sequence (Tarn and Saier, Jr., 1993). The siderophore binding proteins are grouped in a different class than other ligand binding proteins involved in the uptake of other essential nutrients. In general, the different classes of periplasmic proteins of ABC transport systems share relatively little sequence homology and recognize diverse ligands, however, most are closely related in structure (Quiocho and Ledvina, 1996). Many consist of two globular domains connected by short stretches of polypeptide chain. Each lobe consists of a central β -sheet surrounded by α -helices and molecular recognition of ligands arises from slight differences in the number and arrangement of the β -strands and α -helices in the two globular domains. As a result of the differences in domain structure and sequence of the periplasmic receptors, the structure of the binding site is highly variable. In most periplasmic proteins, crossovers of the polypeptide chain between the two domains form the hinge region and the base of the binding cleft. Closure around the substrate in the deep binding cleft formed by the two domains is suggestive of a "Venus fly trap" or "Pac-man" motion (Mao *et al*, 1982; Ames, 1986). This mode of binding allows many interactions to form between the protein and substrate, increasing ligand specificity. The variations between the structures of the prototypical periplasmic binding protein and the *E. coli* periplasmic ferric siderophore binding protein FhuD reveal that different periplasmic ligand binding proteins may exercise distinct mechanisms for ligand binding and release. Since the structure of FhuD is atypical for a periplasmic protein, larger ligands such as ferric siderophores may require a different structure. The specificity of periplasmic ferric siderophore binding proteins is also broader, compared to other periplasmic ligand binding proteins, so the binding pocket is more solvent exposed and some movement of side chains is allowed.

Thus, for the periplasmic ferric siderophore binding family, a distinct structure may be required for function. The use of homology modeling studies, in this case, is limited, since there is relatively little sequence homology between these proteins (< 20%). In lieu of

other structures for this family, we have attempted to identify key residues among these proteins important for function. Point mutations in *E. coli* FhuD have identified key residues important for performance of the protein *in vivo* and *in vitro*. These have been mapped to the three dimensional structure of FhuD to identify disruptions to the secondary and tertiary structure. When these mutations are identified in a sequence alignment of the siderophore binding family of proteins, many are among the conserved residues found in this family. Our data indicates that in the ferric siderophore binding family, there are a number of residues that may play a key role maintaining the overall structures of the proteins.

Results.

Phenotype of the FhuD mutants. The conditions used for the PCR reaction produced a number of *fhuD* mutants with single point mutations in different positions along the polypeptide chain. The change in sequence produced by this method resulted in amino acid conversions that did not necessarily maintain the original properties of the wild type residue. The point mutations to *fhuD* and analysis of the function of the protein made by Drs. Martin Rohrbach and Wolfgang Koster are listed in Table 4.1. Mutated FhuD proteins complemented the mutation in the *fhuD* sequence in *E. coli* K0295 to varying levels. This is indicated by growth on ferrichrome or coprogen as the sole iron source, as well as sensitivity to the antibiotic albomycin (Table 4.1). Degradation of FhuD by proteases has been shown to be prevented or diminished by substrate binding (Koster and Braun, 1990; Rohrbach *et al*, 1995a, b). The amount of proteolysis of the FhuD mutant proteins when substrate is added provides an estimation of the binding properties of the protein (Table 4.1).

Several single mutations to different positions on the polypeptide chain had a large effect on the ability of the protein to grow on ferrichrome or coprogen and have resistance to albomycin. On the other hand, other mutations had little effect on the function of the protein. No mutations were found that enhanced the activity of the protein. There were a number of mutants that were able to resist proteolysis similarly to the wild type protein. However, in some cases, the ability of the mutant to resist proteolytic degradation was diminished or absent.

Many of the mutant FhuD proteins resistant to albomycin also had limited growth on ferrichrome and coprogen in the mutant strain of *E. coli*. This indicates that these proteins have a decreased ability to function *in vivo*. These mutants also tended not to be resistant to proteolysis, so the protein may not be able to bind the ligand in the same manner as the wild type protein. The reverse is true for other mutants since mutant proteins that complemented the *fhuD E. coli* mutant seem to be more resistant to proteolysis. There are also several mutant proteins that did not follow this trend. These mutant proteins did not function *in vivo* but were able to resist proteolysis *in vitro*.

Methods.

Construction of the FhuD mutants. By varying the conditions for the polymerase chain reaction, the *fhuD* gene was amplified according to the procedure outlined by Rohrbach *et al.* (1995a), thereby introducing point mutations at various sites. The sequences of the *fhuD* mutants were determined by the dideoxy method as previously described (Rohrbach *et al.*, 1995a). FhuD mutants were expressed and purified as previously described (Rohrbach *et al.*, 1995a, b).

Functional analysis of the FhuD mutants. The mutant plasmids were introduced into a *fhuD E. coli* K0295 mutant strain, then after protein expression, sensitivity to albomycin and growth on ferrichrome or coprogen as the sole iron source was tested (Rohrbach *et al.*, 1995a,b). The resulting FhuD mutants were analyzed with respect to processing and stability in a protease protection assay as previously described (Koster and Braun, 1990; Rohrbach *et al.*, 1995b).

Identification of the locations of point mutations in FhuD. The locations of each of the point mutations in FhuD were identified in the x-ray crystal structure (Protein Data Bank accession code 1EFD (Clarke *et al.*, 2000)) with respect to their location in the secondary and tertiary structure. The point mutations were colour coded according to the severity of the effect on the function of the protein in the functional assays and classified into regions of the proteins that are important for function.

Sequence analysis and multiple alignments. Sequence similarity searches to *E. coli* were initiated by the BLAST search tool at the NCBI web site (www.ncbi.nlm.nih.gov) (Altschul *et al.*, 1997). The evolutionary tree was produced by the NJ method from a distance matrix based on a multiple alignment obtained with CLUSTAL-X (Thompson *et al.*, 1997).

Results.

Phenotype of the FhuD mutants. The conditions used for the PCR reaction produced a number of *fhuD* mutants with single point mutations in different positions along the polypeptide chain. The change in sequence produced by this method resulted in amino acid conversions that did not necessarily maintain the original properties of the wild type residue. The point mutations to *fhuD* and analysis of the function of the protein made by Drs. Martin Rohrbach and Wolfgang Koster are listed in Table 4.1. Mutated FhuD proteins complemented the mutation in the *fhuD* sequence in *E. coli* K0295 to varying levels. This is indicated by growth on ferrichrome or coprogen as the sole iron source, as well as sensitivity to the antibiotic albomycin (Table 4.1). Degradation of FhuD by proteases has been shown to be prevented or diminished by substrate binding (Koster and Braun, 1990; Rohrbach *et al*, 1995a, b). The amount of proteolysis of the FhuD mutant proteins when substrate is added provides an estimation of the binding properties of the protein (Table 4.1).

Several single mutations to different positions on the polypeptide chain had a large effect on the ability of the protein to grow on ferrichrome or coprogen and have resistance to albomycin. On the other hand, other mutations had little effect on the function of the protein. No mutations were found that enhanced the activity of the protein. There were a number of mutants that were able to resist proteolysis similarly to the wild type protein. However, in some cases, the ability of the mutant to resist proteolytic degradation was diminished or absent.

Many of the mutant FhuD proteins resistant to albomycin also had limited growth on ferrichrome and coprogen in the mutant strain of *E. coli*. This indicates that these proteins have a decreased ability to function *in vivo*. These mutants also tended not to be resistant to proteolysis, so the protein may not be able to bind the ligand in the same manner as the wild type protein. The reverse is true for other mutants since mutant proteins that complemented the *fhuD E. coli* mutant seem to be more resistant to proteolysis. There are also several mutant proteins that did not follow this trend. These mutant proteins did not function *in vivo* but were able to resist proteolysis *in vitro*.

Table 4.1 Phenotype of FhuD mutants

Site of mutation	Sensitivity to albomycin ³	Growth on ferrichrome or coprogen ^b	Protease protection ^o
T181A	(S)	++++	n.d.
F274L	S	++++	n.d.
W68L	R	cop»fer	no
Y65C	R	++	n.d.
I183T	S	++++	n.d.
N242S	(R)	+++++	reduced
V39A	R	+	no
T93N	(R)	++++	n.d.
F99S	R	+++	yes
E213G	(R)	+++	yes
W210R	(S)	+++++	n.d.
D234G	S	+++++	n.d.
L236P	(R)	+++	no
M258V	(S)	+++++	n.d.
F124L	R	+++	yes
F161L	R	++	no
S149G	(R)	++++	yes
N146D	(S)	+++++	n.d.
F169L	(R)	yes

³Degrees of sensitivity: S > (S) > (R) > R (S, sensitive; R, resistant).

^bThe number of crosses reflects the degree of growth promotion (+++++, like wild type).

^on.d., not determined.

Location of the point mutations in the crystal structure of FhuD. The point mutations were fairly evenly distributed in the crystal structure of FhuD (Figure 4.1). In this study, any single residue could be mutated with a resulting full-length stable protein. The mutations to the protein are localized to four different regions; the binding site, the N-domain, the C-domain and the α -helix connecting the two domains (Table 4.2).

The majority of the mutations localized in the binding site had a large effect on the function of the protein. Although the residues that were mutated are not those implicated in hydrogen binding various ferric hydroxamates (Clarke *et al.*, 2000), many of these residues line the binding pocket, forming a surface complimentary to the ligand. W68L and I183T are mutations to important residues for van der Waals interactions between FhuD and the siderophore. Since they stack close to the ligand, there is a large effect on the function of the protein when these residues are mutated. Although the mutations F274L and T181A are not immediately in the vicinity of the binding site, these amino acids are important for maintaining the structural integrity of the stacking interactions between the side chains. Mutations to these residues clearly affect protein function. The mutation N242S is located on a loop near the binding site, not directly involved in forming the binding pocket, so this mutation is tolerated well during protein function.

Mutations in either domain of the protein have a range of effects on the function of the protein in the assays. The mutations in the N-domain localized on the exterior of the protein, T93N and F99S, seem to have only limited effect on the function of the protein. The mutation V39A, which has a large effect on the function of the protein, is located between P-strands in the interior of the N-domain, and may destabilize the secondary structure. In the C-domain, the mutation E213G removes the charge and bulk of a surface exposed side chain, affecting the function of the protein *in vivo* but retaining the ability to protect the protein from proteolysis. The side chains of the mutations W210R and D234G do not significantly affect the formation of P-sheets in the interior of the C-domain, hence the protein function is similar. The mutation L236P is part of a β -strand in the C-domain and the substitution to proline may disrupt the formation of this secondary structure. The mutation M258V is located on a helix on the exterior of the C-domain, with the side chain pointing towards the interior of the protein.

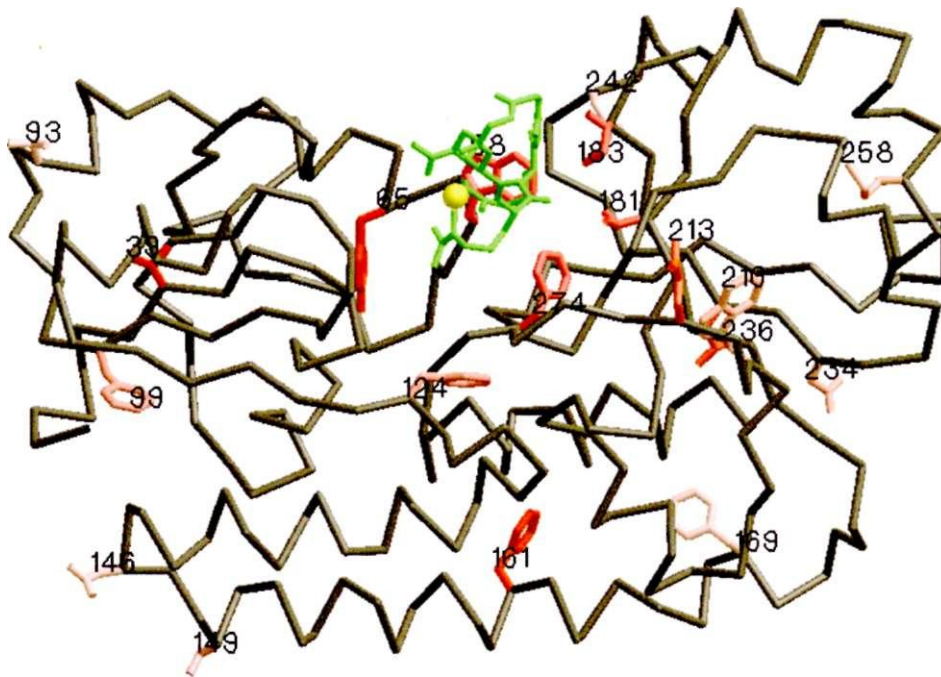


Fig. 4.1 Map of the mutations on the structure of the FhuD gallichrome complex. This is a backbone trace of the protein complex showing the location of mutated residues in the FhuD structure. The side chains of the residues are colour coded, with red residues having a large effect on function *in vivo* and *in vitro* and lighter pink residues having less effect. This figure was created with Setor (Evans, 1993).

Table 4.2 Location of FhuD mutant residues

Site of mutation ¹	Location	Possible effects on the protein structure
T181A	binding site	interactions with peptide backbone of albomycin, ferrichrome and coprogen
F274L	binding site	a hydrophobic group lining the binding pocket
W68L	binding site	a hydrophobic group lining the binding pocket; slight movement when coprogen is bound
Y65C	binding site	a hydrophobic group lining the binding pocket
I183T	binding site	contributes to the shape of the binding site
N242S	loop near binding site	side chain points into the C-domain
V39A	N domain	between α -strands in the interior of the domain
T93N	N domain	surface exposed side chain
F99S	N domain	important in domain packing
E213G	C domain	surface exposed side chain; charge important
W210R	C domain	between (3-strands in the interior of the domain
D234G	C domain	between (3-strands in the interior of the domain
L236P	C domain	part of a (3-strand; the substituted proline could interfere with forming secondary structure
M258V	C domain	within the interior of the domain
F124L	interface between domains	hydrophobic interactions are important between the domains
F161L	centre of connecting helix	hydrophobic contacts between the helix and domains and between domains are present and could be important for stability
S149G	end of connecting helix	surface exposed side chain
N146D	end of connecting helix	surface exposed side chain
F169L	end of connecting helix	side chain interacts with the C-domain

¹in addition to these single mutations, many multiple mutations of FhuD were also analyzed. These are not listed here, as their activity, in terms of the effects to the structure of FhuD is difficult to interpret.

Mutation of this residue to a smaller side chain does not significantly affect the function of the protein to a large extent. The mutation F124L is localized in the base of the binding site, at the interface between the two domains and mutation of this residue has little effect on the function of the protein.

The effect of mutations on the function of the protein along the α -helix connecting the two domains increases as the center of the helix is reached. The mutants N146D, S149G and F169L are located on either end of the helix, having little effect on the function of the protein. However, F161L, is near the center and the side chain interacts with the C-domain, having a dramatic effect on the function of the protein.

Evolutionary relationships. The overall structure and the organization of the *E. coli* FhuD polypeptide chain are different from other known periplasmic binding proteins from ABC transporters. A phylogenetic tree of the periplasmic binding proteins from different bacteria done by Dr. Wolfgang Koster is shown in Figure 4.2. An initial multiple alignment was used as a guide to identify related proteins and develop the family phylogeny. 47 genes were identified in a variety of bacterial species to be involved with the transport of siderophores, heme or vitamin B12. The periplasmic proteins are variable in size, between 25 and 40 kDa. With analysis of only the sequence of some of these proteins, we cannot absolutely cluster them according to their function. There seems to be a common ancestral root and these periplasmic proteins likely make up a large family of binding proteins. There appears to be four distinct subfamilies of three members or more, which includes 23 of the proteins. *E. coli* FhuD is grouped with other FhuD proteins from *Rhizobia sp.*, which are also predicted to bind hydroxamate-type ferric siderophores. Although the remaining members of the family are clearly related, sequence analysis of these proteins provided no evidence that the group could be further subdivided.

Conserved sequence patterns. Analysis of a multiple alignment of the primary sequence of the periplasmic siderophore binding family reveals a number of residues that are conserved (Figure 4.3). There appears to be more sequence conservation in the N-domain region than in the C-domain region. Regions of similar sequence are also conserved in both halves of

the protein. There are a high number of charged residues and proline residues conserved in both domains in the family.

Many of the mutated residues, which were found to be important for the function of *E. coli* FhuD, are conserved in this family. The residues found in the binding site of FhuD are from different sections of the polypeptide chain but tend to be aromatic residues. The residues mutated in the binding site in this study do not appear to be highly conserved amongst the family. However, other residues found lining the binding pocket of *E. coli* FhuD, in particular Glu42, Trp43, Asp61 and Trp217, are conserved in the group. Residues found to form hydrogen bonds between FhuD and its ligands, which include Arg84 and Tyr106, can be found in the other proteins. Interestingly, the positively charged guanidine group from Arg84 is converted to a negatively charged glutamic acid in some proteins. The residues that are found to be important for function in the N- and C-domains also tend to appear in some of the other proteins in the family. The residues found in the connecting helix between the two domains do not seem to be conserved.

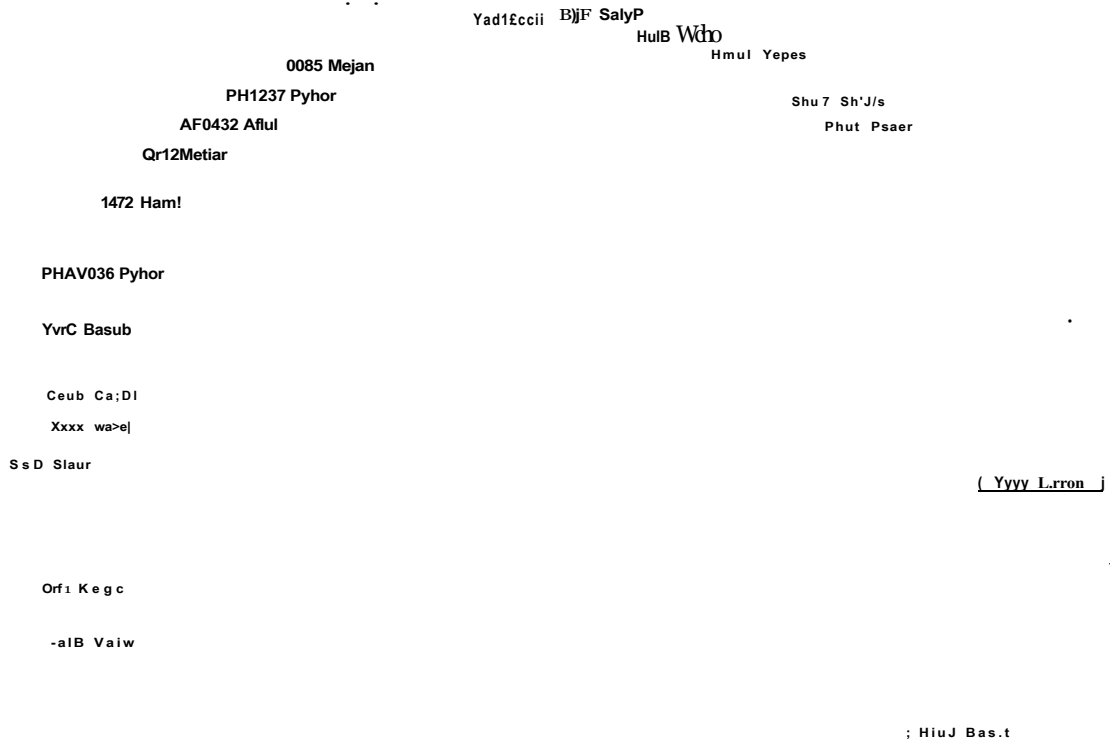


Fig. 42 An unrooted evolutionary tree of the periplasmic ferric siderophore binding proteins from different bacteria. The alignment and phylogenetic analysis was performed with CLUSTAL-X and the tree is drawn with NJPlot (Thompson *et al.*, 1997).

Doma in	N	C
Structure	_HHHHHHH SSSSSS_____S_HHHHHHH_SSSSSS_	
FhuD_Ecoli	87	PNLELLTEMKPSFMVWSAGYG-22 3 VSIDRLAAYKDVDVLCFDHDN-
FhuD_Rhleg		VNFEILVTLKPDIVLTTPLYD_____GIEDLSKITDPDARLIAFDPV-
FhuD_Rhcap		PSLETLALAAPDLILSSSYYS_____VPLERLA-DFPTARIVLTGEI-
0872_Mejan		VNYELIVNLTDPDIVFLGDWKS_____KTKEDLLKINPNFAEFKAFKT-
Yyyy_Limon		PSIEKIANLKPDL11IS-DYQ_____ETKAISSEALPEYAAGADRLF-
YxeB_Basub		ISVBKVMELQPD LIVUM-NEE_____EMKQLSQEVIPEYAADYMFIT-
FhuD_Basub		TSVEKVIDIiNPDLI IVWTTQG_____GYTSSISLEKLPDFAGDYIFAG-
FeuA_Basub		PNIEKILEMKPDVILASTKFP_____SSLEKLSEMNPDIHFVQFSDD-
YfiY_Basub		FNVEAIAELKPDLIIGNKVRQ_____TFSTDSKESIPDMADVLFYF-
ChrA_Erchr		PSLEDIVLLKPD AIVASR FRH_____TNKESIPWDADIPFIFLRSE-
SirA_Staur		PNLEEISKLPDLIVASKVRN_____TSKESIFLMNADHIFWKSDP-
slr1319_Sycys		PNLEKIVALOPDLIIGSP.LRQ_____VSFEQIPQMEADALFYFIYTG-
slr1491_Sycys		INLETLAVLQPD LIIGAVWEM_____ISRESMTEADGDVIFLFTFGH-
slr1492_Sycys		PNLEAILGTNPDLIVGLDS-H_____ISREVLEQADGDVIFLWTGEN-
sll1202_Sycys		?S LEGIFKAKPDLIILSFD-HN_____LSLES LPKLNNANS11ILGYN-
YfmC_Basub		PNLEVISSLPDLI IADAERK_____VSLEQLSKIDPDILFISANEG-
YhfQ_Basub		PSMEKI AS LKPD LIADTTRH_____MTLEQLLKTDPDVIILMTGKT-
ViuP_Vicho		VDLESVYVEQPD LIWSMIGA_____IHYEHLTQLQAETTFLITMTD-
FepB_Ecoli		PSAEAVAAQMPDLILISATGG_____LGGENLAAGLNGESLFLFAGD-
FecB_Ecoli		PSLEAIAALKPDLI IADSSRH_____IGLEQLLAVNPAWLLVAHYRE-
FecB_Mytub		PDLRAIAAAHPDLILIGSQGLT_____GTTAADLAKSPDFSAADADIV-
FecB2_Mytub		IQIDRIAALKPDLIVAINAGV_____PEDEKALLADPEIAAS QATAQ-
Irpl_Codip		IPFEQVADTKPD11LATYSGI_____VSTEKPEE FDDVDV IISYSSG-
YvrC_Basub		VN"-/EKVI S LKPDVLVAHE SSM_____MTDEAIVKLNPD AIVTTDGVK-
2480rf2_Stpyo		TDLEAVTTLKPD LIWGS TEE_____GTVLCLKEILPDNIGDYWW-
YclP_Basub		PDFDKVAE LDPDLI IISA-RQ_____VSYEYISKTNPDYLFVIDRGT-
SstD_Staur		VNFDKIAATKPEVIFISG-RT_____VSNEYVNKENPDVILAMDRGQ-
Xxxx_Cajej		VDFEAINALKPDLI IISG-RQ_____INSEFILEKNPDYIFVIDRNI-
CeuE_Cacol		VDFEAINALKPDLI IISG-RQ_____INSEFILEKNPDYLFWDRNI-
FetB_Negon		PDYET LNAYKPQL111GS-RA_____ISFEYLKEKNPDWLFVLD RSA-
FatBViang		PNMEKIYALKPDLVLMTP-LH_____ISSEFINQANPDILYIIDRTA-
ViuP_Vicho		VDLESVYVE QPDL I WSM - IG_____KQVYGLGE NSFRIDL FS ARE I-
SCF34.13c_StCOe		PNFEKIAALRPDLIVAVY - SE_____LS PERVDLVDVDRV FVINDKA-
HP1561_Hepyi		LNVBLLiKKLSPDLWTFV- GN_____ISVEKIVKHNPEIIFIWWIS P-
HP1562_Hepyi		LNVELLKKLGPDLWTFV- GN_____ISVEKIVKENPEIIFIWWISP-
1472_Hainf		VNIESLLALKPDW FVTN-YA_____VSLENVLEWNP AVILVQDRYP-
PHAV036_Pyhor		PNIEVIASLKPDLIIGTS-LH_____VSVEEIVARDPEVIILSQHPG-
PH1237_Pyhor		PNLEAIMKLPDL11FATY- ID_____IDKEILLKWQPEYIFIDEGGL-
AP0432_Arful		PNAEAI VAVKPDVIFACY- ID_____IDKEKLEWDPDIIFLDENNL-
0085_Mejan		PNPEAI IQVKPDVIFVTY-MP_____VTKEQILKWNPD IIFIDEGGL-
Orf2_Mebar		GNYETVIDMHPDIFIESTATN_____VSIEQVMNWNPEVIITSNPQF-
RumB_Momor		FSVEKALTYQPD LVI FDTGQS_____VNEEQIIADPQFYLMTVADW-
Yadt_Ecoll		MNLERIVALKPDLVIAWRG_____VSREQVLARLPQAIIVITGG- P-
BtuF_Satyp		MNLERIVALKPD L WAWRG_____VIREQVLGRHPHAIIVAGK-T-
HmuT_Codip		SSTENVLKDV PWTEGGHN_____ANAEALAKINPEAIIMMTAGL-
HmuT_Yepes		LNAEGLIAMKPTMLLVSE L_____LSQEGVIASAPDLLLITTDGV-
HemT_Yeent		- - - EG I LAMKPTMLLVSE L_____LSQEGVIASAPDLLLITSDGV-
HutB_Vicho		-AAEGLLTLEPTHLIGSDE_____LSMESMIEMQPDMLVLS GRSL-
ShuTShdys		LSSEGILSLRPSVITWQD_____Y SAES LIAANPEVIWTS QMV-
PhuT_Psaer		LAAEGVLALRPDILIGTEE_____IS VEALAAALDPVAWIADRS L -

Fig. 4.3 (previous page) Sequence alignment of the periplasmic ferric siderophore binding protein family. The segments of the N- and C-domains that are the most conserved are shown for clarity. The conserved residues are in bold text. Above the sequence alignment, the secondary structure observed in *E. coli* FhuD is shown.

Discussion.

The striking architecture of the *E. coli* periplasmic ferric siderophore binding protein FhuD compared to other periplasmic proteins immediately suggests that this type of fold is desired for binding iron complexes. The ligand is cradled in a shallow binding pocket between two domains, largely solvent exposed, with many interactions from aromatic residues lining the binding pocket. However, the importance of the long helix connecting the two domains is yet to be elucidated. Identification of regions and specific residues important for the function of the protein is possible by mapping point mutations along the polypeptide chain to the structure of the protein.

Certain regions of *E. coli* FhuD are more sensitive to point mutations than other areas. Mutations in the binding site of the protein alter the function of the protein to a greater extent than mutations in other areas of the protein. Changes to the aromatic groups that line the binding pocket modify the structural complementarity of the protein to the ligand, decreasing the number of favourable interactions. Substitution of long chain amino acids will also sterically hinder ligand binding. Since there is some movement of the side chains when different hydroxamate-type siderophores are bound (see Chapter 3), substitution of side chains will interfere with the dynamic properties of the binding site.

In addition, particular areas of the N- and C-domains, as well as the helix, are important for protein function. In the two domains, these are residues involved in stabilizing the β -sheet central to the structure of the protein. Disruptions to the packing around the sheet by substituting different amino acids influence the hydrogen bonding network found in this area. In the helix area, hydrophobic interactions between the underside of the two domains and the hydrophobic surface of the amphipathic helix stabilize the structure. Hydrophobic groups on one side of the helix stack into the space

between the helix and each of the two domains. A mutation in the centre of the helix, changing an aromatic group to a leucine greatly alters the function of the protein by destabilizing the interaction between the helix and the C-domain.

In contrast, there are areas of the protein that appear to be unaffected by point mutations. Changes to many of the residues in the N- and C-domains of the protein produce less dramatic effects on the function. These substitutions of solvent exposed side chains seem to be tolerated, maintaining a functional protein. Furthermore, changes to either end of the helix are allowed. These areas form loops connecting the helix to the remainder of the protein and could be somewhat flexible. The side chains of these residues tend to point into the solvent surrounding the protein and are not involved with stacking interactions.

It is beneficial to distinguish between point mutations that affect the function of the protein as a part of the transport system and the ability of the protein to bind ligands. For example, mutants that did not function *in vivo* but functioned *in vitro* may be able to properly bind ligands but not function in the uptake pathway. This could be important in identifying regions of the protein that are used for recognition by the other components of the pathway. One interesting example is the FhuD mutant E213G, which has reduced ability to grow on ferrichrome and coprogen and is partially resistant to albomycin, yet is protected from proteolytic degradation when ligand is bound. This suggests that the charge on the side chains that are solvent exposed may be important for the operation of the protein in the uptake pathway.

The mutations found to be important in the function of *E. coli* FhuD are not necessarily conserved in all the siderophore family members. The highest number of conserved residues occurs between *E. coli* FhuD and its closest neighbours, but conserved motifs are found throughout the family. Several of the conserved sequences found in the N-domains of the proteins are also similar to those found in the C-domains. This indicates that there may have been a gene duplication event early in the evolution of these binding proteins. The topology of the FhuD structure also reflects the homology in sequence between the two domains, with parallels in structure.

The residues found important in the binding site are very similar in the proteins that bind hydroxamate-type siderophores but differ in the other binding proteins. This is not

surprising since the characteristics of the other ligands vary in size and charge. Any residues that form specific interactions, such as hydrogen bonds, between the protein and ligand would not necessarily be conserved since these would be complimentary to each ligand. On the other hand, aromatic groups tend to be common in the binding site of other ligand binding proteins, including those that bind amino acids, sugars and peptides (Quiocho, 1990; Quiocho and Ledvina, 1996). There are several aromatic groups found in the binding site of FhuD that are conserved in most members of the family. Aromatic residues in the protein sequences in the vicinity of the sequence of the binding site residue of FhuD could also be orientated into the pocket with only slight variations in the overall structure.

Members of this siderophore family are clearly distinguishable from all other periplasmic components involved in the uptake of metals and other nutrients. The other components of these ABC transport systems are also classified into their own families. The *E. coli* ATP binding proteins FhuC, FepB, FecE and BtuD are included in the same subfamily as well as the transmembrane proteins FhuB, FepG, FepD, FecC, FecD and BtuC (Linton and Higgins 1999). The fact that sequences of these proteins are quite different from other ABC transport systems suggests that the requirements for this type of high-affinity solute binding impose severe structural constraints on the proteins.

Chapter 5

Spectroscopic and biochemical studies of the *E. coli* periplasmic binding protein FhuD and mutants

Conformational changes in periplasmic binding proteins are important for specific ligand binding and recognition by inner membrane associated proteins. Since the structure of the *E. coli* ferric siderophore binding protein FhuD is different from other periplasmic ligand binding proteins (see Chapter 2), conformational changes experienced by this protein may be unique. The extent of conformational change in FhuD was examined by a number of spectroscopic and biochemical techniques in order to determine the effects of ligand binding, using the siderophores coprogen, Desferal® and ferrichrome. Fluorescence spectroscopy was used to observe the environment of Trp side chains in the protein as well as to monitor the accessibility of aromatic groups in apo and holo protein. Although the fluorescence emission intensity of the protein decreases when ligand binds, there are no significant differences in the accessibility of aromatic groups to external quenching agents. Circular dichroism spectroscopy of apo and holo proteins indicated that there was only a slight change in the secondary structure of the protein. Band shift assays and proteolysis protection assays also indicate that the conformational change of the protein upon ligand binding is very minor. Disruptions in the sequence of the protein can identify residues important for conformational changes and proper ligand binding. Mutant FhuD proteins R84Q and Y106A, which alter two of the groups in the ligand binding pocket, and P167A, which changes a residue in the kinked portion of the connecting α -helix, show atypical conformational changes and different affinities for the siderophores compared to wild type protein. The mutation in the connecting α -helix affected the ability for the protein to change conformation more than the mutations in the residues in the binding pocket.

Introduction.

Many periplasmic binding proteins have considerable conformational flexibility in their structure. In the majority of periplasmic proteins, β -strands connecting the two domains form the hinge region and the base of the binding cleft. The hinge region bends due to small changes in the ϕ and ψ angles of only two or three residues in the β -sheets connecting the two domains. The closure around the substrate in the binding cleft formed by the two domains is suggestive of a "Venus fly trap" or "Pac-man" motion (Mao *et al.*, 1982; Ames, 1986). Each lobe does not significantly change its structure; rather there is a rotation of the two domains about the hinge region. The closure of the two domains is thought to be a dynamic process, with little expenditure of energy (Gerstein *et al.*, 1994; Hayward, 1999). This mode of binding gives rise to numerous interactions between the protein and ligand, providing specificity. Moreover, the final conformation of the receptor-ligand complex is important for making the proper interactions with the inner membrane permease proteins for subsequent release of the tightly bound ligand to the interior of the cell.

It has been shown that the structure of the ferric siderophore binding protein FhuD is different from most periplasmic proteins (Chapter 2). Consequently, there may also be a unique conformational change compared to other periplasmic binding proteins upon ligand binding. The two domains of FhuD, which form a very shallow binding cleft, are connected by a single kinked α -helix. Many hydrophobic interactions are found between side chains of the two domains and between the underside of the domains and the connecting α -helix. Since the α -helix is also a very rigid structure (low crystallographic B-factors), there would appear to be little opportunity for FhuD to further open the two domains. Thus, FhuD may utilize a mechanism for ligand binding that is distinct from other periplasmic binding proteins. In lieu of an unliganded x-ray crystallographic structure of FhuD, evidence for ligand-induced conformational changes can be obtained through various spectroscopic analyses and biochemical of binding studies.

Fluorescence spectra of proteins can be useful to examine conformational changes that occur when a ligand binds. The aromatic amino acids Tyr and Trp are the fluorophores usually monitored by fluorescence spectroscopy, although Trp fluorescence typically dominates the spectrum of proteins (Campbell and Dwek, 1998; Lakowicz, 1999). Trp residues are very sensitive to their local environment and hence their position in a protein, which results in significant differences in the wavelength and intensity of the fluorescence emission spectra. Thus conformational changes can be monitored when the local environment around a Trp residue changes. If the Trp residue experiences more hydrogen bonding or increases its solvent accessibility, the emission spectrum shifts to a longer wavelength (red shift). Conversely, if the Trp residue moves to a more apolar surrounding, such as the interior of a protein, the emission spectra shifts to a shorter wavelength (blue shift), which is generally accompanied by an increase in the intensity. In principle, dissociation constants can be estimated from such changes in the fluorescence spectra.

Addition of fluorescence quenching agents, such as acrylamide, I⁻ and Cs⁺, can also be used to study the solvent accessibility of Trp residues. These molecules do not penetrate nonpolar regions of the protein but quench the fluorescence of Trp residues on the surface of the protein by collisional or dynamic processes. Differences in the ability of these molecules to quench the fluorescence of apo protein versus ligand bound protein can indicate a movement of the Trp residues from a solvent accessible to an inaccessible position.

Other types of spectroscopic and biochemical analyses can also indicate if conformational changes occur when ligand binds to a protein. For example, changes in far-UV circular dichroism (CD) spectra upon ligand binding reflect changes in the secondary structure. If the protein significantly changes size, shape or charge in the holo form, it will migrate differently on a native electrophoresis gel. Limited proteolysis experiments can also help distinguish between different forms of a protein if there is a different degree of protection from degradation by added proteolytic enzymes.

Mutations to FhuD can help identify residues important for the proper functioning of the protein. In this case, a Pro residue in the connecting helix between the two domains was mutated to Ala (P167A) in an attempt to straighten the kink in the helix and evaluate

the effect on conformational changes when ligand binds. Furthermore, two residues important for hydrogen bonding and electrostatic interactions in the siderophore binding site were also mutated (Y106A and R84Q) to examine the effect on ligand binding. These mutants of FhuD were evaluated by spectroscopic experiments and by biochemical assays for evidence of ligand binding and conformational change.

Methods.

Coprogen was a gift from Dr. G. Winkelmann (Universitat Tubingen, Germany). Desferal® (desferoxamine mesylate) was obtained from CIBA-GEIGY Canada. Iron-free ferrichrome was available from Sigma Fine Chemicals. For each siderophore, a 1 mM stock solution of the ferric siderophore complex was made using Fe₂(NO₃)₆ (99.9%, Aldrich Chemical Company) at acidic pH (molecular weight of coprogen is 777 g mol⁻¹, Desferal® is 656.8 g mol⁻¹ and ferrichrome is 687.7 g mol⁻¹). Coprogen, Desferal® and ferrichrome each bind iron in a 1:1 siderophore to iron molar ratio.

Construction of the FhuD mutants. The overexpression strain *E. coli* BL21(DE3) pLysS pMR21 was obtained from Dr. W. Koster (Swiss Federal Institute for Environmental Science and Technology, Switzerland) and Dr. V. Braun (Universitat Tubingen, Germany). All plasmids including pMR21, which contains the His-tag *fhuD* sequence, and mutants were purified using a Qiagen Midi Plasmid Purification Kit (Qiagen). Primers for mutagenesis of *fhuD* were produced by University of Calgary DNA Services and consisted of the following pairs:

P167AFWD: 5'-CGCAGCATGAAAGCCCGCTTTGTG-3' and

P167AREV: 5'-CACAAAGCGGGCTTTCATGCTGCG-3';

R84QFWD: 5'-CGTCGGTTTGCAGACAGAACCTAACC-3' and

R84QREV: 5'-GGTTAGGTTCTGTCTGCAAACCGACG-3';

Y106AFWD: 5'-GGTCGGCAGGAGCTGGCCCTTCACC-3' and

Y106AREV: 5'-GGTGAAGGGCCAGCTCCTGCCGACC-3'.

The QuickChange™ Site-Directed Mutagenesis kit (Stratagene) was used to produce the mutant *fhuD* mutants, with slight modifications. The polymerase chain reaction (PCR) reaction was performed in a Progene thermal cycler (Mandel Scientific) in a 50 µl volume containing 10, 15 or 50 ng of template dsDNA, 125 ng of each primer and 10 mM dNTP mix (2.5 mM of each dNTP). There was no mineral oil added to the reaction since this thermal cycler has a heated lid to prevent evaporation. 0.5 µl *PfuTurbo*™ DNA polymerase (2.5 U/µl; Stratagene) was added to this mixture. The reaction was cycled using 30 s at 95 °C, a 1 min annealing time at 55 °C and a 12 min extension time at 68 °C for 16 cycles. Once the reaction had finished, 0.5 µl of *DpnI* restriction enzyme was added to digest the methylated, nonmutated DNA template and incubated at 37 °C for 1 hour. Subcloning competent *E. coli* DH5α cells were transformed with 5 µl of each mixture. Clones which contained the correct mutations, as sequenced by University of Calgary Core DNA Services, were transformed into the *E. coli* BL21(DE3) pLysS expression strain.

Purification of FhuD and mutants. His-tag FhuD and mutants were purified by metal chelate chromatography (POROS 20MC) charged with nickel, as previously described (Rohrbach *et al.*, 1995a, b) except that the BioCad HPLC metal chelate system (PerSeptive Biosystems) was used. After cell lysis in 50 mM HEPES, 0.5 M NaCl pH 7.6, the protein was bound to the column and washed with 10 volumes of 50 mM HEPES, 0.5 M NaCl pH 7.6 to remove unbound proteins and eluted with a gradient of 0-0.5 M imidazole. The protein was then dialyzed extensively against 10 mM Tris pH 7.5 at 4 °C. The His-tag of the protein was not cleaved off by enterokinase since previous studies showed that the modified protein was functional (Rohrbach *et al.*, 1995b). The extinction coefficient calculated for FhuD is 48790 M⁻¹ (Pace *et al.*, 1995).

Fluorescence spectroscopy. Fluorescence spectra were collected on a Hitachi F-2000 spectrofluorimeter at room temperature in a manner similar to previous published protocols (Rohrbach *et al.*, 1995b). The excitation wavelength was set to 280 nm and emission spectra were recorded from 290 to 400 nm at a scan speed of 60 nm min⁻¹, with bandpasses

set to 10 nm. All samples contained 50 pg of protein (1.53 pM) and 10 mM sodium phosphate buffer, pH 7.5 in a 1 ml sample volume. 0.5 equivalents of ferrichrome were titrated into the sample from a stock solution of 1 mM to 20 times excess ligand. Samples were mixed by inverting the cuvette three times. The fluorescence quenching was expressed as the percent decrease in fluorescence as the siderophores were added.

Fluorescence data were also collected on a Jobin-SPEX Fluorolog 3-21 spectrofluorimeter at 25 °C. The excitation wavelength was 280 nm and the emission was monitored at 338 nm, with slits set to 5 nm. All samples contained 25 pg of protein (0.38 pM) and 10 mM sodium phosphate buffer, pH 7.5 in a 2 ml volume. Siderophores were titrated into the samples in 0.5 equivalents up to 10 times excess ligand. Samples were mixed with a stir bar throughout the experiment. A delay time of 15 s was used between each reading to ensure adequate mixing of the sample. Quenching of FhuD fluorescence was monitored at 338 nm after 10 additions of 10 pi 4 M stock acrylamide, 4 M KI or 4 M CsCl.

Circular dichroism spectroscopy. Circular dichroism spectra were obtained on a Jasco J-715 spectropolarimeter. Far-UV CD spectra were recorded at 25 °C using a cell path length of 0.1 cm at pH 7.5. The concentrations of Tris buffer and protein were 10 mM and 10 pM. Iron loaded siderophores were titrated into the sample by 0.5 equivalent increments from stock solutions of 10 mM to 10 times excess ligand. For each sample, five scans with 0.2 nm step resolution at 50 nm min⁻¹ scan rate, 2 s response time and 20 mdeg sensitivity from 225-185 nm were averaged, the baseline subtracted and a small degree of numerical smoothing applied.

Band shift assays. 25 pg of wild type FhuD was incubated with 0.5, 1, 5 and 10 equivalents of siderophore in 50 pi 10 mM Tris pH 7.5 for 30 min. In order for the samples to stay in the wells of the 12% native PAGE gel, an equal volume of 50% glycerol was added to each sample. Mutant proteins were treated in a similar manner except the samples

were only incubated with a 10-fold excess siderophore. The PAGE gels ran for 3 hours at a constant 80 V to allow proper separation.

Proteolytic protection assays. Wild type FhuD and the FhuD mutants were analyzed with respect to processing and stability in a protease protection assay using trypsin or proteinase K as previously described (Koster and Braun, 1990a; Rohrbach *et al.*, 1995a, b). However, in this experiment, the samples were kept at room temperature after enzyme was added.

Results.

Purification of mutant FhuD proteins. The levels of expression of the mutant FhuD proteins (R84Q, Y106A and PI67A) are very similar to the level obtained for the wild type protein. The purification of the three mutant FhuD proteins is shown in Figure 5.1. The purification procedure used was identical to that of the wild type protein. Approximately 10 mg of mutant protein was obtained per liter of culture. The mutant proteins also appear to have the same stability as the wild type protein due to the absence of extra bands on the SDS-PAGE gel.

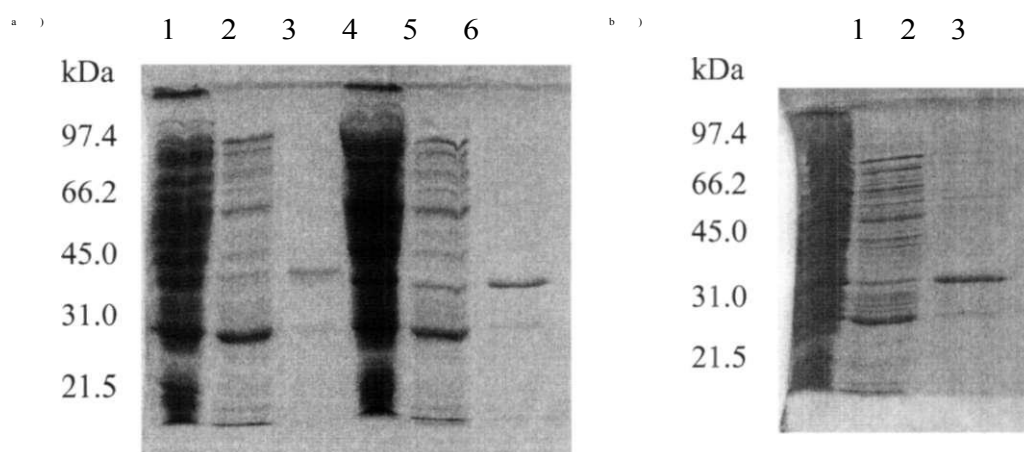
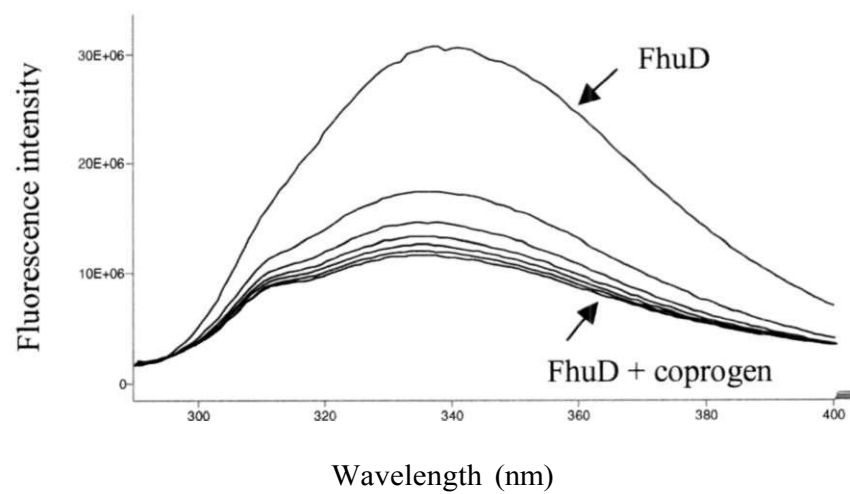


Fig. 5.1 A 12% SDS-PAGE gel following the purification of *E. coli* FhuD mutants, a) Lane 1, cell lysate from R84Q; lane 2, first peak from purification; lane 3, second peak containing R84Q; lane 4, cell lysate from Y106A; lane 5, first peak from purification; lane 6, second peak containing Y106A. b) Lane 1, cell lysate from PI67A; lane 2, first peak from purification; lane 3, second peak containing PI67A. The purified mutant FhuD proteins migrate at slightly different positions on the acrylamide gel due to different charges on each protein.

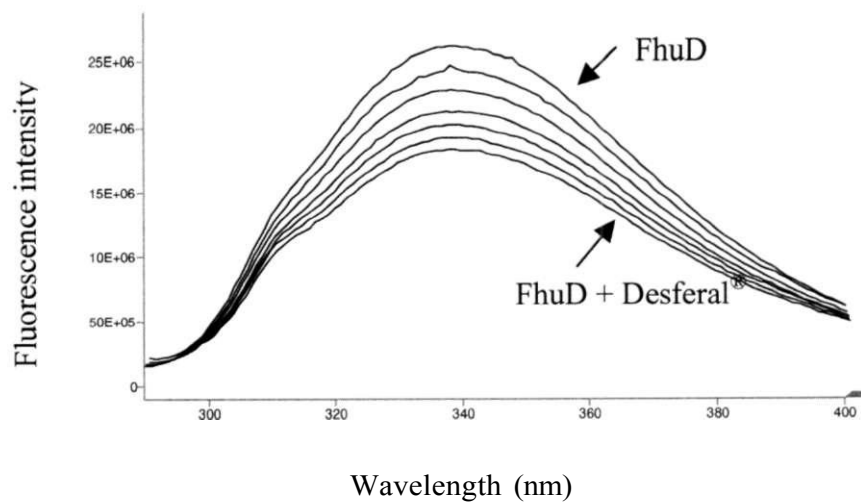
Fluorescence spectroscopy. In addition to examining changes in the environment of the residues in the binding pocket of a protein, dissociation constants can be estimated from changes in the fluorescence spectra of a protein when ligands bind. The fluorescence spectra obtained for the titration of the wild type protein with ferric siderophores were comparable to published results (Rohrbach *et al*, 1995a) using either spectrofluorimeter. The fluorescence maximum is observed around 335 nm, which is consistent with Trp residues buried in a relatively hydrophobic environment. As the concentration of the siderophore is increased, the fluorescence intensity of the sample decreased. There was no shift in the wavelength of the emission maximum after each addition. Addition of excess siderophores to the protein sample does not decrease the level of fluorescence proportionally; rather the protein becomes saturated with ligand and once saturated, the fluorescence emission does not change any further.

The decrease in the fluorescence intensity for the wild type protein is different for each siderophore (Figure 5.2). Coprogen and ferrichrome give rise to the most dramatic decrease of the fluorescence intensity of the wild type protein. In previous studies, the dependence of the fluorescence intensity on the concentration of sample was used to estimate the dissociation constants (Rohrbach *et al*, 1995a). However, when water was titrated into the sample, the fluorescence intensity decreased. This indicates that another quenching mechanism is influencing the spectra and the dissociation constants obtained from this method would be artificially low. Thus only a qualitative estimation of the dissociation constant is reliable. When the Hitachi F-2000 fluorimeter was used, the quenching experienced by the protein when water was added was greater than the quenching obtained with the Jobin-SPEX Fluorolog 3-21 spectrofluorimeter. Given that the sample in the later instrument is stirred and not shaken, the amount of air introduced into the sample is probably less. Thus, oxygen may also be quenching the fluorescence of the protein.

a)



b)



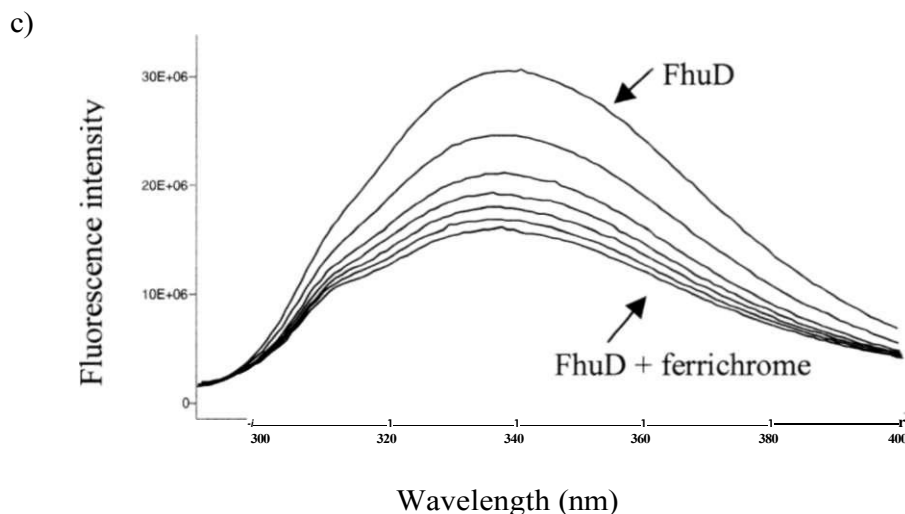


Fig. 5.2 Fluorescence spectra of FhuD in the presence of a) coprogen, b) Desferal® and c) ferrichrome. The top spectrum of each figure is 0.38 pM wild type FhuD in the absence of siderophore. The fluorescence intensity decreases in subsequent curves with the addition of 0.5, 1.0, 1.5, 2.0, 2.5, and 3.0 equivalents of siderophore. These spectra were recorded on a Jobin-SPEX Fluorolog 3-21 spectrofluorimeter.

Changes in the solvent exposure of tryptophan residues in the apo versus holo forms of the proteins can be measured by quenching experiments. Addition of uncharged acrylamide to apo or holo wild type FhuD decreases the fluorescence intensity while addition of charged I^{II} or Cs⁺ did not affect the fluorescence intensity of wild type FhuD. A Stern-Volmer plot of the acrylamide quenching studies shows that there are one or more tryptophan residues accessible to this quenching agent in both the apo and holo forms of the protein (Figure 5.3). When dynamic quenching occurs, the Stern-Volmer curve is expected to be linear. Since the curves have a slight upward curve, it may be possible that there is some static quenching occurring. However, when the apparent quenching constant,

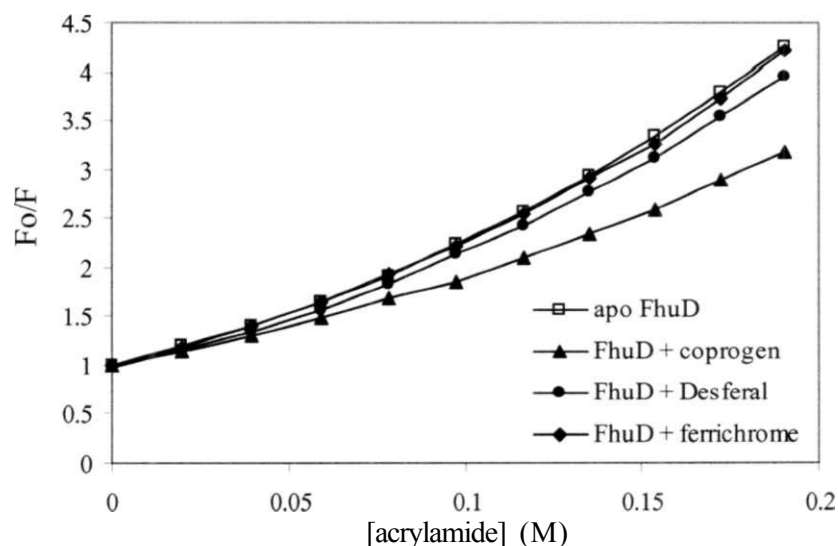
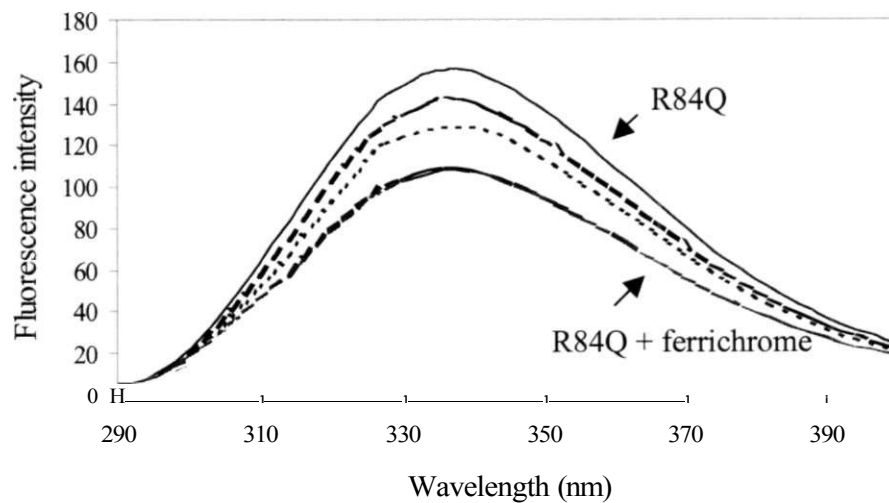


Fig. 5.3 A Stern-Volmer plot of the acrylamide quenching for FhuD and ligand bound FhuD. F_0 is the fluorescence in the absence of acrylamide and F is the fluorescence at each titration point after correction for dilution.

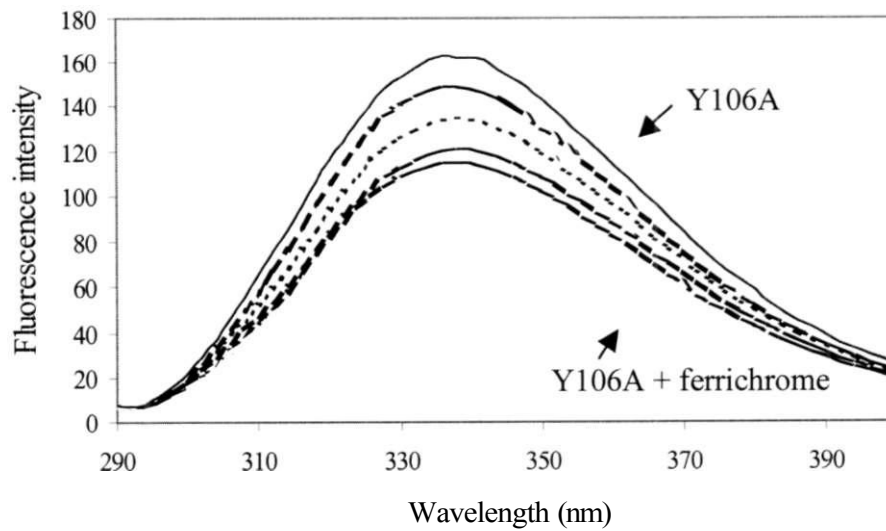
K_{app} , is plotted against the concentration of the quenching agent, the solution for the static and dynamic quenching constants, K_s and K_d , respectively, are imaginary numbers. Thus, as in the case when the protein is titrated with siderophore, the fluorescence of the protein may be quenching by an additional mechanism, influencing the determination of a value for the dynamic quenching constant.

The fluorescence intensity of the FhuD mutant proteins also decreased when siderophores were titrated into the samples (Figures 5.4 to 5.6). However, the changes in fluorescence intensity are less dramatic for the mutants than seen with the wild type protein. The quenching effects of the siderophores are comparable to quenching observed with oxygen (Figure 5.5). Therefore, accurate binding constants could not be determined with this technique in this case. When the fluorescence of PI67A was monitored by the a Jobin-SPEX Fluorolog 3-21 spectrofluorimeter (Figure 5.6), the oxygen quenching effects decreased and the data shows that the siderophores interact with the protein similarly to wild type.

a)



b)



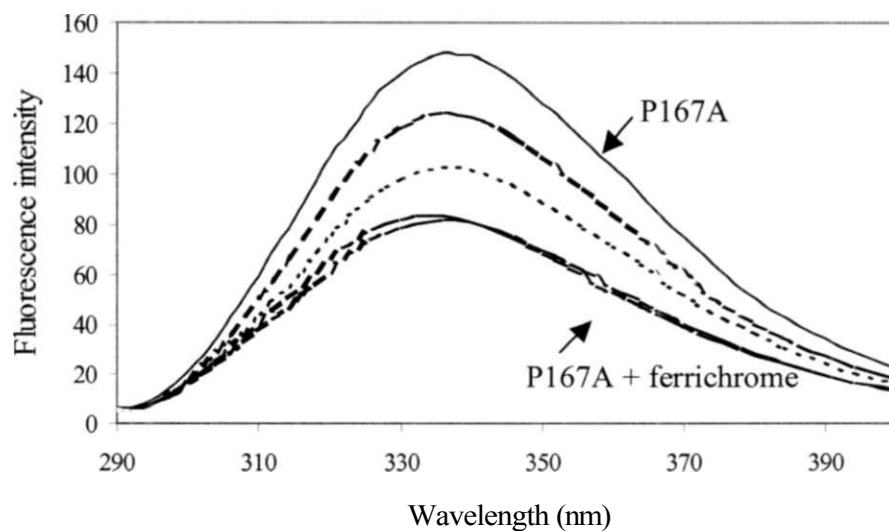


Fig. 5.4 Fluorescence spectra of mutant FhuD proteins in the presence of ferrichrome. In a) R84Q, b) Y106A and c) P167A, the fluorescence decreases as ferrichrome is added. The top spectrum of each figure is 1.53 pM mutant FhuD in the absence of siderophore, and then the fluorescence intensity decreases in each fluorescence curve with the addition of 0.5, 1.0, 1.5, 2.0, 5, and 10.0 equivalents of ferrichrome. These spectra were recorded on a Hitachi F-2000 spectrofluorimeter.

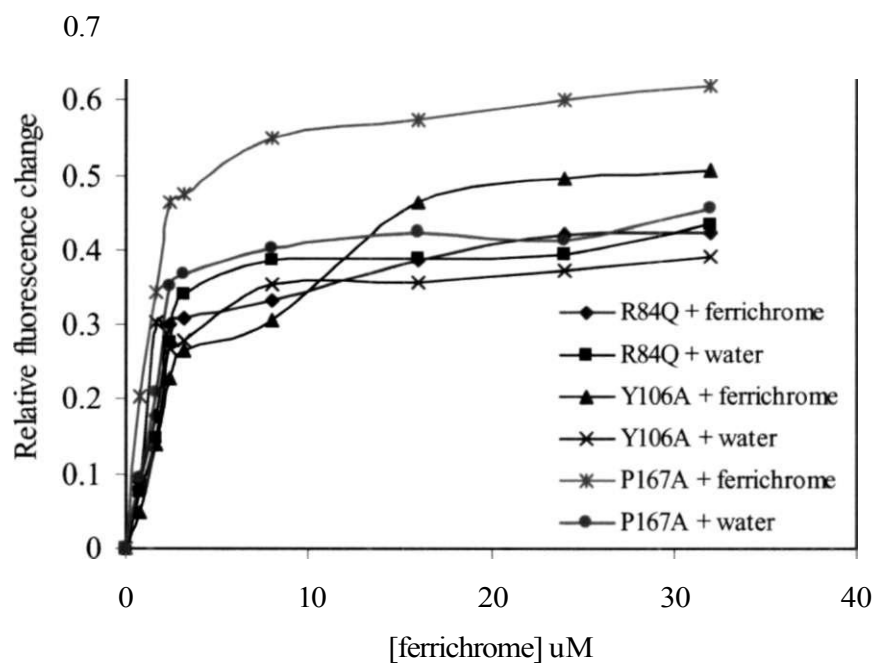
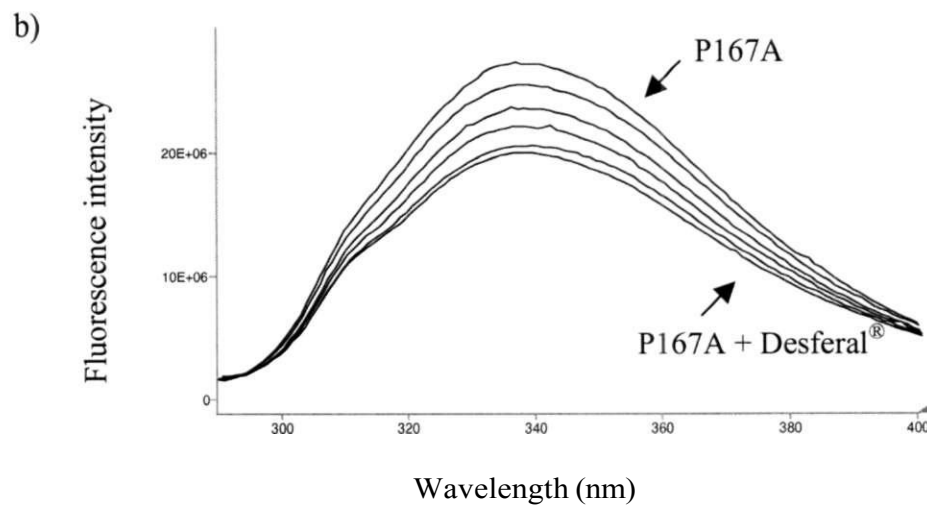
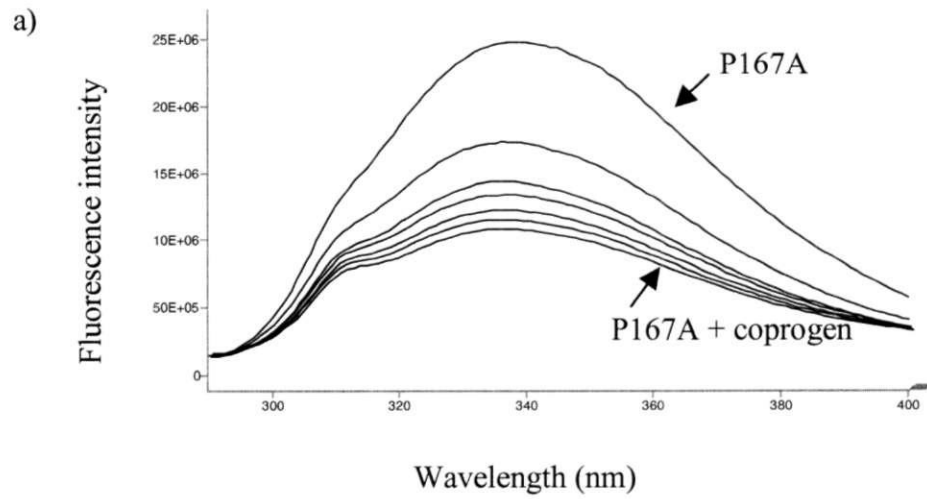


Fig. 5.5 Decrease in the fluorescence intensity of mutant FhuD proteins observed with increasing concentrations of ferrichrome or adding the same amount of water.



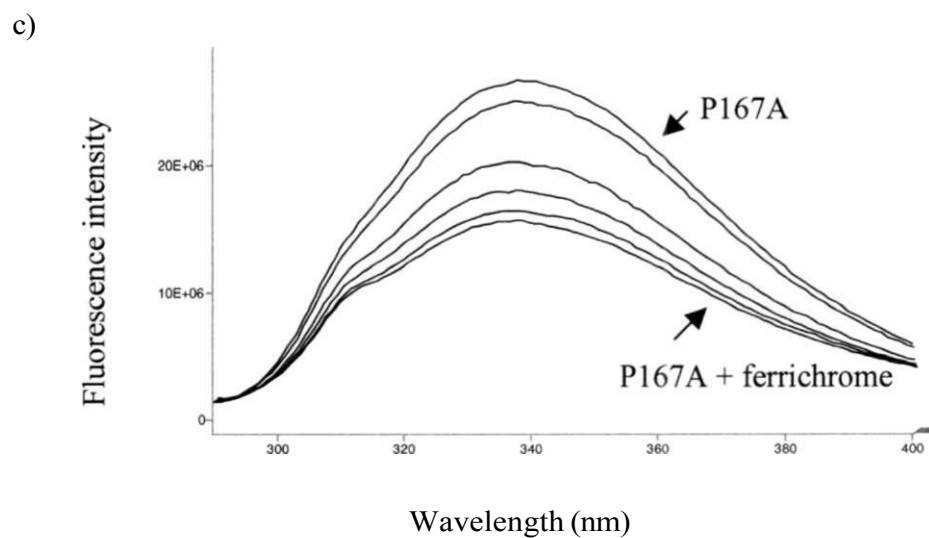


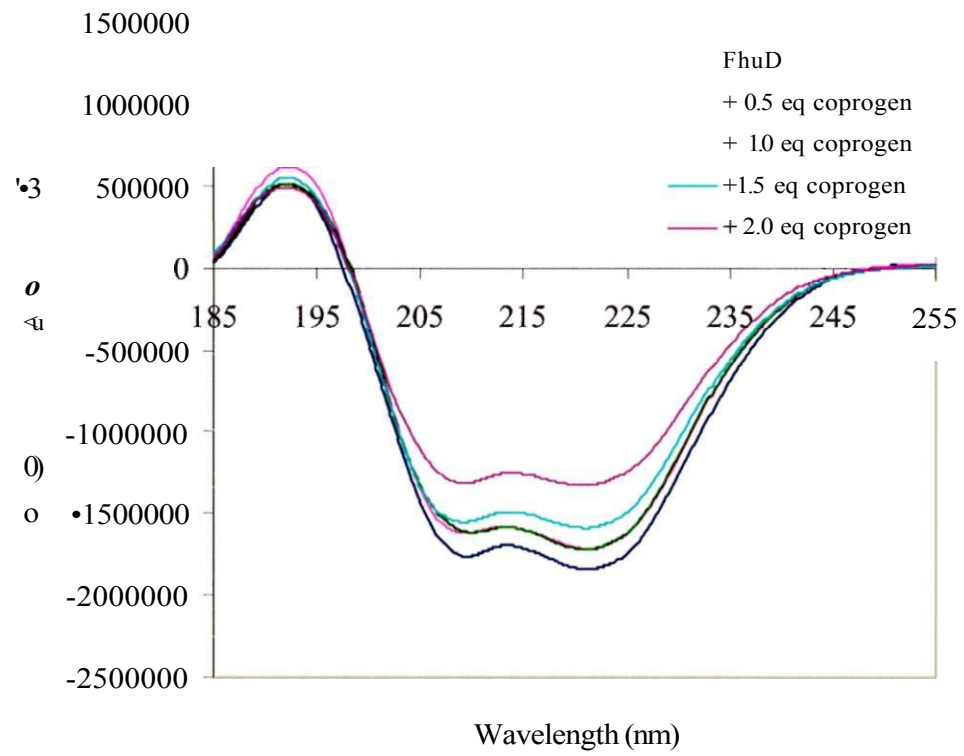
Fig. 5.6 Fluorescence spectra of PI67A in the presence of a) coprogen, b) Desferal and c) ferrichrome. The top spectrum of each figure is 0.38 μ M PI67A in the absence of siderophore, and then the fluorescence intensity decreases in each fluorescence curve with the addition of 0.5, 1.0, 1.5, 2.0, 2.5, and 3.0 equivalents of siderophore. These spectra were recorded on a Jobin-SPEX Fluorolog 3-21 spectrofluorimeter.

Circular dichroism spectroscopy. The far-UV CD spectra of FhuD show that it has a significant proportion of α -helical structure, as shown by the negative ellipticities at 208 nm and 222 nm (Figure 5.7). When siderophores are added to FhuD, there is an increase in the ellipticities, indicating a change in the secondary structure of the protein. Addition of coprogen and ferrichrome changed the molar ellipticity of FhuD to a similar extent. The addition of Desferal®, on the other hand, did not change the molar ellipticity of the sample very much. When siderophores are added in excess (of 2 equivalents), the CD spectrum of the protein does not undergo substantial further changes.

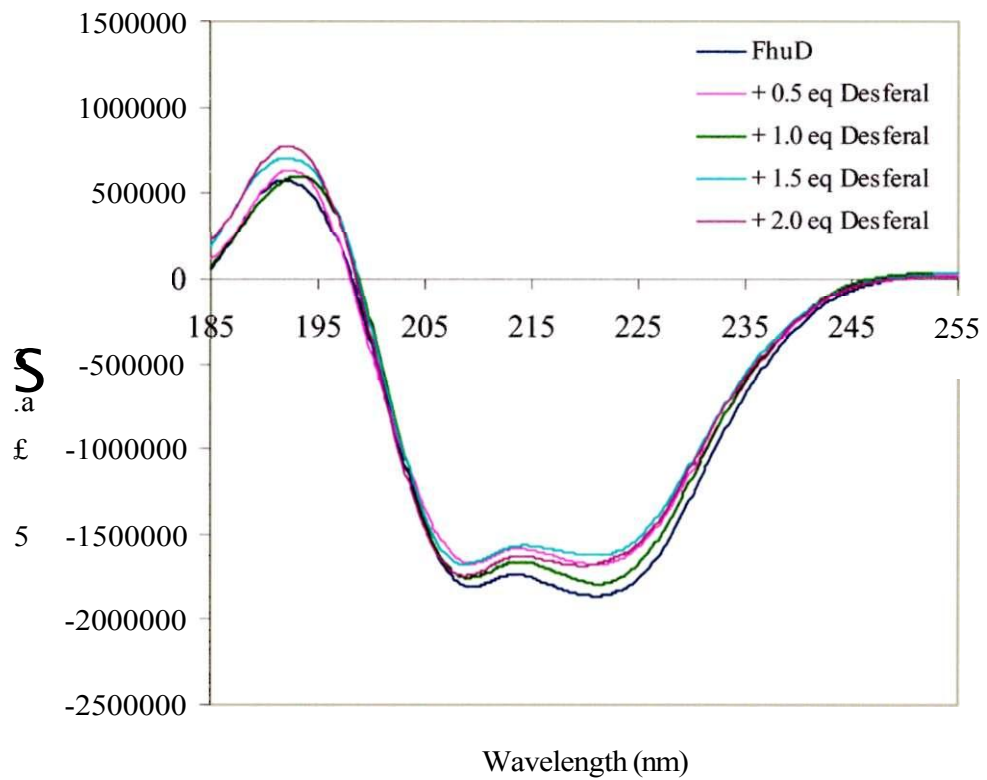
The far-UV spectra of the mutant proteins also show that they have a large proportion of α -helical structure, as shown by the negative ellipticities at 208 nm and 222 nm (Figure 5.8 to 5.10). As each siderophore is titrated into the sample, the ellipticities measured by the spectrometer increase. This indicates that there may be a change in the structure of the protein. Since the change in ellipticity is the same as the change observed for the wild type protein, the structural changes may be similar.

The CD spectra of each mutant protein are affected by the different siderophores to varying degrees. This indicates that certain siderophores do not bind to the protein or that the changes in protein structure are different when certain siderophores bind. Desferal® and ferrichrome change the spectra of R84Q to a greater extent than coprogen. All three siderophores affect the spectra of Y106A to the same degree. In contrast, the spectra of PI 67 A are changed very little when any of the three siderophores are added.

a)



b)



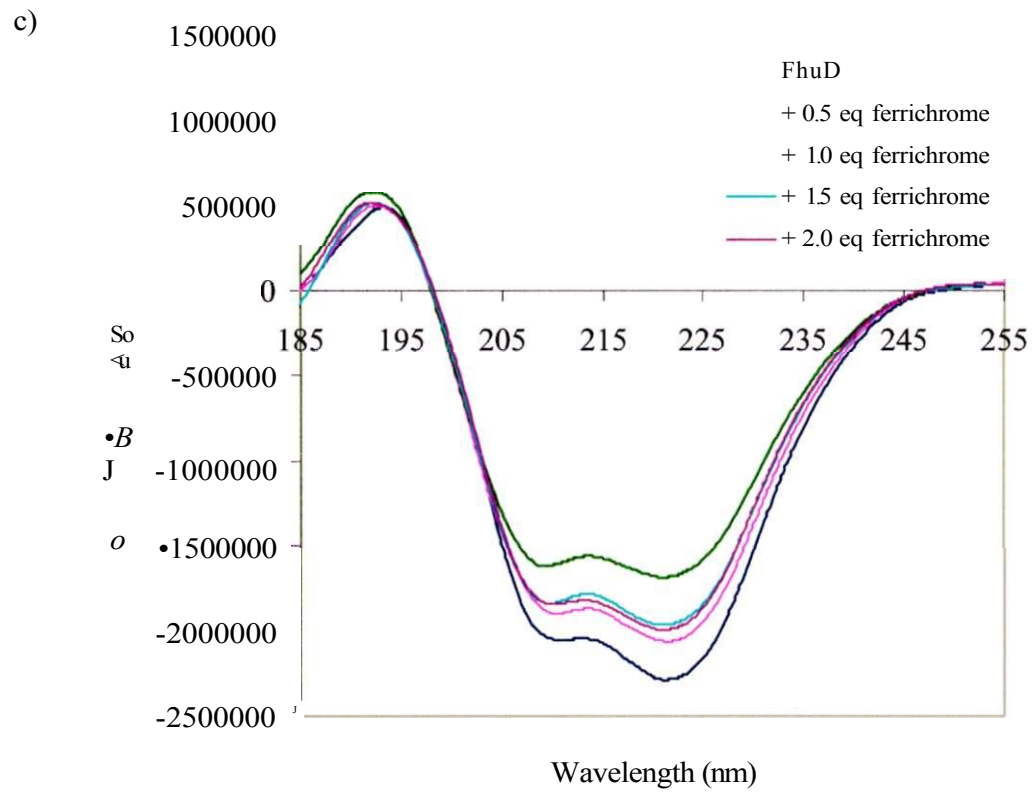
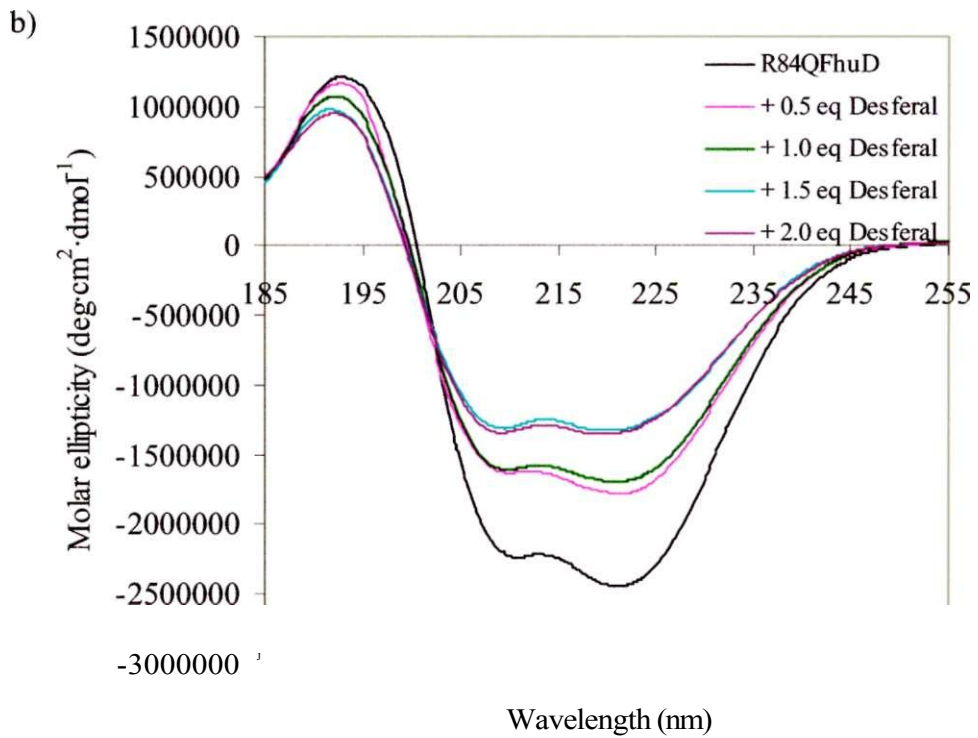
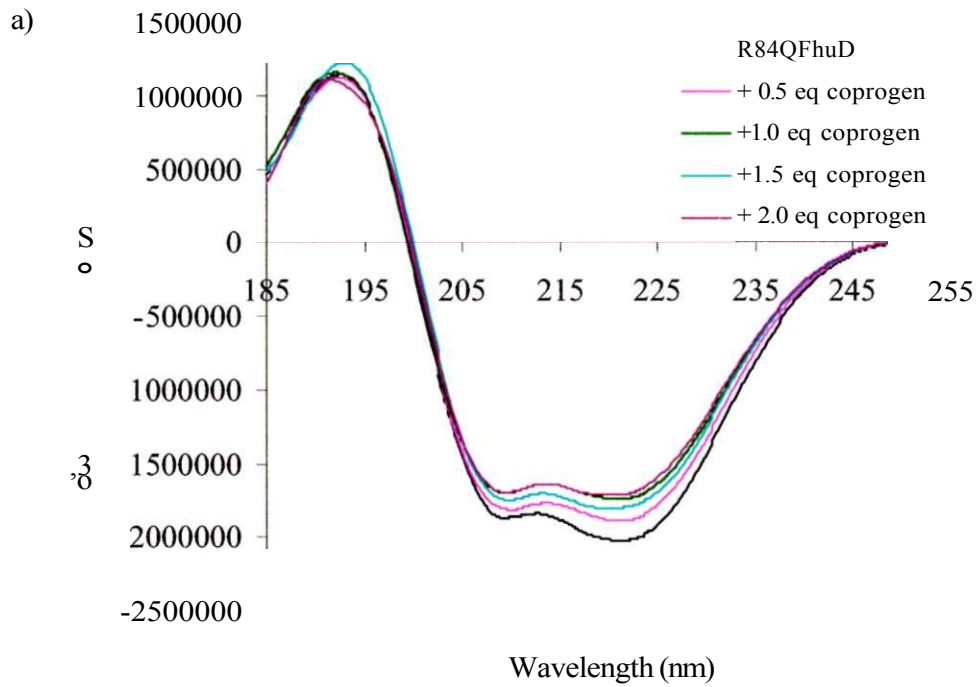


Fig. 5.7 Far-UV circular dichroism spectra of FhuD. As the protein was titrated with a) coprogen, b) Desferal® and c) ferrichrome, the ellipticity of the spectra increased. Additional aliquots of each siderophore (above 2.0 equivalents) did not change the spectra significantly.



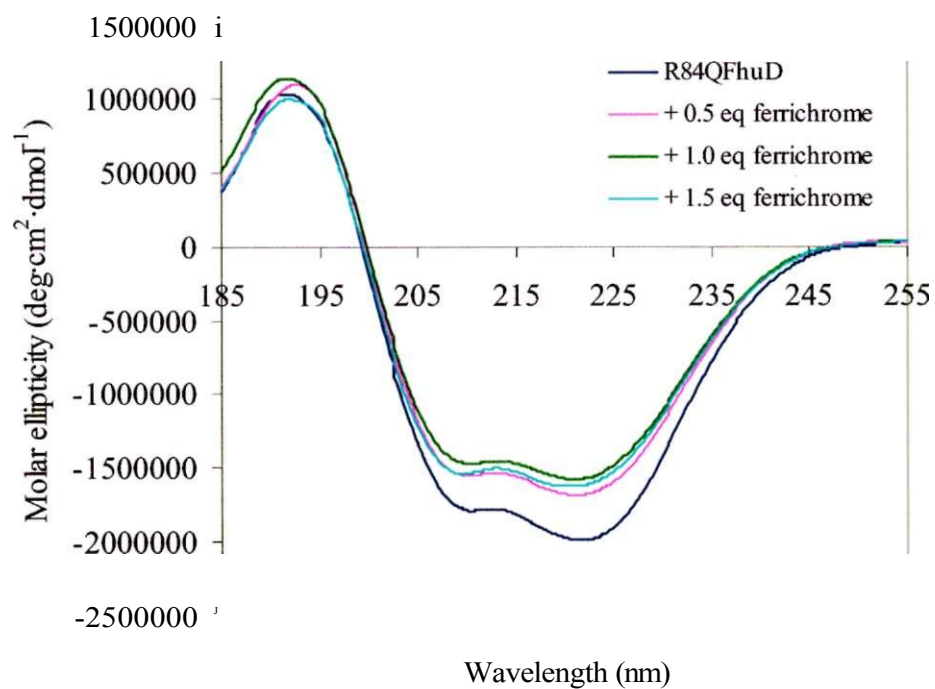
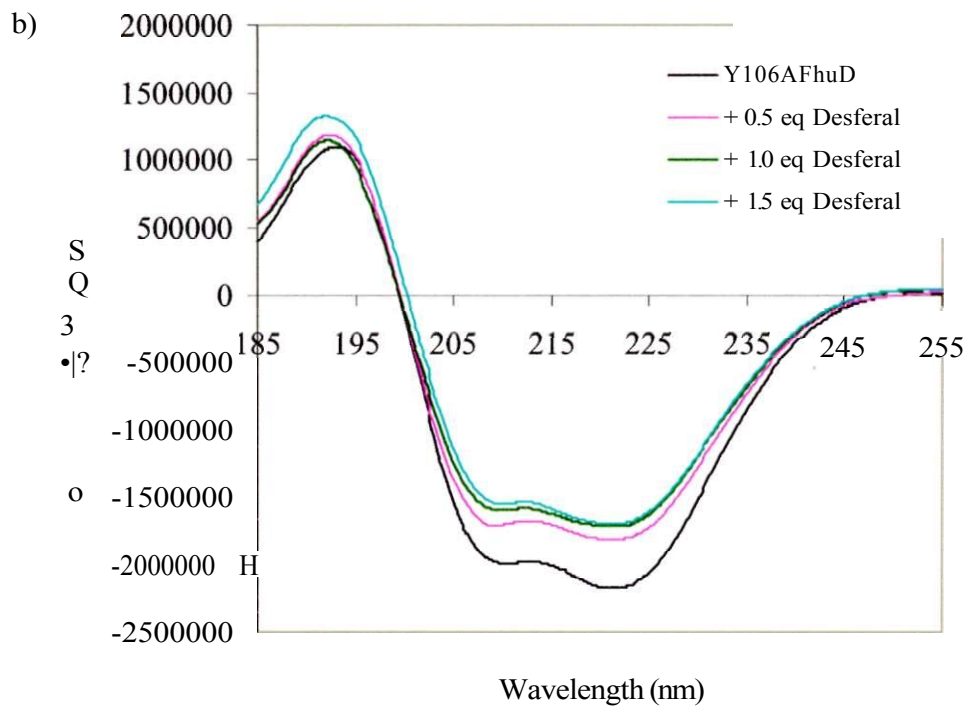
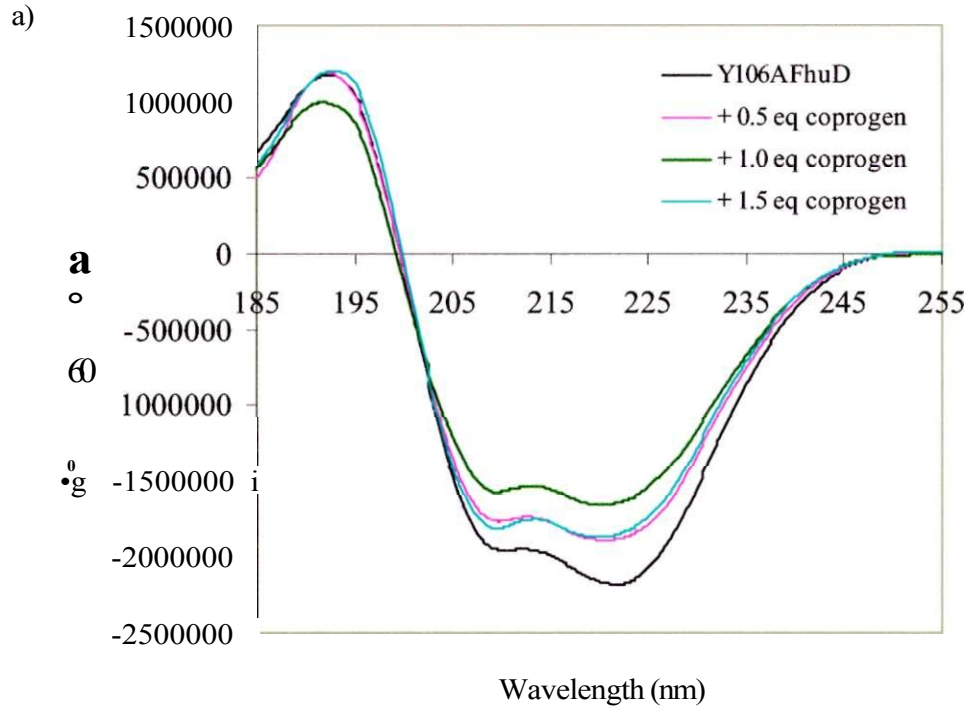


Fig. 58 Far-UV CD spectra of R84Q titrated with a) coprogen, b) Desferal^o and c) ferrichrome. The molar ellipticity of the spectra increased when siderophores were added. Addition of higher levels of the siderophores did not affect the CD spectra further.



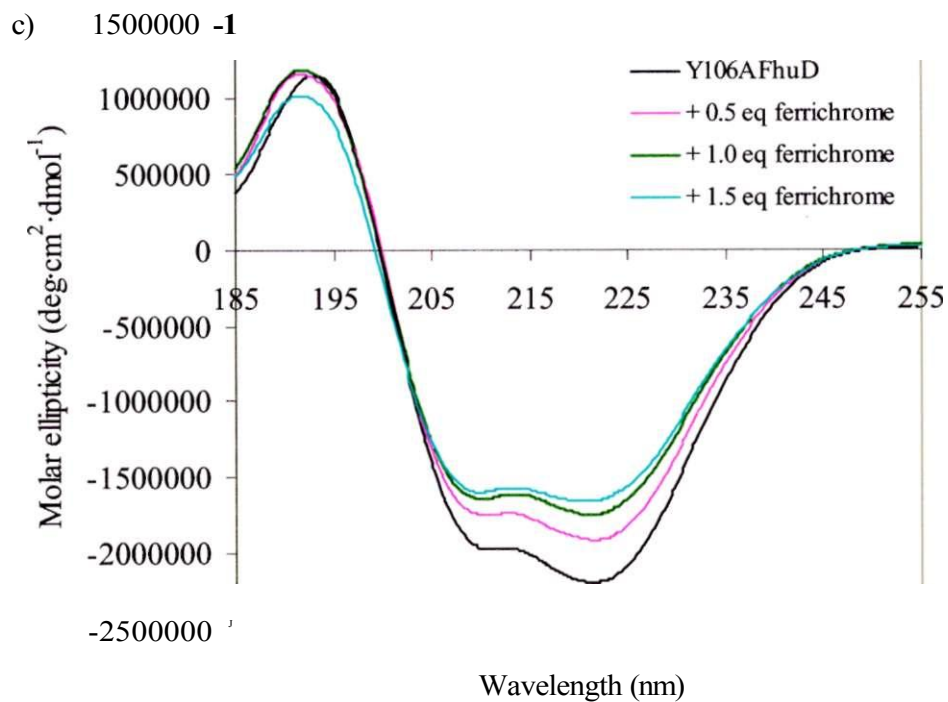
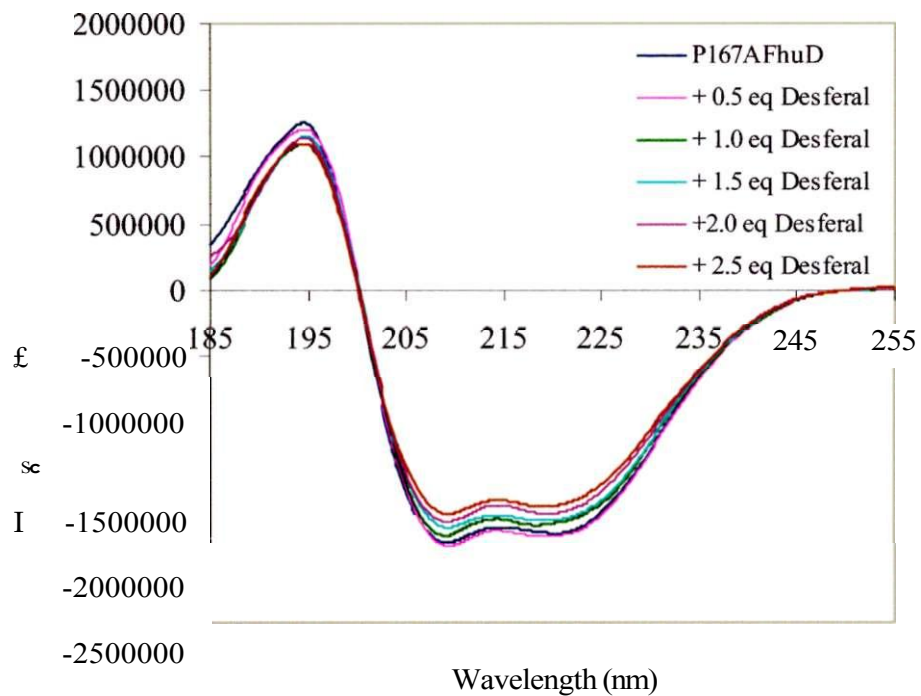
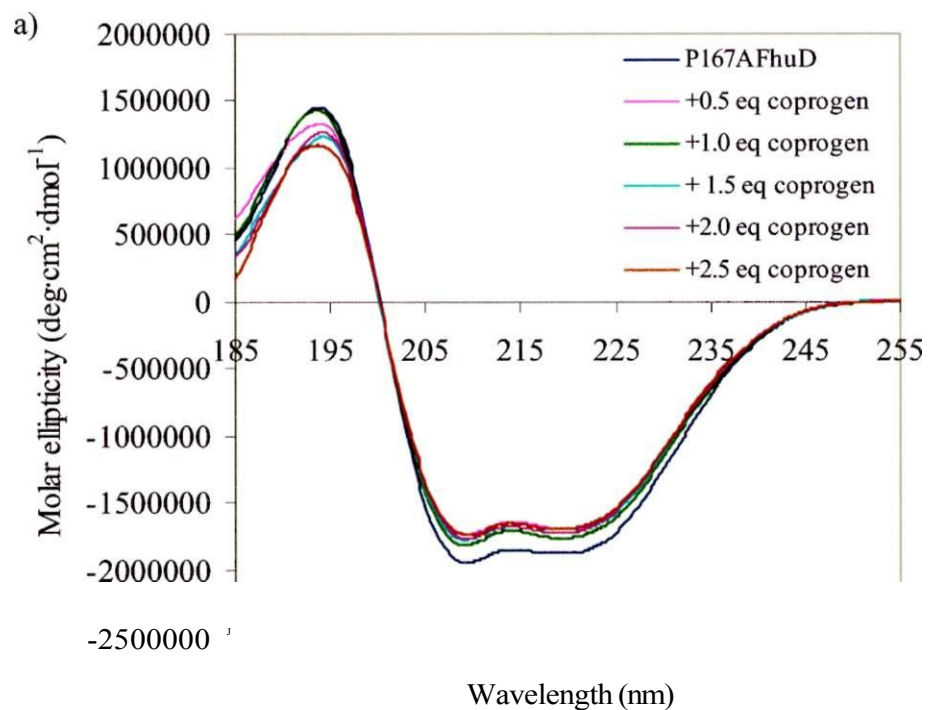


Fig. 5.9 Far-UV CD spectra of Y106A titrated with a) coprogen, b) Desferal and c) ferrichrome. When siderophores were added, the ellipticity of the spectra increased. Addition of further aliquots of siderophore did not affect the CD spectra.



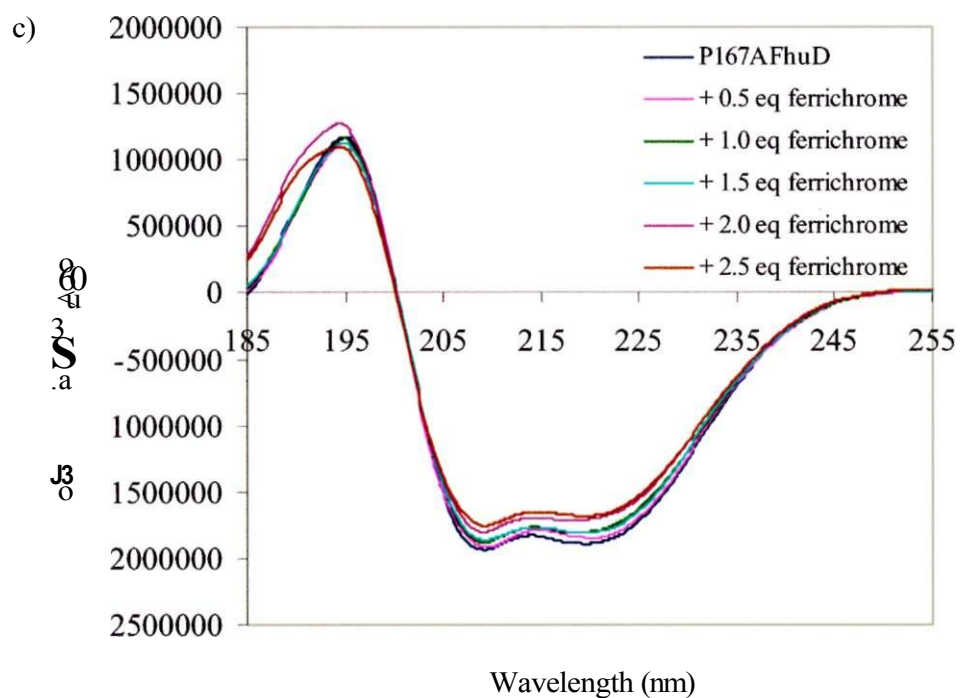


Fig. 5.10 Far-UV CD spectra of PI67A titrated with a) coprogen, b) Desferal and c) ferrichrome. Only a slight increase in ellipticity was observed when siderophores were added. The CD spectra did not change with the addition of excess siderophore.

Native PAGE band shift assays. During the formation of a protein ligand complex, a combination of the increased size of the complex, a change in conformation or a change in charge can result in a different migration on a native electrophoresis gel. This technique has been used successfully with other protein complexes, such as calmodulin with various binding peptides, to demonstrate that the complex has a reduced mobility compared to the protein alone. In Figure 5.11, the relative mobilities of FhuD and the FhuD ferrichrome complex is shown. The protein complex appears to migrate in the same vicinity as the protein alone. This is also true for the FhuD complexes with coprogen and Desferal® (data not shown). The mobilities of the mutant FhuD proteins and complexes are also very similar (Figure 5.12). However, when R84Q is bound to Desferal® or ferrichrome, a slight decrease in the mobility is seen.



Fig. 5.11 Native PAGE of FhuD complexed with ferrichrome. Lane 1, FhuD without ferrichrome; lane 2, FhuD and ferric nitrate; lanes 3-6, FhuD with 0.5, 1, 5 and 10 equivalents of iron loaded ferrichrome. The migration of FhuD is not significantly affected by forming a complex with ferrichrome.

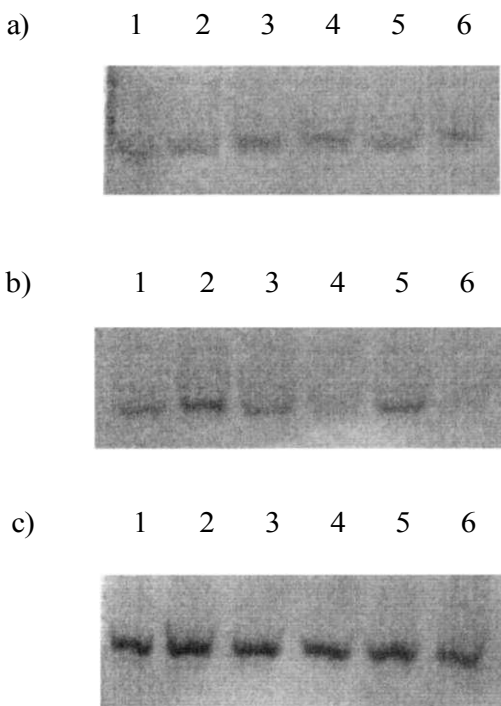


Fig. 5.12 Native PAGE of mutant FhuD proteins. In each, a) R84Q b) Y106A c) P167A, lane 1, 3 and 5 is the apo mutant protein; lane 2, with coprogen; lane 4, with Desferal®; lane 6, with ferrichrome.

Protease protection assays. Previous studies have shown that ligand binding to FhuD decreases its degradation by added proteases (Rohrbach *et al.*, 1995a, b). FhuD is degraded by proteinase K and trypsin in the absence of siderophores (Figure 5.13, lanes 5-8). Digestion of FhuD in the presence of 1 equivalent of ferrichrome seems to decrease the rate of proteolytic cleavage slightly (Figure 5.13, lanes 13-16) but the addition of excess ferrichrome results in little proteolysis (Figure 5.13, lanes 17-20). The other siderophores, coprogen and Desferal®, had a similar effect on the extent of proteolysis of FhuD. This indicates that binding of these ligands stabilizes a proteolytic resistant conformation of the protein that may be different from the apo form (Rohrbach *et al.*, 1995a, b).

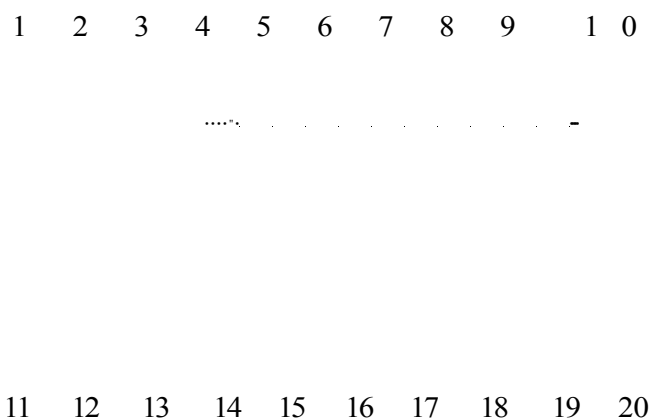


Fig. 5.13 Protection of FhuD from degradation by trypsin in the presence of ferrichrome. In the SDS-PAGE gel, lanes 1-4, control sample with no trypsin added; lanes 5-8, trypsin added to FhuD; lanes 9-12, ferric nitrate added; lanes 13-16, 1 equivalent of ferrichrome added; lanes 17-20, 10 equivalents of ferrichrome added. Samples were taken at 0, 15, 30 and 60 min after trypsin was added.

When the mutant proteins were subjected to the same proteolytic treatment in the presence of excess siderophores, not all were resistant to the enzymes (Figure 5.14). R84Q was only resistant to proteolysis in the presence of Desferal® and ferrichrome. Y106A was resistant to proteolysis only in the presence of Desferal while P167A was resistant to proteolysis in the presence of coprogen and ferrichrome.

Fig. 5.14 (next page) Protection of mutant FhuD proteins from degradation by trypsin in the presence of siderophores. In the SDS-PAGE gel, lanes 1-15, R84Q; lanes 16-31, Y106A; lanes 32-46; P167A. Proteins were incubated without trypsin (lanes 1-3; lanes 16-19; lanes 32-34), with trypsin (lanes 4-6; lanes 20-22; lanes 35-37), with coprogen (lanes 7-9; lanes 23-25; lanes 38-40), with Desferal (lanes 10-12; lanes 26-28; lanes 41-43), and ferrichrome (lanes 13-15; lanes 29-31; lanes 44-46). Samples were taken at 0, 15 and 30 min after adding trypsin.

R84Q-trypsin R84Q+trypsin R84Q+coprogen
 1 2 3 4 5 6 7 8 9



R84Q+Desferal® R84Q+ferrichrome Y106A
 -trypsin
 10 11 12 13 14 15 16 17 18



Y106A Y106A Y106A Y106A
 -Hrypsin +coprogen +Desferal® +ferrichrome
 19 20 21 22 23 24 25 26 27 28 29 30 31



PI 67 A P167A P167A P167A P167A
 -trypsin +trypsin +coprogen +Desferal® +ferrichrome
 32 33 34 35 36 37 38 39 40 41 42 43 44 45 46

Discussion.

Transport of ferric hydroxamate-type siderophore across the periplasmic space first requires specific high affinity binding to the periplasmic protein FhuD, which then releases the siderophore to the inner membrane associated proteins for uptake into the cytoplasm of the cell. Thus, specific interactions between the ligand and protein are required, as well as special contacts between the holo periplasmic protein and the inner membrane associated proteins. In order to meet these requirements, the periplasmic protein could undergo a conformational change when the ligand binds, allowing both domains to participate in ligand binding and to distinguish between the apo and holo forms of the protein. Due to the unique structure of FhuD, the conformational change experienced by the protein when ligand binds is expected to be less dramatic than for other periplasmic ligand binding proteins.

The effect of the binding of the siderophores can be monitored by a variety of experimental techniques. When the siderophore binds to FhuD, the fluorescence intensity decreases, due to quenching of the Trp fluorescence. Since the binding constant for ferrioxamine B ($36 \mu\text{M}$) is greater than the binding constants for coprogen ($0.3 \mu\text{M}$) and ferrichrome ($1.0 \mu\text{M}$) (Rohrbach *et al.*, 1995b), more Desferal® must be added to the protein to obtain a similar fluorescence decrease. However, there is no red or blue shift in fluorescence emission spectra. This indicates that the aromatic residues in the binding site of the protein do not experience a change in their local environment from a polar to non-polar state. Since the ligand binding pocket of FhuD is shallower than other periplasmic proteins negating the need for large movements of side chains blocking the binding site, the arrangement of the residues in the binding pocket is similar in both the apo and holo forms.

The aromatic residues also remain accessible to quenching agents in both the apo and holo forms of the protein. Most of the aromatic residues are clustered in the binding site of the protein, so even though the siderophore is bound, solvent can still access the shallow binding pocket. When coprogen is bound to the protein, the accessibility of the aromatic groups decrease since this siderophore inserts more of the molecule into the protein, clearly limiting the accessibility of the protein to the quenching agent.

The effects of binding siderophore to FhuD are evident in the CD spectra by the increase in the negative ellipticity at 208 nm and 222 nm. This is indicative of a change in the overall structure of the protein, but quantitation of the changes to the secondary structure using CD spectra is difficult to determine. Often, changes to the CD spectra cannot be solely attributed to changes in the secondary structure alone and are due to the spatial reorientation of the structure. This is evident in the dramatic changes in the CD spectra of calmodulin, which are due to reorientation of helices when Ca^{2+} binds rather than an increase in the amount of secondary structure (Bayley and Martin, 1986; Ikura *et al*, 1991; Zhang *et al*, 1995; Kuboniwa *et al*, 1995). Although the native gels of FhuD show very little difference between the two forms of the protein, since it is protected from proteolysis, the apo and holo forms can be distinguished. Thus, interaction between the protein and siderophore seems to change the conformation of FhuD but the nature of the conformational change remains to be determined.

Characterization of the mutant proteins by these techniques shows that mutating residues, either in the binding site or in the connecting α -helix, affects the function of the protein. For each technique, the apo form of the mutant protein produced similar results, so these mutant proteins fold properly. The fluorescence spectra of the mutants show that these three siderophores quench the fluorescence of the mutant proteins to different degrees. However, the determination of a binding constant for each of these proteins is hampered by the presence of oxygen in the sample, which also quenches fluorescence. Since the CD spectra of the mutant proteins also showed the same changes as in the wild type protein, the changes in the secondary structure may be similar. Since the proteins did not experience a large change in migration on a native electrophoresis gel, this change is likely small. In the proteolysis assay, better protection experienced by the mutant proteins when bound to a certain siderophore may be related to better binding or to a slightly more resistant holo form of the protein (Rohrbach *et al*, 1995b).

The effects of the mutations on FhuD not only demonstrates that certain residues are important for conformational change when ligands bind but limits the important areas within the binding site required for ligand interaction. This information can be used during rational design of an antimicrobial agent, since the new compound can be designed to

complement these vital areas. The mutant protein R84Q does not have the charged residue in the binding site but the substituted residue still may contribute to hydrogen bonding of the ligand. This protein demonstrated a preference for Desferal® and ferrichrome but not coprogen. For uncharged hydroxamate-type siderophores, the charge of residue 84 may not affect the recruitment of most siderophores but may be required for the rearrangement of the side chains of the residues in the binding site in order to accommodate the large *trans*-anhydromevalonic acid group of coprogen. Y106A has one less side chain for hydrogen bonding to the siderophore and likely has decreased hydrophobicity and a different shape within the binding pocket. This mutant protein had some affinity for all the siderophores, as shown by the changes in the CD spectra as well as the protease protection studies, suggesting that this area of the protein may not be as important for interaction with the ligand. P167A, with the mutation in the α -helix connecting the two domains of the protein, appeared to be able to bind siderophores, as shown in the slight change in the fluorescence spectra, but the conformational changes associated with ligand binding were less dramatic, as seen in the CD spectra and protease protection experiments. Thus, this mutated region of the protein may affect the hinge region that opens and closes the two domains of the protein. A detailed three-dimensional structure of the apo form of the protein is eagerly anticipated in order to conclusively resolve these issues.

Chapter 6**Characterization of the *E. coli* periplasmic ferric siderophore binding proteins FepB and FecB**

Conformational changes in the structures of periplasmic binding proteins are important for specific ligand binding and recognition by other proteins. Like other A B C transport systems, the ferric siderophore binding proteins FepB and FecB shuttle ligands through the periplasmic space to the inner membrane associated proteins. Both proteins have limited substrate specificity; FepB is able to bind ferric catecholates such as ferric enterobactin (FeEnt) and the related compound GaTRENAM while FecB appears to only bind ferric citrate. Since these proteins have little sequence homology to other periplasmic proteins with known structures, including the ferric siderophore binding protein FhuD, information about their mechanism of function is largely unknown. In an attempt to characterize the conformational changes associated with ligand binding in FepB and FecB, these proteins were examined by a number of techniques. Circular dichroism spectroscopy of apo and holo proteins indicated that there was a slight change in the secondary structure of each of the proteins when ligand bound. Band shift assays and proteolytic protection assays indicated that the conformational change of FepB was greater than the conformational change experienced by FecB. Thus, these proteins may not experience the same conformational changes when ligand binds and may not have identical structural features.

Introduction.

Under iron deficiency, ferric siderophore complexes are transported into Gram-negative bacteria by specific transport systems. In *E. coli* and other Gram-negative strains, transport of siderophores involves a specific outer membrane receptor, a periplasmic transport protein and several inner membrane associated proteins (for reviews of iron transport systems see Guerinot, 1994; Ratledge and Dover, 2000). This arrangement is similar to other periplasmic protein dependent systems, termed ABC transporters (for ATP binding cassette-type transport), which transport amino acids, peptides and sugars into the cell (Tarn and Saier, Jr., 1993; Ames, 1986). Many types of hydroxamate and catechol siderophores, as well as citrate, are utilized by the pathogen, *Escherichia coli*, of which only enterobactin (Ent) is actually synthesized by the bacteria itself. Although there are specific receptors for each hydroxamate-type siderophore (aerobactin, ferrichrome, rhodoturulate, coprogen and ferrioxamine B), and catechol-type compounds (enterobactin and dihydroxybenzylserine), common systems within the periplasm and inner membrane are used which are encoded by the *fhu* (Fecker and Braun, 1983) and *fep* (Shea and McIntosh, 1991; Ozenberger *et al*, 1987; Pierce and Earhart, 1986) operons respectively. Ferric citrate is internalized via the transport system encoded by the *fee* genes (Staudenmaier *et al*, 1989).

Synthetic analogues of siderophores are also transported into the cell by these uptake systems. Several compounds structurally similar to enterobactin have been used to determine the features important for recognition by the outer membrane receptor FepA. Of a variety of compounds tested, MECAM was transported into the cell at the same rate as Ent (Ecker *et al*, 1986) whereas some derivatives of MECAM were not able to support growth under iron-limiting conditions (Heidinger *et al*, 1983). In another study, only the left-handed isomer of Ent and TREN CAM, which has a tertiary amine substituted for the macrocyclic lactone ring (Figure 6.1), were recognized by FepA (Thulasiraman *et al*, 1998). This indicates that the chelating groups as well as the net charge of the molecule are important for recognition.

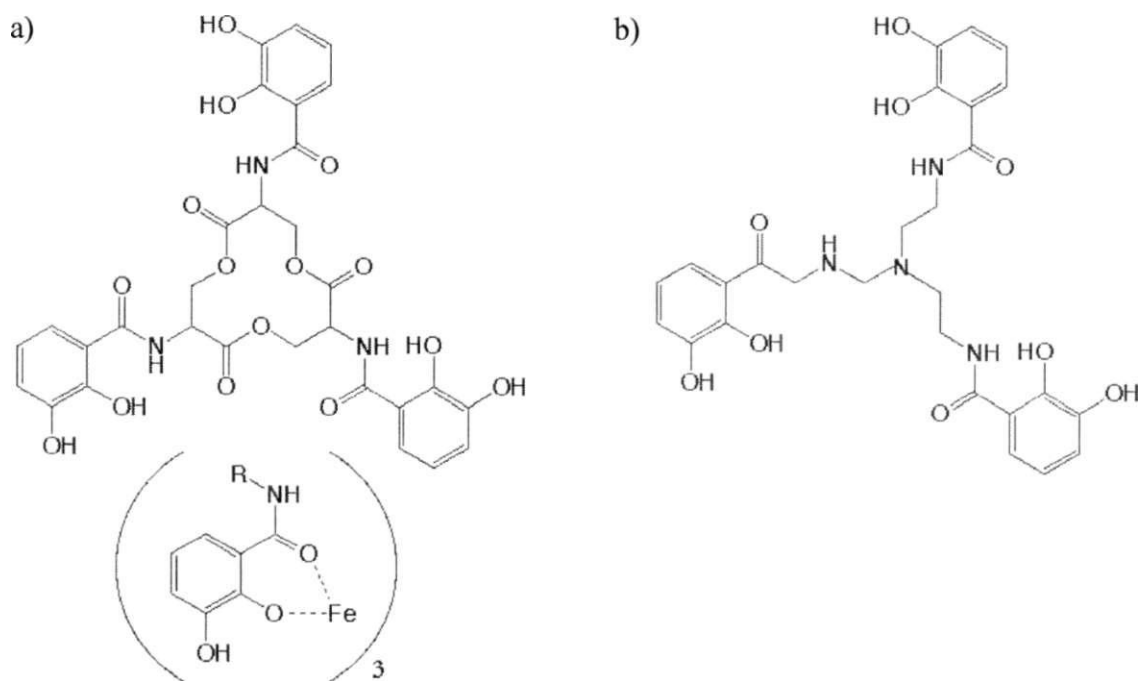


Fig. 6.1 Chemical structures of a) enterobactin (Cohen *et al*, 1998) b) TRENCA M (Thulasiraman *et al*, 1998).

The regulation of these genes is tightly controlled to limit iron uptake, since both ferric (Fe(III)) and ferrous (Fe(II)) iron can act as catalysts to produce deleterious hydroxyl radicals. Much of the control of the iron uptake systems is at the transcription level, negatively regulated by the Fur protein (Elkins and Earhart, 1989; Pressler *et al*, 1988). Fur binds to a consensus sequence (fur box or iron box) in the promoter region in the presence of iron but not in its absence (Litwin and Calderwood, 1993; Guerinot, 1994). In a unique response mechanism, the ferric citrate transport system of *E. coli* is repressed by Fe²⁺-Fur but activated by exogenous ferric citrate by a signal transduction event *via* TonB involving the conformational change of FecA and the consequential activation of FecR, then FecI, which activates transcription of

fecABCDE (Zimmermann *et al.*, 1984; Angerer and Braun, 1998), reviewed in Braun, 1995; Braun, 1997).

Energy for the active transport of ferric siderophores across the outer membrane is obtained from the cytoplasmic proton motive force utilizing the proteins TonB, ExbB and ExbD (reviewed in Braun, 1995). TonB is thought to shuttle between the cytoplasmic and outer membrane during energy transduction, then ExbB and ExbD recycles TonB (Letain and Postle, 1997). Subsequent transport of ferric siderophores across the inner membrane is dependent upon the energy provided by respective cytoplasmic membrane associated components.

Three distinct periplasmic proteins, FhuD, FepB and FecB, are involved in transport of ferric siderophores from the receptor protein across the periplasmic space to the cytoplasmic membrane components. Interestingly, the periplasmic proteins FhuD and FepB have less specificity for iron (III) hydroxamates and catechols, respectively, than the outer membrane receptors (Stephens *et al.*, 1995; Koster and Braun, 1990). The K_d of these interactions are very low, for FepB-FeEnt, the value is in the nanomolar range (Sprenzel *et al.*, 2000) while those for FhuD lie in the micromolar range (Rohrbach *et al.*, 1995a). FecB, thus far, appears to only transport ferric citrate (Pressler *et al.*, 1988). The amino acid sequences of FhuD, FepB and FecB are not significantly homologous to any other bacterial proteins involved in the uptake of amino acids or sugars. However, they share some sequence homology to the periplasmic vitamin B12 binding protein, BtuE, the anguibactin binding protein of *Vibrio anguillarum*, FatB and the siderophore binding protein, FhuD, of *Bacillus subtilis* (Koster W, 1991), with most of the homology in the N-terminal domains of FhuD, FepB, FecB and FatB (see Chapter 4) (Tarn and Saier, Jr., 1993).

Although very diverse in function, essential three-dimensional motifs are present in most bacterial periplasmic binding proteins (Quioco, 1990; Tarn and Saier, Jr., 1993). Periplasmic proteins generally have two similar globular domains, connected by two or three peptide stretches, with the ligand binding site located in the deep cleft between. A conformational change occurs upon ligand binding, whereupon the two domains close to bury the substrate (Quioco, 1990). Rotation of domains to a more compact structure upon metal

ion binding is also seen in the transferrins (Grossmann *et al.*, 1993). However, the structure of the *E. coli* periplasmic hydroxamate siderophore binding protein FhuD is distinct from other periplasmic proteins. The two domains of FhuD form a shallow binding pocket for the ligand. Since this is the first structure of a periplasmic ferric siderophore binding protein, it sets a precedent for the other siderophore binding proteins. The conformational change associated with ligand binding may also be different in FhuD and the other periplasmic ferric siderophore binding proteins.

In order to examine the conformational changes associated with ligand binding to the periplasmic proteins FepB and FecB, a number of techniques were employed. Changes in secondary structure were monitored by far-UV circular dichroism (CD) spectroscopy. Differences in size, shape or charge between the apo and holo forms results in changes in the migration rates on a native electrophoresis gel. Enzyme degradation studies were also used to distinguish between different forms of the proteins. The results of these experiments were compared to FhuD to establish if a common conformational change occurs when ligand binds.

Methods.

Cloning and expression of FepB. All molecular biology techniques were followed as outlined by Sambrook *et al.* (1989). The mature *fepB* sequence from pME13.18 (donated by Dr. C.F. Earhart, University of Texas at Austin (Elkins and Earhart, 1989)) was amplified by PCR using the primers TCFPB: 5'-GCTTTCAGGCATATGGCCGCAGTTCAG-3' and VLREV: 5'-AAGGATCCCAGTAGTAGGTTGAGGCCG-3' (University Core DNA Services, University of Calgary). These primers create unique *NdeI* and *BamHI* sites to allow insertion into the multiple cloning site of pT7-7 (Stan Tabor, Harvard Medical School, Boston, Mass.), creating pFepB7-8. The sequence of pFep7-8 was confirmed by the University Core DNA Sequencing Facility (University of Calgary). *E. coli* BL21(DE3) pLysS (Studier and Moffatt, 1986) cells were transformed with pFepB7-8 for protein production. For protein over-accumulation, cells were grown in LB media at 37 °C until $A_{600nm} = 0.6-0.8$, then induced with IPTG (80 mg/L) for 3 hours. Cells were harvested by centrifugation at 4°C then stored at -20°C.

Purification of FepB. Frozen cells were resuspended in 10 mM Tris pH 7.5 with DNaseI (10 ug/ml) and lysed by two passes through a French pressure cell at 1500 psi. The debris was pelleted at 15000 rpm for 30 min using a Beckman SS-34 rotor and the cell lysate was subjected to 50% ammonium sulphate precipitation. After centrifugation at 15000 rpm for 30 min, the supernatant containing the protein was chromatographed on a Sephacryl S-100 (Pharmacia) column using 10 mM Tris, pH 7.5, and then the pooled fractions were dialyzed extensively against 10 mM Tris, pH 7.5 at 4 °C. The resulting protein solution was loaded on a Q Sepharose column (Sigma Fine Chemicals), equilibrated with 10 mM Tris, pH 7.5. The protein was eluted with a 0-20% NaCl gradient, over 5 column volumes. For crystallization trials, FepB was further purified by anion exchange chromatography using the HQ column of the BioCad HPLC system (PerSeptive Biosystems). Once purified, the protein was dialyzed extensively against 10 mM Tris, pH 7.5 at 4 °C. Purity of the protein was monitored by 12% SDS-PAGE during each purification step. The quantity of the protein was determined using a

molar absorption coefficient, ϵ_{280} , calculated to be 44920 (Pace *et al.*, 1995). The calculated molecular weight of FepB is 32193 Da and migrates on 12 % SDS-PAGE at the appropriate position.

Purification of enterobactin. The *E. coli* strain AN 102 was generously donated by Dr. C.F. Earhart (University of Texas at Austin (Pierce *et al.*, 1983)). This strain (F⁻, pro⁻, leu⁻, trp⁻, fep⁻, thi⁻) is unable to transport Ent and requires proline, leucine, tryptophan, and thiamine for growth. It grows poorly on glucose minimal media and is unable to grow with succinate as the only carbon source (Young, 1976). Since the citrate transport system is available for iron transport in these cells, addition of citrate to succinate and glucose minimal media allows growth to occur.

The M9 salts media used (Sambrook *et al.*, 1989) was supplemented, when required, with 30 mM glucose, 30 mM succinate, 1 p M thiamine, 1.5 mM proline, 0.8 mM leucine, 0.2 mM tryptophan and 10 mM citrate, which were filter sterilized separately. When additional FeSO₄ (0.2 mM) was required, it was autoclaved together with the mineral salts media. To make plates, agar was added to the mineral salts media to a concentration of 15 g L⁻¹. All glassware used in the purification of the enterobactin was acid washed and all buffers were treated with Chelex (Bio-Rad Laboratories, CA) to remove any metal ions before use.

The procedure provided for enterobactin purification by Dr. C.F. Earhart was modified slightly. An agar plate containing the minimal salts media plus glucose, succinate, citrate and other supplements was streaked from the frozen stock of *E. coli* AN 102 and allowed to grow in an incubator at 37 °C for two days. A 20 ml flask of glucose and succinate minimal media with citrate was inoculated with a single colony of AN 102 and is grown at 37 °C with vigorous shaking overnight. A 100 ml subculture of the same media inoculated (1:100) from the 20 ml flask was then shaken overnight at 37 °C. This culture was used to inoculate (1:100) 4 L of M9 media containing glucose, succinate, amino acids and FeSO₄. Since the cells were iron-starved in this media, production of Ent ensues. This culture was grown with vigorous shaking at 37 °C until the peak of Ent production had been reached, approximately 18-20 hours. At this point, the cultures were deep pink from the accumulation of ferric Ent in the media (>10 pg ml⁻¹).

The amount of enterobactin in the media was estimated by withdrawing a 4 ml sample of the media, treating it with H_2SO_4 , and extracting with an equal volume of ethyl acetate. The ethyl acetate fraction was extracted with an equal volume of 0.1 M sodium phosphate buffer pH 7.0 to remove any hydrolysis products of Ent. The concentration of the sample was determined using the molar extinction coefficient for Ent in ethyl acetate at 316 nm, $9390 M^{-1} cm^{-1}$ (O'Brien and Gibson, 1970). The cells were then harvested by centrifugation at 4 °C and the media containing the FeEnt retained for further purification.

In order to keep the Ent in solution, 1/10 volume of ethyl acetate was added to the media. As the pH of the solution is lowered to 3 with concentrated HCl, the colour of the solution disappeared as the iron dissociates from Ent. This solution was extracted three times with a 1/5 volume of ethyl acetate, partitioning Ent and dihydroxybenzylserine (DBS) into the organic phase. Brownish films at the interface of the two phases were kept with the ethyl acetate layer. The ethyl acetate portions containing the products were concentrated in a rotary evaporator to a final volume of approximately 200 ml. The ethyl acetate was then evaporated over 100 ml of 25 mM $FeSO_4$ in 0.1 M sodium phosphate buffer pH 7.0. As the ethyl acetate evaporates, Ent and DBS transferred into the aqueous phase, which turned deep red. The aqueous FeEnt solution was adjusted to pH 7.0 with NaOH and at this point, the concentrated solution was kept overnight at 4 °C.

The aqueous FeEnt solution was extracted three times with equal volumes of ethyl acetate; the FeEnt and FeDBS stayed in the aqueous phase at neutral pH, while impurities soluble in ethyl acetate were removed. The pH of the aqueous solution was adjusted to 1 with concentrated HCl and extracted three times with an equal volume of ethyl acetate. The solution lost its red colour and the Ent and DBS transferred into the organic phase. The ethyl acetate washings were concentrated to 100 ml in the rotary evaporator.

In order to separate the DBS from Ent, the ethyl acetate solution was extracted once with an equal volume of 0.1 M sodium phosphate buffer pH 2.0 and then extracted three times with equal volumes of 0.1 M sodium phosphate buffer pH 7.4. The DBS partitioned into the aqueous phase while the Ent remained in the ethyl acetate phase. The ethyl acetate phase is dried with an appropriate amount of solid $MgSO_4$ and filtered through sintered glass. Once

concentration of Ent was determined, sufficient 1 mM FeCl₃ (or other metal ion, such as Ga₂N₃) in 0.1 M sodium phosphate pH 7.0 was prepared such that the final concentration of FeEnt was 1 mM. Using 4 L of culture, 15 mL of buffer solution is usually adequate. The ethyl acetate was evaporated over the buffer, forcing the Ent into the aqueous phase. FeEnt is then transferred into small aliquots and frozen at -20 °C.

Cloning and expression of FecB. The mature *FecB* sequence from *E. coli* K12 cells was amplified by PCR using the primers RDFWD: 5'-GCCTTTGCCCATATGGTTCAGGAC-3' and RDREV: 5'-CGCGGATCCTTCACAACGGTAAG-3' (University Core DNA Services, University of Calgary). These primers create unique *NdeI* and *BamHI* sites to allow insertion into the multiple cloning site of pT7-7 (Stan Tabor, Harvard Medical School, Boston, Mass.), creating pFecB. The sequence of pFecB was confirmed by the DNA Sequencing Facility (University of Calgary). *E. coli* BL21(DE3)pLysS (Studier and Moffatt, 1986) cells were transformed with pFecB for protein production. For expression, cells were grown in LB media at 30 °C until A_{600nm}=0.6-0.8, then induced with IPTG (80mg/L) for 4h. Growing the cells at 30 °C decreased the formation of protein inclusion bodies and an increased amount of soluble protein was recovered from the cells. Cells were harvested by centrifugation at 4°C then stored at -20°C. All cloning and initial expression studies were done in collaboration with Ryan Deedo (Undergraduate project student, University of Calgary).

Purification of FecB. Frozen cells were resuspended in 10 mM Tris pH 8.5 with DNaseI (10 ug/ml) and lysed by two passes through a French pressure cell at 1500 psi. The debris was pelleted at 15000 rpm for 30 min using a Beckman SS-34 rotor. The lysate was loaded on a DEAE column, equilibrated with 10 mM Tris pH 8.5 at 4 °C. The column was washed with five column volumes of buffer or until the A₂₈₀ was below 0.1. The protein was eluted with a 0-0.25 M gradient of NaCl. FecB eluted at 0.15 M NaCl. Once purified, the protein was dialyzed extensively against 10 mM Tris, pH 8.5 at 4 °C. Purity of the protein was monitored by 12% SDS-PAGE during each purification step. The quantity of the protein was determined using a molar absorption coefficient, 8280, calculated to be 42970 (Pace *et al.*, 1995). The

molecular weight of FecB is 30787 Da and the protein migrates at the proper position on a SDS-PAGE gel.

Circular dichroism spectroscopy. CD spectra were recorded at 25 °C on a Jasco J-715 CD spectropolarimeter using a cell path length of 0.1 cm at pH 7.5. The concentrations of Tris buffer and protein were 10 mM and 10 pM. Iron loaded siderophores or Ga TRENCAM (donated by Dr. K. N. Raymond, University of California Berkley) were titrated into the sample by 0.5 equivalent increments from stock solutions of 10 mM to 10 times excess ligand. For each sample, five scans with 0.2 nm step resolution at 50 nm min⁻¹ scan rate, 2 s response time and 20 mdeg sensitivity from 225-185 nm were averaged, the baseline subtracted and a small degree of numerical smoothing applied.

Non-denaturing PAGE. 25 pg of protein was incubated with 0.5, 1, 5 and 10 equivalents of siderophore in 50 pi 10 mM Tris pH 7.5 for 30 min. In order for the samples to stay in the wells of the 12% native PAGE gel, an equal volume of 50% glycerol was added to each sample. The gels were placed in 25 mM Tris, 0.192 M glycine pH 8.8 running buffer. The PAGE gels ran for 3 hours at a constant 80 V to allow proper separation between the bands of protein.

Proteolytic protection assays. FecB and FepB were analyzed with respect to processing and stability in a protease protection assay as previously described (Koster and Braun, 1990; Rohrbach *et al.*, 1995a, b). However, in this experiment, the samples were kept at room temperature after enzyme was added.

Crystallization of FepB. Crystals of FepB were grown at 20 °C by hanging drop vapour diffusion from 5 pi drops containing 10 mg ml⁻¹ of purified FepB, 4% PEG 8000, 50 mM sodium cacodylate pH 8.8 and 100 mM zinc acetate. The drops were equilibrated against a 1 ml reservoir containing 8% PEG 8000, 100 mM sodium cacodylate pH 8.8 and 200 mM zinc acetate. Large, needle-like crystals grew within one week. For cryo-crystallography

experiments, crystals were soaked in a stabilizing solution identical to the reservoir solution with a final concentration of 30 % (v/v) glycerol.

Diffraction data on FepB crystals was collected on a Rigaku RUH3RHB rotating copper anode x-ray generator equipped with Osmic confocal multilayer x-ray focussing optics and a MAR345 image plate scanner. Data were collected on crystals frozen to -160 °C in a cold gas stream generated by an Oxford Cryostream crystal cooling device. Data were indexed, integrated and scaled using DENZO/SCALEPACK (Otwinowski and Minor, 1997).

Results.

Overproduction of FepB and FecB and purification. In attempts to overexpress the *E. coli* periplasmic protein FhuD, it was found that a functional, mature protein could be produced in the cytoplasm of the cell (Rohrbach *et al*, 1995b). This strategy, where the signal sequence of the protein is not included in the cloned gene, was employed to overproduce FepB and FecB. These proteins, unlike FhuD, do not contain a His-tag sequence, or the like, to facilitate protein purification. Since these tag sequences could potentially interfere with characterization of the protein, it was more desirable to obtain the protein simply in the mature form. Most of the FepB protein produced could be isolated from the soluble portion of the cells. On the other hand, a greater proportion of FecB was insoluble and likely was sequestered in inclusion bodies. Purification from the inclusion bodies was not attempted to avoid problems refolding the protein to a functional state. If the temperature of the culture was decreased to 30 °C, more of the protein produced was soluble, but the amounts accumulated were lower.

After precipitation with 50% ammonium sulfate, FepB remains soluble while many other contaminating proteins are precipitated. This step in the purification protocol of FepB is different than that of Sprencel *et al* (2000), where FepB is precipitated by ammonium sulfate, then dialyzed before purification on a DE-52 column. The method used here is gentler than precipitating the protein with salt, since the protein could potentially be denatured in the latter method. The protein solution was passed through a gel filtration column to desalt the protein before using the strong anion exchange Q Sepharose column. Only one band corresponding to a molecular weight of 32 kDa was purified (Figure 6.2). Usually 12 mg of purified FepB was obtained from 1 L of culture.

Weak anion exchange DEAE matrix was used to purify FecB. R/measurements for FecB from SDS-PAGE estimated a molecular mass of 31.5 kDa. There were several minor bands of lower molecular weight present during protein purification (Figure 6.3). The presence of 0.1 mM PMSF diminished the amount of these bands. At least 9 mg of purified FecB was obtained from 1 L of culture. However, FecB is an unstable protein and after a week stored in solution at a low concentration at 4 °C or at 20 °C, much of the protein was precipitated and

many bands less than 31.5 kDa were present.

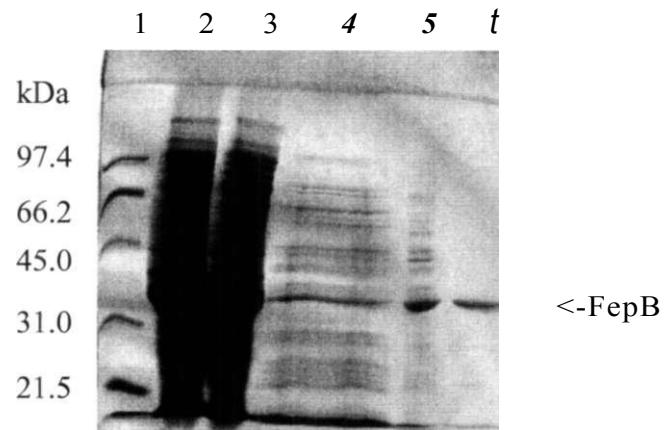


Fig. 62 A 12% SDS-PAGE gel following the purification of *E. coli* FepB. Lane 1, molecular weight standards; lane 2, whole cells; lane 3, cell lysate; lane 4, soluble proteins after the 50% ammonium sulphate precipitation; lane 5, pooled fractions from the gel filtration column; lane 6, pooled fractions from the Q Sepharose column.

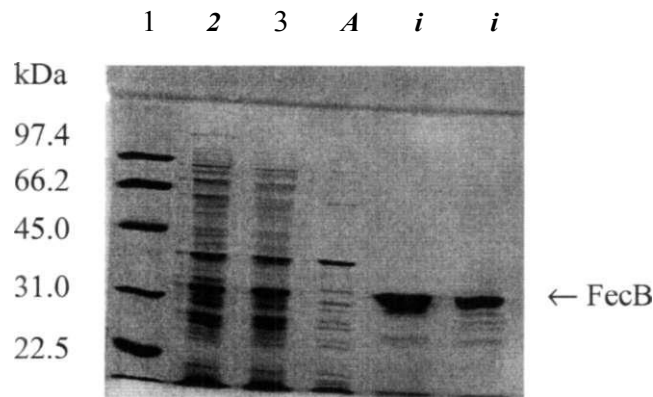
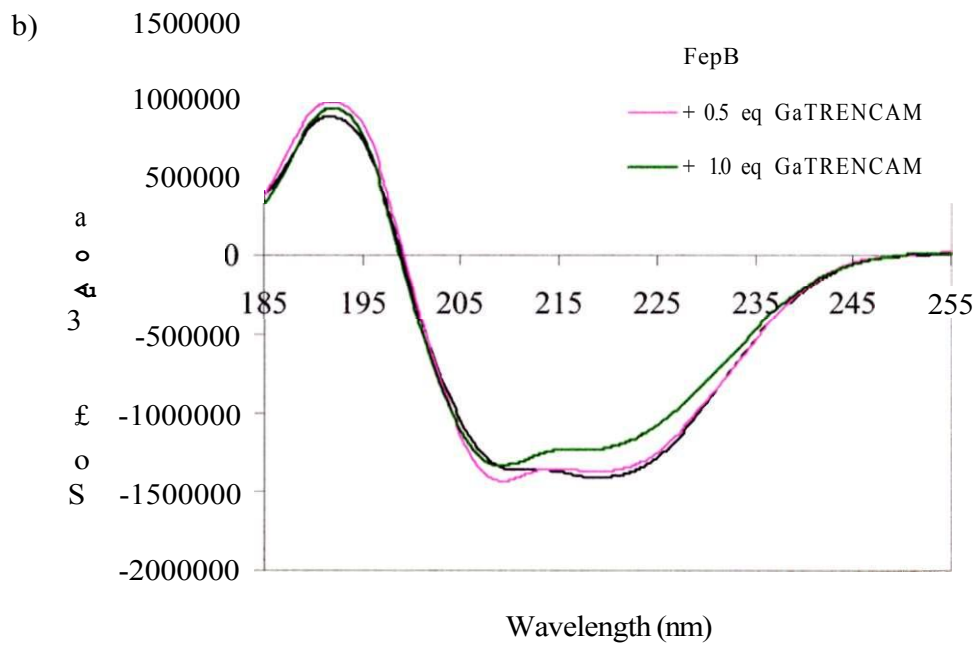
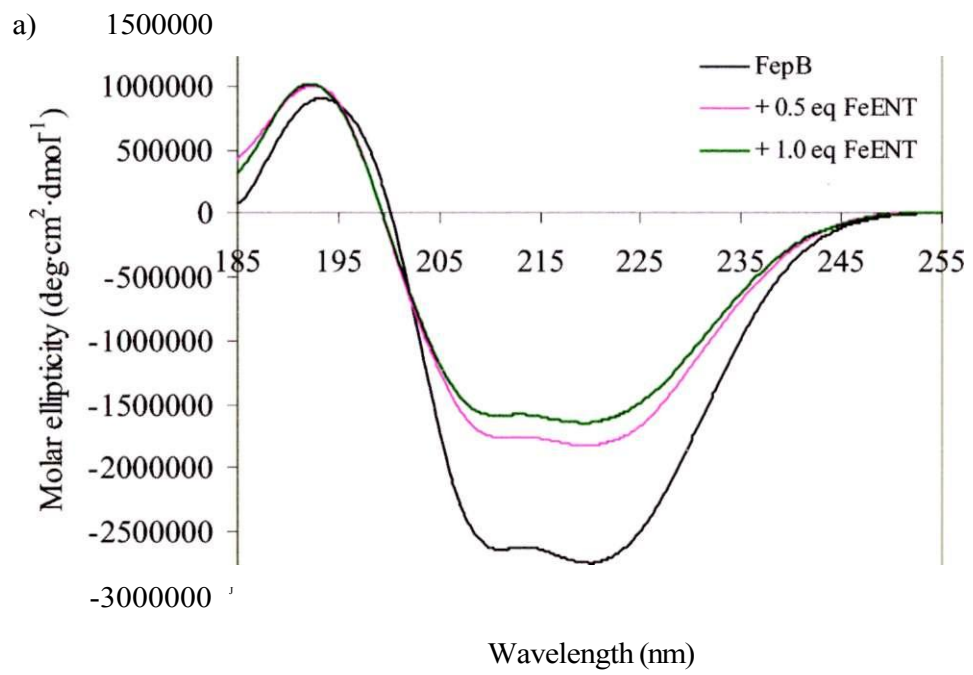


Fig. 6.3 A 12% SDS-PAGE gel monitoring the purification of *E. coli* FecB. Lane 1, molecular weight standards; lane 2, whole cells; lane 3, cell lysate; lane 4, unbound proteins from the DEAE column; lane 5, pooled fractions from the DEAE column; lane 6, dialyzed FecB. Note the presence of smaller molecular weight bands on the protein gel. Addition of 0.1 mM PMSF in subsequent purifications diminished the presence of these bands.

Circular dichroism spectroscopy. The far-UV CD spectra of these periplasmic proteins show that they have a significant proportion of α -helical structure, as shown by the negative ellipticities at 208 nm and 222 nm (Figure 6.4). When siderophores are added to either protein, there is a change in the ellipticities, indicating a change in the helical secondary structure of the protein. When siderophores are added in excess, the CD spectrum of either protein complex does not change considerably.

The changes in the CD spectra of FepB when FeEnt or GaTRENCA M vary in amount. When FeEnt is added, there is a dramatic increase in the ellipticity at 208 nm and 222 nm as shown in Figure 6.4a. If GaTRENCA M is added to the protein solution, the increase in ellipticity is not as pronounced (Figure 6.4b). Since it is already known that both of these ligands are able to bind to FepB, the structural change experienced by FepB could vary in amount or occur by another mechanism. When ferric citrate is added to FecB, there is a large decrease in ellipticity at 208 nm and 222 nm (Figure 6.4c). This change is different than the effect found for FepB and FhuD when titrated with different siderophores.



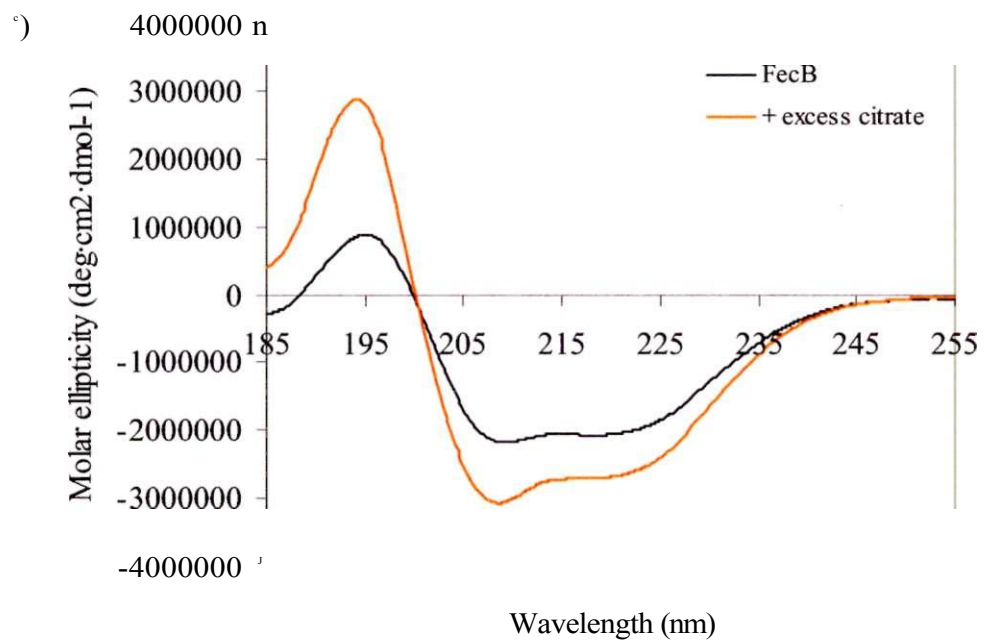


Fig. 64 Far-UV CD spectra of a) FepB titrated with FeEnt, b) FepB with Ga TREN CAM and c) FecB with ferric citrate. The change in ellipticity when ligand is added is very different in each case. The CD spectra did not change with the addition of excess siderophore.

Band shift assays. In the formation of a protein and ligand complex, there may be a change in the size of the complex, in conformation or a difference in charge which results in different migration on a native electrophoresis gel. This technique has been used successfully with other protein complexes, to demonstrate that the protein complex has a mobility unlike the protein alone.

The migration of FepB and complexes through the gel was much slower than when FhuD was electrophoresed on a similar native gel. The p_is of these proteins are different, so the migration rate was expected to be faster for FepB (p_i = 5.12) than FhuD (p_i = 5.9) so the difference in migration between the two proteins could be attributed to differences in conformation. A change in the mobility of the FepB complexes is seen on the native gel. When FeEnt or GaTRENCA M is bound to the protein, the complex migrates faster on the gel (Figure 6.5). This effect is likely due to a change in conformation in the protein when ligand is bound. If the complex forms a more compact structure, it migrates faster through the matrix. This effect cannot be attributed to a change in charge or molecular weight. These features would result in a decrease in the migration since the complex would be positively charged and larger than the apo form of the protein. The apo protein and complexes cannot be resolved on a gel filtration column since the difference in size is very small.

The migration rate of FecB and complexes on the native gel is even slower than the migration of FepB and FecB. This effect can also be attributed to the different p_i of FecB (p_i = 8.2) compared to the other proteins. At the pH of the gel and running buffer, pH 8.3, this protein is less negatively charged than the other proteins. There doesn't appear to be a significant difference in mobility between the apo protein and the protein complex. In this case, the combination of a change in size, conformation and charge in the formation of a complex does not result in a mobility shift (Figure 6.5).

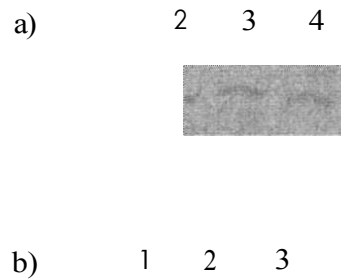


Fig. 6.5 Mobility differences between apo and holo proteins on a native PAGE, a) FepB complexed to siderophores, lanes 1 and 2, FepB; lane 3, FepB complexed with FeEnt; lane 4, FepB complexed to GaTRENAM. b) FecB complexed with ferric citrate, lane 1, FecB; lane 2, FecB with 1 equivalent ferric citrate; lane 3, FecB with excess ferric citrate. Excess ligand was added to the protein, allowed to form a complex, and then the complex was dialyzed to remove any unbound ligand. The FepB complexes migrate slightly faster in the polyacrylamide matrix.

Protease protection assays. Previous studies of degradation by added proteases have shown that the formation of a complex between FhuD and ferric siderophores protects the protein from degradation (Rohrbach *et al.*, 1995a, b). This indicates that binding of these ligands stabilize a proteolytic resistant conformation of the protein that may be different from the apo form (Rohrbach *et al.*, 1995a, b). FepB is degraded by trypsin and proteinase K in the absence of siderophores (Figure 6.6, lanes 4-6). Digestion of FepB in the presence of FeEnt or GaTRENAM decreases the rate of proteolytic cleavage slightly (Figure 6.6, lanes 7-12). There is an extra band that appears during the degradation of FepB but even without siderophore added, it is quite resistant to degradation by trypsin and proteinase K. Even when the reaction is allowed to proceed longer, there is not much more degradation observed. FecB, on the other hand, is a very unstable protein and is quickly degraded in both the presence and absence of ferric citrate.



Fig 6.6 Protection of FepB from degradation by trypsin in the presence of siderophores. Lanes 1-3, control sample with no trypsin added; lanes 4-6, trypsin added to FepB; lanes 7-9, FeEnt added; lanes 10-12, GaTRENAM added. Samples were taken at 0, 15 and 30 min after trypsin was added.

Crystallization Trials. The FepB crystals obtained with the hanging drop crystallization method are shown in Figure 6.7. They grow from the nucleation site in long thin needles. These crystals diffract to 3.0 Å, but cannot be indexed to a single space group. Several layers of crystals stack on one another, so the diffraction patterns obtained do not result from a single crystal. Attempts to crystallize FepB with enterobactin or Ga TREN CAM and FecB with and without ferric citrate were not successful.

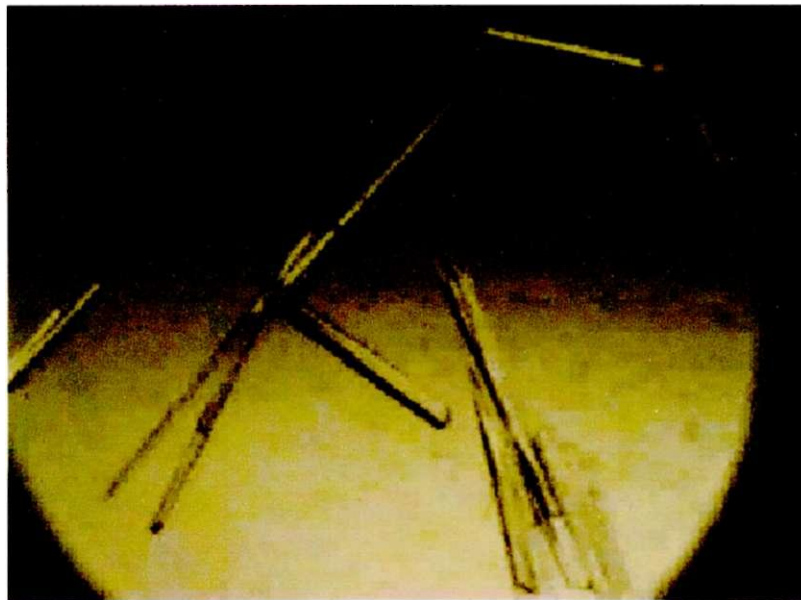


Fig. 6.7 FepB crystals grown in a hanging drop. The crystals are colourless and form long needles.

Discussion.

Although the level of amino acid sequence homology between periplasmic ligand binding proteins is relatively low, their three-dimensional structures are often very similar (Quiocho and Ledvina, 1996). These key structural features may be required for the common function they perform within the periplasm of the cell. Certain characteristics of the periplasmic protein structure are retained in order to bind ligands with high affinity and transport them to the inner membrane associated proteins. The unusual structure of the *E. coli* ferric hydroxamate binding protein FhuD reveals another means to function in the same capacity. The native structures of the other *E. coli* ferric siderophore binding proteins FepB and FecB could resemble that of the related FhuD or may be similar to the structure of other periplasmic binding proteins. However, the behaviour of these proteins sets them apart from both possibilities. Nonetheless, a common feature between all periplasmic proteins for proper function in the cell, as discussed in Chapter 5, is that it is likely that a conformational change occurs when the ligand binds to the protein.

The function of the catecholate binding protein FepB is analogous to other periplasmic binding proteins; to shuttle ligands from one side of the periplasmic space to the other side. Several distinct characteristics of FepB set it apart from its colleagues. Sprencel *et al.* (2000) suggest that FepB is unlike the amino acid and sugar binding proteins since it is expressed at lower levels, has such a high affinity for ligands and may have a lipid posttranslationally attached. They also believe that FepB is unlike FhuD since it is more selective when binding ligands. FepB binds FeEnt (natural form or the enantiomer) but does not bind the similar catecholate agrobactin (Sprencel *et al.*, 2000) or vibrobactin (Wyckoff *et al.*, 1999). More specificity between the protein and ligand implies that the size of the binding site is limited and there are more interactions in the binding site. If the binding site is deeper than the shallow pocket of FhuD, where only part of the molecule is bound, more interactions could occur between the protein and ligand. In addition, the negative charge of the ligand may influence the manner in which the ligand is bound in FepB, by neutralizing the charge or dissipating it through a network of hydrogen bonds. On the other hand, like FhuD, the fluorescence of the tryptophans of FepB decreased in the presence of ligands but the maxima did not shift

wavelength (Sprenzel *et al.*, 2000). Thus, both proteins apparently do not experience a great change in the environment of their tryptophans.

In this study, the conformational change that occurs when FepB binds siderophores is unlike FhuD. The changes observed in the secondary structure are more dramatic than in FhuD, but quantitation of the changes to the secondary structure using CD spectra is difficult to determine. As well, the protein converts to a more compact form in the complex that is visible as a band shift on native acrylamide gels and a decrease in the hydrodynamic radius. If the ligand is buried in the holo form of the structure, binding may stabilize a more compact form.

To date, the description of FecB is less complete compared to the other siderophore binding proteins in the periplasm. Since *fecB* is part of the *fee* operon and encodes a periplasmic protein, it is implicated in citrate transport in the periplasm of the cell (Staudenmaier *et al.*, 1989). This protein also has some sequence homology to FepB and FhuD. Like FhuD and FepB, the levels of FecB are also very low in the cell (Ames, 1986). The *fee* uptake system, induced by the presence of exogenous citrate, requires a high turnover of the proteins involved in citrate uptake. The inherent instability of FecB may be a part of the response mechanism of the cell to citrate. Since this protein appears to be specific only for citrate, the binding site of the ligand may be designed differently than the other periplasmic binding proteins. From this study, it was found that the conformational changes that occur when FecB binds citrate are limited. Very little difference is seen in size or shape in the assays, similar to the results found for FhuD in Chapter 5.

The characteristics of each of the periplasmic siderophore binding proteins are tailored to their role in the cell. Each protein design is exploited in different ways to operate efficiently in the cell. FhuD can easily scavenge the periplasm, scanning for many different potential ligands with its shallow binding pocket, conserving energy by making small conformational changes. FepB would only be present in the periplasm when Ent is produced endogenously, to specifically bind the ligand, undergoing a large conformational change. FecB is also produced in response to a certain stimulus, specifically binds that ligand and is quickly degraded after use. The overall structure and mechanism of binding of these periplasmic proteins are matched to their function.

Chapter 7

Concluding Remarks

With the possible exception of lactobacilli, all known bacteria absolutely require iron to live. While iron is the fourth most abundant element in the Earth's crust, it is found mainly as insoluble ferric (Fe^{3+}) hydroxides. To overcome the problem of iron scarcity, pathogenic bacteria have evolved efficient strategies for procuring iron from human and animal hosts by extracting the metal from proteins such as transferrin, lactoferrin, and hemoglobin. To liberate iron from eukaryotic iron-binding proteins, a wide variety of microbes synthesize and secrete low-molecular-weight (500 to 1000 Da) organic chelators called siderophores. Siderophores function by complexing and removing iron from the host proteins or by scavenging it from precipitates of ferric hydroxide, making it available for microbial use. Many types of hydroxamate and catechol-like siderophores, as well as citrate, are utilized by *Escherichia coli*, of which only enterobactin is actually synthesized by the bacteria itself. In *E. coli* and other Gram-negative strains, transport of siderophores involves a specific outer membrane receptor, a periplasmic transport protein and several inner membrane associated proteins. This arrangement is similar to other periplasmic protein dependent ATP-binding cassette (ABC) transporters, which transport amino acids, peptides and sugars into the cell (Nikaido and Saier, 1992). Although there are specific outer membrane receptors in *E. coli* for each hydroxamate-type siderophore (aerobactin, ferrichrome, rhodoturulate, coprogen and ferrioxamine B) and catechol-like compound (enterobactin and dihydroxybenzylserine), common systems within the periplasm and inner membrane are used which are encoded by the *fhu* and *fep* operons respectively (Fecker and Braun, 1983; Shea and McIntosh, 1991). Ferric citrate is internalized via the transport system encoded by the *fee* genes (Staudenmaier *et al*, 1989).

FhuD is the periplasmic binding protein involved in the uptake of hydroxamate-type siderophores and is considered to be a potential drug target. The three dimensional x-ray crystal structure of FhuD from *E. coli* complexed with the ferrichrome homolog gallichrome was determined at 1.9 Å resolution using MAD phasing (Clarke *et al*, 2000). This represents the first structure of an ABC-type periplasmic binding protein involved in

the uptake of siderophores. The protein is shaped like a kidney bean, with two globular domains connected by a long helix. This is unlike most periplasmic ligand binding proteins (PLBPs), which usually have several strands linking two domains together (Quioco, 1990; Quioco and Ledvina, 1996). This helix forms a rigid architecture that may hinder the large conformational changes typically observed in PLBPs upon ligand binding. The gallichrome binds in a shallow hydrophobic pocket between the two domains of the protein. Crystal structures of FhuD complexed with other siderophores, including coprogen, the iron chelation drug Desferal® and the antibiotic albomycin were also solved by x-ray crystallography. These show that binding occurs in a similar manner, with slight movement of amino acid side chains within the binding pocket. These structures will be further refined by modeling the siderophores as rigid bodies to prevent changes in bond lengths and angles.

The function of periplasmic binding proteins is based upon their ability to specifically bind their ligands and shuttle them to the inner membrane associated proteins. Conformational flexibility in structure can facilitate ligand binding and recognition of the holo complex by other members of the transport system. In many periplasmic proteins, β -strands connecting the two domains of the protein form a hinge region and the base of the binding cleft. The hinge bends due to small changes in the ϕ and ψ angles of only two or three residues in the β -sheets connecting the two domains. The protein envelops the substrate in the binding cleft with the two domains like a "Venus fly trap" (Mao *et al*, 1982; Ames, 1986) or "Pac-man". Many interactions form between the protein and ligand, providing specificity. In addition, the final closed conformation of the receptor-ligand complex is important for making the proper interactions with the inner membrane permease proteins.

It is remarkable that FhuD functions in the same capacity as other periplasmic proteins, particularly other iron transport proteins, since the structure of the protein is so different than the norm. Attempts to crystallize the apo form of FhuD to determine the differences between the apo and holo forms were unsuccessful. The range of motion experienced by FhuD when binding substrate could be limited, even more than in the structurally related proteins PsaA and TroA, due to the presence of the hydrophobic

interface between domains. The α -helix connecting the two domains of the protein inhibits the amount of separation between the domains. The number of hydrogen bonds integrated into the helical structure is greater than in a sheet structure so the energy barrier required, even for minor changes in the peptide backbone angles, is higher. There are also many hydrophobic interactions between the inside of the helix and the bottom of the domains. In addition, the binding pocket of FhuD is entirely distinct from the most structurally related metal binding proteins, PsaA and TroA, as well as other periplasmic iron transport proteins. To accommodate the large ferric siderophore complex, the binding site in FhuD is considerably more solvent exposed and wider than those for uncomplexed metal ions. Therefore, the contact surface of the protein is limited to a small surface of each the domains. Since the siderophore remains solvent exposed in FhuD, it is not enveloped by the protein and there are not as many interactions. This is in contrast to the iron bound by the periplasmic *Haemophilus influenzae* ferric iron binding protein, which is buried, coordinated by several side chain residues, a phosphate ion and a water (Bruns *et al*, 1997). From the numerous spectroscopic and diagnostic studies presented, it is evident that the two forms of FhuD, the apo and holo forms, are distinguishable. Interaction with the inner membrane proteins may also facilitate domain motion in order to release the ligand. Attempts to co-crystallize or soak peptides, corresponding to the areas of FhuB found to interact with FhuD (Table 7.1) (provided by Dr. H. Killmann, Universitat Tubingen), were not productive. However, the differences between the two forms is small; although significant enough for function within the cell. With this in mind, FhuD could be implicated in a distinctive mode of iron transport in Gram-negative bacteria.

Table 7.1 FhuB peptides used in crystallization

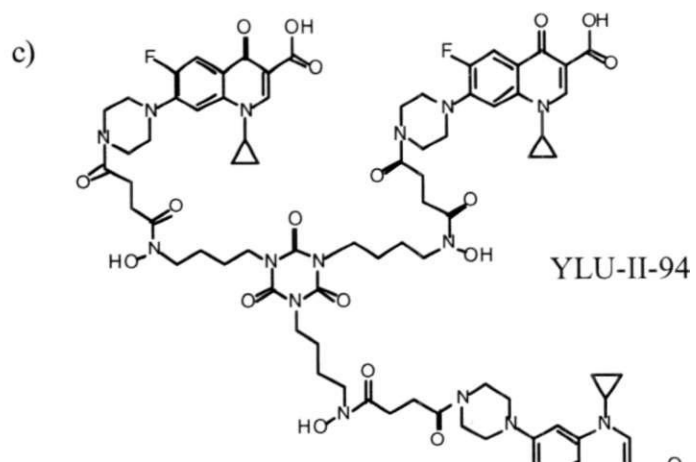
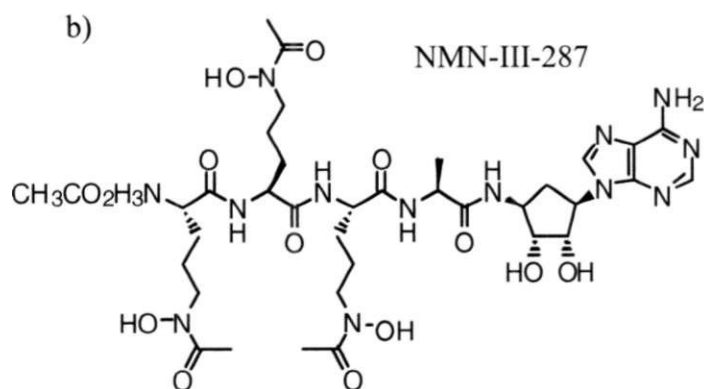
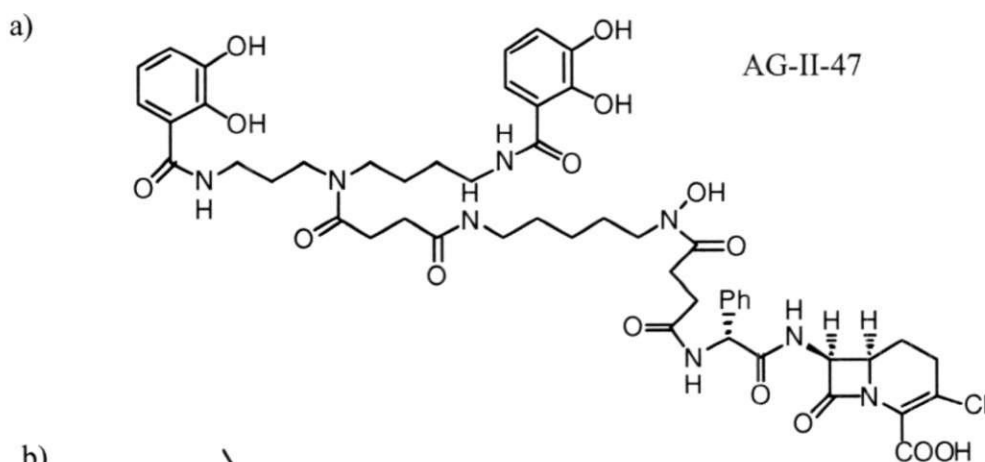
Name of peptide	Sequence	Molecular weight (g/mol)
2.7bi	Biotinylated-ASMFLWSTGTL-NH ₂	1751.16
T7.1	H-RRWLTILPLG-NH ₂	1223.54
T7.2	H-CRRWLTILPL-NH ₂	1269.62

Mutations to FhuD in the binding site, R84Q and Y106A, and the helix connecting the two domains, P167A, showed that these residues are important for the function of the protein. The affinity for hydroxamate type siderophores decreased in these proteins, as determined by the change in fluorescence spectra when ligand was added. The conformational changes of FhuD mutants also were also very limited when ligand bound. An interesting observation about the mutant proteins is that they did not crystallize under the same conditions as the wild type protein. In fact, crystals for the mutant proteins, either with or without ligand, were not obtained during the duration of this thesis. This indicates that the mutant proteins are significantly different than the wild type FhuD, since other types of proteins with more conservative mutations easily crystallize.

The conformational changes of the other periplasmic siderophore binding proteins FepB and FecB are slightly different than those observed for FhuD. FepB seems to convert to a more compact form when ligand is bound, similar to changes observed in "classical" periplasmic binding proteins. This form of the protein is easily distinguished from the apo form by various types of spectroscopy and other experiments. Analysis of FecB shows that the differences between the apo and holo forms of the protein are less discernible. Since FecB is such an unstable protein *in vitro*, some of these analyses were inconclusive. Thus, the mechanism for ligand recognition and therefore structure of these proteins may be distinct from FhuD. Of course, further structural studies of these proteins are required for more conclusive results.

One of the more interesting applications from this study is to design novel bacteriostatic agents. Co-crystallization of FhuD with a number of hydroxamate-like siderophore-antibiotics (Figure 7.1) (provided by Dr. M.J. Miller, University of Notre Dame) was fruitless. It was not clear if these compounds were not able to bind to FhuD or if they were too large, interfering with packing in the crystal. As an additional investigation, the process of structure-based drug design, which uses structural information in order to design novel ligands that bind tightly and selectively to a particular protein, was undertaken (Martin, 1992; Verlinde and Hoi, 1994; Bohm, 1996). There are a number of different methods now available that can suggest novel structures that can serve as lead

compounds or act as a stimulus for creativity. Computational methods exist to either a library of existing molecules or to design a molecule *de novo*.



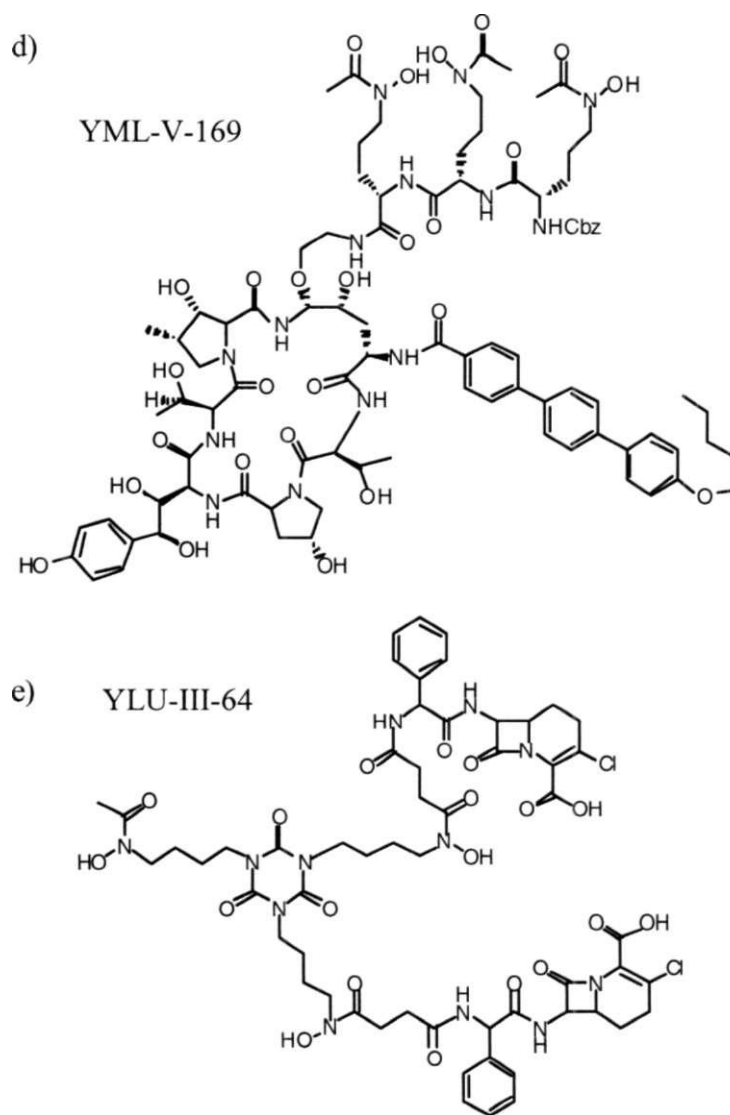


Fig. 7.1 Siderophore-antibiotic conjugates from the Miller group used in crystallization trials, a) AG-II-47 is a mixed ligand siderophore which may be able to use multiple iron transport pathways (Ghosh *et al*, 1996). b) NMN-III-287 (Ghosh *et al.*, 1999) and c) YML-V-169 are trihydroxamate tripeptide conjugates of synthetic alanyl azanoraristeromycin and echinocandin B, respectively, d) YLU-II-94 and e) YLU-III-64 are multiwarhead siderophore conjugates.

An easy program to use to create new ligands for the binding pocket of a protein is LigBuilder (Wang *et al*, 2000). This program builds a new molecule in the binding site using a library of organic fragments according to chemical rules. In the first stage of the process, POCKET, key interaction sites between the ligand and the binding pocket are identified. Either of two modules can be used to build the molecule into the site. The GROW strategy attaches additional units from the fragment library to a "seed" molecule placed in the binding site. With the LINK module, the program attempts to attach several pieces that have been placed in the binding pocket that maximize the interactions with the target protein. Finally, the structures are evaluated using ANALYZE, which estimates binding affinities for the ligand by an empirical scoring function and bioavailabilities by a set of chemical rules.

Novel ligands for FhuD were generated using the LigBuilder program from the crystal structure. The binding site of FhuD contains two residues which hydrogen bond to the siderophores used in this study and is lined with numerous hydrophobic molecules. From the analysis of the crystal structures of FhuD bound to various siderophores in Chapter 3, the protein recognizes the iron bound to the hydroxamate ligands of the siderophore. For this preliminary investigation of structure-based drug design, the iron binding core area of the siderophores, consisting of the iron atom and the three hydroxamate ligands, was used as a starting structure for generating new molecules. The POCKET module was first used to analyze the binding site for key regions of interactions (Figure 7.2). In addition to the predictable interactions found in the binding pocket proper, an interaction site was found by the program more in the interior of the protein. This is the area where coprogen inserts its functional group in the crystal structure. Next, GROW was used to add fragments to the sites identified on the seed molecule as growing sites (Figure 7.3). In all, 200 new compounds were created which conform to the binding site of FhuD. The default parameters for each stage of the ligand design were used. It was not expected that a compound similar to any of the siderophores would be produced since the space outside the binding site, where the majority of the molecule resides, was not included in the allowable area for the molecule. Many different parameters could be optimized to produce

a more biologically relevant molecule. However, the potential for drug design using this type of program is clearly evident.



Fig 7.2 Key interaction sites of the binding pocket of FhuD. The protein and ligand are shown in wireframe with the interaction sites modeled as a surface in the binding pocket.

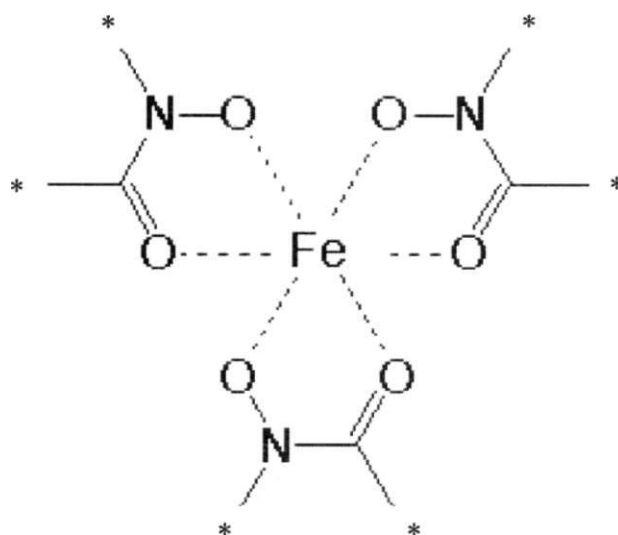


Fig 7.3 The seed structure used by GROW. This is the iron binding core of the siderophore that is recognized by FhuD. Growing sites are labelled by *.

A discussion of the results of these experiments is not complete without an indication of the sources of error of these techniques and suggestion of improvements to the method. Although several sources of error are indicated in each chapter, a few are worth mentioning here. The major limitation with protein x-ray crystallography is that it produces a static model of the structure of the protein. In this technique, the concentration of protein is unrealistically high and crystal packing may interfere with the proper conformation of the protein. Ideally, the structure would be determined in an environment not unlike that found *in vivo* but technology has not advanced far enough for this to be possible. Be that as it may, it is accepted that the crystal structure is a reasonable approximation of the structure of the protein. When determining the binding constants using the intrinsic fluorescence of the protein, several factors can interfere. When the protein is excited at a certain wavelength, even one chosen to selectively excite one population of fluorophore, the energy can be transferred to other fluorophores. This results

in fluorescence emission from a variety of sources. This could be limited by specifically labelling residues found in the binding site with a fluorophore, whose emission and excitation spectra do not overlap with any other fluorophores present, to examine the effects of ligand binding. Another problem encountered with the fluorescence experiments with FhuD is that oxygen was acting as a quenching agent during the titration of siderophore or acrylamide. This interfered with an accurate determination of the binding constants for different siderophores and the solvent exposure of the tryptophan residues. Using the Jobin-SPEX Fluorolog 3-21 spectrofluorimeter, which is a more sensitive instrument, equipped with a stir plate improved the accuracy of the results. However, to limit the amount of oxygen present in the sample, degassed solutions should be used and the solutions gently agitated with a bent rod.

Combining the information from the structure of FhuD and some biochemical analysis, as well as data from the experiments with the related proteins FepB and FecB, the mechanism utilized by the periplasmic ferric siderophore binding proteins to recognize ligands is clearer. As we can see, the information acquired from the structure of a protein does not always provide us with absolute answers to how the protein functions. Rather, it is a starting point for more investigation.

References

- Abdallah, M.A. 1991. Pyoverdins and pseudobactins. *In* Handbook of Microbial Iron Chelates. G.Winkelmann, editor. CRC, Boca Raton. 139-53.
- Adhikari, P., S.A.Berish, A.J.Nowalk, K.L.Veraldi, S.A.Morse, and T.A.Mietzner. 1996. The *fbpABC* locus of *Neisseria gonorrhoeae* functions in the periplasm-to-cytosol transport of iron. *J. Bacteriol.* 178:2145-2149.
- Adhikari, P., S.D.Kirby, A.J.Nowalk, K.L.Veraldi, A.B.Schryvers, and T.A.Mietzner. 1995. Biochemical characterization of a *Haemophilus influenzae* periplasmic iron transport operon. *J. Biol. Chem.* 270:25142-25149.
- Althaus, E.W., C.E.Outten, K.E.Olson, H.Cao, and T.V.O'Halloran. 1999. The ferric uptake regulation (Fur) repressor is a zinc metalloprotein. *Biochemistry* 38:6559-6569.
- Altschul, S.F., T.L.Madden, A.A.Schaffer, J.Zhang, Z.Zhang, W.Miller, and D.J.Lipman. 1997. Gapped BLAST and PSI-BLAST: a new generation of protein database search programs. *Nucleic Acids Res.* 25:3389-3402.
- Ames, G.F. 1986. Bacterial periplasmic transport systems: structure, function and evolution. *Annu. Rev. Biochem.* 55:397-425.
- Andrews, S.C. 1998. Iron storage in bacteria. *Adv. Microb. Physiol* 40:281-351.
- Angerer, A. and V.Braun. 1998. Iron regulates transcription of the *Escherichia coli* ferric citrate transport genes directly and through the transcription initiation proteins. *Arch. Microbiol.* 169:483-490.
- Angerer, A., S.Enz, M.Ochs, and V.Braun. 1995. Transcriptional regulation of ferric citrate transport in *Escherichia coli* K-12. FecI belongs to a new subfamily of sigma 70-type factors that respond to extracytoplasmic stimuli. *Mol. Microbiol.* 18:163-174.

- Angerer,A., S.Gaisser, and V.Braun. 1990. Nucleotide sequences of the *sfuA*, *sfuB*, and *sfuC* genes of *Serratia marcescens* suggest a periplasmic-binding-protein-dependent iron transport mechanism. *J. Bacteriol.* 172:572-578.
- Ankenbauer,R., S.Sriyosachati, and C.D.Cox. 1985. Effects of siderophores on the growth of *Pseudomonas aeruginosa* in human serum and transferrin. *Infect. Immun.* 49:132-140.
- Ankenbauer,R.G. 1992. Cloning of the outer membrane high-affinity Fe(III)-pyochelin receptor of *Pseudomonas aeruginosa*. *J. Bacteriol.* 174:4401-4409.
- Ankenbauer,R.G. and H.N.Quan. 1994. FptA, the Fe(III)-pyochelin receptor of *Pseudomonas aeruginosa*: a phenolate siderophore receptor homologous to hydroxamate siderophore receptors.*Bacteriol.* 176:307-319.
- Anton,M. and K.J.Heller. 1991. Functional analysis of a C-terminally altered TonB protein of *Escherichia coli*. *Gene* 105:23-29.
- Archibald,F. 1983. *Lactobacillus plantarium*, an organism not requiring iron. *FEMS Microbiol Lett* 19:29-32.
- Armstrong,S.K. and M.A.Mcintosh. 1995. Epitope insertions define functional and topological features of the *Escherichia coli* ferric enterobactin receptor. *J. Biol. Chem.* 270:2483-2488.
- Arnoux,P., R.Haser, N.Izadi, A.Lecroisey, M.Delepierre, C.Wandersman, and M.Czjzek. 1999. The crystal structure of HasA, a hemophore secreted by *Serratia marcescens*. *Nat. Struct. Biol.* 6:516-520.
- Arroyo,C.M., S.D.Kirby, R.J.Werrlein, R.L.McCarthy, T.S.Moran, and J.R.Keeler. 1994. Reactive oxygen species produced in metal-catalyzed oxidation of bis(trifluoromethyl)disulfide and protection by ZE. *J. Toxicol. Environ. Health* 41:329-344.

- Atkin, C.L. and J.B. Neilands. 1968. Rhodotorulic acid, a diketopiperazine dihydroxamic acid with growth-factor activity. I. Isolation and characterization. *Biochemistry* 7:3734-3739.
- Bagg, A. and J.B. Neilands. 1987a. Ferric uptake regulation protein acts as a repressor, employing iron (II) as a cofactor to bind the operator of an iron transport operon in *Escherichia coli*. *Biochemistry* 26:5471-5477.
- Bagg, A. and J.B. Neilands. 1987b. Molecular mechanism of regulation of siderophore-mediated iron assimilation. *Microbiol. Rev.* 51:509-518.
- Baumler, A.J. and K. Hantke. 1992. A lipoprotein of *Yersinia enterocolitica* facilitates ferrioxamine uptake in *Escherichia coli*. *J. Bacteriol.* 174:1029-1035.
- Beal, F.B. 1998. Two iron-regulated putative ferric siderophore receptor genes in *Bordetella bronchiseptica* and *Bordetella pertussis*. *Res. Microbiol* 149:189-201.
- Beal, F.B. and G.N. Sanden. 1995. A *Bordetella pertussis* *fepA* homologue required for utilization of exogenous ferric enterobactin. *Microbiology* 141 (Pt 12):3193-3205.
- Beall, B. and T. Hoenes. 1997. An iron-regulated outer-membrane protein specific to *Bordetella bronchiseptica* and homologous to ferric siderophore receptors. *Microbiology* 143:135-145.
- Bearden, S.W. and R.D. Perry. 1999. The Yfe system of *Yersinia pestis* transports iron and manganese and is required for full virulence of plague. *Mol. Microbiol.* 32:403-414.
- Becker, K., Koster W, and V. Braun. 1990. Iron(III)hydroxamate transport of *Escherichia coli* K12: single amino acid replacements at potential ATP-binding sites inactivate the FhuC protein. *Mol. Gen. Genet.* 223:159-162.
- Belf, P.E., C.D. Nau, J.T. Brown, J. Konisky, and R.J. Kadner. 1990. Genetic suppression demonstrates interaction of TonB protein with outer membrane transport proteins in *Escherichia coli*. *J. Bacteriol.* 172:3826-3829.

- Bereswill, S., F. Lichte, T. Vey, F. Fassbinder, and M. Kist. 1998. Cloning and characterization of the *fur* gene from *Helicobacter pylori*. *FEMS Microbiol. Lett.* 159:193-200.
- Berish, S.A., D.R. Kapczynski, and S.A. Morse. 1990a. Nucleotide sequence of the Fbp gene from *Neisseria meningitidis*. *Nucleic Acids Res.* 18:4596.
- Berish, S.A., S. Subbarao, C.Y. Chen, D.L. Trees, and S.A. Morse. 1993. Identification and cloning of a *fur* homolog from *Neisseria gonorrhoeae*. *Infect. Immun.* 61:4599-4606.
- Berish, S.A., T.A. Mietzner, L.W. Mayer, C.A. Genco, B.P. Holloway, and S.A. Morse. 1990b. Molecular cloning and characterization of the structural gene for the major iron-regulated protein expressed by *Neisseria gonorrhoeae*. *J. Exp. Med.* 171:1535-1546.
- Bitter, W., J.D. Marugg, L.A. de Weger, J. Tommassen, and P.J. Weisbeek. 1991. The ferric-pseudobactin receptor PupA of *Pseudomonas putida* WCS358: homology to TonB-dependent *Escherichia coli* receptors and specificity of the protein. *Mol. Microbiol.* 5:647-655.
- Bitter, W., J. Tommassen, and P.J. Weisbeek. 1993. Identification and characterization of the *exbB*, *exbD* and *tonB* genes of *Pseudomonas putida* WCS358: their involvement in ferric-pseudobactin transport. *Mol. Microbiol.* 7:117-130.
- B6hm, B., H. Boschert, and W. Koster. 1996. Conserved amino acids in the N- and C-terminal domains of integral membrane transporter FhuB define sites important for intra- and intermolecular interactions. *Mol. Microbiol.* 20:223-232.
- Bohm, H.J. 1996. Current computational tools for *de novo* ligand design. *Curr. Opin. Biotechnol.* 7:433-436.
- Bohnke, R. and B.F. Matzanke. 1995. The mobile ferrous iron pool in *Escherichia coli* is bound to a phosphorylated sugar derivative. *Biometals* 8:223-230.

- Bonhivers, M., A. Ghazi, P. Boulanger, and L. Letellier. 1996. FhuA, a transporter of the *Escherichia coli* outer membrane, is converted into a channel upon binding of bacteriophage T5. *EMBOJ.* 15:1850-1856.
- Bonnah, R.A. and A.B. Schryvers. 1998. Preparation and characterization of *Neisseria meningitidis* mutants deficient in production of the human lactoferrin-binding proteins LbpA and LbpB. *J. Bacteriol.* 180:3080-3090.
- Boos, W. and J.M. Lucht. 1996. *Escherichia coli* and *Salmonella typhurium*. A S M Press.
- Bradbeer, C. 1993. The proton motive force drives the outer membrane transport of cobalamin in *Escherichia coli*. *J. Bacteriol.* 175:3146-3150.
- Braun, M., H. Killmann, and V. Braun. 1999. The beta-barrel domain of FhuADelta5-160 is sufficient for TonB- dependent FhuA activities of *Escherichia coli*. *Mol. Microbiol.* 33:1037-1049.
- Braun, V. 1989. The structurally related *exbB* and *tolQ* genes are interchangeable in conferring to «5-dependent colicin, bacteriophage, and albomycin sensitivity. *J. Bacteriol.* 171:6387-6390.
- Braun, V. 1995. Energy-coupled transport and signal transduction through the gram-negative outer membrane via TonB-ExbB-ExbD-dependent receptor proteins. *FEMS Microbiol. Rev.* 16:295-307.
- Braun, V. 1997. Avoidance of iron toxicity through regulation of bacterial iron transport. *Biol. Chem.* 378:779-786.
- Braun, V. 1997. Surface signaling: novel transcription initiation mechanism starting from the cell surface. *Arch. Microbiol.* 167:325-331.
- Braun, V. 1998. Pumping iron through cell membranes. *Science* 282:2202-2203.

- Braun, V. and C. Herrmann. 1993. Evolutionary relationship of uptake systems for biopolymers in *Escherichia coli*: cross-complementation between the TonB-ExbB-ExbD and the TolA-TolQ-TolR proteins. *Mol Microbiol* 8:261-8.
- Braun, V. and H. Killmann. 1999. Bacterial solutions to the iron-supply problem. *Trends Biochem. Sci.* 24:104-109.
- Braun, V., J. Frenz, K. Hantke, and K. Schaller. 1980. Penetration of colicin M into cells of *Escherichia coli*. *J. Bacteriol.* 142:162-168.
- Braun, V., K. Gunter, and K. Hantke. 1991. Transport of iron across the outer membrane. *Biol. Met.* 4:14-22.
- Braun, V., K. Gunthner, K. Hantke, and L. Zimmermann. 1983. Intracellular activation of albomycin in *Escherichia coli* and *Salmonella typhimurium*. *J. Bacteriol.* 156:308-315.
- Braun, V., K. Hantke, and W. Koster. 1998. Bacterial iron transport: mechanisms, genetics, and regulation. *Met. Ions. Biol. Syst.* 35:67-145.
- Brickman, T.J. and M.A. McIntosh. 1992. Overexpression and purification of ferric enterobactin esterase from *Escherichia coli*. Demonstration of enzymatic hydrolysis of enterobactin and its iron complex. *J. Biol. Chem.* 267:12350-12355.
- Brickman, T.J. and S.K. Armstrong. 1995. *Bordetella pertussis* fur gene restores iron repressibility of siderophore and protein expression to deregulated *Bordetella bronchiseptica* mutants. *J. Bacteriol.* 177:268-270.
- Brickman, T.J. and S.K. Armstrong. 1999. Essential role of the iron-regulated outer membrane receptor FauA in alcaligin siderophore-mediated iron uptake in *Bordetella* species. *J. Bacteriol.* 181:5958-5966.
- Briskof G., K. Taraz, and H. Budzikiewicz. 1986. [Pyoverdin-type siderophores from *Pseudomonas aeruginosa*]. *Z. Naturforsch. [C]* 41:497-506.

Brunger, A.T., P.D.Adams, G.M.Clore, W.L.DeLano, P.Gros, R.W.Grosse-Kunstleve, J.S.Jiang, J.Kuszewski, M.Nilges, N.S.Pannu, R.J.Read, L.M.Rice, T.Simonson, and G.L.Warren. 1998. Crystallography & NMR system: A new software suite for macromolecular structure determination. *Acta Crystallogr. D. Biol. Crystallogr.* 54:905-921.

Bruns, C.M., A.J.Nowalk, A.S.Arva, M.A.McTigue, K.G.Vaughan, T.A.Mietzner, and D.E.McRee. 1997. Structure of *Haemophilus influenzae* Fe(+3)-binding protein reveals convergent evolution within a superfamily. *Nat. Struct. Biol.* 4:919-924.

Bruske, A.K. and K.J.Heller. 1993. Molecular characterization of the *Enterobacter aerogenes tonB* gene: identification of a novel type of *tonB* box suppressor mutant. *J. Bacteriol.* 175:6158-6168.

Bruske, A.K., M.Anton, and K.J.Heller. 1993. Cloning and sequencing of the *Klebsiella pneumoniae tonB* gene and characterization of *Escherichia coli*-*K. pneumoniae* TonB hybrid proteins. *Gene* 131:9-16.

Bsat, N., A.Herbig, L.Casillas-Martinez, P.Setlow, and J.D.Helmann. 1998. *Bacillus subtilis* contains multiple Fur homologues: identification of the iron uptake (Fur) and peroxide regulon (PerR) repressors. *Mol. Microbiol.* 29:189-198.

Buchanan, S.K., B.S.Smith, L.Venkatramani, D.Xia, L.Esser, M.Palnitkar, R.Chakraborty, D.van der Helm, and J.Deisenhofer. 1999. Crystal structure of the outer membrane active transporter FepA from *Escherichia coli*. *Nature Struct. Biol.* 6:56-63.

Bult, C.J., O.White, G.J.Olsen, L.Zhou, R.D.Fleischmann, G.G.Sutton, J.A.Blake, L.M.FitzGerald, R.A.Clayton, J.D.Gocayne, A.R.Kerlavage, B.A.Dougherty, J.F.Tomb, M.D.Adams, C.I.Reich, R.Overbeek, E.F.Kirkness, K.G.Weinstock, J.M.Merrick, A.Glodek, J.L.Scott, N.S.M.Geoghagen, and J.C.Venter. 1996. Complete genome sequence of the methanogenic archaeon, *Methanococcus jannaschii*. *Science* 273:1058-1073.

- Burkhardt, R. and V. Braun. 1987. Nucleotide sequence of the *fhuC* and *fhuD* genes involved in iron (III) hydroxamate transport: domains in FhuC homologous to ATP-binding proteins. *Mol Gen. Genet.* 209:49-55.
- Butterton J.R., J.A. Stoebner, S.M. Payne, and S.B. Calderwood. 1992. Cloning, sequencing, and transcriptional regulation of *viuA*, the gene encoding the ferric vibriobactin receptor of *Vibrio cholerae*. *J. Bacteriol* 174:3729-3738.
- Byers, B.R. and J.E. Arceneaux. 1998. Microbial iron transport: iron acquisition by pathogenic microorganisms. *Met. Ions. Biol Syst.* 35:37-66.
- Campbell, I.D. and R.A. Dwek. 1984. Biological Spectroscopy. Benjamin/Cummings Publishing Company, Inc., Don Mills.
- Carmef G., D. Hellstern, D. Henning, and J.W. Coulton. 1990. Insertion mutagenesis of the gene encoding the ferrichrome-iron receptor of *Escherichia coli* K-12. *J. Bacteriol.* 172:1861-1869.
- Carson, S.D., C.E. Thomas, and C. Elkins. 1996. Cloning and sequencing of a *Haemophilus ducreyi* fur homolog. *Gene* 176:125-129.
- Chen, C.J., P.F. Sparling, L.A. Lewis, D.W. Dyer, and C. Elkins. 1996. Identification and purification of a hemoglobin-binding outer membrane protein from *Neisseria gonorrhoeae*. *Infect. Immun.* 64:5008-5014.
- Chin, N., J. Frey, C.F. Chang, and Y.F. Chang. 1996. Identification of a locus involved in the utilization of iron by *Actinobacillus pleuropneumoniae*. *FEMS Microbiol. Lett.* 143:1-6.
- Clarke, T.E., L.W. Tari, and H.J. Vogel. 2001. Structural Biology of Iron Uptake Systems. *Curr. Top. Med. Chem.* 1:(in press).
- Clarke, T.E., S. Y. Ku, D.R. Dougan, H.J. Vogel, and L.W. Tari. 2000. The structure of the ferric siderophore binding protein FhuD complexed with gallichrome. *Nat. Struct. Biol.* 7:287-291.

- Cockayne,A., P.J.Hill, N.B.Powell, K.Bishop, C.Sims, and P.Williams. 1998. Molecular cloning of a 32-kilodalton lipoprotein component of a novel iron-regulated *Staphylococcus epidermidis* ABC transporter. *Infect. Immun.* 66:3767-3774.
- Cohen,S.M., M.Meyer, and K.M.Raymond. 1998. Enterochelin protonation and iron release: Hexadentate tris-salicyclate ligands as models for triprotonated ferric enterobactin. *J. Am. Chem. Soc.* 120:6277-6286.
- Constantine,K.L., A.De Marco, M.Madrid, C.L.Brooks, III, and M.Llinas. 1990. The solution conformations of ferrichrome and deferriferrichrome determined by ¹H-NMR spectroscopy and computational modeling. *Biopolymers* 30:239-256.
- Cope,L.D., R.Yogev, U.Muller-Eberhard, and E.J.Hansen. 1995. A gene cluster involved in the utilization of both free heme and heme:hemopexin by *Haemophilus influenzae* type b. *J. Bacteriol.* 177:2644-2653.
- Cornelis,G.R., T.Biot, d.R.Lambert, T.Michiels, B.Mulder, C.Sluiters, M.P.Sory, M.Van Bouchaute, and J.C.Vanooteghem. 1989. The *Yersinia yop* regulon. *Mol. Microbiol.* 3:1455-1459.
- Cornelissen,C.N. and P.F.Sparling. 1994. Iron piracy: acquisition of transferrin-bound iron by bacterial pathogens. *Mol. Microbiol.* 14:843-850.
- Coulanges,V., P.Andre, O.Ziegler, L.Buchheit, and D.J.Vidon. 1997. Utilization of iron-catecholamine complexes involving ferric reductase activity in *Listeria monocytogenes*. *Infect. Immun.* 65:2778-2785.
- CoultonJ.W., P.Mason, and D.D.Allatt. 1987. *fhuC* and *fhuD* genes for iron (III)-ferrichrome transport into *Escherichia coli* K-12. *J. Bacteriol.* 169:3844-3849.
- Cox,C.D. 1982. Effect of pyochelin on the virulence of *Pseudomonas aeruginosa*. *Infect. Immun.* 36:17-23.

- Cox, C.D. 1985. Iron transport and serum resistance in *Pseudomonas aeruginosa*. *Antibiot. Chemother.* 36:1-12.
- Coy, M. and J.B.Neilands. 1991. Structural dynamics and functional domains of the *fur* protein. *Biochemistry* 30:8201-8210.
- Crichton, R.R. 1991. Inorganic biochemistry of iron metabolism. Ellis Horwood, New York, N. Y.
- Crosa, J.H. 1989. Genetics and molecular biology of siderophore-mediated iron transport in bacteria. *Microbiol. Rev.* 53:517-530.
- Crosa, J.H. 1997. Signal transduction and transcriptional and posttranscriptional control of iron-regulated genes in bacteria. *Microbiol Mol. Biol. Rev.* 61:319-336.
- Cunliffe, H.E., T.R.Merriman, and I.L.Lamont. 1995. Cloning and characterization of *pvdS*, a gene required for pyoverdine synthesis in *Pseudomonas aeruginosa*: PvdS is probably an alternative sigma factor. *J. Bacteriol.* 177:2744-2750.
- Daniel, J.C., S.Haentjens, M.C.Bissinger, and R.J.Courcol. 1999. Characterization of the *Acinetobacter baumannii* Fur regulator: cloning and sequencing of the *fur* homolog gene. *FEMS Microbiol. Lett.* 170:199-209.
- Dean, C.R. and K.Poole. 1993a. Expression of the ferric enterobactin receptor (PfeA) of *Pseudomonas aeruginosa*: involvement of a two-component regulatory system. *Mol. Microbiol.* 8:1095-1103.
- Dean, C.R. and K.Poole. 1993b. Cloning and characterization of the ferric enterobactin receptor gene (*pfeA*) of *Pseudomonas aeruginosa*. *J. Bacteriol.* 175:317-324.
- Dean, C.R., S.Neshat, and K.Poole. 1996. PfeR, an enterobactin-responsive activator of ferric enterobactin receptor gene expression in *Pseudomonas aeruginosa*. *J. Bacteriol.* 178:5361-5369.

- de Lorenzo, V., A. Bindereif, B. H. Paw, and J. B. Neilands. 1986. Aerobactin biosynthesis and transport genes of plasmid ColV-K30 in *Escherichia coli* K-12. *J. Bacteriol.* 165:570-578.
- de Lorenzo, V., S. Wee, M. Herrero, and J. B. Neilands. 1987. Operator sequences of the aerobactin operon of plasmid ColV-K30 binding the ferric uptake regulation (*fur*) repressor. *J. Bacteriol.* 169:2624-2630.
- de Luca, N. G., M. Wexler, M. J. Pereira, K. H. Yeoman, and A. W. Johnston. 1998. Is the *fur* gene of *Rhizobium leguminosarum* essential? *FEMS Microbiol. Lett.* 168:289-295.
- De Marco, A. and M. Llinas. 1979. Complete assignment of carbon signals in a stereospecific peptide via selective and single off-resonance proton decoupling experiments. Analysis of the carbon-13 nuclear magnetic resonance spectrum of alumichrome at 67.88 MHz. *Biochemistry* 18:3846-3854.
- Doukhan, L., M. Predich, G. Nair, O. Dussurget, I. Mandic-Mulec, S. T. Cole, D. R. Smith, and I. Smith. 1995. Genomic organization of the mycobacterial sigma gene cluster. *Gene* 165:67-70.
- Drenth, J. 1999. Principles of protein x-ray crystallography. Springer-Verlag, New York.
- Dyer, D. W., E. P. West, and P. F. Sparling. 1987. Effects of serum carrier proteins on the growth of pathogenic neisseriae with heme-bound iron. *Infect. Immun.* 55:2171-2175.
- Ecker, D. J., B. F. Matzanke, and K. N. Raymond. 1986. Recognition and transport of ferric enterobactin in *Escherichia coli*. *J. Bacteriol.* 167:666-673.
- Elkins, M. F. and C. F. Earhart. 1989. Nucleotide sequence and regulation of the *Escherichia coli* gene for ferrienterobactin transport protein FepB. *J. Bacteriol.* 171:5443-5451.
- Elshorsf B., M. Hennig, H. Forsterling, A. Diener, M. Maurer, P. Schulte, H. Schwalbe, C. Griesinger, J. Krebs, H. Schmid, T. Vorherr, and E. Carafoli. 1999. NMR solution structure

of a complex of calmodulin with a binding peptide of the Ca pump. *Biochemistry* 38:12320-12332.

Elshorst,B., M.Hennig, H.Forsterling, A.Diener, M.Maurer, P.Schulte, H.Schwalbe, C.Griesinger, J.Krebs, H.Schmid, T.Vorherr, and E.Carafoli. 1999. NMR solution structure of a complex of calmodulin with a binding peptide of the Ca²⁺ pump. *Biochemistry* 38:12320-12332.

Enz,S., V.Braun, and J.H.Crosa. 1995. Transcription of the region encoding the ferric dicitrate-transport system in *Escherichia coli*: similarity between promoters for *fecA* and for extracytoplasmic function sigma factors. *Gene* 163:13-18.

ErnsfJ.F., R.L.Bennett, and L.I.Rothfield. 1978. Constitutive expression of the iron-enterochelin and ferrichrome uptake systems in a mutant strain of *Salmonella typhimurium*. *J. Bacteriol.* 135:928-934.

Escolar,L., J.Perez-Martin, and V.deLorenzo. 1998. Binding of the *fur* (ferric uptake regulator) repressor of *Escherichia coli* to arrays of the G A T A A T sequence. *J. Mol. Biol.* 283:537-547.

Escolar,L., J.Perez-Martin, and V.deLorenzo. 1999. Opening the iron box: transcriptional metalloregulation by the Fur protein. *J. Bacteriol.* 181:6223-6229.

Escolar,L., V.deLorenzo, and J.Perez-Martin. 1997. Metalloregulation *in vitro* of the aerobactin promoter of *Escherichia coli* by the Fur (ferric uptake regulation) protein. *Mol. Microbiol.* 26:799-808.

Evans,S.L., J.E.Arceneaux, B.R.Byers, M.E.Martin, and Ff.Aranha. 1986. Ferrous iron transport in *Streptococcus mutans*. *J. Bacteriol.* 168:1096-1099.

Evans,S.V. 1993. SETOR: hardware-lighted three-dimensional solid model representations of macromolecules. *J. Mol. Graph.* 11:134-138.

- Fecker,L. and V.Braun. 1983. Cloning and expression of the *fhu* genes involved in iron(III)-hydroxamate uptake by *Escherichia coli*. *J. Bacteriol.* 156:1301-1314.
- Ferguson,A.D., E.Hofmann, J.W.Coulton, K.Diederichs, and W.Welte. 1998. Siderophore-mediated iron transport: crystal structure of FhuA with bound lipopolysaccharide. *Science* 282:2215-2220.
- Ferguson,A.D., V.Braun, H.P.Fiedler, J.W.Coulton, K.Diederichs, and W.Welte. 2000b. Crystal structure of the antibiotic albomycin in complex with the outer membrane transporter FhuA. *Protein Sci.* 9:956-963.
- Ferguson,A.D., W.Welte, E.Hofmann, B.Lindner, O.Hoist, J.W.Coulton, and K.Diederichs. 2000a. A conserved structural motif for lipopolysaccharide recognition by procaryotic and eucaryotic proteins. *Structure. Fold. Des* 8:585-592.
- Fetherston,J.D., S.W.Bearden, and R.D.Perry. 1996. YbtA, an AraC-type regulator of the *Yersinia pestis* pesticin/yersiniabactin receptor. *Mol. Microbiol.* 22:315-325.
- Fetherston,J.D., V.J.Bertolino, and R.D.Perry. 1999. YbtP and YbtQ: two ABC transporters required for iron uptake in *Yersinia pestis*. *Mol. Microbiol.* 32:289-299.
- Fischer,E., B.Strehlow, D.Hartz, and V.Braun. 1990. Soluble and membrane-bound ferrisiderophore reductases of *Escherichia coli* K-12. *Arch. Microbiol.* 153:329-336.
- Fischer,E., K.Gunter, and V.Braun. 1989. Involvement of ExbB and TonB in transport across the outer membrane of *Escherichia coli*: phenotypic complementation of *exb* mutants by overexpressed *tonB* and physical stabilization of TonB by ExbB. *J. Bacteriol.* 171:5127-5134.
- Fontecave,M., J.Coves, and J.L.Pierre. 1994. Ferric reductases or flavin reductases? *Biometals* 7:3-8.

- Franza, T., C. Sauvage, and D. Expert. 1999. Iron regulation and pathogenicity in *Erwinia chrysanthemi* 3937: role of the Fur repressor protein. *Mol. Plant Microbe Interact.* 12:119-128.
- Frishman, D. and P. Argos. 1996. Incorporation of non-local interactions in protein secondary structure prediction from the amino acid sequence. *Protein Eng* 9:133-142.
- Frishman, D. and P. Argos. 1997. The future of protein secondary structure prediction accuracy. *Fold. Des* 2:159-162.
- Frolow, F., A. J. Kalb, and J. Yariv. 1994. Structure of a unique twofold symmetric haem-binding site. *Nat. Struct. Biol.* 1:453-460.
- Gaisser, S. and V. Braun. 1991. The *tonB* gene of *Serratia marcescens*: sequence, activity and partial complementation of *Escherichia coli* tonB mutants. *Mol. Microbiol.* 5:2777-2787.
- Gerstein, M., A. M. Lesk, and C. Chothia. 1994. Structural mechanisms for domain movements in proteins. *Biochemistry* 33:6739-6749.
- Ghigo, J. M., S. Letoffe, and C. Wandersman. 1997. A new type of hemophore-dependent heme acquisition system of *Serratia marcescens* reconstituted in *Escherichia coli*. *J. Bacteriol.* 179:3572-3579.
- Goldberg, M. B., S. A. Boyko, J. R. Butterton, J. A. Stoebner, S. M. Payne, and S. B. Calderwood. 1992. Characterization of a *Vibrio cholerae* virulence factor homologous to the family of TonB-dependent proteins. *Mol. Microbiol.* 6:2407-2418.
- Ghosh, A., M. J. Miller, E. De Clercq, and J. Balzarini. 1999. Synthesis and biological evaluation of a carbocyclic azanoraristeromycin siderophore conjugate. *Nucl. Nucl.* 18:217-225.

- Ghosh, A., M.Ghosh, C.Niu, F.Malouin, U.Moellmann, and M.J.Miller. 1996. Iron transport-mediated drug delivery using mixed-ligand siderophore-P-lactam conjugates. *Chem. Biol.* 3:1011-1019.
- Gray-Owen,S.D. and A.B.Schryvers. 1996. Bacterial transferrin and lactoferrin receptors. *Trends Microbiol.* 4:185-191.
- Gray-Owen,S.D., S.Loosmore, and A.B.Schryvers. 1995. Identification and characterization of genes encoding the human transferrin-binding proteins from *Haemophilus influenzae*. *Infect. Immun.* 63:1201-1210.
- Griffiths,E. 1991. Iron and bacterial virulence~a brief overview. *Biol. Met.* 4:7-13.
- Groeger,W. and W.Koster. 1998. Transmembrane topology of the two FhuB domains representing the hydrophobic components of bacterial ABC transporters involved in the uptake of siderophores, haem and vitamin B12. *Microbiology* 144:2759-2769.
- GrossmannJ.G., M.Neu, R.W.Evans, P.F.Lindley, H.Appel, and S.S.Hasnain. 1993. Metal-induced conformational changes in transferrins. *J. Mol. Biol.* 229:585-590.
- GuerinofM.L. 1994. Microbial iron transport. *Annu. Rev. Microbiol* 48:743-772.
- Gunter-Seeboth,K. and T.Schupp. 1995. Cloning and sequence analysis of the *Corynebacterium diphtheriae* *dtxR* homologue from *Streptomyces lividans* and *S. pilosus* encoding a putative iron repressor protein. *Gene* 166:117-119.
- HalfH.K. and J.W.Foster. 1996. The role of *fur* in the acid tolerance response of *Salmonella typhimurium* is physiologically and genetically separable from its role in iron acquisition./ *Bacteriol.* 178:5683-5691.
- Hancock,R.W. and V.Braun. 1976. Nature of the energy requirement for the irreversible adsorption of bacteriophages T1 and phi80 to *Escherichia coli*. *J. Bacteriol.* 125:409-415.

- Hannavy, K., G.C. Barr, C.J. Dorman, J. Adamson, L.R. Mazengera, M.P. Gallagher, J.S. Evans, B.A. Levine, I.P. Trayer, and C.F. Higgins. 1990. TonB protein of *Salmonella typhimurium*. A model for signal transduction between membranes. *J. Mol. Biol.* 216:897-910.
- Hanson, M.S., S.E. Pelzel, J. Latimer, U. Muller-Eberhard, and E.J. Hansen. 1992. Identification of a genetic locus of *Haemophilus influenzae* type b necessary for the binding and utilization of heme bound to human hemopexin. *Proc. Natl. Acad. Sci. U. S. A* 89:1973-1977.
- Hantke, K. 1981. Regulation of ferric iron transport in *Escherichia coli* K12: isolation of a constitutive mutant. *Mol. Gen. Genet.* 182:288-292.
- Hantke, K. 1983. Identification of an iron uptake system specific for coprogen and rhodotorulic acid in *Escherichia coli* K12. *Mol. Gen. Genet.* 191:301-306.
- Hantke, K. and V. Braun. 1978. Functional interaction of the *tonA/tonB* receptor system in *Escherichia coli*. *J. Bacteriol.* 135:190-197.
- Harle, C., I. Kim, A. Angerer, and V. Braun. 1995. Signal transfer through three compartments: transcription initiation of the *Escherichia coli* ferric citrate transport system from the cell surface. *EMBOJ.* 14:1430-1438.
- Harrison, P.M. and P. Arosio. 1996. The ferritins: molecular properties, iron storage function and cellular regulation. *Biochim. Biophys. Acta* 1275:161-203.
- Hartmann, A., H.P. Fiedler, and V. Braun. 1979. Uptake and conversion of the antibiotic albomycin by *Escherichia coli* K-12. *Eur. J. Biochem.* 99:517-524.
- Hayward, S. 1999. Structural principles governing domain motions in proteins. *Proteins* 36:425-435.
- Heesemann, J., K. Hantke, T. Vocke, E. Saken, A. Rakin, I. Stojiljkovic, and R. Berner. 1993. Virulence of *Yersinia enterocolitica* is closely associated with siderophore production,

expression of an iron-repressible outer membrane polypeptide of 65,000 Da and pesticin sensitivity. *Mol. Microbiol.* 8:397-408.

Heidinger, S., V. Braun, V. L. Pecoraro, and K. N. Raymond. 1983. Iron supply to *Escherichia coli* by synthetic analogs of enterochelin. *J. Bacteriol.* 153:109-115.

Heidrich, C., K. Hantke, G. Bierbaum, and H. G. Sahl. 1996. Identification and analysis of a gene encoding a Fur-like protein of *Staphylococcus epidermidis*. *FEMS Microbiol. Lett.* 140:253-259.

Heinrichs, D. E. and K. Poole. 1993. Cloning and sequence analysis of a gene (*pchR*) encoding an AraC family activator of pyochelin and ferripyochelin receptor synthesis in *Pseudomonas aeruginosa*. *J. Bacteriol.* 175:5882-5889.

Heinrichs, D. E. and K. Poole. 1996. PchR, a regulator of ferripyochelin receptor gene (*fptA*) expression in *Pseudomonas aeruginosa*, functions both as an activator and as a repressor. *J. Bacteriol.* 178:2586-2592.

Heller, K. J., R. J. Kadner, and K. Gunther. 1988. Suppression of the *btuB451* mutation by mutations in the *tonB* gene suggests a direct interaction between TonB and TonB-dependent receptor proteins in the outer membrane of *Escherichia coli*. *Gene* 64:147-153.

Hershko, C. 1992. Iron chelators in medicine. *Mol. Aspects Med.* 13:113-165.

Hickey, E. K. and N. P. Cianciotto. 1994. Cloning and sequencing of the *Legionella pneumophila* *fur* gene. *Gene* 143:117-121.

Higgins, C. F. 1992. ABC transporters: from microorganisms to man. *Annu. Rev. Cell Biol.* 8:67-113.

Holm, L. and C. Sander. 1993. Protein structure comparison by alignment of distance matrices. *J. Mol. Biol.* 233:123-138.

Holm, L. and C. Sander. 1996. Alignment of three-dimensional protein structures: network server for database searching. *Methods Enzymol.* 266:653-662.

Hossain, M.B., M.A.F. Jalal, and van der Helm D. 1986. *Acta Crystallogr. C.* 42:1305.

Hossain, M.B., M.A.F. Jalal, B.A. Benson, C.L. Barnes, and D. van der Helm. 1987. Structure and Conformation of Two Coprogen-type Siderophores: Neocoprogen I and Neocoprogen II. *J. Am. Chem. Soc.* 109:4948-4954.

Hung, L.W., I.X. Wang, K. Nikaido, P.Q. Liu, G.F. Ames, and S.H. Kim. 1998. Crystal structure of the ATP-binding subunit of an ABC transporter. *Nature* 396:703-707.

Husson, M.O., D. Legrand, G. Spik, and H. Leclerc. 1993. Iron acquisition by *Helicobacter pylori*: importance of human lactoferrin. *Infect. Immun.* 61:2694-2697.

Ikura, M., G.M. Clore, A.M. Gronenborn, G. Zhu, C.B. Klee, and A. Bax. 1992. Solution structure of a calmodulin-target peptide complex by multidimensional NMR. *Science* 256:632-638.

Ikura, M., G.M. Clore, A.M. Gronenborn, G. Zhu, C.B. Klee, and A. Bax. 1992. Solution structure of a calmodulin-target peptide complex by multidimensional NMR. *Science* 256:632-638.

Ikura, M., S. Spera, G. Barbato, L.E. Kay, M. Krinks, and A. Bax. 1991. Secondary structure and side-chain ¹H and ¹³C resonance assignments of calmodulin in solution by heteronuclear multidimensional NMR spectroscopy. *Biochemistry* 30:9216-9228.

Jaskula, J.C., T.E. Letain, S.K. Roof, J.T. Skare, and K. Postle. 1994. Role of the TonB amino terminus in energy transduction between membranes. *J. Bacteriol.* 176:2326-2338.

Kammler, M., C. Schon, and K. Hantke. 1993. Characterization of the ferrous iron uptake system of *Escherichia coli*. *J. Bacteriol.* 175:6212-6219.

Kampfenkel, K. and V. Braun. 1992. Membrane topology of the *Escherichia coli* ExbD protein. *J. Bacteriol.* 174:5485-5487.

Kampfenkel, K. and V. Braun. 1993a. Membrane topologies of the TolQ and TolR proteins of *Escherichia coli*: inactivation of TolQ by a missense mutation in the proposed first transmembrane segment. *J. Bacteriol.* 175:4485-4491.

Kampfenkel, K. and V. Braun. 1993b. Topology of the ExbB protein in the cytoplasmic membrane of *Escherichia coli*. *J. Biol. Chem.* 268:6050-6057.

Karlsson, M., K. Hannavy, and C. F. Higgins. 1993. A sequence-specific function for the N-terminal signal-like sequence of the TonB protein. *Mol. Microbiol.* 8:379-388.

Killmann, H. and V. Braun. 1994. Energy-dependent receptor activities of *Escherichia coli* K-12: mutated TonB proteins alter FhuA receptor activities to phages T5, T1, phi 80 and to colicin M. *FEMS Microbiol. Lett.* 119:71-76.

Killmann, H., C. Herrmann, H. Wolff, and V. Braun. 1998. Identification of a new site for ferrichrome transport by comparison of the FhuA proteins of *Escherichia coli*, *Salmonella paratyphi B*, *Salmonella typhimurium*, and *Pantoea agglomerans*. *J. Bacteriol.* 180:3845-3852.

Killmann, H., G. Videnov, G. Jung, H. Schwarz, and V. Braun. 1995. Identification of receptor binding sites by competitive peptide mapping: phages T1, T5, and phi 80 and colicin M bind to the gating loop of FhuA. *J. Bacteriol.* 177:694-698.

Killmann, H., R. Benz, and V. Braun. 1993. Conversion of the FhuA transport protein into a diffusion channel through the outer membrane of *Escherichia coli*. *EMBO J.* 12:3007-3016.

Kim, I., A. Stiefel, S. Plantor, A. Angerer, and V. Braun. 1997. Transcription induction of the ferric citrate transport genes via the N-terminus of the FecA outer membrane protein, the

Ton system and the electrochemical potential of the cytoplasmic membrane. *Mol. Microbiol.* 23:333-344.

Kim, J. and D.C. Rees. 1992. Structural models for the metal centers in the nitrogenase molybdenum-iron protein. *Science* 257:1677-1682.

Kleywegt, G.J. and T.A. Jones. 1998. Databases in protein crystallography. *Acta Crystallogr. D. Biol. Crystallogr.* 54:1119-1131.

Koebnik, R., A.J. Baumler, J. Heesemann, V. Braun, and K. Hantke. 1993b. The TonB protein of *Yersinia enterocolitica* and its interactions with TonB-box proteins. *Mol. Gen. Genet.* 237:152-160.

Koebnik, R., K. Hantke, and V. Braun. 1993a. The TonB-dependent ferrichrome receptor FcuA of *Yersinia enterocolitica*: evidence against a strict co-evolution of receptor structure and substrate specificity. *Mol. Microbiol.* 7:383-393.

Koster, W. 1991. Iron(III) hydroxamate transport across the cytoplasmic membrane of *Escherichia coli*. *Biol Met* 4:23-32.

Koster, M., V. J. van de Leong, and P.J. Weisbeek. 1993. Identification and characterization of the *pupB* gene encoding an inducible ferric-pseudobactin receptor of *Pseudomonas putida* WCS358. *Mol. Microbiol.* 8:591-601.

Koster, M., W. van Klompenburg, W. Bitter, J. Leong, and P. Weisbeek. 1994. Role for the outer membrane ferric siderophore receptor PupB in signal transduction across the bacterial cell envelope. *EMBOJ.* 13:2805-2813.

Koster, W. and B. Bohm. 1992. Point mutations in two conserved glycine residues within the integral membrane protein FhuB affect iron(III) hydroxamate transport. *Mol Gen Genet* 232:399-407.

Koster, W. and V. Braun. 1986. Iron hydroxamate transport of *Escherichia coli*: nucleotide sequence of the *fhuB* gene and identification of the protein. *Mol Gen Genet* 204:435-42.

K5ster,W. and V.Braun. 1989. Iron-hydroxamate transport into *Escherichia coli* K12: localization of FhuD in the periplasm and of FhuB in the cytoplasmic membrane. *Mol Gen Genet* 217:233-9.

Koster,W. and V.Braun. 1990a. Iron (III) hydroxamate transport into *Escherichia coli*. Substrate binding to the periplasmic FhuD protein. *J Biol Chem* 265:21407-10.

K6ster,W. and V.Braun. 1990b. Iron(III) hydroxamate transport of *Escherichia coli*: restoration of iron supply by coexpression of the N- and C-terminal halves of the cytoplasmic membrane protein FhuB cloned on separate plasmids. *Mol Gen Genet* 223:379-84.

Kuboniwa,H., N.Tjandra, S.Grzesiek, H.Ren, C.B.Klee, and A.Bax. 1995. Solution structure of calcium-free calmodulin. *Nat. Struct. Biol.* 2:768-776.

Kuhn,S., V.Braun, and W.Koster. 1996. Ferric rhizoferrin uptake into *Morganella morganii*: characterization of genes involved in the uptake of a polyhydroxycarboxylate siderophore. *J. Bacteriol.* 178:496-504.

LakowiczJ.R. 1999. Principles of Fluorescence Spectroscopy. Kluwer Academic/Plenum Publishers, New York.

Larsen,R.A., G.E.Wood, and K.Postle. 1994. The conserved proline-rich motif is not essential for energy transduction by *Escherichia coli* TonB protein. *Mol. Microbiol.* 12:857.

Laskowski,R.A., M.W.MacArthur, D.S.Moss, and J.M.Thornton. 1993. PROCHECK: A program to check the stereochemical quality of protein structures. *J. Appl. Cryst.* 26:283-291.

Lathrop,J.T., B. Y. Wei, G.A.Touchie, and R.J.Kadner. 1995. Sequences of the *Escherichia coli* BtuB protein essential for its insertion and function in the outer membrane. *J. Bacteriol.* 177:6810-6819.

- Lawrence, M.C., P.A. Pilling, V.C. Epa, A.M. Berry, A.D. Ogunniyi, and J.C. Paton. 1998. The crystal structure of pneumococcal surface antigen PsaA reveals a metal-binding site and a novel structure for a putative ABC-type binding protein. *Structure*. 6:1553-1561.
- Lee, Y.H., R.K. Deka, M.V. Norgard, J.D. Radolf, and C.A. Hasemann. 1999. *Treponema pallidum* TroA is a periplasmic zinc-binding protein with a helical backbone. *Nat. Struct. Biol.* 6:628-633.
- Leoni, L., A. Ciervo, N. Orsi, and P. Visca. 1996. Iron-regulated transcription of the *pvdA* gene in *Pseudomonas aeruginosa*: effect of Fur and PvdS on promoter activity. *J. Bacteriol.* 178:2299-2313.
- Letain, T.E. and K. Postle. 1997. TonB protein appears to transduce energy by shuttling between the cytoplasmic membrane and the outer membrane in *Escherichia coli*. *Mol. Microbiol.* 24:271-283.
- Letoffe, S., F. Nato, M.E. Goldberg, and C. Wandersman. 1999. Interactions of HasA, a bacterial haemophore, with haemoglobin and with its outer membrane receptor HasR. *Mol. Microbiol.* 33:546-555.
- Letoffe, S., V. Redeker, and C. Wandersman. 1998. Isolation and characterization of an extracellular haem-binding protein from *Pseudomonas aeruginosa* that shares function and sequence similarities with the *Serratia marcescens* HasA haemophore. *Mol. Microbiol.* 28:1223-1234.
- Lewis, L.A., E. Gray, Y.P. Wang, B.A. Roe, and D.W. Dyer. 1997. Molecular characterization of *hpuAB*, the haemoglobin-haptoglobin- utilization operon of *Neisseria meningitidis*. *Mol. Microbiol.* 23:737-749.
- Litwin, C.M. and S.B. Calderwood. 1993a. Role of iron in regulation of virulence genes. *Clin. Microbiol. Rev.* 6:137-149.

Litwin, C.M. and S.B. Calderwood. 1993b. Cloning and genetic analysis of the *Vibrio vulnificus fur* gene and construction of a *fur* mutant by *in vivo* marker exchange. *J. Bacteriol.* 175:706-715.

Litwin, C.M. and S.B. Calderwood. 1994. Analysis of the complexity of gene regulation by *fur* in *Vibrio cholerae*. *J. Bacteriol.* 176:240-248.

Litwin, C.M., S.A. Boyko, and S.B. Calderwood. 1992. Cloning, sequencing, and transcriptional regulation of the *Vibrio cholerae fur* gene. *J. Bacteriol.* 174:1897-1903.

Llinas, M. and K. Wuthrich. 1978. A nitrogen-15 spin-lattice relaxation study of alumichrome. *Biochim. Biophys. Acta* 532:29-40.

Llinas, M., D.M. Wilson, and J.B. Neilands. 1977. Peptide strain. Conformation dependence of the carbon-13 nuclear magnetic resonance chemical shifts in the ferrichromes. *J. Am. Chem. Soc.* 99:3631-3637.

Llinas, M., D.M. Wilson, M.P. Klein, and J.B. Neilands. 1976. ¹³C nuclear magnetic resonance of the ferrichrome peptides: structural and strain contributions to the conformational state. *J. Mol. Biol.* 104:853-864.

Llinas, M., M.P. Klein, and J.B. Neilands. 1970. Solution conformation of ferrichrome, a microbial iron transport cyclohexapeptide, as deduced by high resolution proton magnetic resonance. *J. Mol. Biol.* 52:399-414.

Llinas, M., M.P. Klein, and J.B. Neilands. 1972. The solution conformation of the ferrichromes. II. Proton magnetic resonance of metal-free ferricrocin and ferrichrysin, conformational implications. *Int. J. Pept. Protein Res.* 4:157-166.

Locher, K.P. and J.P. Rosenbusch. 1997. Oligomeric states and siderophore binding of the ligand-gated FhuA protein that forms channels across *Escherichia coli* outer membranes. *Eur. J. Biochem.* 247:770-775.

- Locher, K.P., B.Rees, R.Koebnik, A.Mitschler, L.Moulinier, J.P.Rosenbusch, and D.Moras. 1998. Transmembrane signaling across the ligand-gated FhuA receptor: crystal structures of free and ferrichrome-bound states reveal allosteric changes. *Cell* 95:771-778.
- Ma, J.F., U.A.Ochsner, M.G.Klotz, V.K.Nanayakkara, M.L.Howell, Z.Johnson, J.E.Posey, M.L.Vasil, J.J.Monaco, and D.J.Hassett. 1999. Bacterioferritin A modulates catalase A (KatA) activity and resistance to hydrogen peroxide in *Pseudomonas aeruginosa*. *J. Bacteriol.* 181:3730-3742.
- Mademidis, A., H.Killmann, W.Kraas, I.Flechsler, G.Jung, and V.Braun. 1997. ATP-dependent ferric hydroxamate transport system in *Escherichia coli*: periplasmic FhuD interacts with a periplasmic and with a transmembrane/cytoplasmic region of the integral membrane protein FhuB, as revealed by competitive peptide mapping. *Mol. Microbiol.* 26:1109-1123.
- Mahe, B., C.Masclaux, L.Rauscher, C.Enard, and D.Expert. 1995. Differential expression of two siderophore-dependent iron-acquisition pathways in *Erwinia chrysanthemi* 3937: characterization of a novel ferrisiderophore permease of the ABC transporter family. *Mol. Microbiol.* 18:33-43.
- Mao, B., M.R.Pear, J.A.McCammon, and F.A.Quiocho. 1982. Hinge-bending in L-arabinose-binding protein. The "Venus's-flytrap" model. *Biol. Chem.* 257:1131-1133.
- Martin, S.R. and P.M.Bayley. 1986. The effects of Ca^{2+} and Cd^{2+} on the secondary and tertiary structure of bovine testis calmodulin. A circular-dichroism study. *Biochem. J.* 238:485-490.
- Martin, Y.C. 1992. 3D database searching in drug design. *J. Med. Chem.* 35:2145-2154.
- Matzanke, B.F., I.Berner, E.Bill, A.X.Trautwein, and G.Winkelmann. 1991. Transport and utilization of ferrioxamine-E-bound iron in *Erwinia herbicola* (*Pantoea agglomerans*). *Biol. Met.* 4:181-185.

- McLachlan, D.R., T.P. Kruck, W.J. Lukiw, and S.S. Krishnan. 1991. Would decreased aluminum ingestion reduce the incidence of Alzheimer's disease? *CMAJ*. 145:793-804.
- Meador, W.E., A.R. Means, and F.A. Quijoch. 1992. Target enzyme recognition by calmodulin: 2.4 Å structure of a calmodulin-peptide complex. *Science* 257:1251-1255.
- Meador, W.E., A.R. Means, and F.A. Quijoch. 1993. Modulation of calmodulin plasticity in molecular recognition on the basis of x-ray structures. *Science* 262:1718-1721.
- Michaud-Soret, I., A. Adrait, M. Jaquinod, E. Forest, D. Touati, and J.M. Latour. 1997. Electrospray ionization mass spectrometry analysis of the apo- and metal-substituted forms of the Fur protein. *FEBS Lett.* 413:473-476.
- Mietzner, T.A. and S.A. Morse. 1994. The role of iron-binding proteins in the survival of pathogenic bacteria. *Annu. Rev. Nutr.* 14:471-493.
- Mietzner, T.A., S.B. Tencza, P. Adhikari, K.G. Vaughan, and A.J. Nowalk. 1998. Fe(III) periplasm-to-cytosol transporters of gram-negative pathogens. *Curr. Top. Microbiol. Immunol.* 225:113-135.
- Mills, M. and S.M. Payne. 1995. Genetics and regulation of heme iron transport in *Shigella dysenteriae* and detection of an analogous system in *Escherichia coli* 0157:H7. *J. Bacteriol.* 177:3004-3009.
- Miyazaki, H., H. Kato, T. Nakazawa, and M. Tsuda. 1995. A positive regulatory gene, *pvdS*, for expression of pyoverdinin biosynthetic genes in *Pseudomonas aeruginosa* PAO. *Mol. Gen. Genet.* 248:17-24.
- Modun, B. and P. Williams. 1999. The staphylococcal transferrin-binding protein is a cell wall glyceraldehyde-3-phosphate dehydrogenase. *Infect. Immun.* 67:1086-1092.
- Modun, B., J. Morrissey, and P. Williams. 2000. The staphylococcal transferrin receptor: a glycolytic enzyme with novel functions. *Trends Microbiol.* 8:231-237.

- Modun,B., R.W.Evans, C.L.Joannou, and P.Williams. 1998. Receptor-mediated recognition and uptake of iron from human transferrin by *Staphylococcus aureus* and *Staphylococcus epidermidis*. *Infect. Immun.* 66:3591-3596.
- Moeck,G.S. and J.W.Coulton. 1998. TonB-dependent iron acquisition: mechanisms of siderophore-mediated active transport. *Mol. Microbiol.* 28:675-681.
- Moore,G.R., F.H.Kadir, F.K.al Massad, N.E.Le Bran, A.J.Thomson, C.Greenwood, J.N.Keen, and J.B.Findlay. 1994. Structural heterogeneity of *Pseudomonas aeruginosa* bacterioferritin. *Biochem. J.* 304 (Pt 2):493-497.
- Morris,A.L., M.W.MacArthur, E.G.Hutchinson, and J.M.Thornton. 1992. Stereochemical quality of protein structure coordinates. *Proteins* 12:345-364.
- NeilandsJ.B. 1995. Siderophores: structure and function of microbial iron transport compounds. *J. Biol. Chem.* 270:26723-26726.
- Newton,S.M., J.S.Allen, Z.Cao, Z.Qi, X.Jiang, C.Sprencel, J.D.Igo, S.B.Foster, M.A.Payne, and P.E.Klebba. 1997. Double mutagenesis of a positive charge cluster in the ligand-binding site of the ferric enterobactin receptor, FepA. *Proc Natl Acad Sci USA* 94:4560-5.
- Nicholls,A., K.Sharp, and B.Honig. 1992. GRASP Manual. Columbia University, New York, New York.
- Nikaido,H. and M.H.Saier, Jr. 1992. Transport proteins in bacteria: common themes in their design. *Science* 258:936-942.
- O'BrienJ.G. and F.Gibson. 1970. The structure of enterochelin and related 2,3-dihydroxy-N-benzoylserine conjugates from *Escherichia coli*. *Biochim. Biophys. Acta* 215:393-402.
- Ochs,M., A.Angerer, S.Enz, and V.Braun. 1996. Surface signaling in transcriptional regulation of the ferric citrate transport system of *Escherichia coli*: mutational analysis of

the alternative sigma factor FecI supports its essential role in iron transport gene transcription. *Mol. Gen. Genet.* 250:455-465.

Ochs, M., S. Veitinger, I. Kim, D. Welz, A. Angerer, and V. Braun. 1995. Regulation of citrate-dependent iron transport of *Escherichia coli*: fecR is required for transcription activation by FecI. *Mol. Microbiol.* 15:119-132.

Ochsner, U.A. and M.L. Vasil. 1996. Gene repression by the ferric uptake regulator in *Pseudomonas aeruginosa*: cycle selection of iron-regulated genes. *Proc. Natl. Acad. Sci. U. S. A.* 93:4409-4414.

Ochsner, U.A., A.I. Vasil, and M.L. Vasil. 1995. Role of the ferric uptake regulator of *Pseudomonas aeruginosa* in the regulation of siderophores and exotoxin A expression: purification and activity on iron-regulated promoters. *J. Bacteriol.* 177:7194-7201.

Ochsner, U.A., Z. Johnson, and M.L. Vasil. 2000. Genetics and regulation of two distinct haem-uptake systems, *phu* and *has*, in *Pseudomonas aeruginosa*. *Microbiology* 146:185-198.

Oguiza, J.A., A.T. Marcos, M. Malumbres, and J.F. Martin. 1996. Multiple sigma factor genes in *Brevibacterium lactofermentum*: characterization of *sigA* and *sigB*. *J. Bacteriol.* 178:550-553.

Oguiza, J.A., X. Tao, A.T. Marcos, J.F. Martin, and J.R. Murphy. 1995. Molecular cloning, DNA sequence analysis, and characterization of the *Corynebacterium diphtheriae* *dtxR* homolog from *Brevibacterium lactofermentum*. *J. Bacteriol.* 177:465-467.

Ogunnariwo, J.A. and A.B. Schryvers. 1996. Rapid identification and cloning of bacterial transferrin and lactoferrin receptor protein genes. *J. Bacteriol.* 178:7326-7328.

Osawa, M., H. Tokumitsu, M.B. Swindells, H. Kurihara, M. Orita, T. Shibamura, T. Furuya, and M. Ikura. 1999. A novel target recognition revealed by calmodulin in complex with Ca²⁺ - calmodulin-dependent kinase kinase. *Nat. Struct. Biol.* 6:819-824.

- Otwinowski,Z. and W.Minor. 1997. Processing of x-ray diffraction data collected in oscillation mode. *Methods Enzymol.* 276:307-326.
- Ozenberger,B.A., M.S.Nahlik, and M.A.Mcintosh. 1987. Genetic organization of multiple *fep* genes encoding ferric enterobactin transport functions in *Escherichia coli*. *J Bacteriol* 169:3638-46.
- Pace,C.N., F.Vajdos, L.Fee, G.Grimley, and T.Gray. 1995. How to measure and predict the molar absorption coefficient of a protein. *Protein Sci.* 4:2411-2423.
- Page,W.J. and M.Huyer. 1984. Derepression of the *Azotobacter vinelandii* siderophore system, using iron-containing minerals to limit iron repletion. *J. Bacteriol.* 158:496-502.
- Patzer,S.I. and K.Hantke. 1998. The ZnuABC high-affinity zinc uptake system and its regulator Zur in *Escherichia coli*. *Mol. Microbiol.* 28:1199-1210.
- Payne,S.M. 1988. Iron and virulence in the family *Enterobacteriaceae*. *Crit Rev. Microbiol.* 16:81-111.
- Payne,S.M. 1993. Iron acquisition in microbial pathogenesis. *Trends Microbiol.* 1:66-69.
- Persson,B. and P.Argos. 1994. Prediction of transmembrane segments in proteins utilising multiple sequence alignments. *J. Mol. Biol.* 237:182-192.
- Pettersson,A., A.Maas, and J.Tommassen. 1994. Identification of the *iroA* gene product of *Neisseria meningitidis* as a lactoferrin receptor. *J. Bacteriol.* 176:1764-1766.
- Pettersson,A., L.P.van der, J.T.Poolman, and J.Tommassen. 1993. Molecular characterization of the 98-kilodalton iron-regulated outer membrane protein of *Neisseria meningitidis*. *Infect. Immun.* 61:4724-4733.
- Pettersson,A., T.Prinz, A.Umar, B.J.van der, and J.Tommassen. 1998. Molecular characterization of LbpB, the second lactoferrin-binding protein of *Neisseria meningitidis*. *Mol. Microbiol.* 27:599-610.

- Pierce J.R. and C.F. Earhart. 1986. *Escherichia coli* K-12 envelope proteins specifically required for ferrienterobactin uptake. *J. Bacteriol.* 166:930-936.
- Pierce J.R., C.L. Pickett, and C.F. Earhart. 1983. Two *fep* genes are required for ferrienterochelin uptake in *Escherichia coli* K-12. *J. Bacteriol.* 155:330-336.
- Pohl, E., R.K. Holmes, and W.G. Hol. 1998. Motion of the DNA-binding domain with respect to the core of the diphtheria toxin repressor (DtxR) revealed in the crystal structures of apo- and holo-DtxR. *J. Biol. Chem.* 273:22420-22427.
- Pohl, E., R.K. Holmes, and W.G. Hoi. 1999. Crystal structure of the iron-dependent regulator (IdeR) from *Mycobacterium tuberculosis* shows both metal binding sites fully occupied. *J. Mol. Biol.* 285:1145-1156.
- Pohl, E., X. Qui, L.M. Must, R.K. Holmes, and W.G. Hol. 1997. Comparison of high-resolution structures of the diphtheria toxin repressor in complex with cobalt and zinc at the cation-anion binding site. *Protein Sci.* 6:1114-1118.
- Poole, K., S. Neshat, K. Krebs, and D.E. Heinrichs. 1993. Cloning and nucleotide sequence analysis of the ferripyoverdine receptor gene *fpvA* of *Pseudomonas aeruginosa*. *J. Bacteriol.* 175:4597-4604.
- Postle, K. 1993. TonB protein and energy transduction between membranes. *J. Bioenerg. Biomembr.* 25:591-601.
- Postle, K. and J.T. Skare. 1988. *Escherichia coli* TonB protein is exported from the cytoplasm without proteolytic cleavage of its amino terminus. *J. Biol. Chem.* 263:11000-11007.
- Postle, K. and R.F. Good. 1983. DNA sequence of the *Escherichia coli* tonB gene. *Proc. Natl. Acad. Sci. U. S. A* 80:5235-5239.
- Pressler, U., H. Staudenmaier, L. Zimmermann, and V. Braun. 1988. Genetics of the iron dicitrate transport system of *Escherichia coli*. *J. Bacteriol.* 170:2716-2724.

Prince, R.W., C.D. Cox, and M.L. Vasil. 1993. Coordinate regulation of siderophore and exotoxin A production: molecular cloning and sequencing of the *Pseudomonas aeruginosa* *fur* gene. *J. Bacteriol.* 175:2589-2598.

Pugsley, A.P., W. Zimmerman, and W. Wehrli. 1987. Highly efficient uptake of a rifamycin derivative via the FhuA-TonB- dependent uptake route in *Escherichia coli*. *J. Gen. Microbiol* 133 (Pt 12):3505-3511.

Qiu, X., C.L. Verlinde, S. Zhang, M.P. Schmitt, R.K. Holmes, and W.G. Hol. 1995. Three-dimensional structure of the diphtheria toxin repressor in complex with divalent cation co-repressors. *Structure.* 3:87-100.

Qiu, X., E. Pohl, R.K. Holmes, and W.G. Hol. 1996. High-resolution structure of the diphtheria toxin repressor complexed with cobalt and manganese reveals an SH3-like third domain and suggests a possible role of phosphate as co-corepressor. *Biochemistry* 35:12292-12302.

Quioco, F.A. 1990. Atomic structures of periplasmic binding proteins and the high-affinity active transport systems in bacteria. *Philos. Trans. R. Soc. Lond B Biol. Sci.* 326:341-351.

Quioco, F.A. and P.S. Ledvina. 1996. Atomic structure and specificity of bacterial periplasmic receptors for active transport and chemotaxis: variation of common themes. *Mol. Microbiol.* 20:17-25.

Ratledge, C. and L.G. Dover. 2000. Iron metabolism in pathogenic bacteria. *Annu. Rev. Microbiol.* 54:881-941.

Raymond, K.N. and C.J. Carrano. 1979. Coordination chemistry and microbial iron transport. *Acc. Chem. Res.* 12:183-190.

Richardson, P.T. and S.F. Park. 1995. Enterochelin acquisition in *Campylobacter coli*: characterization of components of a binding-protein-dependent transport system. *Microbiology* 141:3181-3191.

- Rohrbach, M.R., V. Braun, and W. Koster. 1995a. Ferrichrome transport in *Escherichia coli* K-12: altered substrate specificity of mutated periplasmic FhuD and interaction of FhuD with the integral membrane protein FhuB. *J. Bacteriol.* 177:7186-7193.
- Rohrbach, M.R., S. Paul, and W. Koster. 1995b. *In vivo* reconstitution of an active siderophore transport system by a binding protein derivative lacking a signal sequence. *Mol Gen Genet* 248:33-42.
- Roosenberg J.M., Y.M. Lin, Y. Lu, and M.J. Miller. 2000. Studies and syntheses of siderophores, microbial iron chelators, and analogs as potential drug delivery agents. *Curr. Med. Chem.* 7:159-197.
- Roussel, A. and C. Cambillau. 1989. TURBO-FRODO. In Silicon Graphics Geometry Partner Directory. Silicon Graphics, Mountain View, California. 77-88.
- Rutz, J.M., J. Liu, J.A. Lyons, J. Goranson, S.K. Armstrong, M.A. McIntosh, J.B. Feix, and P.E. Klebba. 1992. Formation of a gated channel by a ligand-specific transport protein in the bacterial outer membrane. *Science* 258:471-475.
- Saito, T., M.R. Wormald, and R.J. Williams. 1991. Some structural features of the iron-uptake regulation protein. *Eur. J. Biochem.* 197:29-38.
- Saken, E., A. Rakin, and J. Heesemann. 2000. Molecular characterization of a novel siderophore-independent iron transport system in *Yersinia*. *Int. J. Med. Microbiol* 290:51-60.
- Sambrook J., E.F. Fritsch, and T. Maniatis. 1989. Molecular cloning: A Laboratory Manual. Cold Spring Harbour Laboratory Press, New York.
- Saurin, W., W. Koster, and E. Dassa. 1994. Bacterial binding protein-dependent permeases: characterization of distinctive signatures for functionally related integral cytoplasmic membrane proteins. *Mol. Microbiol.* 12:993-1004.

Sauvage,C, T.Franza, and D.Expert. 1996. Analysis of the *Erwinia chrysanthemi* ferrichrysoactin receptor gene: resemblance to the *Escherichia coli* *fepA-fes* bidirectional promoter region and homology with hydroxamate receptors. *J. Bacteriol.* 178:1227-1231.

Schaffer,S., K.Hantke, and V.Braun. 1985. Nucleotide sequence of the iron regulatory gene *fur*. *Mol. Gen. Genet.* 200:110-113.

SchalkJ.J., P.Kyslik, D.Prome, A.van Dorsseleer, K.Poole, M.A.Abdallah, and F.Pattus. 1999. Copurification of the FpvA ferric pyoverdine receptor of *Pseudomonas aeruginosa* with its iron-free ligand: implications for siderophore-mediated iron transport. *Biochemistry* 38:9357-9365.

Schiering,N., X.Tao, H.Zeng, J.R.Murphy, G.A.Petsko, and D.Ringe. 1995. Structures of the apo- and the metal ion-activated forms of the diphtheria *tox* repressor from *Corynebacterium diphtheriae*. *Proc. Natl. Acad. Sci. U. S. A* 92:9843-9850.

SchmittM.P. and R.K.Holmes. 1993. Analysis of diphtheria toxin repressor-operator interactions and characterization of a mutant repressor with decreased binding activity for divalent metals. *Mol. Microbiol.* 9:173-181.

Schmitt,M.P., B.G.Talley, and R.K.Holmes. 1997. Characterization of lipoprotein IRP1 from *Corynebacterium diphtheriae*, which is regulated by the diphtheria toxin repressor (DtxR) and iron. *Infect. Immun.* 65:5364-5367.

Schmitt,M.P., M.Predich, L.Doukhan, I.Smith, and R.K.Holmes. 1995. Characterization of an iron-dependent regulatory protein (IdeR) of *Mycobacterium tuberculosis* as a functional homolog of the diphtheria toxin repressor (DtxR) from *Corynebacterium diphtheriae*. *Infect. Immun.* 63:4284-4289.

Schneider,E. and S.Hunke. 1998. ATP-binding-cassette (ABC) transport systems: functional and structural aspects of the ATP-hydrolyzing subunits/domains. *FEMS Microbiol. Rev.* 22:1-20.

- Schneider,R. and K.Hantke. 1993. Iron-hydroxamate uptake systems in *Bacillus subtilis*: identification of a lipoprotein as part of a binding protein-dependent transport system. *Mol. Microbiol.* 8:111-121.
- Schoffler,H. and V.Braun. 1989. Transport across the outer membrane of *Escherichia coli* K12 via the FhuA receptor is regulated by the TonB protein of the cytoplasmic membrane. *Mol. Gen. Genet.* 217:378-383.
- Schryvers,A.B. and B.C.Lee. 1989. Comparative analysis of the transferrin and lactoferrin binding proteins in the family *Neisseriaceae*. *Can. J. Microbiol.* 35:409-415.
- Schryvers,A.B. and I.Stojiljkovic. 1999. Iron acquisition systems in the pathogenic *Neisseria*. *Mol. Microbiol.* 32:1117-1123.
- Schryvers,A.B. and L.J.Morris. 1988a. Identification and characterization of the transferrin receptor from *Neisseria meningitidis*. *Mol. Microbiol.* 2:281-288.
- Schryvers,A.B. and L.J.Morris. 1988b. Identification and characterization of the human lactoferrin-binding protein from *Neisseria meningitidis*. *Infect. Immun.* 56:1144-1149.
- Schultz-Hauser,G., W.Koster, H.Schwarz, and V.Braun. 1992. Iron(III) hydroxamate transport in *Escherichia coli* K-12: FhuB-mediated membrane association of the FhuC protein and negative complementation of *offhuC* mutants. *J. Bacteriol.* 174:2305-2311.
- Shea,C.M. and M.A.Mcintosh. 1991. Nucleotide sequence and genetic organization of the ferric enterobactin transport system: homology to other periplasmic binding protein-dependent systems in *Escherichia coli*. *Mol Microbiol* 5:1415-28.
- Shilton,B.H., H.A.Shuman, and S.L.Mowbray. 1996. Crystal structures and solution conformations of a dominant-negative mutant of *Escherichia coli* maltose-binding protein. *J. Mol. Biol.* 264:364-376.

Sigel,S.P. and S.M.Payne. 1982. Effect of iron limitation on growth, siderophore production, and expression of outer membrane proteins of *Vibrio cholerae*. *J. Bacteriol.* 150:148-155.

Skare,J.T. and K.Postle. 1991. Evidence for a TonB-dependent energy transduction complex in *Escherichia coli*. *Mol. Microbiol.* 5:2883-2890.

SkareJ.T., B.M.Ahmer, C.L.Seachord, R.P.Darveau, and K.Postle. 1993. Energy transduction between membranes. TonB, a cytoplasmic membrane protein, can be chemically cross-linked *in vivo* to the outer membrane receptor FepA. *J. Biol. Chem.* 268:16302-16308.

SokofP.A. 1987. Surface expression of ferripyochelin-binding protein is required for virulence of *Pseudomonas aeruginosa*. *Infect. Immun.* 55:2021-2025.

Sokol,P.A. and D.E.Woods. 1984. Relationship of iron and extracellular virulence factors to *Pseudomonas aeruginosa* lung infections. *J. Med. Microbiol.* 18:125-133.

Sprencel,C, Z.Cao, Z.Qi, D.C.Scott, M.A.Montague, N.Ivanoff, J.Xu, K.M.Raymond, S.M.Newton, and P.E.Klebba. 2000. Binding of ferric enterobactin by the *Escherichia coli* periplasmic protein FepB. *J. Bacteriol.* 182:5359-5364.

Staggs,T.M. and R.D.Perry. 1995. Fur regulation in *Yersinia species*. *Mol. Microbiol.* 17:601.

Staudenmaier,H., B.Van Hove, Z.Yaraghi, and V.Braun. 1989. Nucleotide sequences of the *fecBCDE* genes and locations of the proteins suggest a periplasmic-binding-protein-dependent transport mechanism for iron(III) dicitrate in *Escherichia coli*. *J. Bacteriol.* 171:2626-2633.

Stephens,D.L., M.D.Choe, and C.F.Earhart. 1995. *Escherichia coli* periplasmic protein FepB binds ferrienterobactin. *Microbiology* 141:1647-1654.

- Stintzi,A., Z.Johnson, M.Stonehouse, U.Ochsner, J.M.Meyer, M.L.Vasil, and K.Poole. 1999. The *pvc* gene cluster of *Pseudomonas aeruginosa*: role in synthesis of the pyoverdine chromophore and regulation by PtxR and PvdS. *J. Bacteriol.* 181:4118-4124.
- Stoebner,J.A. and S.M.Payne. 1988. Iron-regulated hemolysin production and utilization of heme and hemoglobin by *Vibrio cholerae*. *Infect. Immun.* 56:2891-2895.
- StojiljkovicJ. and K.Hantke. 1992. Hemin uptake system of *Yersinia enterocolitica*: similarities with other TonB-dependent systems in gram-negative bacteria. *EMBO J.* 11:4359-4367.
- Stojiljkovic,I. and K.Hantke. 1994. Transport of haemin across the cytoplasmic membrane through a haemin- specific periplasmic binding-protein-dependent transport system in *Yersinia enterocolitica*. *Mol. Microbiol.* 13:719-732.
- Stojiljkovic,I. and K.Hantke. 1995. Functional domains of the *Escherichia coli* ferric uptake regulator protein (Fur). *Mol. Gen. Genet.* 247:199-205.
- StojiljkovicJ. and N.Srinivasan. 1997. *Neisseria meningitidis tonB, exbB, and exbD* genes: Ton-dependent utilization of protein-bound iron in *Neisseriae*. *J. Bacteriol.* 179:805-812.
- StojiljkovicJ., A.J.Baumler, and K.Hantke. 1994. Fur regulon in gram-negative bacteria. Identification and characterization of new iron-regulated *Escherichia coli* genes by a *fur* titration assay. *J. Mol. Biol.* 236:531-545.
- StojiljkovicJ., J.Larson, V.Hwa, S.Anic, and M.So. 1996. HmbR outer membrane receptors of pathogenic *Neisseria* spp.: iron- regulated, hemoglobin-binding proteins with a high level of primary structure conservation. *J. Bacteriol.* 178:4670-4678.
- Studier,F.W. and B.A.Moffatt. 1986. Use of bacteriophage T7 RNA polymerase to direct selective high-level expression of cloned genes. *J. Mol. Biol.* 189:113-130.

Sun, T.P. and R.E. Webster. 1987. Nucleotide sequence of a gene cluster involved in entry of E colicins and single-stranded DNA of infecting filamentous bacteriophages into *Escherichia coli*. *J. Bacteriol.* 169:2667-2674.

Tam, R. and M.H. Saier, Jr. 1993. Structural, functional, and evolutionary relationships among extracellular solute-binding receptors of bacteria. *Microbiol. Rev.* 57:320-346.

Theif E.C. 1987. Ferritin: structure, gene regulation, and cellular function in animals, plants, and microorganisms. *Annu. Rev. Biochem.* 56:289-315.

Thomas, C.E. and P.F. Sparling. 1994. Identification and cloning of a *fur* homologue from *Neisseria meningitidis*. *Mol. Microbiol.* 11:725-737.

Thomas, C.E. and P.F. Sparling. 1996. Isolation and analysis of a *fur* mutant of *Neisseria gonorrhoeae*. *J. Bacteriol.* 178:4224-4232.

Thompson, J.D., T.J. Gibson, F. Plewniak, F. Jeanmougin, and D.G. Higgins. 1997. The CLUSTAL_X windows interface: flexible strategies for multiple sequence alignment aided by quality analysis tools. *Nucleic Acids Res.* 25:4876-4882.

Thompson, J.D., T.J. Gibson, F. Plewniak, F. Jeanmougin, and D.G. Higgins. 1997. The CLUSTAL-X windows interface: flexible strategies for multiple sequence alignment aided by quality analysis tools. *Nucleic Acids Res.* 25:4876-4882.

Thulasiraman, P., S.M. Newton, J. Xu, K.N. Raymond, C. Mai, A. Hall, M.A. Montague, and P.E. Klebba. 1998. Selectivity of ferric enterobactin binding and cooperativity of transport in gram-negative bacteria. *J. Bacteriol.* 180:6689-6696.

Tolmasky, M.E., A.M. Wertheimer, L.A. Actis, and J.H. Crosa. 1994. Characterization of the *Vibrio anguillarum fur* gene: role in regulation of expression of the FatA outer membrane protein and catechols. *J. Bacteriol.* 176:213-220.

Tolmasky, M.E., L.A. Actis, and J.H. Crosa. 1988. Genetic analysis of the iron uptake region of the *Vibrio anguillarum* plasmid pJM1: molecular cloning of genetic determinants encoding a novel trans activator of siderophore biosynthesis. *J. Bacteriol.* 170:1913-1919.

Torres, A.G. and S.M. Payne. 1997. Haem iron-transport system in enterohaemorrhagic *Escherichia coli* 0157:H7. *Mol. Microbiol.* 23:825-833.

Traub J., S. Gaisser, and V. Braun. 1993. Activity domains of the TonB protein. *Mol. Microbiol.* 8:409-423.

Tsolis, R.M., A.J. Baumber, F. Heffron, and I. Stojiljkovic. 1996. Contribution of TonB- and Feo-mediated iron uptake to growth of *Salmonella typhimurium* in the mouse. *Infect. Immun.* 64:4549-4556.

Tsolis, R.M., A.J. Baumber, I. Stojiljkovic, and F. Heffron. 1995. Fur regulon of *Salmonella typhimurium*: identification of new iron-regulated genes. *J. Bacteriol.* 177:4628-4637.

Van der Helm, D., J.R. Baker, D.L. Eng-Wilmot, M.B. Hossain, and R.A. Loghry. 1980. Crystal structure of ferrichrome and a comparison with the structure of ferrichrome A. *J. Am. Chem. Soc.* 102:4224-4231.

Van Hove, B., H. Staudenmaier, and V. Braun. 1990. Novel two-component transmembrane transcription control: regulation of iron dicitrate transport in *Escherichia coli* K-12. *J. Bacteriol.* 172:6749-6758.

Vasif M.L. and U.A. Ochsner. 1999. The response of *Pseudomonas aeruginosa* to iron: genetics, biochemistry and virulence. *Mol. Microbiol.* 34:399-413.

Venturi, V., C. Ottevanger, M. Bracke, and P. Weisbeek. 1995a. Iron regulation of siderophore biosynthesis and transport in *Pseudomonas putida* WCS358: involvement of a transcriptional activator and of the Fur protein. *Mol. Microbiol.* 15:1081-1093.

Venturi, V., P. Weisbeek, and M. Koster. 1995b. Gene regulation of siderophore-mediated iron acquisition in *Pseudomonas*: not only the Fur repressor. *Mol. Microbiol.* 17:603-610.

- Verlinde, C.L. and W.G.Hol. 1994. Structure-based drug design: progress, results and challenges. *Structure*. 2:577-587.
- Wandersman, C. and I.Stojiljkovic. 2000. Bacterial heme sources: the role of heme, hemoprotein receptors and hemophores. *Curr. Opin. Microbiol.* 3:215-220.
- Wang, R., Y.Gao, and L.Lai. 2000. LigBuilder: A Multipurpose Program for Structure-Based Drug Design. *J. Mol. Model.* 6:498-516.
- Webster, R.E. 1991. The *tol* gene products and the import of macromolecules into *Escherichia coli*. *Mol. Microbiol.* 5:1005-1011.
- Wyckoff, E.E., A.M.Valle, S.L.Smith, and S.M.Payne. 1999. A multifunctional ATP-binding cassette transporter system from *Vibrio cholerae* transports vibriobactin and enterobactin. *J. Bacteriol.* 181:7588-7596.
- Yeoman, K.H., F.Wisniewski-Dye, C.Timony, J.B.Stevens, N.G.deLuca, J.A.Downie, and A.W.Johnston. 2000. Analysis of the *Rhizobium leguminosarum* siderophore-uptake gene *fhuA*: differential expression in free-living bacteria and nitrogen-fixing bacteroids and distribution of an *jhuA* pseudogene in different strains. *Microbiology* 146:829-837.
- Young, J.G. 1976. Preparation of Enterochelin from *Escherichia coli*. *Prep. Biochemistry* 6:123-131.
- Zhang, M., T.Tanaka, and M.Ikura. 1995. Calcium-induced conformational transition revealed by the solution structure of apo calmodulin. *Nat. Struct. Biol.* 2:758-767.
- Zimmermann, L., K.Hantke, and V.Braun. 1984. Exogenous induction of the iron dicitrate transport system of *Escherichia coli* K-12. *J. Bacteriol.* 159:271-277.